An investigation of an innovative power pack and motor for a compressed air car of practical performance.

Henry Robert Ditmore

School of Electronics and Computer Science

An Investigation of an Innovative Power Pack and Motor for a Compressed Air Car of Practical Performance

H. R. Ditmore

A thesis submitted in partial fulfilment of the requirements of the University of Westminster for the degree of Doctor of Philosophy

January 2011

Abstract

This thesis investigates the design and potential of an automobile that is powered by compressed air supplied from an on board store charged by a separate compressor. That store is a carbon fibre sphere of 250 litres capacity and, once charged with compressed air to 30MPa, has a specific energy density the equal of conventional Ni-Mh electrochemical batteries. It is shown that this store can be built to a safe international standard and it is reasonable that the store can be expected to have a life equivalent to the life of the vehicle. In contrast, all electric vehicle batteries can be expected to have a life of 3 – 5 years.

The range and efficiency of the vehicle are contributed to by a lightweight heat pipe based heat exchanger that takes heat from ambient air and uses it to raise the temperature of the compressed air stream that is initially at 60K below ambient temperatures. The compressed air stream's temperature is raised to within 10K of the ambient temperature and that increase in enthalpy makes a significant difference to the performance of the system. It is shown that this is equivalent to at least a 13% increase in storage capacity. The inclusion of this heat exchanger increases the system energy density to equal the best Ni-Mh electrochemical batteries.

Almost all electric battery vehicles have a regenerative braking system that collects a proportion of the vehicles braking energy, normally lost to the environment. This project has investigated a unique design of regenerative braking system that uses a heat pipe heat exchanger to collect the heat resulting from braking. Those heat pipes then transfer the heat to a water/alcohol based heat store. Further heat pipes transfer the heat to the compressed air flow once the vehicle is moving and re-uses that energy to further increase the energy available to the compressed air motor/prime mover. The first system tested was an open system that allowed the hot air to escape to the atmosphere after one pass through the heat exchanger. Whilst being an easily implemented system it proved to be inefficient at capturing the heat of braking and it was replaced by a closed system in which the hot air was recirculated through the brake and heat exchanger. This final system achieved an efficiency of 70% with potential for further improvements. It is believed that this is the first system of its type to be used in this kind of application.

In order to maximise the range of any future compressed air driven vehicle it was necessary to design a new kind motor. The basic design is that of a rotary multi-vane expander. In order to maximise the motor's efficiency, whilst dealing with the wide range of motoring demands that a commuting vehicle can expect to make upon its motor, it was necessary to make several elements of the motor's geometry adaptable. Some of these can vary their geometry whilst the motor is in operation. Initial tests suggest an efficiency of 88% has been achieved but higher efficiencies are expected with further work.

Contents

List of Figures

List of Tables

Nomenclature

A	Area (m^2)
C_p	Specific Heat, Constant Pressure (kJ/kg.K)
D	Characteristic diameter of the expander (m)
D_S	Specific Diameter (see equation 7.2 - p179)
E_g	Energy supplied to Consumer
E_s	Energy stored (J)
F	Force (N)
F_L	Aerodynamic drag (N)
F_{RO}	Rolling resistance (N)
F_{ST}	Climb resistance (N)
F_W	Driving resistance (N)
g	Gravitational acceleration
h	Specific enthalpy (kJ/kg)
m	Mass (kg)
$\dot{m}$	Mass flow rate (kg/s)
N	Expander rotational speed (rpm)
N	Number of moles
N_S	Specific speed (see equation 7.1 - p179)
P	Pressure (Pa)
Pb	Burst pressure of finished cylinder (bar)
Ph	Test pressure of finished cylinder (bar)

Pmax	Maximum pressure (bar)
P_o	Pressure, original (Pa)
P_W	Motive power (W)
Pw	Working pressure of cylinder (bar)
Q	Expander outlet volume flow (m^3/s)
Q	Heat Transfer (k/J)
$\dot{Q}$	Heat Transfer Rate (k/W)
R_u	Universal Gas Constant (kJ/kmol.K)
S	Entropy (kJ/K)
T	Temperature C° or K
V	Volume (m^3)
V_f	Volume, final (m^3)
V_o	Volume, original (m^3)
W_{in}	Work Input (kJ)
W_{out}	Work Output (k/J)
$(\Delta h)_{is}$	Isentropic enthalpy drop across the expander (J/kg)
η_{mech}	Mechanical efficiency (%)
ρ	Density (kg/m^3)
σ_p	Maximum allowable tensile stress (Pa)

Abbreviations

RPE	Reciprocating Piston Expander
RoPE	Rotary Piston Expander
MVE	Multi-vane Expander
VCR	Variable Compression Ratio
VER	Variable Expansion Ratio
VPT	Variable Port Timing
HEV	Hybrid Electric Vehicle
ICE	Internal Combustion Engine
ZEV	Zero Emissions Vehicle
CARB	California Air Resources Board
CA	Compressed Air
CAES	Compressed Air Energy Storage

D.O.D.	Depth of Discharge (%)
AR	Aspect Ratio
BNCB	British national Coal Board
BDC	Bottom Dead Centre
IEA	International Energy Agency

Acknowledgements

The author would like to express his thanks to Dr Christopher Marquand who enabled this project to be initiated and remained a supporter during the many years of its delayed fruition. Thanks are also deserved by Dr Wah Cheng Lee who stepped in as supervisor in the last year of the project and provided much needed help in refining the thesis. Additional thanks are due to Dr Andrezej Tarczynski for further support in the final year of the project. Personal thanks are due to Shirley Blakemore for her understanding and personal support throughout this project.

A more general thanks is due to the former Department of Technology and Design, (University of Westminster) for its financial support in the early years of the project, and its academic staff for their general assistance.

1. Introduction

Compressed air energy storage (CAES) is an old technology that was in common use over a century ago to reduce the load demands on compressors supplying power to factories and some street car systems in the USA. These systems used compressed air as a method of short range power transmission, the primary motive power coming from heavy steam or electric motor driven compressors. Air motors of the time were powerful, compact and reliable in comparison to the smaller IC engines and electric motors then possible, but, as the rival technologies developed compressed air energy fell out of common use. They are now largely restricted to situations where a potentially combustible environment requires a low temperature energy source with no risk of sparking.

These early systems were never particularly transportable (the street-car systems drew electricity from overhead power lines) but now maturing technologies (lightweight materials, heat pipes etc) and an increased understanding of air motor losses make a practical transportable CAES system a possibility. Such a system would have a number of advantages over current rival systems, particularly the electric battery powered car.

This thesis presents an investigation into a transportable CAES and air motor system design that overcomes many of the problems associated with such systems and may allow the widespread use of compressed air, from a variety of sources, as motive power.

1.1 Aims

This thesis is intended to demonstrate theoretically and practically that a motor car of acceptable performance, solely driven by onboard stored compressed air, is a realistic concept. The primary aims are to:

- Investigate, evaluate the design of a lightweight pressure cell and arrive at an optimum design.
- Design and build a compact heat pipe heat exchanger test rig to investigate the possibility of using heat pipes as a reheat mechanism for cold compressed air.
- Evaluate the potential methods of achieving a regenerative braking system intended to use the energy of braking to return energy to the compressed air stream or storage cell.
- Design build and investigate a number of practical design solutions to previously identified sources of losses in a type of compressed gas motor called an eccentric vane motor or a multi vane expander (MVE).

1.2 Thesis Structure

The thesis chapters will, largely, follow the aims of the project as outlined above but with additional explanatory material.

Chapter 2 contains a review of the use of compressed gases as an energy storage medium and the current level of technology applied to vehicles using such systems for motive power.

Chapter 3 is an overview of the thermodynamic background of CAES, the envisioned air car cycle and the theoretically derived energy storage capabilities of the transportable compressed air store. These are in turn related to the energy requirements of an appropriate automobile.

Chapter 4 deals with the intended design for the compressed air store relating it to the relevant international standard and the safety tests it must meet. Also the intended manufacturing processes are explored in order to verify the vessel's practicality. The final part of this chapter estimates the weight of the intended design and gives a preliminary estimate of the systems energy density.

Chapter 5 details the design of the primary heat exchanger, the design of the heat pipe test rig and the experimental results from that rig. Those results are factored into the energy density calculations for a final estimate of the system energy density.

Chapter 6 explores a unique but practical design of regenerative braking system and the results from an initial test rig.

Chapter 7 deals with the design, building and testing of a compressed air motor. The design is in the form of a multi-vane expander with adaptive geometry, that can be changed whilst the motor is in operation. The loss pathways and mechanical elements requiring improvement, in this basic motor form, have been identified elsewhere and each is dealt with in order to maximise efficiency.

2. Compressed Gas Energy Storage in Context

2.1 Introduction

The following chapter is a review of CAES, and some other compressed gases, as used in both stationary and mobile installations. A general look at history of compressed air in personal transport will be followed by a review of the problems faced by current, and proposed, personal transport systems. It is intended that these sections will clarify the position and justification for this project. Finally, criteria for evaluating the proposed Compac will be discussed.

2.2 Why Store Energy?

Our general power requirements, both as individuals and as a society, vary a great deal across a number of time scales. It is well known that the ending of a popular TV programme can result in an electrical power demand surge as viewers boil water for a drink. This surge takes place on a time scale of minutes. More manageable is the change in demand resulting from the change in behaviour from winter to summer. All of these changes must be met by supply systems constructed from elements with response times ranging from tens of minutes, in the case of gas turbine plant, to hours or days for nuclear plant.

In addition to response times there is the problem of plant efficiency. Most plant operate at their most efficient level within a limited range of speeds and loads etc. so it is in the economic interests of the operator to operate the plant in the highest efficiency range. With a varying load and no means to store energy generated at low demand times, operators must often order plant large enough to deal with high demand but then operate it at low efficiency during low demand times.

A new problem has been the insertion of intermittent renewable energy sources into the national grid. Attempts to mitigate global warming by reducing CO_2 output have resulted in a number of countries greatly increasing the proportion of renewables in their supply. The problem with this is that most renewable sources are intermittent in nature, wind being the most obvious example. Continental European experience, especially in Denmark, has shown that grid stability can be adversely affected when the proportion of intermittent renewable sources reaches about 18%. The most recent British Energy Review, published on 15th Feb 2002, sets a target of generating 20%

of UK energy from renewable sources by 2020, and has been criticised as not addressing the problem of intermittent supply.

Given that renewable power generation cannot be constant, and that customers are unlikely to modify their power demands to accommodate suppliers, then there must be an element in the system that can transmit energy from times of over supply to times of high demand. This element must be some form of energy storage.

2.2.1 Large Scale Energy Storage Examples

The most popular form of large-scale energy storage is pumped hydro storage, often combined with a normal hydroelectric plant. The turnaround efficiency of a pure pumped hydro plant is the ratio of the energy generated and supplied to the consumer (E_g) to the energy consumed whilst pumping (E_p) - E_g/E_p. A pure pumped-storage plant, designed for daily or weekly storage, has a turnaround efficiency in the range 70-85% but is limited to terrain that has a large area, close to and above the pumping facility, capable of being adapted to water storage. The greater the distance from the facility the storage area is then the lower the turnaround efficiency due to pumping losses in the piping. A good example is the 1800 MW Dinorwic pumped hydro storage power station which is a hollowed out mountain that can deliver 1320 MW within 10 seconds of demand and is capable of "black start". That means it is possible for it to start generating without any external power supply

Excellent though these systems can be their provision is constrained by local geography and the limited availability of suitable sites. They can be added to

reservoirs but the different operating regimes often cause problems. However, CAES requires only a stable airtight cavity in the ground. Simple though this sounds, the execution may be complex and expensive.

A number of studies carried out in the USA have shown that there are no technical limitations to the widespread application of CAES, but since large volumes of air have to be stored, conventional vessels are quite impractical and underground storage in impermeable material is essential. Unfortunately, leak-tight rock is hard to find so the two following examples use a cavern excavated in an impermeable salt layer.

2.2.1.1 CAES, Huntorf, Germany.

The Huntorf CAES was commissioned in Dec 1978 and is rated at 290MW with an air storage capacity of $3x10^5$ m^3 distributed across two caverns [Mattick et al, 1975]. Based on a Swedish patent, a simplified schematic of the system is shown in Figure 2.1 below.

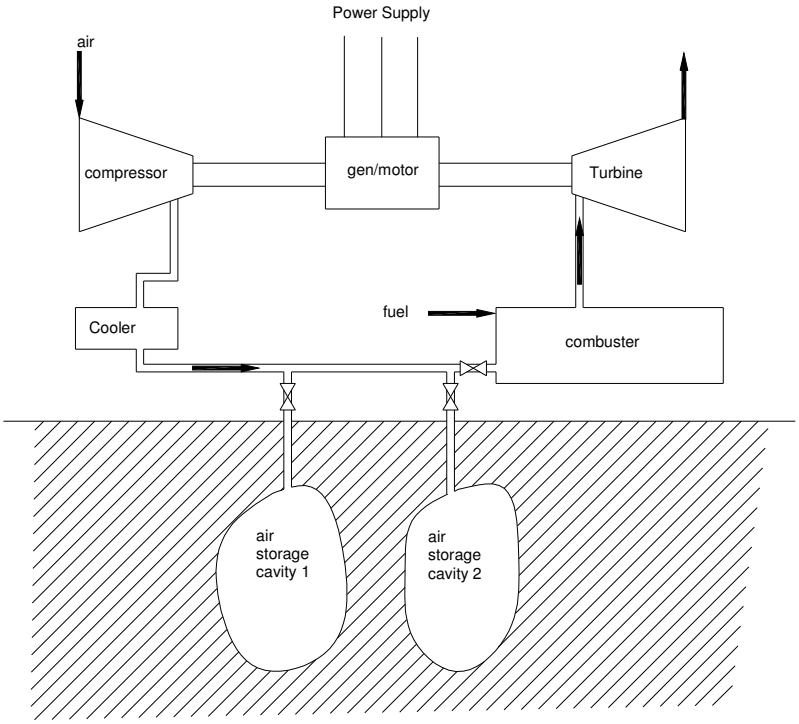

Figure 2.1 - Simplified layout of Huntorf CAES facility

In this case the salt caverns have been excavated by the technology of 'solution mining' in which fresh water is injected into a salt layer in order to dissolve the salt. The saturated brine is then extracted and disposed of. This is an attractive method of constructing the storage caverns, as it is cheap and well understood having been used for oil and gas storage. Although virtually leak-tight (leakage losses are estimated at 10^{-5} –10^{-6} m^3 per day) the caverns have their problems, primary amongst which are:

- Brine disposal, common to the chemical industry, but still a problem.
- The salt is plastic and creeps under the subterranean pressure, distorting and reducing the chamber.
- Salt crystals detach from the chamber walls and contaminate the turbine.

The latter two place limitations on the operation of the caverns. The pressure range is limited to 66 – 46 bar and the pressure change rate is limited to 10 bar/h. The

minimum pressure of 46 bar is because the turbine is run at a constant inlet pressure of 46 bar. Because of this unusually high inlet pressure the turbine stage is, in fact, a two stage expansion through a high and low pressure turbine.

The facility is designed to generate peak power for two hours a day and to be recharged over eight hours. During compression the air is cooled to 50 °C for efficiency, and geological reasons. There is no provision to scavenge and reuse the heat that is discarded either from the compressor or the turbine stages.

2.2.1.2 CAES, McIntosh, Alabama

After a little under three years of construction the Alabama Electric co-operative took delivery of the 110 MW McIntosh CAES, in 1991 [Lamarre,1991]. This facility was intended to be an improved version of the Huntorf plant. The improvement was based upon the addition of a 'recuperator '. This device is a heat exchanger intended to increase the plants thermodynamic performance by using waste heat, from the exhaust stacks, to pre-heat air from the storage cavern before it enters the combustor chamber. The heat from cooling the CAES compression stages is still rejected to the atmosphere.

This type of plant, the same as Huntorf, feeds the combustion gases directly to the turbine section and so needs high quality fuel to reduce particulate contamination that might damage the turbine. Normally the fuel is gas or oil and is relatively expensive. The addition of the recuperator reduces the fuel consumption by some

25% [Lamarre, 1991] whilst the remaining basic components are similar to those found in Huntorf.

The air storage cavern is 500 m below the ground in a salt deposit that is 8 miles deep and 1.5 miles in diameter. The cavern itself is 300 m deep and 80 m in diameter with a volume of 5.32 x 10^6 m^3 so there is plenty of room for additional caverns if necessary. So far the plant has proved successful, being able to change load at a rate of 33 MW a minute, which, on a percentage basis, is three times faster than any other type of plant.

The pressure range, of the storage cavern, is similar to the Huntorf system at 74 - 45 bar and allows a mass delivery rate of 170kg/s. It would be advantageous to operate the caverns at a higher pressure to increase storage capacity. However, 70+ bar is the current economic maximum as this is the practical maximum pressure that can be developed with the present design of compressor that can be directly coupled to a gas turbine. It is possible to obtain much higher pressures but much larger equipment of a different design would be required and it is currently deemed uneconomic.

2.3 Compressed Gases and CAES in Transport

Self contained compressed air powered vehicles have a history almost as old as stationary systems. Knight's American Mechanical Dictionary [Knight,1876A] refers to a number of compressed air locomotives and goes on to say "One of these (compressed air locomotives) was invented by BOMPAS (English Patent, 1828) ….. An engine, similar in most material respects to the above, was made by

Baron Von Rathlen in 1848, and was driven by its compressed air motor from Putney to Wandsworth (England) at a rate of ten or twelve miles per hour." It is not clear if this last vehicle ran on rails but the same reference refers, in detail, to a vehicle design developed by Parsey in 1847.This is shown in Fig 2.2. Whilst not obviously an independent road travelling vehicle Knight claims that, at the time of his publication, this project was being "revived for impelling street-cars".

In general literature, several comments have been noted in reference to a US patent for a compressed air powered vehicle was issued to a Charles Buell in 1885. However, no further details have been discovered.

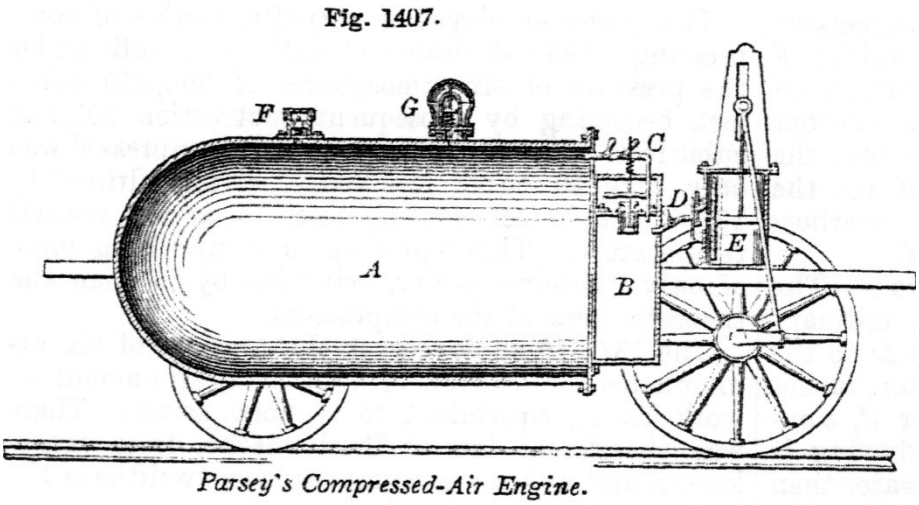

Fig 2.2 Parsey's Compressed Air Engine

As IC engines and electric motors developed compressed air fell out of favour, mainly because the riveted steel tanks that formed the compressed air stores were large and heavy and couldn't be trusted to contain high pressures safely.

External combustion in the form of steam power fared rather better and is mentioned in this context as it shares many of the advantageous characteristics of compressed air. Indeed, dry steam at pressure, has a similar behaviour to compressed air and requires similar mechanical techniques to control and extract energy as will be seen later. Otherwise the similarities in the systems are limited due to the requirement to deal with the phase change from steam to water and high temperature differences.

The following sub-sections deal with the case histories of the most notable attempts to use pressurised gases for motive power and indicate the current performance requirements and benefits of a modern compressed air car. For brevity I will, henceforth, refer to the compressed air car as a Compac.

2.3.1 The Stanley Steamer

The relatively high power to weight ratio possible with steam power at the start of the 20th century resulted in steam powered cars holding a number of speed records. In 1906 a special vehicle built by the Stanley Steam Automobile Co became the first car to exceed two miles a minute, 127.66 mph to be precise. The following year the same driver, Fred Marriott, tried to beat his own record in another Stanley. His vehicle was travelling at an estimated 190 mph when his vehicle passed over a depression in the sand of Ormand Beach, Florida. The wind pressure against the flat-bottomed car lifted it into the air and the car reputedly rolled end over end for more than a mile. Marriott survived but his impressive speed never entered the record books. However, the earlier record stood for a number of years and, perhaps more interestingly from the point of view of this thesis, was not beaten until the late forties

by a car of the same weight. That these competitive power to weight ratios were possible using only iron and steel shows one of the inherent advantages of using high pressure gases as a source of power.

The record breaking Stanleys used sophisticated steam engines that were, admittedly, approaching the limits of their development. However, the commercially available Stanley of 1906 was a much simpler machine using a straightforward double acting twin cylinder expansion engine coupled directly to the rear axle with no intervening gearbox. The boiler was a simple pressurised multi-tube design with no condenser, so water consumption was reputedly a gallon a mile. Subsequent models acquired a condenser and flash steam generator with greater efficiency and power but ultimately the cars strengths and weaknesses remained the same. On the plus side, with high torque available from zero revs, the car was easy to drive with no gears to select or clutch to control. With no fuel being combusted within the motor maintenance is low and reliability is high. On the downside steamers require a lengthy and complicated procedure to start (and to stop in the case of early designs). Some steamers in use in the forties had automated electric start with 12v fans and pumps but still took a minute to produce usable pressure and remained slow to respond to changes in power demand. Though their smooth and silent power made steamers a delight to drive, it was this last problem that ensured IC engines would prevail commercially.

2.3.2 **The Oil Crisis Inventors**

During the early 1970's the developing world oil cartel known as the Oil Producing and Exporting Countries (OPEC) restricted the supply of oil in order to drive up the price. The USA and its citizens took this as a personal insult and, as a result, interest in fuel efficiency and alternative fuels soared. Alongside work on methanol fuels, electric batteries and variations on the steam theme, interest in Compacs restarted after languishing for nearly a century. Being perceived as a simple process, it was attractive to the more amateur investigators some of whom were highly misguided individuals. However, a number of individuals were able and sensible engineers who produced machines with performance comparable to the electric battery vehicles of their time.

A typical example is Terry Miller, an aircraft mechanics instructor, who constructed a four-cylinder sequential expansion motor in which the air is passed from a cylinder of small capacity to cylinders of successively larger capacity until most of the energy of expansion has been used. This is an arrangement similar to that used in the steamers of half a century earlier. The compressed air was supposedly stored in breathing air cylinders of the 'scuba' type. Storage pressure and capacity are not mentioned in the reports of the time but 200 bar was readily achievable and 10 litres per cylinder a normal size. However a picture of the rather crude open frame three wheeled vehicle seems to show a rather larger sausage shaped tank of what appears to be some 350mm diameter and unknown length. This is far beyond portable breathing cylinder dimensions and might be of the type used by American and European navies which can be as large as 0.25 m^3, though still capable of holding 200 bar. If it were a fabricated tank of the type often used for air receivers then the

containable pressure would be of an indeterminate, but much lower, value. Whatever the storage tanks capacity, a range of 17 miles for the prototype system and 45 miles for the commercial version was claimed for the 1400 lb. vehicle. Given the technology involved these figures are believable although the quoted recharging time of four minutes seems optimistic. Unusually, for his time, Miller appreciated the difference between a locally non-polluting vehicle that simply shifted the polluting emissions to a power station, and a genuine emission free system. His system was recharged through a windmill powered compressor. It is unlikely that there was enough wind about at any time to directly recharge even a small tank in four minutes so it is more probable that a static high-pressure store was gradually recharged by the windmill. When required the lower pressure on-car store would be recharged by connecting it to the high-pressure store, perhaps waiting until the pressures of the two stores had equalised. In this mode a recharge time of four minutes is conceivable but more technically demanding in terms of equipment. On the other hand, perhaps he was just exaggerating.

Another feasible design was that produced by Vittorio Sorgato who chose to go for a lightweight one-man design. The actual weight is not quoted in the Popular Science report of Mar 1975 but the accompanying picture shows a vehicle of the approximate size of a Fiat 500 but with a fibreglass body and space frame chassis. The car stored its compressed air at 200 bar in nine small cylinders fitted under the frame. The motor was a five-cylinder, three-hp radial design, which worked through a simple reduction gearbox and rear-wheel differential drive. The vehicle could maintain a top speed of 30 mph for duration of two hours resulting in a sixty mile range. Recharging was through a conventional compressor and took an hour or two.

There were a number of other designs available to convert existing engines to compressed air and all would probably work, though how well and for how long doesn't seem to have been tested or recorded.

What seems to characterise the designs of these 'oil crisis' inventors is the lack of any significant inventive step. All the systems use a cocktail of elderly designs, concepts and existing equipment adapted from elsewhere, perhaps not surprising considering the limited resources of the individuals concerned. However, despite many references to the low temperature of the systems nobody seems to have attempted to warm the gas flow to increase the available energy, the low (often sub zero) temperature being regarded as a good thing. Regenerative braking was a technique perceived as useful in electric battery vehicles and would have been familiar to anyone interested in the subject at the time. Yet none of the practical Compac designs even considered the matter. Some of the more impractical designs did consider using compressors as brakes but the conflicting demands of predictable braking and practical compressor operation ensured none of these ever made it onto the road.

The OPEC cartel was unstable at the best of times and eventually the restricted supply that maintained the high oil prices started to fail as members pursued their selfish interests by trying to sell more oil whilst the price was high. By the 1980's the oil prices had fallen to the early seventies prices (allowing for inflation) and the impetus for alternative fuels research subsided. Various groups continued their work but the next surge in interest was driven by the increasing environmental awareness that demanded an improved urban air quality.

2.3.3 The California Air Resources Board, 1992

In 1992 the California Air Resources Board (CARB) gave notice that, in 1998, 2% of all cars sold in California must be of the 'zero emission' type [CARB, 1992]. The percentage was to rise to 10% by 2003. These targets have now been relaxed, for reasons that will be dealt with later, but at the time they had the effect of galvanising research into zero emission vehicles (ZEV).

The reason for this concern amongst vehicle makers is that California occupies a special position amongst the states of the US (at least in this respect). The primary reason was that California is the single largest, and richest, state containing some 20% of the USA's population. A secondary reason is that in 1990 the Federal Government ceded special powers to the California State Legislature to set its own environmental laws, in view of the particularly poor state of the air quality in many Californian cities. No other state has these special powers. California therefore has the political and financial power to control 20% of the personal automobile market in the USA and it was felt that where California travelled today the rest of the US would follow tomorrow. This judgment was soundly based as most US cities and, most major cities of the world, were suffering from poor air quality. If the Californian legislation was successful it was likely that the rest of the USA, and perhaps other countries, would enact similar laws.

Every vehicle manufacturer selling in the USA launched research projects to design their own ZEV as failure to comply with the laws would be dealt with by large fines, proportional to how far each manufacturer fell short of their individual targets.

Large manufacturers are often poor at innovation and so many smaller groups, in companies and universities, set about their own projects hoping to generate viable solutions to many of the problems faced by a potential zev. In 1992 zev effectively meant 'electrochemical battery car' as no significant projects were concerned with any other class of vehicle. However, the lifetime and energy density of the Lead-Acid battery of the time was considered to be barely adequate and in need of improvement. Electrochemistry is an extraordinarily complex subject and it soon became clear that improving the L-A battery, or making practical batteries out of the alternatives, would be a long road. Flywheel storage/generators and fuel cells are the major alternatives that were, and are, being explored and as such tend to focus on the electric motor for motive power. A few groups looked at CAES and liquefied gases as practical with modern improvements.

2.3.4 Pneumacom – 'Spirit of Joplin'

In 1994 the Pneumacom Company of Joplin, Missouri announced the road testing of a zev powered by compressed air and named 'Spirit of Joplin' [Pneumacom, 1994]. Interestingly, the president of Pneumacom is a Terry Miller. This may be the same Terry Miller mentioned in 2.3.2 above.

The base vehicle was a 1988 Chevrolet Sprint with the fuel tank and drive train removed. The fuel tank was replaced by three air cylinders constructed of glass fibre and carbon fibre and contained air at a pressure of 20 MPa or 200 bar. The capacity of these cylinders is not known directly but it is likely that they were commercially available items. Lightweight air cylinders are not much use to scuba divers, as they

already have to wear ballast belts to achieve neutral buoyancy, but a new class of worker was beginning to use them. These workers were firemen, chemical workers, nuclear workers and anyone that would have to wear the new standard Class A HazMat (hazardous materials) full enclosure suit. Heavy steel cylinders are a liability for these workers and so carbon fibre cylinders became available as soon as their price fell into the range of these relatively wealthy organisations. The capacity of these commercially available cylinders are in the range of 10 -15 litres so it is likely that the maximum capacity of the 'Spirit' was approximately 45 litres.

The compressed air was fed to two engines with steel bores and polymer jackets, each driving one of the front wheels of the car. The left engine has two double-acting cylinders, one 50mm in diameter and the other with a 63mm bore, both with a 254mm stroke. The air enters the first cylinder at 3.5 MPa, expands to drive the piston and is then exhausted to a holding chamber, subsequently to be fed to the second, larger chamber. The air is then fed from the left engine to the first cylinder of the right side engine, which has a bore of 76mm. The exhaust from this cylinder drives the fourth cylinder, which has a bore of 105mm. It is presumed that these cylinders have the same stroke as that of the left engine but it was not stated. The air eventually leaves this last cylinder at 25% above atmospheric pressure.

The piston rods on each engine turn a 140-tooth gear wheel, which in turn drives a 20-tooth gear on the front wheel. This fixed gear ratio allows the engine to drive the car at a top speed of about 60 kph.

In March of 94 the car underwent a 12-hour test being driven around Joplin with stops only to change drivers and recharge the air cylinders. It was claimed that a charge lasted two and half-hours and a recharge took only four minutes.

It may well be that a charge lasted two and a half-hours but the average speed or range achieved in that time was never stated. If the earlier guess, at the capacity of the compressed air store, is correct, a number of other generous assumptions (weight 1400lb, low rolling resistance, etc) would place the maximum range in the order of 30 miles/50 kilometres and the average speed at 12 mph/20 kph. It seems likely that the engineers were being economical with the truth as they were seeking additional funding at the time.

It is interesting to note that the superficial specification of a four-cylinder sequential expansion engine, med/low weight and range of approx. 30 miles, is very similar to that of the Terry Miller air car of almost 20 years earlier. Apart from the carbon fibre air tanks and steel/polymer piston cylinders the design thinking is the same.

Nothing further has been published about this project, at the time of writing, and it seems likely that the project is in abeyance, if not defunct.

2.3.5 University of Washington – 'The Cryocar'

In 1997 the University of Washington announced details of a ZEV research project based on a piston-engined vehicle with nitrogen as the working fluid stored on-board

in its cold, unpressurised, liquid form. The project was very well financed with a $750k grant from the US Department of Energy

Initially, jokingly, named the ‘Smogmobile’ by the research team, it was suggested that the process of liquefying nitrogen from air could also be used as a method for filtering out pollutants, though this might add to operational costs. The name was taken from a L’il Abner cartoon about a car that was fuelled by pollution. Subsequently its name was either ‘The Cryocar’ or the LN2000. Specifically LN2000 seems to be the actual vehicle being worked upon whereas Cryocar seems to have been the generic name for their design and the overall project. As Cryocar is far more descriptive it will be used henceforth.

The concept of a car powered from the boiling of liquid nitrogen is not entirely new as theoretical work in this direction was published in the early 1970’s & 1980’s [Boese and Hencey, 1972] [Boese, 1981] and the Cryocar project builds upon this work [Williams, J., 1997/1 & 2]. More recent theoretical work by Chen et al [2010] suggest that the potential energy density of liquid Nitrogen is 2.45 times that of compressed air. However, they also found that compressed air could deliver greater work and power and was generally more efficient due to the much higher energy costs of Nitrogen liquefaction.

Interestingly, there was similar work carried out in the 1970’s by the British National Coal Board (BNCB) in association with the University of Salford. This work isn’t referenced in any of the Cryocar papers, probably because they were unaware of it, as the work does not appear to have been well publicised. The only reference to this

work so far unearthed (a photocopy of a cutting from Automotive Engineering, Jan 1976) [BNCB, 1976]contains only basic details, no references and no names of researchers and so hasn't been considered as an authoritative reference.

The BNCB proof of concept vehicle was a small one-man go-cart type affair with a vacuum insulated storage vessel in which the liquid was stored at its boiling point. The evaporating nitrogen was fed to a heat exchanger which in turn fed a 2.75 hp four-cylinder motor. These vehicles were intended for transport in underground mines where the non-flammable non-toxic fuel had important safety advantages. The Salford University work appears to be largely theoretical but focused on transportable heat stores rather than heat exchangers, and turbines rather than reciprocating piston engines.

The essential inventive step of the Cryocar was the design of a compact heat exchanger able to vaporise the liquid nitrogen without becoming choked by the build-up of frost. In this respect they were reasonably successful as only small amounts of frost formed at the lower mass flow rates [Williams, 1997/1 & 2]. Frost started to form above 100g/s with a max design flow rate of 300g/s.

The aluminium vehicle body was that of a former electric battery postal service van known as a Grumman-Olson Kubvan. The final weight wasn't given but the former pack of lead-acid batteries was stated as being over 450 kg so the vehicle must have been strong enough to carry this plus its postal load.

The system was that some 80 litres of liquid N_2 was stored in a commercially purchased Dewar capable holding the liquid at 24 bar but actually held at 1 bar. The storage temperature was 77K. From the Dewar the liquid was pumped to the heat exchangers where the pressure was 24 bar. The major heat exchanger consisted of 45 finned copper tube elements arranged in a block measuring approximately 300mm x 300mm x 900mm and weighing 109 kg. At the maximum mass flow of 300 g/s this raised the temperature of the fluid to 240K with an ambient air temperature of 292K. The outlet from the heat exchanger connects directly to the motor. This motor was an 11.1 kW radial piston air motor, designed and manufactured by Cooper Power Tools to power a winch for raising ships anchors. The motor had a cast iron block with five 75 mm cylinders and steel pistons. The motor was attached to the front wheel drive by a 5-speed manual transmission.

The vehicle's performance was limited as it could only manage a fifth of a mile per gallon of liquid Nitrogen. The operating pressures and temperatures were not stated but the motor was believed to be operating at only 20% efficiency. Range is also not stated but an 80-litre tank and 0.2 miles per gallon suggest about 4 miles. Subsequent comments reveal that they are hoping to build a more efficient motor, and to use a 100-gallon tank, to match the 250 mile range of conventional ICE powered vehicles.

Reasons for the inefficiency of the motor are not stated, but, as the motor is of the piston variety it should have had limited leakage. It is likely that the major loss was due to a high input pressure being required to maintain torque and thus much pressure energy would be discarded in the exhaust if the motor's expansion ratio was insufficient.

Despite the poor range of the Cryocar it was a promising technology. However, the still existing website claims that the project is no longer active due to a lack of funding. The date of last modification, for that site, was 8/10/2002 and presumably that was the approximate date that the project closed.

2.3.6 Guy Negre & the 'e.Volution'

In January 1998 it was announced by press release that an engineer by the name of Guy Negre, owner of the development company CQDF Air Solution, had built a dual fuel, compressed air/petrol, taxi. This vehicle was to make its inaugural run the following month and was to be built, in Mexico by the Mexican government, at a rate of 40,000 vehicles. The vehicle apparently was kick-started by a combined compressed air/petrol mixture and switched to pure compressed air operation once running. It seemed like a feasible idea even if the description of the vehicles operation and technology left a lot of questions unanswered. However, over ten years later no examples of the vehicle have been made available for independent testing although a prototype was available for viewing, and a test drive, at the company's laboratory in Brignoles, France. No manufacturing facility is known to have been constructed anywhere.

The compressed air store was a 15-litre carbon fibre cylinder at 200 bar and was said to be able to provide one hour motoring of "normal" town driving. No range was specified.

A reproduction of the initial press release diagram of the engine's layout is contained in Figure 2.3.

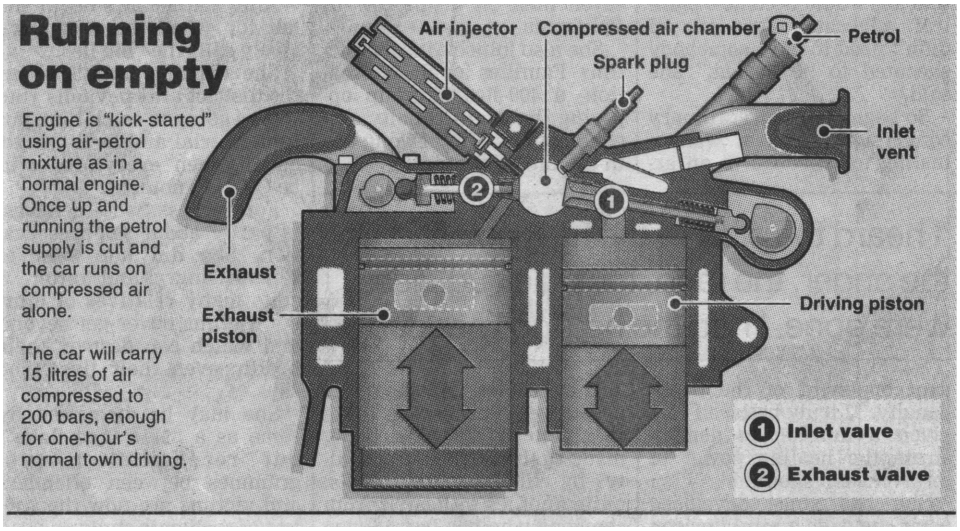

Figure 2.3 First e.Volution press release.

Although it was not made clear, it appears that the mode of operation was that compressed air and a "fuel" were injected into a plenum chamber connected to a small cylinder and a large cylinder by separate, camshaft controlled, poppet valves. The fuel/air mixture was ignited by a spark plug in the plenum chamber, the small cylinder poppet valve opened and the expanding gases drove the piston down. At BDC the poppet valve connecting the plenum chamber to the large cylinder opens and the exhaust gases from the small cylinder now expand into the large cylinder via the plenum chamber whilst being driven out of the small cylinder by the rising piston. Presumably as the large piston nears BDC an exhaust valve (not shown in diagram) opens and the cycle starts again. This is all speculative as there was no operational description provided. Apart from the supposed missing exhaust valve there is no way shown for fuel to enter the cycle and there is an entirely unexplained "inlet" vent. If the air supply was from the compressed air store what is this valve for? At the time it was assumed that the discrepancies were due to poor technical reporting and that later reports would clear up the questions. This has not been the case and since then even those limited operational details have changed.

In July 2000 a new series of reports provided additional details for what was a clearly changed vehicle. The vehicle was now a pure compressed air vehicle with an air store of 300 litres at 300 bar, quite a respectable increase in capacity that gave a believable range of 124 miles/200 km. The old dual fuel version was available as a separate alternative that ran on compressed air at low speeds (below 60 kph) and switched automatically to a traditional fuel at higher speeds. However, the three chamber arrangement remained for the pure compressed air version albeit with rather functional descriptions. The smaller cylinder is now described as being for compression, the plenum chamber is described as for combustion, and the larger cylinder as for expansion. The seeming paradox of a combustion chamber in a pure compressed air engine is not addressed. The weight of the five person car is quoted at 700 kg but it is not stated whether this is the charged or empty weight. It is likely that this is the empty weight as 300 litres of air at 300 bar weighs 98 kg and it would be an incredibly light vehicle for its size (3.3m x 1.75m x 1.72m) at only 600 kg.

At this point the vehicle is being marketed by Zero Pollution Motors Inc and Motor Developments International (MDI), both Guy Negre companies, as the MDI TOP (Taxi zerO Pollution) and as the e.Volution. In those July 2000 press reports the vehicle is predicted to go on sale in South Africa sometime in 2002.

In a press report dated 19/2/2001 it is made clear that, for reasons of high cost of manufacturing the carbon fibre air store, the manufacturing focus of the company has moved to South Africa. The compressed air store is probably the single most expensive item in the vehicle and would certainly cost £1000+ to manufacture in

Europe or the USA. For a vehicle that is intended to retail for under £7000 that component cost is prohibitive. South Africa has a high technology arms manufacturing sector that frequently uses the fibre and tape winding technology that is necessary for fabricating a large compressed air store from composite materials. Alongside the expertise is a low exchange rate economy, which means the expertise comes relatively cheap. The move to South Africa makes sense but there is still no evidence of vehicles being manufactured.

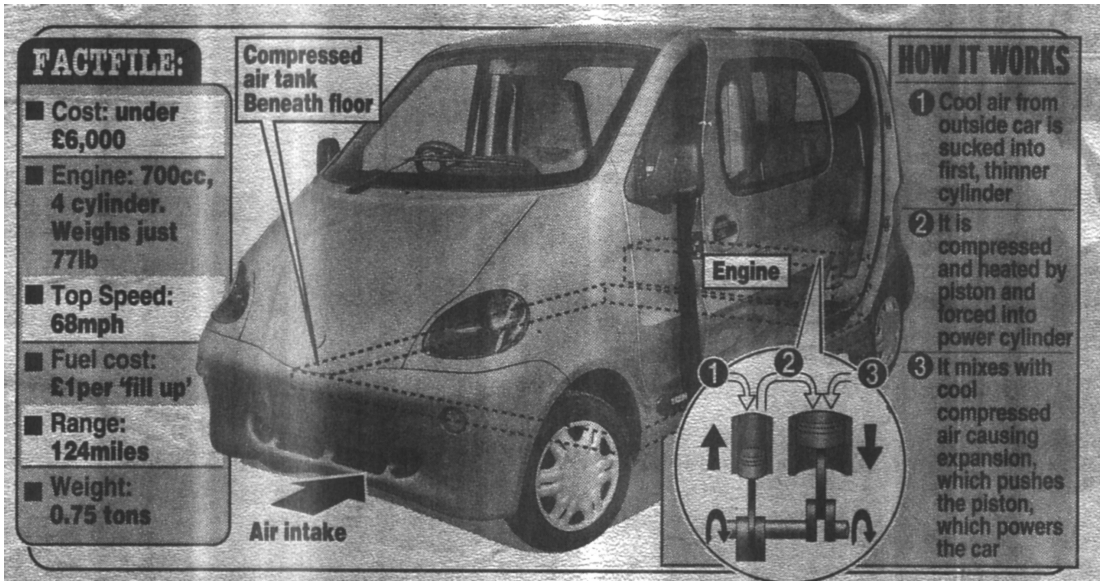

Figure 2.4 e.Volution press release 4/9/02

A press release is shown in figure 2.4 and is taken from the Daily Mail 4th September 2002[Daily Mail, 2002]. The text of the article refers to a "glass fibre" tank and may be sloppy reporting or may be evidence that Guy Negre is retreating from the cost of a carbon fibre tank. More disturbing, from a thermodynamic point of view, is that the press release clearly describes the motors operation as the large piston receiving air

both from the store and from the small “compressor” piston. Both pistons are connected to the same crankshaft so the large piston drives the small piston which in turn drives the large piston. The real source of energy and motive force is the compressed air with the small piston supplying nothing except additional friction. During the 1970’s oil crisis a number of inventors coupled a compressor to their air motors creating thinly veiled perpetual motion machines. This appears to be an echo of that type of thinking. Unless fuel is being burnt in the compressor cylinder this design element only provides additional drag and reduces the efficiency of the engine.

At this point it should be mentioned that this author has been contacted by two separate engineers after they have had a lengthy interview with Guy Negre, in his office in France. They both told the same story. They were not allowed a close view of the vehicle nor its mechanical parts. They were told that the large piston powered a crankshaft that drove the wheels and the small piston. That small piston then compressed air to the point that it would overheat and “explode”. No fuel was involved. The heat from the small cylinder was then channelled to the compressed air flow driving the large cylinder. They both reported that they were told that the spark plug and plenum chamber were in the drawings to misdirect would be copiers and, otherwise, had no function. Neither queried the questionable thermodynamics of this design.

What are the possible explanations for these variations in specification and possible flaws in design?

The designers may be charlatans seeking the £150,000 that they are reputedly asking for a single licence to use their technology. However, this seems unlikely as Negre, and his son, were highly skilled technicians in the motor sport industry and gave up their positions to push their e.Volution project forward, spending a lot of money long before there was any chance of a cash return. It seems more likely that the changing specification is a natural result of product development and the design flaws come from non-academic engineers thinking in terms of individual mechanical elements rather than overall thermodynamic cycles. It is also possible that the e.Volution hasn't really changed since its original design and it is still a dual fuel hybrid and not a compressed air car at all. Also when such a personal investment has been made in a project it may be hard to recognise the defects in one's "baby".

Ultimately, it is not central to the purpose of this thesis to judge the people or the company but to evaluate their overall design. Their compressed air store is the largest yet constructed for a Compac, though it should be noted that, at the time of writing, no independent person has been allowed to see the store. Their car body is certainly the lightest and most well developed yet used for a Compac. All eminently respectable work. That the engine being used is a piston engine of, probably, moderate efficiency simply places them alongside the bulk of the pioneers in this chapter. The e.Volution is probably the best air car yet constructed and deserves to be recognised as such.

2.4 The Case for Compressed Air Cars

In the I.E.A. report *Cars and Climate Change* [IEA,1993] the authors concluded that, for reasons of technical difficulty and of cost effectiveness, the use of most alternative fuels is likely to continue to be in niche markets such as commercial and government fleets. CNG and Diesel were the only fuels likely to make any impact on the gasoline market. Though written over fifteen years ago little seems to have changed except, perhaps, advanced batteries seem even further away.

The case for pursuing the development of a Compac rests in many ways upon the failings of its rival systems, the various forms of electric car, and these will be examined in the following sub-sections. However the Compac has some unique attributes that ensure this system deserves development as an alternative motive power system.

2.4.1 Low Ignition Risk

A very promising niche for Compacs is use in explosive environments. As was mentioned in 2.3.5 one of the motives for developing a liquid nitrogen car was for use in underground mines. This proposed use was not carried forward, perhaps because excessive levels of nitrogen can cause unnoticed suffocation in confined areas. The pure Compac doesn't suffer from this risk and retains the advantage of being operable without high temperatures or electricity. Though a domestic vehicle would benefit from these, they are not necessary to start, move or control the system. All functions can be carried out by low temperature mechanical components. These characteristics make the Compac uniquely suitable for use in volatile or explosive

environments. Currently heavily shielded electric cars or modified diesel vehicles are used but are still excluded from the areas of highest risk. With static electricity reduction techniques applied to the vehicle, a Compac need be no greater a source of risk than its passengers.

The market for such a vehicle is very widespread. Environments such as mines, petrochemical installations and natural gas installations are the obvious candidates, but stores of combustible powders (such as flour silos) and virtually any underground cavity carry a high risk. A number of years ago several VIPs were killed, and many injured, whilst on a tour of a large concrete lined tunnel intended to carry water from one reservoir to another. The subsequent investigation concluded that a large volume of methane, a normal constituent of the ground, had accumulated in the tunnel and had been ignited by an unknown source, possibly one of the vehicles in use by the party. If a new watertight tunnel can be a high risk area then, without forced ventilation, almost anywhere underground can be.

It is also the case that workers in these areas are often restricted to pneumatic tools when they need to use power tools. As a transportable pneumatic power source a Compac would have considerable advantages over a compressor that would have to be sited outside the high risk area.

2.4.2 Simple Recharge Technology

Every time energy is converted from one form to another inefficiencies creep into the process to ensure we get a degradation of the quality of the energy. Less well founded theoretically but commonly true is the fact that converting energy between the different families of high quality energy – Mechanical, Electrical, Chemical – tends to require more complex equipment and processes than converting energy within a family. For example, converting the pressure (Mechanical) energy of compressed air to the kinetic (Mechanical) energy of motion can be done with a simple piston and valve arrangement. Whereas converting the chemical energy of a hydrocarbon fuel to kinetic energy could be done in a similar mechanism but with the addition of fuel control and ignition mechanisms. Converting from one of these groups to Thermal energy is generally rather simple.

As a result of this general tendency it requires relatively simple, and thus reliable, mechanisms to obtain compressed air from the mechanical forms of ambient energy, wind and hydro. This makes compressed air a particularly useful medium for collecting and storing energy at “off grid” sites.

2.5 Problems with Existing ZEV Systems

2.5.1 Weight

Table 2.1 below shows a comparison of the specific energy density of the various, currently available, electro chemical battery systems. The NiMh value has been taken from Fetchenko [2010] in which the originators of the NiMh system, the Ovonics Battery Company, state their present NiMh Hybrid electric vehicle (HEV)

energy density as 45 Wh/kg. They go on to state that their Advanced NiMh HEV battery will achieve 80 Wh/kg. The value shown is an intermediate value weighted towards the forthcoming battery. Petrol has been included to put them in perspective. Whilst petrol might only be used by a thermal system with a "tank to wheels" efficiency of 25%, and the batteries energy will be used by a system with a "battery terminals to wheels" efficiency of about 80%, the disparity in energy stored is remarkable.

Table 2.1 Specific Energy Density of Battery Systems

Battery	**Energy Density Wh/kg**
Lead Acid	25-40
Nickel Cadmium	60-65
NiMh	65-70
Lithium Ion	150-160
Petrol	11,600

2.5.2 Cost

Cost is probably the next most important criteria for comparison but it is less easy to arrive at a genuinely comparable system cost. £s per MJ stored would probably be preferred but battery robustness causes a large variation in price even within battery types. Generally, within the ZEV community £10,000- £15,000 is considered to be the normal price for the battery pack of an electric vehicle. It is expected that the compressed air system would have a similar cost and it is not intended to take the financial comparison any further, for the purposes of this report. However, it should be noted that the "on the road" price of an entire IC vehicle is often less than this. For the foreseeable future all ZEV vehicles will require a premium price to be paid.

An exception to the above price comparison is the Lithium Ion battery. In table 2.1 this system had the best specific energy density, double that of the next best systems. Despite this benefit, these batteries are rarely used in vehicles for reason of their high cost, typically five times that of other systems. A well known example is the Tesla electric sports car. Based on a small Lotus sports car, it has an on the road price of about £85,000. The bulk of this price tag is the cost of the battery pack.

2.5.3 Operational Life

As mentioned above, robustness is a significant factor in the selection of a battery system. "Robustness" effectively means battery life in terms of charge/discharge cycles. All electro chemical batteries operate through a system of chemically dismantling and rebuilding the anode and cathode in every charge/discharge cycle. Because no process is 100% perfect, each cycle results in the build quality of the anode and cathode gradually deteriorating and reducing its electro chemical effectiveness. This means specific energy density, power density and efficiency are all reducing from the moment of first use. Build quality makes a substantial difference to the rate of this deterioration but all electrochemical batteries are limited to a life span of 1000-1500 cycles. Depending on use, this usually means a life of 3-6 years. The expected life of a Compac's system is expected to be that of the life of the car, perhaps longer with recycling of components.

2.5.4 Efficiency

It is not often appreciated that electro chemical batteries have poor efficiencies, defined as the ratio of energy output of the battery to the energy input required to restore the initial state of charge. This figure varies from a peak of about 80% when

the battery is new, and at room temperature, to less than 50% when old or in sub zero temperatures [Dhameja, 2002] [Ehsani et al, 2009]. This is one of the reasons an IC engine is hard to start on icy mornings and why electric vehicles are not popular in areas that suffer low winter temperatures.

At stable temperatures the Compac system pressure cell is 100% efficient in that it delivers the same amount of energy as was input. Assuming there are no leaks, there are no losses in storage. Further, it is hardly affected by normal temperature changes. At 30MPa the reduction in enthalpy is approx 2.5 – 3.0% per 10K reduction in temperature from 300K to 270K.

2.5.5 Fuel Cells

Hydrogen fuel cells have substantial potential but that has yet to be realised as the problems opposing that potential are equally substantial. At the time of the millennium it was commonly supposed that fuel cells would undermine the development of most other automotive power trains but this optimism hasn't been fulfilled. The reasons are well known and won't be dealt with in detail here but are listed below.

1. **Hydrogen fuel.** Effectively an artificial fuel that uses energy in its manufacture and its low carbon, and environmental, credentials vary substantially with the source of that energy.
2. **Hydrogen Distribution Infrastructure.** There is still considerable doubt about the possibility of having liquid Hydrogen refuelling stations along the lines of current gasoline stations. Liquid Hydrogen, at 1bar, is a cryogenic fluid that must be kept at approx -253ºC/20K. Gaseous Hydrogen has an

air-fuel ignition ratio in the range 5%-95% and is hard to contain reliably. Either form is difficult and dangerous to use.

3. **On Vehicle storage.** For the reasons in 2. above, the vehicle fuel tank is pressure tight and insulated. Consequently the tank is large if Hydrogen is stored in its liquid form at relatively low pressures. Alternatives are storing Hydrogen in metal hydrides (very heavy) or at very high pressures (800 bar).
4. **Fuel cell reliability.** Current preferred fuel cell technology, for automotive use, is the proton exchange membrane (PEM) form. This is, mechanically, very complex and lacks the robustness and moderate weight required of a practical system.
5. **Fuel Cell Cost.** The PEM fuel cell uses Platinum as an element in the membranes at the centre of its technology. This is the most expensive of the precious metals and is likely to remain so for the foreseeable future and is central to the costs of this technology

Items 1-3 above are probably accessible to design and development but 4 & 5 seem to be inherent in the technology. In Daimler Chrysler's in house magazine [Hightech Report, 1999] Chris Borroni-Bird, senior manager of technology strategy planning, wrote of the Necar 5 fuel cell car project, and fuel cells in general, "a fuel cell drive system still costs about 10 times as much as a gasoline powered engine, an estimate based on mass production quantities of fuel cell components". The company's goal was cost parity and a commercially available fuel cell car within 5 years. 10 years later, this hasn't been achieved by any company and looks unlikely in the near future. This point was put to a senior fuel cell engineer in a question and answer session at the Low Carbon Vehicles 2009 conference at the IMechE in London. His

response was that he thought that parity of cost would be achieved but that it was several years away, possibly ten years.

2.5.6 Health Risks of All Forms of Electric Power

Health risks from overhead power lines have received a great deal of popular coverage but there is little scientific evidence to support the assertions of its supporters. Far more well founded, but less well known, are the risks from Extremely Low Frequency (ELF) magnetic fields. The range of frequencies in this category is 3-3000Hz but of greatest interest here are the frequencies in the range 50-100Hz known as power frequency magnetic fields.

There have been numerous epidemiological studies of the health risk of this range of magnetic fields, many using the convenient cohorts of railway personnel in their country. The various kind of railway technicians are frequently exposed to this class of magnetic field but other railway personnel, whilst sharing their general environment, do not share the same EMF exposure and so provide a convenient control group for comparison.

The most recent good quality study [Minder & Pfluger, 2001] was carried out in Switzerland. The study authors carried out a comparison of “line engineers”, an occupation with a high average exposure of 25.9μT (microTesla), with a low average exposure occupation (station masters, 1μT). The study demonstrated a similar mortality rate, for brain tumours, between the two groups. However, for leukaemia a mortality rate ratio of 2.4 was found for the line engineers compared to the station

masters. Also, they found a dose response, to the cumulative exposure, of 0.9% per μT-year.

This work received invited commentary [Savitz, 2001] to the effect that it "added modest support for an association between EMF exposure and leukaemia. However, given the large size and high quality of a number of previous studies of occupational EMF exposure and cancer, additional studies similar to past ones are unlikely to yield important new insights". In short, the latest study gave results that supported past studies but provided nothing new. In 2002, The International Agency for Research on Cancer (IARC), a division of the World Health Organisation (WHO), raised power frequency magnetic fields to category 2B of its 5-fold categorisation system. This means it is regarded as "a possible human carcinogen". This category is for substances for which the evidence is considered to be limited in humans and less than sufficient in animals, and is shared by chloroform, DDT and Lead. The next category (2A) of "Probable carcinogens" contains formaldehyde, PCBs and UV-C.

That appears to be the position today. The major difficulty is that the "historical exposure" of each individual has to be reconstructed and this introduces a degree of uncertainty. It is unlikely that there will be any change in the foreseeable future as a cohort of people with a more clearly defined historical exposure does not appear to exist and human experiments are unethical. Similar studies for ionising radiation required exposed workers to carry dosimeter equipment for years but no similar equipment exists for emfs.

2.5.6.1 Power Frequency EMF in Transport.

The previous section would have been irrelevant to this thesis if such fields did not exist in electrically powered vehicles. Fortunately, there is one report [Dietrich & Jacobs, 1999] that has comprehensively assessed such emfs across several electrically powered vehicles. The report was very wide ranging covering virtually all forms of common transport but also included five anonymous electric vehicles. The report presents a complex picture with varying emfs at different levels throughout the vehicles. However, some of the vehicles had strong fields in the 0-300Hz range, at ankle level, coming from the motors, the power controllers and chargers. Given that the leukaemia studies found a dose response relationship with emf exposure it would appear to be wise to ensure that long term electric vehicle users will be shielded from these fields. If this is not done then the difficult to achieve experiments, mentioned above, will begin with the widespread use of electrically powered vehicles.

2.5.6.2 ELF Magnetic Field Shielding.

Shielding usually takes the form of conductive metal barriers, or enclosures, that are also magnetically permeable. These attributes promote induced currents that produce a blocking field and guide the source field away from the protected area. Though straightforward in most cases, the 0-300 Hz range appear to cause difficulties for this method of shielding, though it is not clear why. Existing shielding alloys can have a limited effect, particularly when there are several sources involved. Active electronically controlled shields are effective but are expensive.

3. Energy Storage Capabilities and Energy Requirements

3.1 The Air Car Cycle

All of the compressed gas systems, outlined in chapter 2, can be regarded as variations related to the gas turbine cycle known as the Brayton cycle, in its closed cycle form illustrated in Fig 3.1 and the open cycle in Fig 3.2

A gas is drawn into the compressor at point 1, where both its temperature and pressure increase. The high pressure is required for the process, but increasing the temperature will be beneficial as it increases the enthalpy. Accordingly, the gas is passed through the first heat exchanger, between points 2 & 3, and heat is added, from an external source, before it passes to the expansion turbine. As the gas flow expands through the turbine, between points 3 & 4, it cools. Finally, the cooled air flows through the heat exchanger, points 4 to 1, to cool the charge further to reduce the work required for compression and to complete, and restart, the cycle.

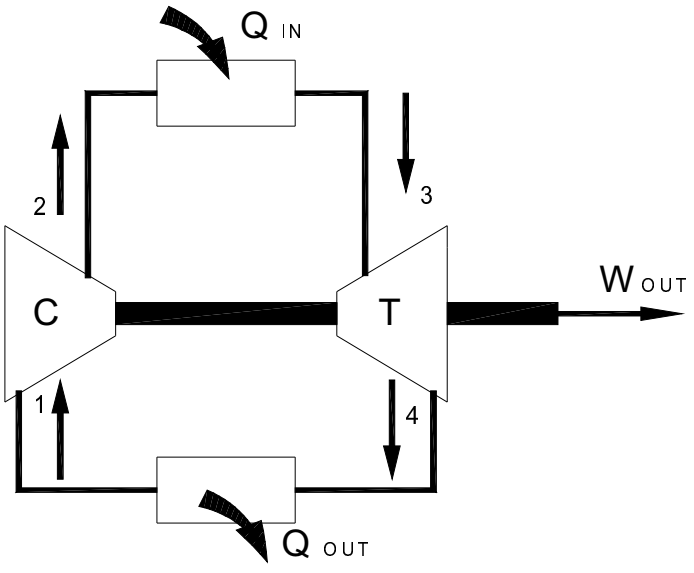

Fig 3.1 The (Closed) Brayton cycle

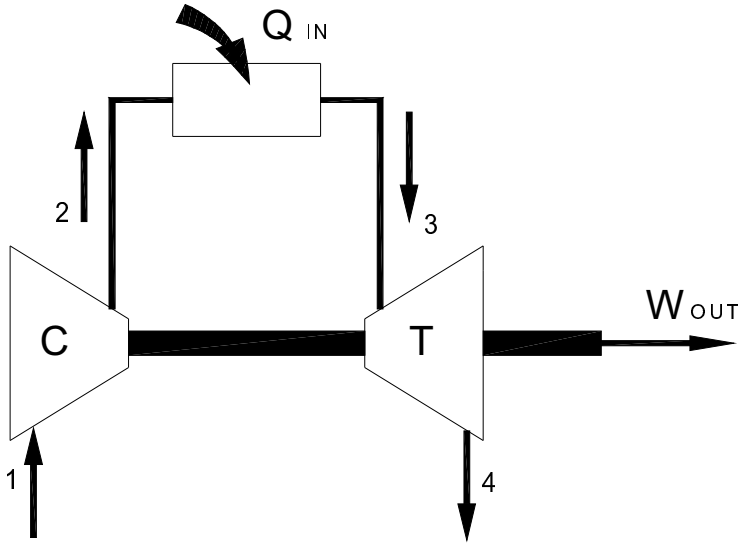

Fig 3.2 The Open Brayton Cycle

In the proposed air car cycle, see Fig 3.3, the relationship to the Brayton cycle is clear. Apart from the storage cell, the same mechanical elements are present

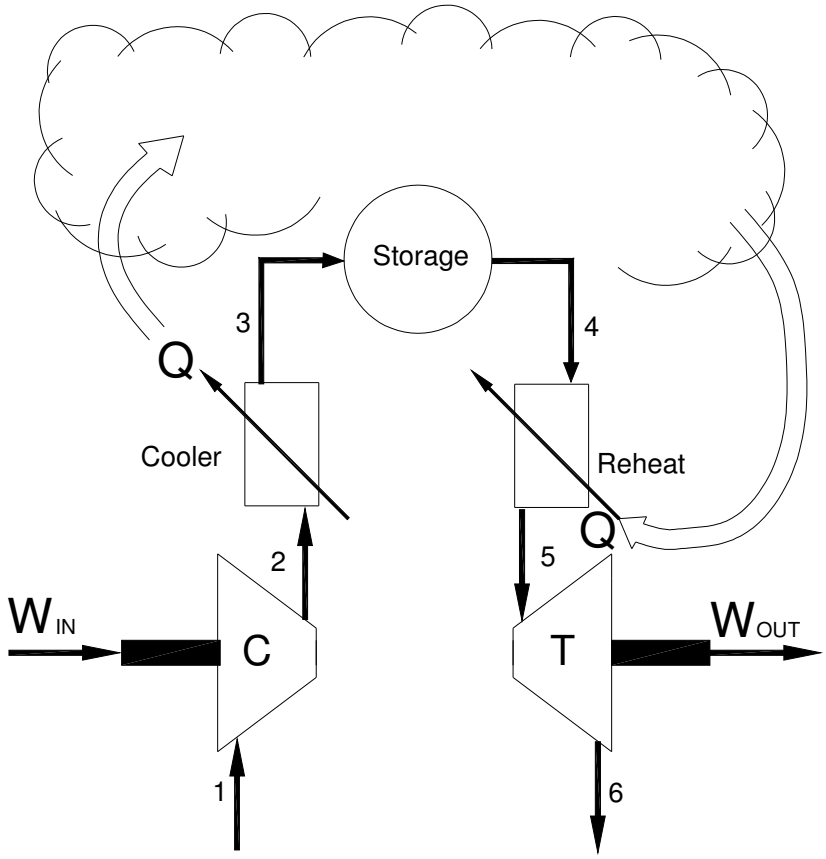

Fig 3.3 The Air Car Cycle

Air is drawn from the environment into the compressor at point 1. The compressed air stream is cooled by the heat exchanger, and the heat rejected to the atmosphere, between points 2 & 3. Air storage takes place between 3 & 4. When required, the air is delivered to the turbine via the second heat exchanger, between points 4 & 5, which boosts the enthalpy of the compressed air stream by raising its temperature using the atmosphere as the heat source. It is this step, between points 4 & 5 that has been omitted in all air cars to date. The same elements are present with the addition of the storage function and the removal of the connection between the compressor and turbine.

To clarify this cycle further, the T-s and P-V diagrams are shown in Figs 3.4 and 3.5.

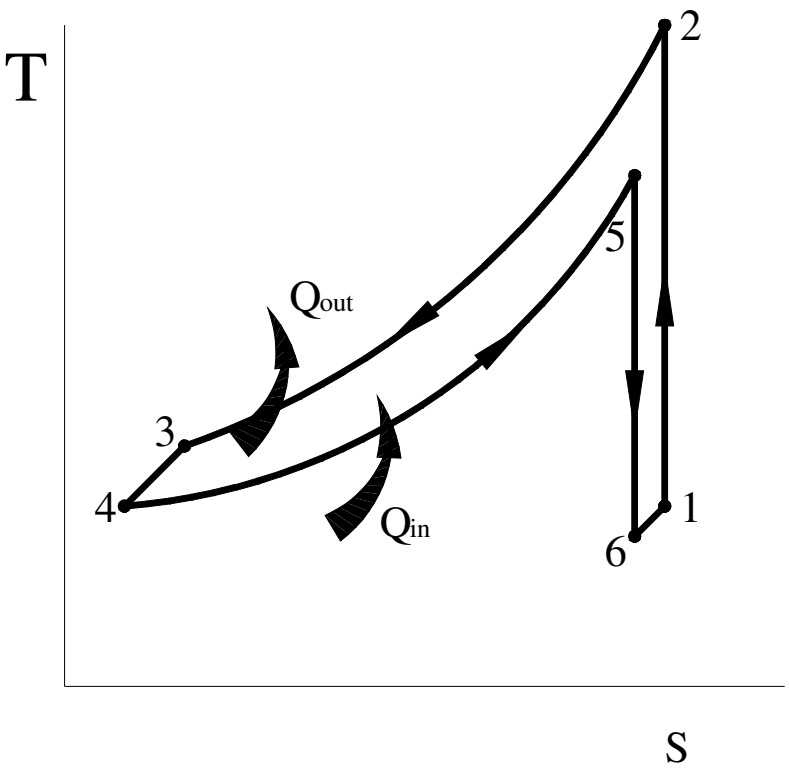

Fig 3.4 Compressed Air Car Temp-Entropy Diagram

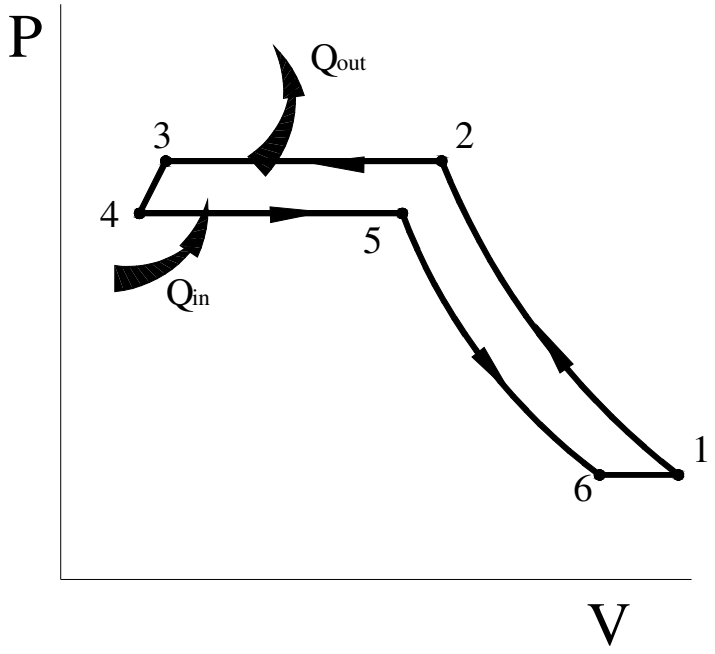

Fig 3.5 Compressed Air Car Pressure-Volume Diagram

1 – 2 Isentropic Compression

2 – 3 Constant Pressure Heat Rejection

3 – 4 Storage with Residual Heat rejection

4 – 5 Constant Pressure Heat Addition

5 – 6 Isentropic Expansion in Motor

In reality, in sections 1 – 3, there would be several stages of compression and heat rejection, probably three or four. Section 3 – 4 represents the assumption that the compressed air will be delivered to the storage cell at slightly above ambient temperature and will experience a heat loss whilst approaching equilibrium with the environment.

3.2 The Compressed Air Power Pack

For a compressed air driven car to be competitive, with an electro-chemical battery car, it must, at the very least, be able to cover the same distances between recharges. Hence a minimum specification was established at the outset as shown in table 3.1.

Table 3.1

Minimum Specified Requirement for a Compressed Air Car

Criteria	Value
Power Pack Energy Density	40 watt hours/kg
Power Pack Life	1500 cycles
Motor Power Output	35kW
Motor Power to Weight Ratio	500 W/kg

The Power pack energy density is derived from the best value for currently available lead acid batteries [Dhameja, 2002a]. A higher value is achieved by Ni-Cad and NiMh but, for cost reasons, these are rarely used in road going vehicles.

The power pack life is the best for any available electro-chemical battery but is an undemanding target as the pressure receiver design suffers no deterioration as a result of the pressure cycle.

The motor power output and power to weight ratios are not the best available values, for the electric motors, but any electric motor that could meet both these values would be considered to be of higher than average quality. It is unlikely that this

project will be able to match the best available electric motors, which have benefited from years of development, but it is expected that these "good" values will be met.

To meet these requirements it was considered that a compressed air storage capacity of the order of 250 litres, at 30 MPa, would be necessary. Higher pressures are reasonably attainable and desirable but 30MPa was chosen as this is the maximum pressure used by breathing air cylinders and thus for which compressors, and recharging facilities, are readily available. This makes this a practical pressure for experimentation due to the ease of sourcing equipment.

3.2.1 Energy Storage Capacity of Compressed Air

The following section closely follows Jensen [1980 & 1984], a close copy of which can be found in Ter-Gazarian [1994].

The calculation of energy stored in compressed gases is based on the ideal gas law:

$PV = nR_uT$

where

P = Pressure

V = Volume

n = number of moles in the Volume

R_u= Universal Gas Constant – 8.314kJ/(kmol.K)

T = Temperature

The conventional way of describing the process of compressed gas energy storage is through a piston/cylinder arrangement as shown in Fig 3.6.

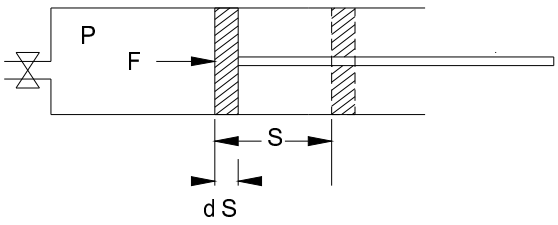

Figure 3.6 Piston Driven by Compressed Gas

No real process of this type is adiabatic so some degree of heat transfer must be involved. According to the first law of thermodynamics (Eq. 3.1),

$$\Delta U = Q + W \qquad \text{Eq. 3.1}$$

The change in internal energy ΔU is equal to the sum of the heat Q and the useful work W. The work done by the piston, whilst moving to the right over distance S in Fig 3.6, ignoring friction, can be derived from the definition of pressure (Eq. 3.2).

$$P = F/A \qquad \text{Eq. 3.2}$$

Hence

$$W = \int F\,ds = \int P\,A\,ds = \int P\,dV \qquad \text{Eq. 3.3}$$

This integral would be straightforward to solve if the process was isobaric, i.e. if P was constant. For this to occur, the valve would have to be open to a very large pressure vessel that would not change its pressure whilst pressurising the small change in volume in the piston/cylinder. The work done by the gas would be

$$W = \int_{v1}^{v2} dV = P(V_2 - V_1) \qquad \text{Eq. 3.4}$$

Here $V_2 - V_1$ is the change in volume caused by the piston movement. If the piston were to be driven in the opposite direction, to the left, the applied force would result in the storage of an amount of energy corresponding to $P(V_2 - V_1)$.

If the process is carried out at a constant temperature, rather than a constant pressure, that is isothermal rather than isobaric, then the ideal gas law, of equation 3.1, becomes the Boyle-Mariotte law in the form of equation 3.5

$$PV = NR_uT = \text{constant} \qquad \text{Eq. 3.5}$$

and so

$$W = \int_{v1}^{v2} PdV = NR_uT \int_{v1}^{v2} \frac{dV}{V} = nR_uT \ln (V_2/V_1) \qquad \text{Eq. 3.6}$$

For clarity this can be re-written as

$$W = vR_u T \int_{vo}^{v} \frac{dV}{V} = P_o V_o \ln(V_o/V) \qquad \text{Eq. 3.7}$$

As this equation assumes perfect heat transfer, and ignores friction, work done is equivalent to energy stored, if the compressed gas is stored. Thus, the calculation of energy stored in compressed air is given by equation 3.8.

$$P_o V_o \ln(V_o/V_f) = E_s \qquad \text{Eq.3.8}$$

Where

P_o = Starting pressure (Pa)

V_o = Starting volume (m^3)

V_f = Final volume (m^3)

E_s = Energy stored (J)

P_o is taken as 1 bar (101,325 Pa)

Final volume is fixed at 250 litres (0.25 m^3)

Starting volume is calculated from the final mass of air stored. The density of air at 300 bar and 300K is 314.03 kg/m^3 [Sychev, et al, 1987] giving a mass stored of 78.5kg. This would be 67.7m^3 at ambient temp and pressure.

The final calculation is 101,325J x $67.7m^3$ x ln(67.7/0.25) = 38.42 x 10^6 J = 38.4MJ

To put this value in perspective, this is slightly less than the energy/heating value stored in a kilogram of gasoline but is equivalent to, or greater than, the energy stored by many current examples of electric vehicle [Dhameja, 2002b].

3.2.1.1 Higher Pressures

The practical element of this thesis will concentrate on a storage pressure of 30MPa as this is the highest practical at the present time. However, it is already possible that much higher pressures, and large pressure vessels, may be utilised on a daily basis in automobiles. In a bid to overcome the problems with Hydrogen storage for fuel cells, Daimler, BMW and Honda are experimenting with carbon fibre pressure vessels, of the order of 50 litres capacity, that store hydrogen at 80 MPa. If such technology becomes reliable and affordable, then it could be utilised for compressed air storage, greatly increasing the energy density. The overall weight of the storage system will be dealt with in a later chapter but Fig 3.7 and 3.8 and Table 3.2 show the results of applying equation 3.8 to the same final volume of air, (energy density excludes pressure vessel weight), but at a range of pressures above and below 30MPa. The complete table of figures is contained in Appendix A. The slightly uneven quality of the graph lines is reflected in the actual values and probably arises from air's mildly non-linear relationship between pressure and density [Sychev, et al., 1987B]. This is because air is a mixture rather than a pure gas and the density values have to be empirically derived.

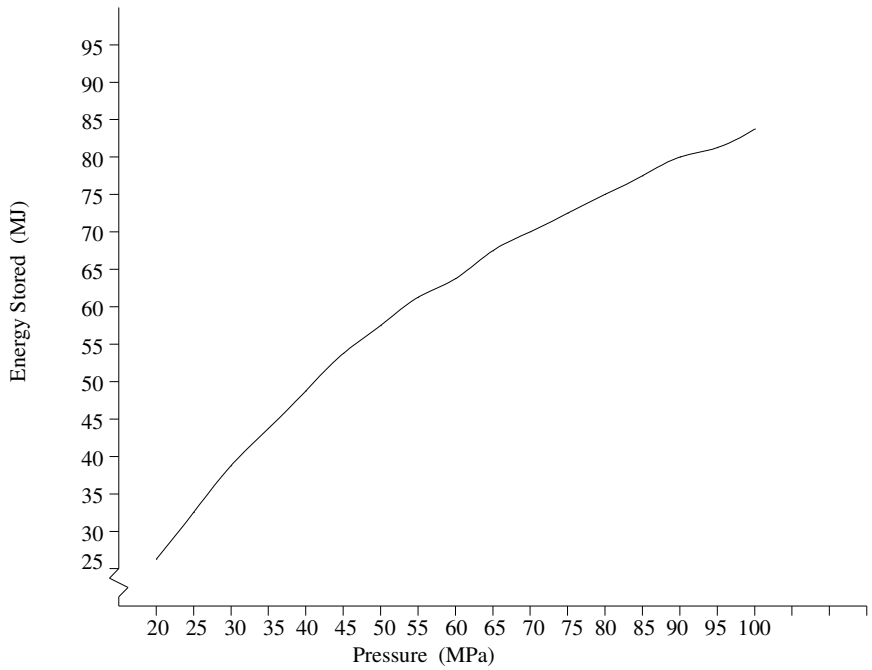

Fig 3.7 Energy Stored in 250 litres

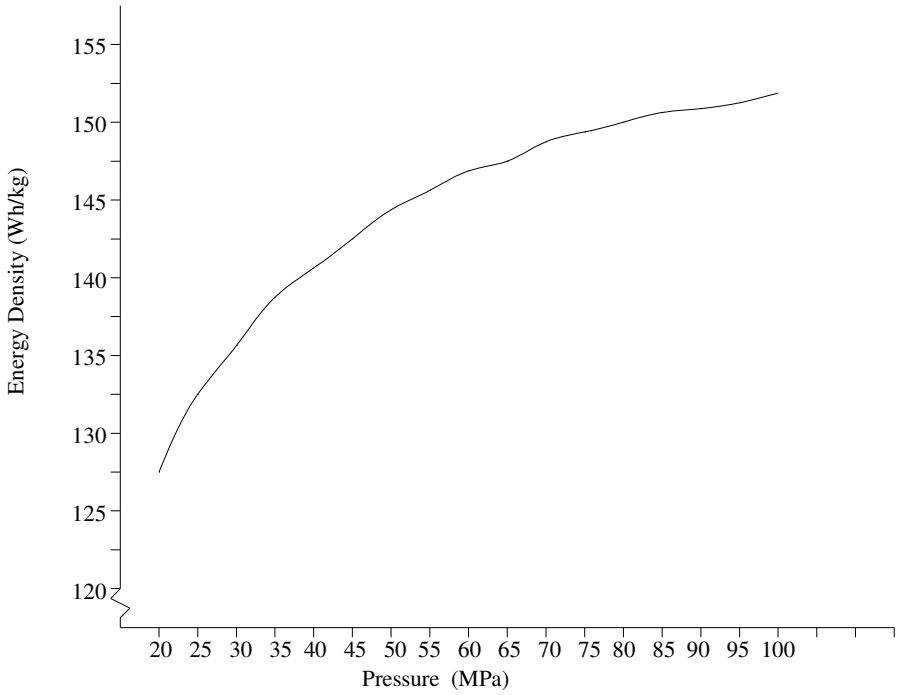

Fig 3.8 Energy Density of Air

Table 3.2 Compressed Air: Energy Stored at High Pressures

Pressure (MPa)	Mass (kg)	Energy Stored (J)	Spec. Energy density (Wh/kg)
20	56.23	25871214	127.8
25	67.99	32411208	132.4
30	78.51	38409677	135.9
35	87.87	43852074	138.6
40	96.20	48770517	140.8
45	103.63	53215454	142.6
50	110.30	57241487	144.2
55	116.32	60900922	145.4
60	121.77	64246114	146.6
65	126.75	67317293	147.5
70	131.33	70152236	148.4
75	135.55	72784105	149.2
80	139.47	75237844	149.8
85	143.14	77537644	150.5
90	146.57	79700456	151.0
95	149.80	81742089	151.6
100	152.85	83678707	152.1

Whilst the Energy Stored graph continues to rise at 100MPa , there is a clear flattening of the Energy Density graph at this pressure and may be taken to indicate reducing benefits of going to such high pressures. This is supported by Carvalho [2008] who performed an exergy analysis to calculate the work potential of air at different pressures when expanded in a variable-volume closed system. He showed that the rate of exergy increase reduced with increased air pressure implying diminishing returns with increased air storage pressure.

3.2.2 Real Processes

Equation 3.8 is still useful despite the fact that real processes do not maintain constant temperatures or pressures. In Figs 3.9 - 3.11, the area under the line graph curves represent Work (W). Fig 3.9 represents equation 3.8 above where

compression, or expansion, follows a constant temperature isotherm represented by the curve T1. Vs = small volume and Vl = large volume.

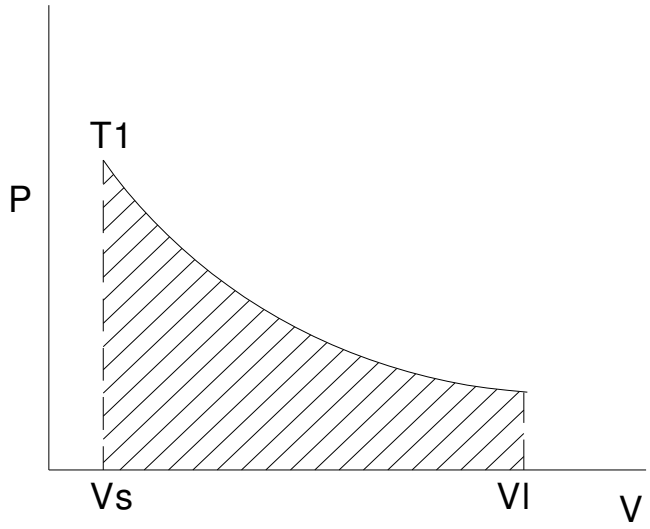

Fig 3.9 Isothermal Compression/Expansion

The curve in Fig 3.10, whilst arbitrary, follows a more realistic pathway taking account of the temperature and pressure increase that occurs in the compression process. Now W is the area under the arbitrary slope between the isotherm T1 and the higher temperature isotherm T2. Assuming Vs and Vl represent the same volumes in each graph, it is clear that the area under the arbitrary real slope is greater than that simply under the isotherm T1.

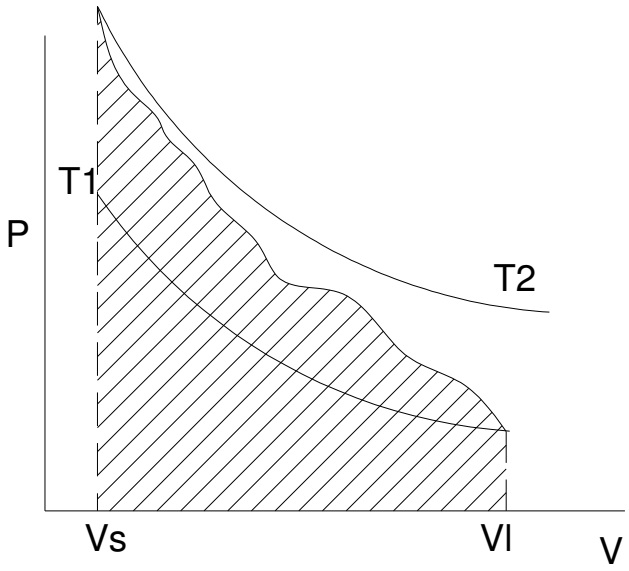

Fig 3.10 Realistic compression pathway

An even more realistic, but more complex, pathway is shown in fig. 3.11. If the curve T1 is accepted as being the ambient temperature, then it is clear that a multistage compression process, ultimately ending in a thermally conductive storage cell, will return to equilibrium at the ambient temp.

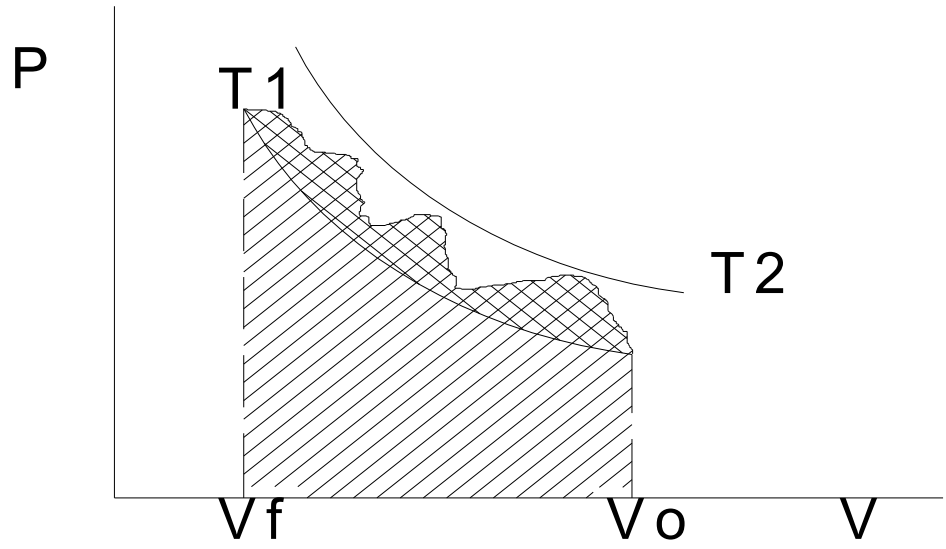

Fig 3.11 Realistic Compression / Storage Pathway

In this scenario, the compression process starts at the ambient temperature and ends at the same temperature. It is equivalent to the compression process happening very slowly and always following the isotherm T1. The realistic curve follows several compression / cooling cycles and, mostly, rises above the ambient temperature isotherm but, given enough time, the realistic curve must return to the ambient temperature isotherm.

The practical effect of this is that the area below the ambient temperature isotherm T1 represents the energy stored whilst the area between the realistic curve and T1

represents the excess work of compression as represented by equation 3.9 [Ter-Gazarian, 1994B].

$$W = C_p \delta T \qquad \text{Eq. 3.9}$$

Where C_p is the specific heat of constant pressure and δT the change in temperature of the working fluid. Therefore equation 3.8 represents the energy stored at ambient temperatures and equation 3.9 represents the excess work resulting from the temperature of the working fluid / compressed air rising above the ambient temperature and causing temporary excess back pressure until the temperature returns to ambient.

Whilst this thesis will not be dealing with the matter of efficient compressor design and operation, equation 3.9 makes it clear that minimising the compressed air temperature rise, during the compression process, is crucial to the efficient operation of any practical compressed air car system.

3.3 Comparison to Electrochemical Batteries

It is proposed that the storage cylinders be built of aluminium cylinders reinforced with a wound carbon fibre composite. It is yet to be decided whether use a single cell or to use multiple cylinders that can be stored more conveniently. A single cell in the form of a sphere would be the lightest option. An FEA (Mechanica/Pro Engineer) analysis of a spherical carbon fibre cell has estimated the cell weight as 45kg. This design allowed for a pressure safety factor of two. However, a more detailed and conservative analysis, using a safety factor of 3, an aluminium liner and stronger

carbon fibres, is detailed in section 4.3. This design has a weight of 57.9kg. Making an allowance for the weight of the regulator valve, and including the air mass, provides a basic weight for a fully operating cell, of 250 litres capacity, as 140kg. Using these figures yields an expected specific energy density of 76Wh/kg. Table 2.1 is reproduced in table 3.3 with the addition of this figure in order to compare this proposed system to the available electro-chemical battery systems and it can be seen that the performance of the CA cell is competitive.

Table 3.3 Specific Energy Density of Battery Systems

Battery	**Energy Density Wh/kg**
Lead Acid	25-40
Nickel Cadmium	60-65
NiMh	65-70
Lithium Ion	150-160
Comp Air (30MPa)	76

However, for the purposes of the test rig, two ordinary 12 litre breathing air cylinders are employed, again charged to a pressure of 30 MPa.

It should be noted that although the CA cell compares well by specific energy density, it isn't so competitive in the area of volumetric energy density. As this is usually considered to be of secondary importance it is not a criteria usually quoted and large battery systems are not readily comparable by volume. However, a 250 litre spherical CA cell would be approximately 800mm in diameter and this should be manageable even within a compact vehicle. A "sausage" shaped cylinder would

be more manageable but would become heavier as its aspect ratio lengthened. However, the matter of the storage cell design will be dealt with in more detail in the next chapter.

It should also be noted that it isn't necessary to expand the compressed air, from the pressure at which it is stored in the cylinder, through the rotary motor, down to atmospheric, in order to generate the required power output. Whilst a high pressure motor has a superior power to weight ratio, sealing of the system at the higher pressures would be difficult and leakage losses would reduce overall system efficiency. Also adapting the flow rate to compensate for the falling maximum pressure, whilst maintaining power output, adds unnecessary complexity to the system. It is proposed to utilise the compressed air at a maximum pressure of 1MPa (10 bar), at the inlet to the motor. It is expected that, in normal operation, pressures would be lower than this. The high storage pressure is employed to reduce the size of the cylinders for a given mass of air.

There is a further thermodynamic advantage to using a lower operating pressure. The greater the pressure difference, between the storage cylinder and the inlet to the motor, the greater the temperature gradient between the compressed air stream and ambient air, assuming the storage cylinder is at ambient temperature. This makes it easier to pass heat from the ambient air, through the heat exchanger, into the pressurised air stream.

3.3.1 The Effect of Temperature Reduction on Batteries

In an earlier chapter, it was mentioned that all currently available types of electrochemical batteries suffer a serious loss of power and available energy when operating at low temperatures. When operating at 0°C, a reduction of 50% is typical when compared with the same battery's performance at 20 - 25°C [Dhameja, 2002c][Ehsani, 2009].

The performance of the compressed air battery is virtually unaffected by operation at low temperatures, as long as the temperature is relatively stable. However, if the compressed air battery is recharged whilst the ambient temperature is relatively high and that temperature then falls a substantial amount, this can have a noticeable effect. When the storage cell reaches equilibrium at the lower temperature the specific enthalpy, and pressure, will have fallen as a result. This is an unusual scenario but night time temperatures can be 20K lower than day time temperatures in some areas so an investigation of this point is worthwhile. Equation 3.8 is of no value here as it does not take account of any temperature changes. A comparison of measured specific enthalpy values, as they change with temperature, is possible [Sychev, 1987] and this is shown as a graph in Figure 3.12.

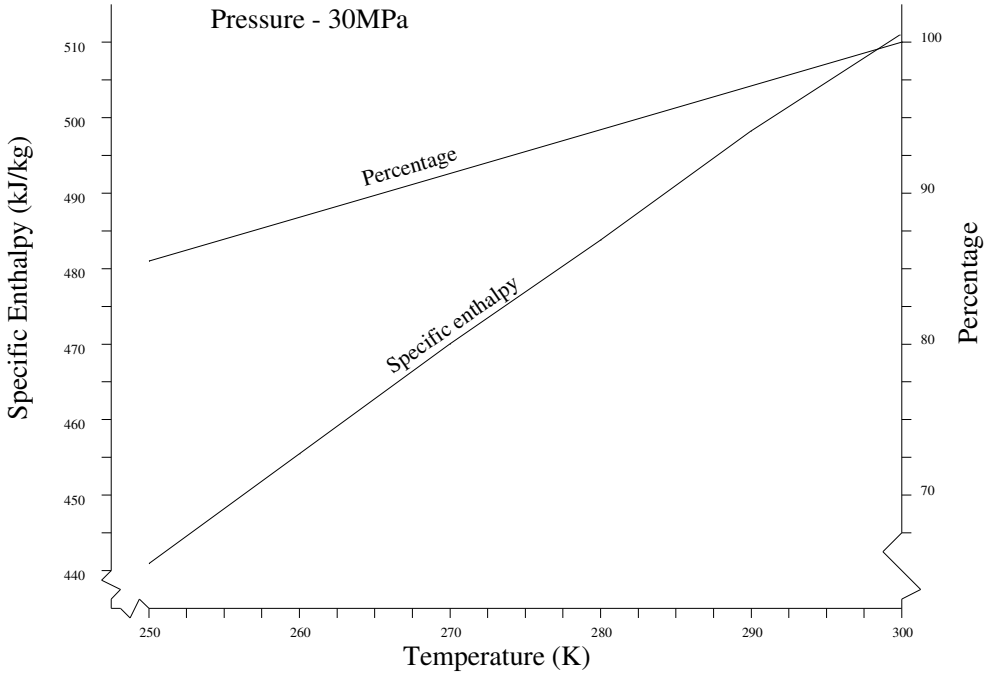

Fig 3.12 Enthalpy Change with Temperature for Air

It can be seen that the reduction in enthalpy, in the range 300 – 280K, is little more than 5% and is less than 15% for a 50K reduction in ambient temperature. Whilst such a change cannot be ignored, in a system that has such a small amount of energy to start with, it is substantially better than all available electrochemical batteries.

The above deals with the matter of energy available from compressed air but doesn't refer to the matter of power. This is because the power available is a function of the system pressure regulator and the volume flow it allows. Essentially, power is controlled by the system design and isn't directly affected by temperature.

3.4 Automotive Power Requirements

The power required from a vehicle's motor, to maintain any specified speed is given by the motive force equation 3.10 [Bosch, 2008a].

$$P_W = (F_W \cdot v)/3600 \qquad \text{Eqn. 3.10}$$

Where F_W (Newtons) is equal to the total driving resistance force from equation 3.11 [Bosch, 2008], and *v* is velocity in km/h.

$$F_W = F_{RO} + F_L + F_{ST} \qquad \text{Eqn. 3.11}$$

The elements of equation 3.11 are detailed below.

Rolling resistance

$F_{RO} = f \times m \times g \times \cos \alpha$

(*f*) Coefficient of rolling resistance. This results from the energy absorbed by the tyre as it deforms against the road surface and varies with the type of vehicle, vehicle speed and road surface, and is determined empirically. For a domestic passenger vehicle, with radial ply tyres on a Tarmacadam surface at a speed of 50 – 100 km/h, a value of 0.015 is typical but can be significantly lower [Bosch, 2008a].

(*m*) Vehicle mass in kg. For the purposes of this calculation, a value of 1000kg is to be used. This could be an arbitrary decision but it is based on the lightweight, but otherwise standard, vehicles of large manufacturers. For example, the Ford 1.3 Ka has a kerb weight of 870kg and it is expected that the Compac drive train would be of less weight than the conventional SI drive train. A gross vehicle weight of 1000kg would include two passengers and some luggage.

(*g*) The acceleration due to gravity and the normal value of 9.81 m/s^2 is used.

(α) Gradient angle. For the purposes of this calculation the vehicle is considered to be on a level road. Therefore, as the gradient is 0° and cos α is 1, this element can be omitted from the calculation.

Aerodynamic drag

$F_L = 0.5 . p \times c_w \times A \times$ (road speed (v) + Head wind velocity (v_o) $)^2$

(p) Air density (kg/m^3). The value used is 1.16 kg/m^2, the same as that used in the energy storage calculations.

(c_w) Drag coefficient. This value is experimentally determined for each vehicle design. The value of 0.4 will be used here as this is a fairly conservative value. Lower values are common but tend to be for larger vehicles than envisaged here.

(A) Cross sectional area. A conservative value of 2 m^2 will be used. As a comparison, the Ford Escort value for A is 1.9 m^2.

Climb resistance

$F_{ST} = m \times g \times$ sin (gradient angle a)

The equation for climb resistance, $F_{ST,}$ will not be directly included in the calculations here as it would introduce a large degree of subjectivity. Whilst the equation is reasonably precise, there is no "standard hill" to base the equation upon and one would have to be conjured up. When calculating a range for the vehicle this element will be excluded. However, when calculating the power requirement an

approximation, equation 3.12 [Bosch, 2008a], will be used that is, purportedly, subject to less than 2% error for inclines up to 20% (approximately 11° angle).

$F_{ST\,(approx)} = 0.01 \times m \times g \times p$ Eqn. 3.12

(where $p = 20$ for a 20% incline)

Another good reason for excluding F_{ST} from cruise/range calculations is that on the downward slope of a hill the resistance becomes negative and aids acceleration. On the basis that most things that go up must come down, the losses are substantially diminished by the gains.

Using the above values

F_{RO} = Rolling resistance =

coefficient of rolling resistance (f) . vehicle mass (m) . gravity (g)

becomes 0.015 x 1000 x 9.81 = 147.15 N

F_L = Aerodynamic drag =

0.5 . air density (p) . drag coefficient (c_w) . Cross sectional area (csa) . V(road speed (v) + Head wind velocity (v_o))^2

becomes (at 50km/h) $0.5 \times 1.16 \times 0.4 \times 2.0 \times 13.89^2 = 89.5$ N

(at 90 km/h) $0.5 \times 1.16 \times 0.4 \times 2.0 \times 25^2 = 290$ N

and $F_{ST\,(approx)} = 0.01 \times m(\text{kg}) \times g \times p$

becomes 0.01 . 1000 . 9.81 . 20 = 1962 N

Therefore,

at 50 km/h F_W will be 2,200 N inc climb resistance

and at 90 km/h F_W will be 2,400 N inc climb resistance.

Excluding climb resistance, for cruise conditions, these values become

At 50 km/h - 263.65 N

and at 90 km/h - 437.15 N

Putting these values into the motive power equation 3.10, results in the following power requirements:-

At 50 km/h (inc. climb resistance) = (2,200 x 50)/3600 = 30.5 kW

At 90 km/h (inc. climb resistance) = (2,400 x 90)/3600 = 60 kW

At 50 km/h (exc. climb resistance) = (263.65 x 50)/3600 = 3.29 kW

At 90 km/h (exc. climb resistance) = (437.15 x 90)/3600 = 10.93 kW

The 30.5 kW (50 km/h inc. climb resistance) power requirement would appear to be a minimum as a vehicle that cannot negotiate a gradient is unlikely to be considered acceptable. This is the basis for the 35kW motor power value in table 3.1.

3.5 Potential Range of the Compressed Air Car

An estimate of a vehicle's range is usually derived from motoring tests based on a prescribed drive cycle. An alternative is to simulate the drive cycle on a computer and this has been carried out by Bozic & Milton [2011] using the FTP-75 test cycle for a compressed air hybrid vehicle with impressive results. This isn't possible at the

present stage of this project but a straightforward calculation on the basis of the above figures will give a broad indication of the vehicles potential range.

The range will be calculated for two speeds, 50 km/h/30mph and 90 km/h/54mph, and, for sake of simplicity, in the present calculation the efficiency of the drive train will be considered as 100%. This calculation will be revisited in the chapters dealing with the reheat heat exchangers, and the motor design and testing, where the effect of an experimentally derived efficiency will be considered.

The kinetic energy (E_K) of the vehicle is given by ½ mv^2. It is assumed that this energy will need to be absorbed/subtracted from the stored energy (E_S) before the range is calculated. Then the range is calculated by dividing the power requirement(P_W) for that speed, into the remaining energy stored to obtain the time (in seconds) remaining for energy use at that rate. Then the range is simply converting that amount of time into hours and multiplying by the given speed.

Thus the equation is

$$R = \left(\frac{\left((E_S - E_K) / P_W \right)}{3600} \right) V \qquad \text{Equation 3.13}$$

The kinetic energy of a 1000kg vehicle

At 50km/h (13.89m/s) is 0.5 x 1000 x 13.89^2 = 96,466 J

At 90km/h (25.0m/s) is 0.5 x 1000 x 25.0^2 = 312,500 J

The energy stored is 38.41MJ

The motive power required at 50km/h is 3.29kW.

The motive power required at 90km/h is 10.93kW

For 50km/h, the calculation is

(38.41MJ - 96,500J)/3290W = 11,645secs = 3.23 hrs

3.23 hrs at 50km/h = 161.74km

For 90km/h, the calculation is

(38.41MJ - 312,500J)/10930W = 3,485secs = 0.97hrs

0.97 hrs at 90km/h = 87km

These range values are indicative but the lack of any efficiency element precludes any further discussion until the relevant later chapters.

All of the above results are summarised in table 3.4 below.

Table 3.4 Summary of Results

	V (50km/h)	V(90km/h)
Total Drive Resistance (Inc F_{ST})	2,200N	2,400N
Total Drive Resistance (Exc F_{ST})	263.65N	437.15N
Rolling Resistance (F_{RO})	147.15N	147.15N
Aerodynamic Drag (F_L)	89.5N	290N
Climb Resistance (F_{ST})	1962N	1962N
Motive Power (Inc F_{ST})	30.5kW	60.0kW
Motive Power (Exc F_{ST})	3.29kW	10.93kW
Vehicle Kinetic Energy	94.5kJ	312.5kJ
Vehicle Range (Exc F_{ST})	161.74km	87km

4. Compressed Air Storage Cell

This chapter deals with the intended design for the compressed air storage cell. It will be shown that the necessary technology is mature but still quite complicated and the fine detail and manufacture of the design is beyond the scope of this project. The broader view of the design geometry and weight will be considered as will the practicality of the design and how the design will be affected by the legislative environment within which this system will have to operate.

4.1 Pressure Cell Geometry and Material

Much of the general design of this cell is decided in advance by the need to perform its function whilst being of the lightest weight.

This automatically requires that the construction material have a high strength to weight ratio. The highest current strength to weight performance is achieved by carbon fibre composites, and the best of those is the fibre known as Torayca T1000 with an ultimate tensile strength of 7GPa [Toray, 2008] and a Youngs modulus of 300 GPa.

Apart from the construction material, the shape of the cell is the most important element of the geometric design that affects weight. As a thin walled pressure vessel the weight of the vessel is closely related to its volume and surface area. Given that, for the purpose of this project, the volume of the cell has been fixed at 250 litres, a shape must be chosen that has the minimum surface area/volume ratio. A sphere is

known to be the shape with the lowest surface area/volume ratio. A sphere of 250 litres capacity has an internal diameter of 0.78m.

In short, to minimise the weight of a 250 litre pressure vessel, the vessel must be a 780mm internal diameter sphere of carbon fibre, probably Torayca T1000. There are a number of considerations in respect of other elements e.g. internal and external protective layers, inlets and ancillary equipment, but the major design elements are set by the cells function.

4.1.1 Conventional Construction of Carbon Fibre Pressure Vessels

Carbon fibre pressure vessels are now a mature technology, at least in the case of breathing air cylinders. The first commercially available carbon fibre cylinders were certified, by the UK Health and Safety Executive in Jan 1994, for use as part of self-contained breathing apparatus (SCBA) used by firemen and other emergency services. Since then the technology's uses have expanded to portable storage of alternative fuels such as CNG, LPG and Hydrogen, life raft inflators and even paintball guns. Though the materials may change in detail, the form of construction is usually as in figure 4.1 below. The very similar Figure 4.2 is a hydrogen storage cylinder designed to operate at 800 bar. This was used by Daimler Benz (then Daimler Chrysler) as a hydrogen fuel tank for their ongoing hydrogen fuel cell car project.

Figure 4.1 Standard Form of Construction of a Carbon Fibre Pressure Vessel (Courtesy of Luxfer Gas Cylinders)

1. Threaded Inlet, for mounting of valves, is usually a continuous part of (3)
2. Smooth, inert internal finish. Main purpose is corrosion reduction.
3. Thin aluminium liner. Prevents corrosion or mechanical damage to internal surface of carbon fibre wrap.
4. Carbon fibre/Epoxy resin overwrap. Main structural element.
5. Glass fibre/epoxy resin overwrap. Main purpose is as a protective layer preventing damage to the outer surface of the carbon fibre overwrap.
6. Smooth resin outer layer

Figure 4.2 Hydrogen (800 bar) Fuel Tank (Courtesy Daimler Benz)

The most common examples of this type of cylinder are quite small in volume, 9-12 litres for the SCBA equipment. The larger, Daimler Benz, cylinder wasn't credited with a volume but is probably about 50 litres. The proposed pressure vessel is unusually large but, reputedly, the same construction has been used for large fuel tanks in missiles and rockets, although there is little published on this use. A recent search of Science Direct produced only one reference [Higuchi, 2005] and there was surprisingly little on the internet, even of the usual apocryphal standard. This notwithstanding, the demand for such pressure vessels must be substantial as the ISO has constructed a standard for them [ISO,2002].

4.2 Standard ISO11119-3:2002 for Large Capacity Pressure Vessels

The following is the abstract of part 3 of that standard:-

“ISO1119-3:2002, Gas cylinders of composite construction -- Specification and test methods -- Part 3: Fully wrapped fibre reinforced composite gas cylinders with non-load-sharing metallic or non-metallic liners.

ISO 11119-3 specifies requirements for composite gas cylinders up to and including 450 l water capacity, for the storage and conveyance of compressed or liquefied gases with test pressures ranging up to and including 650 bar.

ISO 11119-3 applies to:

1. Fully wrapped composite cylinders with a non-load-sharing metallic or non-metallic liner (i.e. a liner that does not share the load of the overall cylinder design) and a design life from 10 years to non-limited life.
2. Composite cylinders without liners (including cylinders without liners manufactured from two parts joined together) and with a test pressure of less than 60 bar.

The cylinders are constructed:

1. in the form of a disposable mandrel overwrapped with carbon fibre or aramid fibre or glass fibre (or a mixture thereof) in a resin matrix to provide longitudinal and circumferential reinforcement;
2. in the form of two filament wound shells joined together.

ISO 11119-3 does not address the design, fitting and performance of removable protective sleeves."

Parts 1 & 2 are for similar pressure vessels but using structural liners.

The relevant tests and pressures are summarised below and from these springs the structural performance requirements.

Table 4.1 — ISO 11119-3 symbols and their designations

Symbol	Designation	unit
Pb	Burst pressure of finished cylinder (2Ph)	bar
Ph	Test Pressure (1.5 Pw)	bar
Pmax	Maximum developed pressure at 65ºC	bar
Pw	Working pressure (2/3rds Ph – Section 7.2.4 e)	bar

4.2.1 Summary of ISO11119-3 Performance Tests

A manufacturer supplies a batch of 30 examples of the cylinders (referred to as cylinders in the standard but as "vessels" in the summary below) to be subject to the following tests.

Test 1 Hydraulic proof pressure test

Hydraulic tests require that the vessel be filled with water and which is then raised to the specified pressure. The test requires that the hydraulic pressure in the cylinder be increased gradually until the test pressure, Ph, is reached. The cylinder test pressure shall be held for at least 30 seconds to ascertain that there are no leaks and no failure.

If leakage occurs in the piping or fittings, the cylinders may be re-tested after repair of such leakages.

Fail = leaks, failure to hold pressure or visible permanent deformation after the cylinder is depressurised.

Test 2 Hydraulic volumetric expansion test

This test requires that the hydraulic pressure in the cylinder be increased gradually and regularly until the test pressure, Ph, is reached. The cylinder test pressure shall be held for at least 30 secs to ascertain that there are no leaks and no failure.

The elastic expansion shall be measured between 10% of test pressure, Ph, and the test pressure, Ph.

The vessel shall be rejected if either:
(a) it shows an elastic expansion in excess of 110 % of the average elastic expansion for the batch
(b) if there are leaks or failure to hold pressure.

Test 3 Burst test

Three vessels shall be tested hydraulically, to destruction, by pressurising at a rate of no more than 5 bar/sec. The test shall be carried out under ambient conditions. The burst pressure or pressure at failure, Pb, shall be not less than 2 times the test pressure, Ph, of the composite cylinder design

Test 4 Ambient cycle test for cylinders with test pressure ≥60 bar

Two cylinders shall be subjected to a hydraulic pressure cycle test, from a low pressure to test pressure, Ph.

The test shall be carried out using a non-corrosive fluid under ambient conditions, subjecting the cylinders to successive reversals at an upper cyclic pressure that is equal to the hydraulic test pressure, Ph. The value of the lower cyclic pressure shall not exceed 10 % of the upper cyclic pressure, but shall have an absolute maximum of 30 bar. The frequency of reversals shall not exceed 0, 25 Hz (15 cycles/min). The temperature on the outside surface of the cylinder shall not exceed 50 °C during the test.

The cylinders shall withstand N pressurisation cycles to the test pressure, Ph, without failure by burst or leakage where

N = y × 250 cycles per year of design life;

y is the number of years of design life and is a whole number which is not less than 10 years.

The test shall continue for a further N, cycles, or until the cylinder fails by leakage, whichever is the sooner. In either case the cylinder shall be deemed to have passed the test. However, should failure during this second part of the test be by burst, then the cylinder shall have failed the test.

Test 5 Vacuum test

When this test is carried out, one vessel shall be subjected to a vacuum test prior to the environmental cycle test.

The vessel shall be subjected to a series of cycles from atmospheric pressure to a vacuum. The test cycle is that the contents (inert gas or air) shall be reduced from atmospheric pressure to a pressure of 0,2 bar absolute at ambient temperature. The vacuum shall then be maintained at this level for at least 1 min. after which the pressure in the cylinder shall be returned to atmospheric pressure. The total number of cycles shall be 50.

After cycling, the interior of the liner shall be inspected for damage. Any evidence of disbonding, folding or other damage shall be noted. If the cylinder then passes the environmental cycle test (see Test 6) it shall also be considered as having passed the vacuum test.

Test 6 Environmental cycle test

When the vacuum test (Test 5) is carried out, the vacuum-tested cylinder shall be used for the environmental cycle test.

Condition the cylinder and contained pressurising medium for 48 h at atmospheric pressure, at a temperature between 60 °C and 70 °C and at a relative humidity greater than or equal to 95 %. Hydraulically apply 5 000 cycles from a pressure approximately equal to atmospheric pressure to two-thirds of the test pressure, Ph. The cylinder skin temperature shall be maintained at between 60 °C and 70 °C by regulating the environmental chamber and the cycling frequency. The cycling frequency shall not exceed 5 cycles/min. Release the pressure and stabilise the cylinder at 20 °C approximately. Stabilise the cylinder and the contained pressurizing medium until the temperature is between 50 °C and 60 °C. The

hydraulic pressurizing medium external to the cylinder under test shall commence the cycle testing at ambient temperature. Apply 5 000 cycles from a pressure approximately equal to atmospheric pressure to two-thirds of the test pressure, Ph. The cylinder skin temperature shall be maintained at between 50 °C and 60 °C by regulating

the environmental chamber and the cycling frequency. The cycling frequency shall not exceed 5 cycles/min. Release the pressure and stabilise the vessel at approximately 20 °C. Hydraulically apply 30 cycles from a pressure approximately equal to atmospheric pressure to the test pressure, Ph, under ambient conditions.

On completion of these tests the cylinder shall be subjected to the burst test (Test 3). The burst pressure, Pb, shall be not less than the test pressure, Ph, × 1,4 of the composite cylinder design.

Test 7 High temperature creep test

For a design life of up to 20 years, two vessels shall be hydraulically pressurised to test pressure, Ph, and shall be maintained at this pressure for 1,000 h. For a design life equal to or greater than 20 years, the test shall run for 2,000 h. The test shall be conducted at a minimum temperature of 70 °C and a relative humidity of less than 50 %. After this test, the cylinders shall be subjected to the leak test (see Test15) and the burst test (Test.3).

The vessel shall not exhibit any visible deformation or loose fibres (unravelling); the cylinder shall satisfy the criteria of the leak test (see Test15); the burst pressure, Pb, shall be equal to or greater than 2 times the test pressure, Ph.

Test 8 Flaw test

(Note: this seems to apply solely to “cylinders” with parallel sections and may not apply to spheres)

Two cylinders shall be tested in accordance with the following procedure.

One longitudinal flaw is cut into each cylinder, in the mid-length of the cylindrical wall of the cylinder. The flaw shall be made with a 1 mm thick cutter to a depth equal to at least 40 % of the composite thickness and to a length between the centres of the cutter equal to five times the composite thickness. A second transverse flaw of the same dimensions is cut into each cylinder in the mid-length of the cylindrical wall

approximately 120° around the circumference from the other flaw. One cylinder shall be subjected to the burst test specified in Test.3. The other cylinder shall be subjected to the ambient cycle test specified in Test 4, but the upper cyclic pressure shall

be 2/3 of the test pressure, Ph, and the test shall be suspended after 5 000 cycles if the cylinder has not failed.

First cylinder: burst pressure, Pb, shall be equal to or greater than the test pressure, 4/3Ph.

Second cylinder: the cylinder shall withstand at least 1000 pressure cycles to 2/3 of the test pressure, Ph, without leakage. If the cylinder fails by leakage after 1 000 cycles it shall be deemed to have passed the test. However, should failure during this second half of the test be by burst, then the cylinder shall have failed the test.

Test 9 Drop test

(Note again that parts of this test can only be carried out on a cylinder)

For cylinders over 50 litres water capacity.

One empty cylinder, fitted with sealing device to protect threads and sealing surfaces, shall be subjected to a sequence of drops from a maximum height of 1.8 m on to a smooth flat concrete surface.

1. horizontally on to the cylinder sidewall;
2. vertically on to the cylinder base – however maximum potential energy of 1 220 Nm (900 ft-lb.) shall not be exceeded;
3. vertically on to other end of cylinder – however maximum potential energy of 1 220 Nm (900 ft-lb.) shall not be exceeded;

(Note: These are the units used in the Standard, not Joules as expected)

4. at an angle of 45° to strike the shoulder of the cylinder – however the drop height shall be such that the centre of gravity of the cylinder is 1.8 m from the floor with the shoulder a minimum of 0,6 m from the floor. The cylinder shall then be subjected to 12 000 pressurisation cycles in accordance with the procedure specified in Test 4 but the upper cyclic pressure shall be 2/3 of the test pressure, Ph.

The cylinders shall withstand 3000 pressurization cycles to 2/3 of the test pressure, ph, without failure by burst or leakage. The test shall continue for a further 9 000 cycles, or until the cylinder fails by leakage, whichever is the sooner. In either case the cylinder shall be considered to have passed the test. However should failure during this second part of the test be by burst, then the cylinder shall have failed the test.

Test 10 High velocity impact (gunfire) test

One vessel shall be filled to 2/3 of the test pressure, Ph, with air or nitrogen.

The vessel shall be positioned in such a way that the point of impact of the projectile shall be in the vessel side wall at a nominal angle of 45° and such that the bullet would also exit through the vessel side wall. The bullet shall penetrate one wall of the vessel at least. If this does not occur, the energy of the bullet shall be increased until penetration is achieved. Vessels with diameter of above 120 mm shall be impacted by a 7.62 mm (0.3 calibre) armour-piercing projectile (of length between 37 mm and 51 mm) with a nominal speed of about 850 m/s. The bullet shall be fired from a distance of not more than 45 m. The dimensions of the entrance and exit openings shall be measured and recorded. After the test the cylinder shall be rendered unserviceable.

A fail will be recorded if the vessel does not remain in one piece

Test 11 Fire resistance test

Required if a pressure-relief device is fitted to prevent failure in case of fire in service.

One cylinder shall be fitted with a valve as follows:

a) with the valve intended for use (if known) or

b) with a valve fitted with bursting disc set to operate at between Ph and 1,15 Ph.

The cylinder shall be charged with air or nitrogen or with the gas intended for use to 2/3 of the test pressure, Ph.

A suitable fire can be created with either wood, gas or other hydrocarbon fuel (see ISO 11439 for details of the construction of the fire).

For “cylinders” the test varies with orientation but the following is representative.

One cylinder shall be placed in a horizontal position with the lowest part of the cylinder approximately 0,1 m from the top of the firewood, in the case of a wood fire, or 0,1 m from the surface of the liquid in a fuel-based fire. The cylinder and valve shall be exposed to fire engulfment along its whole length, but the relief device shall be shielded from direct flame impingement. The fire shall be capable of enveloping the entire length of the cylinder, when in the horizontal position, and producing a temperature ≥ 590 °C, measured 25 mm below the cylinder, within 2 min. The cylinder shall be exposed to the fires until vented.

The cylinder shall not burst during a period of 2 min from the start of the fire test. It may vent through the pressure relief device or leak through the cylinder wall or other surfaces. NOTE: This test does not imply that only one pressure relief device assembly provides fire protection for the valve/prd (pressure relief device) system.

Test 12 Permeability test

This test is only required for composite cylinders with non-metallic liners and for cylinders without liners and involves weighing the pressurised vessel to estimate gas loss through the vessel walls. It is not considered to be relevant to the current system.

Test 13 Torque test on cylinder neck boss

The cylinder shall be fitted with an appropriate valve and tightened to 150 % of the maximum torque recommended in ISO 13341, for the relevant boss material in ISO 11439 or as recommended by the manufacturer where this part of ISO 11119 does not apply. The valve shall be removed after the first installation and the neck thread and boss inspected. The valve shall then be re-installed as specified above and the vessel pressurised to 2/3 Ph for 2hrs. A test for leaks (bubble test) in the cylinder neck area shall be conducted for 10mins.

The neck thread and boss shall show no significant deformation and shall remain within drawing and gauge tolerance.

Leakage greater than 1 bubble/2 min in the bubble leak test shall constitute a failure of the test.

Test 14 Salt water immersion test

This test is mandatory for all cylinders intended for underwater applications and is optional in the case of other uses. It is not considered relevant here.

Test 15 Leak test

Related to test12 and is not considered to be relevant here.

Test 16 Pneumatic cycle test

One cylinder shall be charged to the test pressure, Ph, × 2/3. The cylinder pressure shall be held at the test pressure, Ph, × 2/3 for 72 h. The cylinder shall then be subjected to 100 pneumatic pressure cycles between atmospheric pressure and the test pressure, Ph, × 2/3. Each cycle shall be completed over a period between 55 min and 65 min. After cycling, the cylinder pressure shall be held at the test pressure, Ph,

× 2/3 for 72 h the pressure shall be released by venting through the fully-opened valve. The cylinder shall then be visually inspected on the internal surfaces for signs of blistering or liner collapse. After visual inspection, the cylinder shall be subjected to the ambient cycle test (See test 4).

If the internal surfaces show evidence of blisters or the liner has collapsed the vessel shall have failed the test.

Test 17 Water boil test

This test is only required for cylinders without liners and which are manufactured from two parts joined together and is not considered relevant here.

4.2.2 Pressure Vessel Specification as it Arises from the Test Requirements

Section 7.2.4.e of the Standard required that the working pressure, Pw, be no more than 2/3rds of the test pressure, Ph. As Pw is the starting point of the vessels design, this is set first and is 300bar/30MPa. The reason for this value is that it is the highest pressure for which equipment is commonly available. This makes the test pressure, Ph, 450bar/45MPa.

Tests 1 & 2 Vessel shall be leak free at 450bar/45MPa.

Test 3 Vessel shall not burst until the pressure exceeds 2 x Ph = 900bar.

Test 4 Designed life not less than 10 yrs @ 250 cycles PY.

Tests 5, 6 & 7 Can only be reliably met by continuous aluminium liner.

Test 8 Flaw test – may not apply to sphere.

Test 9 & 10 Impact and Gun Fire tests Implies a solid body with no joins or weak points.

Test 11 A pressure relief valve is, probably, a requirement and must be able to operate at a maximum of the test pressure Ph x 1.15 (518 bar). A fire resistant outer layer should be able to resist a fire for 2 mins.

Test 12 No mechanical relevance.

Test 13 No leaks at working pressure.

Test 14 & 15 No mechanical relevance.

Test 16 Pneumatic cycle test. This requires a continuous aluminium liner.

Test 17 No mechanical relevance.

Several tests consider the possibility of the liner delaminating as a result of high pressure penetrating between the liner and the pressure vessel and deforming the liner when the interior pressure falls. The most reliable response to this is a continuous metal liner, usually constructed by upsetting and hydroforming, of an aluminium alloy. The alloy recommended elsewhere [HSE, 2002] is AA 6061.

Tthe structural requirements for the carbon fibre body could be met by resin pre impregnated (pre preg) carbon fibre sheets being laid over a pattern this would allow the possibility of weak or permeable joints. These could fail in extreme circumstances unless a higher safety factor is used. Carbon fibre pressure vessels are all now made by a variation of the process called fibre winding. In a basic version of this process a single tow of pre impregnated carbon fibre is wound onto a mandrel, in this case the aluminium liner. A variety of winding patterns are possible and each has its own structural benefits. The pattern design is a complex matter and best left to an experienced designer but, at the end of the curing process, the body of the vessel is far more homogenous with a low chance of any weak spots. It is this process that

meets the requirement of the gun fire test (Test 10) of the vessel not breaking up under a high speed impact. As the crack creating forces try to propagate the crack through the material they are constantly being blocked by fibres across the crack path, whatever the direction of the crack.

4.2.2.1 Fibre Winding Production Method

The process of fibre winding has some other benefits apart from being particularly crack resistant. Paramount amongst these is the high fibre volume fraction that is now possible with this method. Until about a decade ago a common fibre volume fraction was 50%. It was desirable to increase the fibre fraction as this increased the tensile strength of the composite [Cohen, 2001] in proportion. In fibre winding the method for increasing the fibre volume fraction was to increase the tension of the tow when winding it onto the mandrel. This worked well up to 55-60% but when using higher tensions to reach the higher volume fractions, the strength of the composite started to fall. It was believed that the higher tensions were damaging the tow, made up of many thousands of individual fibres, as it was wound onto the mandrel. Several methods have been devised to overcome this problem, using tapes or multiple tows, but these still place the carbon fibre under high tension.

A successful method that doesn't strain the fibre is the " fibre placement" method developed by Cincinnati Machine Inc. A large but otherwise fairly normal fibre winding machine is shown in figure 4.3. Smaller machines differ only in respect of the tailstock often not being required as the headstock is stiff enough to handle smaller mandrels. This machine also has the compaction roller head that is shown in

more detail in figure 4.4. This head feeds the tow, or tape, to the mandrel as with other systems, but finally presses the tow into the work piece with a “compaction roller”.

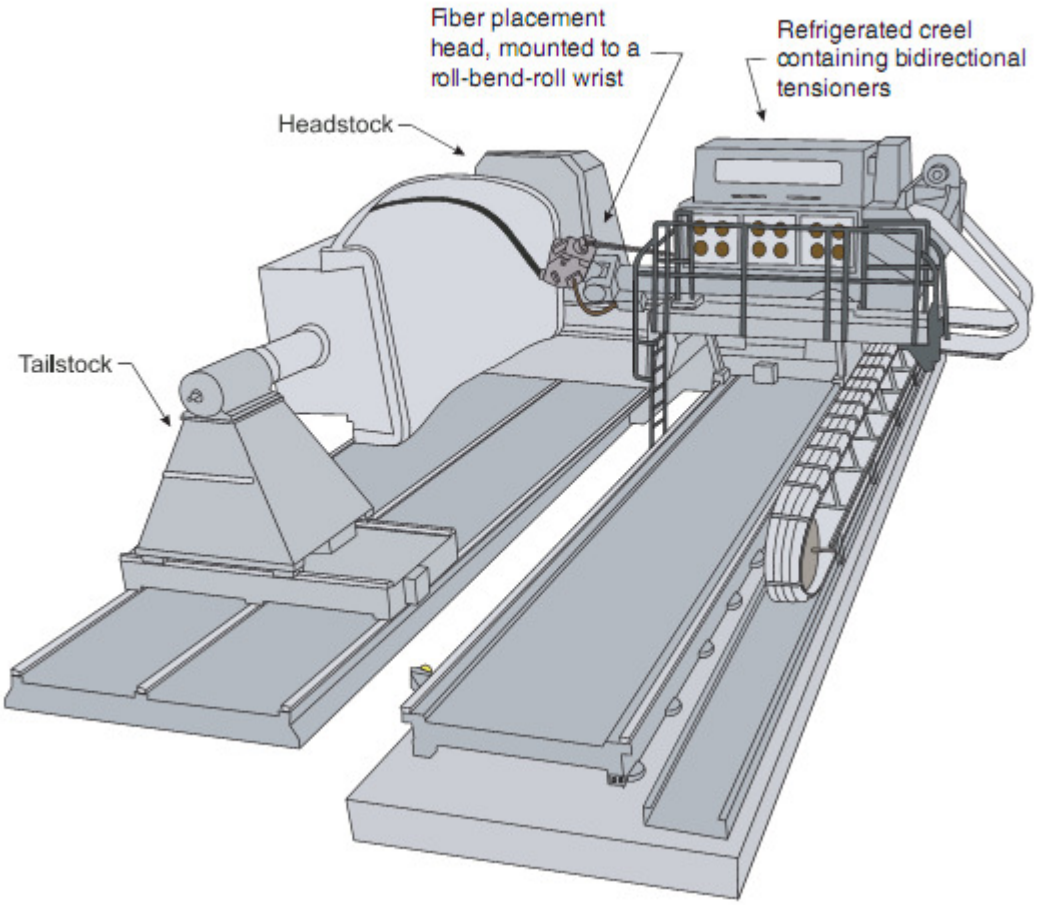

Figure 4.3 Cincinnati Machine Inc. Fibre Winding System

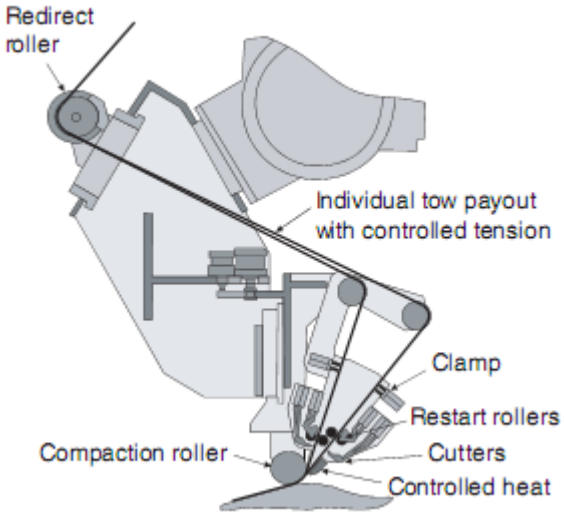

Figure 4.4 Fibre Placement Compaction Roller Head

These methods, and others like them, enable manufactures to make composites with fibre volume fractions of the order of 80% [GRP Tubing, 2009]. These fibre volume fractions have not yet been tested, or have referred to in the professional literature, but this is an area where craft skill often precedes engineering analysis.

4.3 Weight of Spherical Pressure Vessel

The previous sections have been about placing the concept of a large spherical pressure vessel in context, showing that it is not an exotic and impractical technology.

At a more prosaic level, the estimate of the systems specific energy density requires an estimate of the weight of the proposed pressure vessel.

A full weight analysis has been found for a CF wrapped pressure vessel [Kawahara,1996]. This was for a titanium lined vessel of 4105 in^3/67.27 litres and

used T1000 carbon fibres for the overwrap. Its purpose was to contain helium, at the pressure of 30 MPa, as an energy store for an unspecified spacecraft. The total weight for the vessel was just under 10kg. Expanding that value proportionally, to 250 litres, would result in a weight of 37.2 kg. As the surface/volume ratio falls with increasing volume this design could be expected to deliver an even lower weight, although the effects of hoop stress increasing with the radius might counteract that. However, it would be overoptimistic to use this design as it only uses a safety factor of 1.5 with a minimum burst pressure is 46 MPa.

As mentioned in Section 3.3 an FEA analysis of a carbon fibre vessel was carried out using Pro Engineer/Mechanica. This yielded a weight value of 45kg but was for a pressure safety factor of two and did not include a liner. This reduced the weight of the design, but it was also based on the tensile strength of the weaker (and cheaper) T700 carbon fibre which made the design heavier. This safety factor was based on the requirements, and formula, of a now superseded British Standard BS5045 (Transportable Gas Containers).

The ISO standard 11119-3 is intended to set the standard for transportable long life pressure vessels, for “10 yrs to non-limited life”. It is likely that any practical compressed air vehicle will have to meet this standard which, as can be seen from table 4.1 above, uses a safety factor of 3 times the working pressure. Although there is no specific demand for a metal liner (lightweight polymers are allowed) this is considered to be best practice and will be used in the final calculation of weight. No guidance is given on the thickness of non-structural metal liners but a recent specification [US-DOT, 2007] makes a reference to test sample thicknesses that

implies an upper limit for non-structural liners of 4.8mm/ 3/16in. A lower limit seems to be about 1.5mm, so the medium seems to be 3mm.

The volume of the aluminium liner is the volume of the outer diameter A_{vo} minus the volume of the inner diameter A_{vi}. As already stated, the internal diameter of a 250 litre sphere is 780mm. A 3mm wall will give an outer diameter of 786mm. The density, ρ_{α}, is in the range 2600 – 2700 kg/m^3 [John, 2003], 2700 kg/m^3 will be used.

The calculation is carried out using equation 4.1

$$\left(\left(\frac{\pi A_{vo}^3}{6}\right) - \left(\frac{\pi A_{vi}^3}{6}\right)\right)\rho a \qquad \text{Eqn. 4.1}$$

which becomes $((\pi \times 0.786^3)/6) - ((\pi \times 0.780^3)/6) = 0.00578$ m^3

$0.00578 \times 2700 = 16.2$ kg

The approximate weight of the aluminium liner is 16.2 kg.

A similar calculation will provide the weight of the carbon fibre overwrap, but first a calculation of the wall thickness is necessary.

The initial tensile strength of the Torayca T1000 fibres is 7 GPa. This is its isotropic value for all the fibres arranged in one direction. In an effectively two dimensional layout with fibres arranged in all possible two dimensional directions, this tensile strength falls to 1/3rd of its isotropic value [John, 2003b]. Good fibre layout patterns can improve on this. Assuming a 70% fibre volume fraction the composite shall be assumed to have 70% of its two dimensional value which is 1.633 GPa.

As the safety factor is 3 the internal pressure shall be taken as 90 MPa.

The maximum principle stress in the wall of a thin walled spherical pressure vessel is given by the well known arrangement for hoop stress in equation 4.2 below [Popov, 1978] and was confirmed as accurate by the FEA model in Pro Engineer/Mechanica. These FEA tools are no longer available to this project but the earlier experience confirmed that equation 4.2 is more than accurate enough for current purposes.

$$\sigma_p = \frac{pr}{2t} \qquad \text{Eqn 4.2}$$

Where

p = max. internal pressure = 90Mpa

r = internal radius = 0.393m

σ_p = max. allowable tensile stress = 1.633GPa

t = minimum carbon fibre wall thickness

Rearranging for 2t and solving gives a (rounded up) value of 22mm and so a wall thickness of 11mm.

This gives a carbon fibre sphere inner diameter of 0.786m (the same as A_{vo}) and an outer diameter of 0.808m. Taking the density of the CFRP as 1900 kg/m^3, the highest in the range of densities [John, 2003b], and substituting these figures into equation 4.1 results in a value of 45.6 kg. Including the 16.1 kg weight of the liner brings the total weight, of the pressure storage cell, to 61.8 kg. A number of conservative judgements have been made in order to arrive at this value and,

accordingly, it could reasonably be expected that a professionally optimised design would reduce this value significantly

A summary of these design requirements is contained in table 4.2.

Table 4.2 Design Requirements and Values

Characteristic	Design Requirement
Pressure Cell Capacity	250 litres
Internal Diameter Of Liner	0.78m
External Diameter of Liner	0.786m
Internal Diameter of CF Overwrap	0.786m
External Diameter of CF Overwrap	0.808m
Liner Material	Aluminium Alloy AA 6061
Carbon Fibre Type	Toray Industries, Torayca T1000
Torayca T1000 Tensile Strength	7GPa
Estimated Tensile Strength of Fibre Wound Composite	1.633GPa (70% of 1/3rd of initial fibre strength)
Normal Working Pressure (Pw)	30MPa
Test Pressure (Ph)	45MPa (1.5 x Pw)
Burst Pressure (Pb)	90MPa (2 x Ph)
Weight of Liner	16.1kg
Weight of Carbon Fibre Overwrap	41.7kg
Total Weight	57.9kg

5. Primary Heat Exchanger

5.1 Overview

As a consequence of the Boyle-Marriotte law, when compressed air is stored at high pressure and ambient temperatures, the process of depressurisation results in a substantial drop in its temperature. For the intended storage pressures and operating pressures used here (30MPa, 1Mpa-101kPa) the temperature difference is approximately 60ºC. With an ambient temperature of 20ºC the released air would fall to a temperature of approximately -40ºC and this temperature has been observed in the course of the heat exchanger (HX) experiments. Creutzig et al [2009] evaluated the performance compressed air cars and assumed that expansion would be adiabatic. They described this assumption as "conservative" and it was fundamental to their poor assessment of Compacs. In reality it is a rather negative assessment as it is very unrealistic and serves to reduce the calculated final output of any compressed air storage system to a theoretical minimum.

Assuming compression has been carried out with a good HX this temperature gradient does not represent an energy loss but does present an opportunity to increase the energy in the system. If the cold compressed air stream is passed through a lightweight air/air heat exchanger it can be warmed by heat from the ambient air before it enters the motor, its enthalpy will be increased and that energy can be used to drive the motor. The basic question is – is it a practical proposition to warm the compressed air stream up to close to the ambient temperature using a lightweight HX?

This chapter deals with the development of the requirements for such a HX and the construction of the experimental rig for testing the above question and refining the proposed design. For the reasons outlined in the following sections a multiple heat pipe based design was chosen.

5.2 Heat Exchanger Performance Requirements

The general requirements for the HX are that it be as light as possible and, potentially at least, of low cost and tough enough to withstand normal road use. This would be the equivalent to the common automotive water/air HX usually referred to as a radiator and of a similar size and weight. Compact and efficient heat exchangers have been in use for some time but their construction is complex and, in consequence, they are handmade and expensive, as in the case of the liquid nitrogen LN2000 car [Williams, 1997/2]. No weight or dimensions are available for this HX but a photograph indicates it to be approximately 750mm x 500mm x 500mm and is constructed of 45 fin and tube elements. This was a good design but it would be too large and heavy for the envisaged small car application. It needed to be this large because it was doing the more demanding task of evaporating liquid nitrogen at a rate of 300g/s whilst also avoiding frosting up. Given that the initial temperature of the compressed air would be of the order of -40ºC this was also a problem to be considered here.

A further consideration is that the HX should not detract from the specific energy storage performance of the overall system. In chapter 3 it was calculated that a carbon fibre cell could store energy at 80Wh/kg and the HX should be considered as complementing that performance. Whilst the HX isn't storing energy it is adding to

the total energy available from the system and can only function whilst the compressed air store is delivering energy. Therefore the HX should only be considered to be acceptable if the rate of energy it delivers does not fall short of the equivalent of adding more storage capacity. A HX is not directly comparable to an energy store but with a simple assumption, in regard to operating time, a useful comparison is possible.

The store is designed to contain 38.5MJ and is estimated to weigh in the region of 130kg. If it is assumed that all of the energy will be used up in one hour of motoring this would be a rate of 10.5kW which is a specific output of 80W/kg. This is the specific output of the system without the HX and therefore the HX should have a similar, or greater, output if its use is to be fully justified.

In respect of this particular criterion there will be no comparison with other HXs as it is not commonly quoted feature. Indeed, in the main source used for these matters [Hesselgreaves, 2001a], no mention of it was found and the general question of "weight" received very little consideration. Whilst it can be understood that a HX criterion such as this cannot be characterised by a single number, a graph of performance might be expected but doesn't appear to be readily available. Perhaps this is to be expected for static HXs but the automobile industry uses a number of HXs in their vehicle design and some automotive sources refer to "reduced radiator weight" as a good thing but none specifically relate heat dissipation performance to weight.

It should be mentioned, at this point, that the HX does improve the energy efficiency of the system since it provides energy that has not been generated at the cost of some fuel somewhere. For this reason alone the inclusion of a HX will not be solely justified by its specific output as calculated above.

An estimate of the total output results from the desired change in specific enthalpy (Δh = kJ/kg) and the expected mass flow ($\dot{m}$ = kg/s).

At the inlet, to the HX, the pressure is 10 bar and the temperature approximately 240K. At these conditions h_{orig} is 490.1 kJ/kg and the specific heat C_p 1.031 kJ/kg.K

At the outlet the pressure will be unchanged and the maximum temperature would be that of the ambient air, say 300K (it is accepted that it is unlikely that actual output temperatures will be greater than 295k). At these conditions h_{final} is 551.96 kJ/kg. and the specific heat C_p is 1.021 kJ/kg.K

Interpolating the two specific heats results in 1.029 kJ/kg.K. As a check of accuracy

h_{orig} 490.1 + (ΔT (60) . 1.029 kJ/kg.K) = 551.86 kJ/kg. (close to h_{final})

Taking $\dot{m}$ to be the entire contents of the compressed air store (78.5kg) over a period of one hour gives flow rate of 21.8g/s.

0.0218kg/s . 60 . 1.029 = 1.3459kJ/s = 1.35kW

This indicates that the HX will be required to deliver approximately 1.35 kW across an initial temperature gradient of 60K. It is unlikely this would be achieved as the temperature gradient would be reduced in the final stages of heat transfer. However,

it does indicate that the HX will weigh approximately 17kg if the specific output target is achieved.

Finally, a target for the degree of "compactness" should be set. In the field of compact heat exchangers the ratio of m^2 of heat transfer surface to m^3 of overall HX volume (m^2/m^3) is the conventional measure. This is less important than the absolute dimensions but serves as a measure by which to compare the design with others. A ratio of several thousand is possible amongst micro scale HXs designed for micro-processors but 200 – 300 is standard amongst macro scale HXs [Hesselgreaves, 2001b] so this is a more reasonable target for the moment.

The absolute dimensions of the final design of HX will have to wait until the performance of the test rig is evaluated, but it is expected that it would be of a similar volume to an automobile radiator.

The above values are summarised in table 5.1 below.

Table 5.1 Summary of HX Requirements

Operating Temp. Range	20+°C to -40°C
Operating Pressure	1MPa/10bar
Test Pressure	2MPa/20bar
Specific Output	80W/kg
Total Output (in operating temp. range)	1350W
Maximum Weight (approx)	17kg
Compactness	200-300 m^2/m^3

5.3 Heat Exchanger - Initial Design Considerations

It was initially hoped to modify a conventional “flat tube and fin” automotive radiator for the purposes of this project. It was required to handle 1MPa/10 bar but with a safety factor of 2 so its maximum pressure would be 2MPa/ 20 bar. A strong aluminium radiator was acquired but some basic static pressure water tests resulted in visible distortion at 1MPa/10 bar and visible leakage from the tube/header tank join. An attempt was made to source a more robust radiator but enquiries indicated that these requirements were considerably outside the normal construction standards for even truck radiators. At this point the idea of modifying a radiator was abandoned.

Figure 5.1 shows a high pressure aluminium radiator that was developed by Serck Heat Transfer Ltd a few years ago. The radiator was intended to operate at 20 bar and would have been very interesting if available to this project. However, it wasn’t developed commercially which indicates that this type of HX does not have a clear commercial market. Also, it was intended as a water /air HX

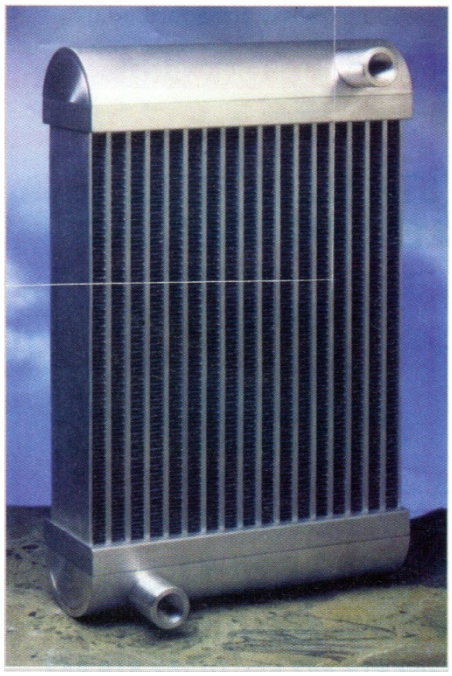

Fig 5.1 High Pressure Radiator - Serck Heat Transfer Ltd

Commissioning, or building, our own plate or flat tube and fin HX for this project was not an option. To build our own design required specialist skills and equipment not available to the project. Commissioning a design and build project from an outside contractor was equally beyond the resources of the project. The tube and fin heat exchanger for the liquid nitrogen vehicle had been the major element of that project (project cost $350,000) and presumably had consumed a proportional amount of the project funding.

A product in the form of copper pipes, with cold moulded fins, is available but the fins were quite small and the pipes were intended for use as a water/air HX. Some crude calculations suggested that a large number of these pipes (about 80 x 300mm tubes) would be required. It would probably be a superior solution to fit ordinary plumbing pipes with large soldered-on fins. This was seriously considered but was eventually put aside because of the large amount of delicate soldering work it entailed and the final design solution (heat pipes) arrived at seemed more achievable.

5.3.1 Heat Pipes

In the process of sourcing a HX many HX components were considered (e.g. the cold moulded copper tubes mentioned above) and one of these were heat pipes. The manufacturers, then Isoterix Ltd now named Thermacore Europe Ltd, claimed that their products had a thermal conductivity 1000 times greater than that of copper [Isoterix, 2002]. Whilst this was not necessarily accepted without question, it did suggest that these could be used as the core of an efficient HX. Two non-finned heat pipes (one alcohol based and one water based) were obtained and tested in comparison to a copper bar of similar dimensions. The test was simply placing one end of the bar and heat pipes in the same container of hot (55°C) water, lightly insulating the above water section and recording the temperature change at the very top. Within 10 seconds the water heat pipe was at 50°C and the alcohol heat pipe achieved the same temperature a few seconds later. The copper bar did heat up but never reached this temperature nor matched the performance of the heat pipes.

This test was hardly conclusive as a comparison between heat pipes and finned copper pipes as heat exchangers. The effect of the detailed final HX design was hard to predict without much more data. The heat pipe HX seemed more achievable but, in retrospect, the eventual heat pipe HX design had some features that would have made the finned copper pipe design easier to build. The final decision, to use heat pipes, was based, in part, on the fact that the heat pipes were very interesting devices and some practical experience of them was desirable.

5.3.2 Heat Pipe Basics

Heat Pipes are an improvement on the thermosyphon principle in which a small amount of liquid is stored in a sealed tube, often at low pressure. Heat is supplied to the lower (evaporator) end of the tube so that the liquid evaporates and quickly travels to the upper (condenser) end of the tube which is cool. Here the vapour condenses on the tube wall, giving up its heat, and returns to the evaporator end under the influence of gravity, see figure 5.2(a). The thermosyphon has to be close to vertical for it to work effectively and the evaporator is always the lower end.

A heat pipe operates in a very similar fashion except that an additional element called the wick is placed on the tube wall covering the middle section but not the evaporator/condenser sections. The effect of the wick is to add “capillary action” to the condensate transport mechanism increasing thermal conductivity when the heat pipe is in the normal position of condenser – high & evaporator - low. The capillary action is sufficiently strong to overcome the effect of gravity so that, if required, the heat pipe may operate (less effectively) in an inverted position, as in figure 5.2(b), or any angle between the two positions.

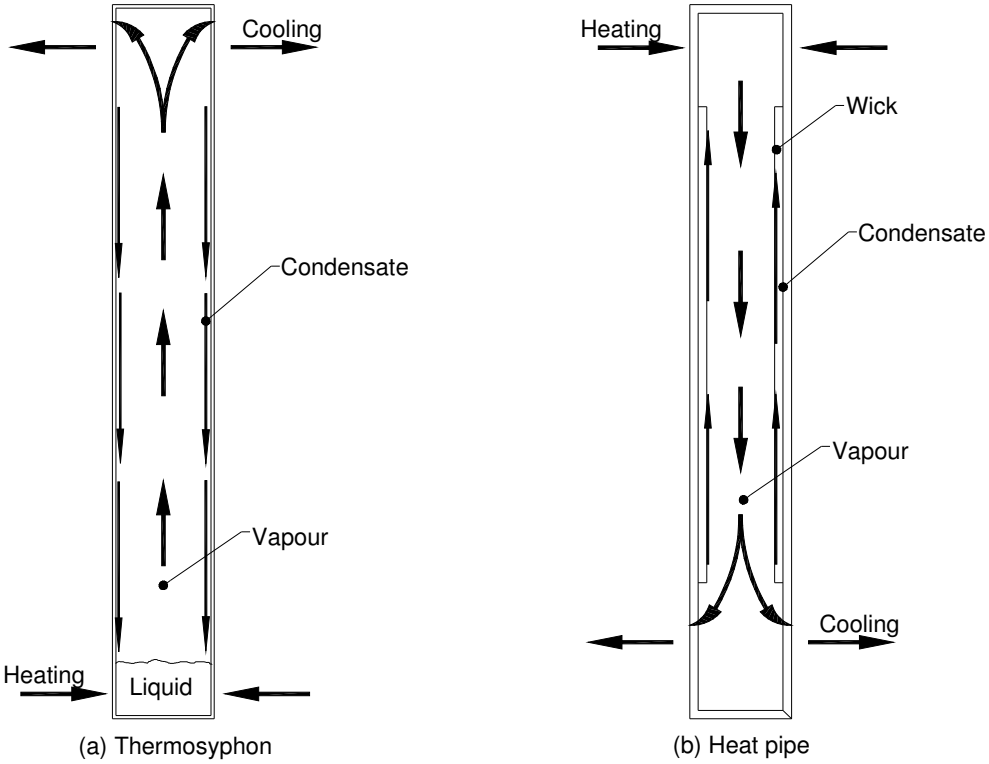

Figure 5.2 Thermosyphon/Heat Pipe Operation

There are a variety of working fluids used in heat pipes according to the temperature ranges they are expected to be working within. As mentioned above, tests and calculations based on the ideal gas equation suggested that the minimum temperatures that should be expected would be approximately 60°C below ambient. So, for an ambient temperature of 20 heat pipes that cope with -40°C would be necessary. This lower range is dealt with by heat pipes using ethanol as a working fluid. The heat pipes selected for use in this project are ethanol and water based, both operating at below atmospheric pressure in order to lower the working fluids boiling point.

Apart from a high thermal conductivity, heat pipes are also characterised by

(a) The capability to act as a heat flux transformer and

(b) The condenser presenting an almost isothermal surface.

Flux (heat absorption/rejection in W/m^2) transformation is achieved by varying the ratio of evaporator surface area to condenser surface area. This is usually achieved by the application of finning and insulation.. However, this only occurs effectively because of the isothermal characteristics of the condenser surface. The condenser surface will tend to operate at a uniform temperature (the condensation/boiling point of the working fluid). If more cooling is applied then more fluid will condense at that point but then be quickly transported to the evaporator, before freezing, to collect more heat. An automatic, temperature moderated , heat transfer balancing act takes place and continues unless there is a major difference between the heating and cooling loads. This has the effect that a heat pipe condenser may operate in temperatures below the freezing point of its working fluid for as long as the heat load at the evaporator is sufficient to maintain the cycle.

This isn't much of a consideration in regard to ethanol as its melting point is -112°C and its boiling point is (at atmospheric pressure) 78°C. For the low pressure heat pipes the boiling point was about -20°C. Whilst ethanol heat pipes can operate at low temperatures they have the disadvantage of a lower thermal conductivity due to the relatively low specific heat and enthalpy of vaporisation, of ethanol compared to water, Water C_p 4.18kJ(kg-K) compared to ethanol C_p 2.5 kJ(kg-K) and Water $h_{f\,g}$ 2442kJ/kg compared to ethanol h_{fg} 841kJ/kg, [Cengal,1989a]. The lowest temperature (-40°C) is slightly below the "useful range" (-20°C to 90°C) of the low

pressure ethanol heat pipes but, for as long as the heat flux at the evaporator is sufficient, the heat pipe will continue to operate. The useful range of the low pressure water heat pipes was 5°C to 50°C . When dealing with the compressed air stream this required that the ethanol heat pipes be placed upstream of the water based heat pipes in order to prevent significantly sub zero temperatures reaching the water heat pipes and causing them to shut down through freezing. It was decided to try the water heat pipes as is advantageous to use them as early in the process as is possible because they are almost twice as effective as the ethanol heat pipes at transporting heat.

The water heat pipes would not cease to operate immediately when exposed to sub zero temperatures as there is heat entering the system at the evaporator. Freezing only takes place when the heat extracted at the condenser exceeds the maximum heat available to the evaporator. This will be the result of the air mass flows and the temperatures of those flows. These, of course, will vary according to circumstances and testing the various possible configurations, of heat pipe, to see how they cope with different mass flows and temperatures is the purpose of the test rig.

5.3.3 Finning

The purpose of finning is to increase the heat transfer capability of the heat pipe whilst maintaining the balance of heat transfer when the heat transfer coefficients differ substantially. For gases at a medium pressure this is typically 60W/m^2.K whilst for liquids it is 2000 W/m^2.K [Hesselgreaves, 2001c]. At the operational temperatures and pressures air reasonably approximates to an ideal gas [Cengal, 1989b]. For this reason, and for simplicity, it was assumed that the compressed air

stream would behave reasonably linearly in that the coefficient would be proportional to the pressure of the air. The exact values were not important at this point as it was intended to simply balance the heat transfer by designating a large length of the heat pipe as “evaporator” and a smaller length as “condenser”, and finning and separating the two accordingly. The decision to be made was simply what should the relative proportions be. The high pressure manifold would be operating between a minimum pressure of about 200kPa(2bar) and a maximum pressure of 1MPa(10bar). At 200kPa it is expected that the heat transfer coefficient will double and balancing would require that only half as much of heat pipe length be exposed to the compressed air stream as to the ambient air stream. This would be a split of two thirds of the finning applied to the evaporator and one third to the condenser. Similar reasoning would lead to smaller condenser lengths at higher pressures but it was felt that the greater problem would be heating the compressed air stream rather than extracting heat from the ambient air. Generally speaking, larger condenser section were better than smaller, so a split of two thirds for the evaporator to one third for the condenser was considered to be a good working compromise.

The size of the fins was set as a square, of 40mm length of a side, for similarly practical reasons. The fins had to be manufactured and fitted individually to the heat pipes and the heat pipe fin assembly then individually fitted to the compressed air manifold. Fins in the form of a 40mm square appeared to be a reasonable compromise between small (ease of handling) and large (better heat capture/transfer). The fins were cut from 0.5 mm aluminium sheet. Subsequent experience indicates this to have been a good choice.

5.3.3.1 Fin Fitting

Though a relatively minor aspect of the test rig, the method of fitting the fins needs to be clarified as it has a significant impact on the efficiency and capabilities of the rig.

Once heat pipes are constructed their normal operation means it is very difficult to solder any metal objects to them. The heat is quickly conducted away. This might be overcome by applying a great amount of heat whilst insulating the sections not being worked on but the possibility of damaging the heat pipe was high.

It was always intended to fix the fins to the heat pipe by making a push tight hole in the fin, sliding it into position and fixing it in place with a thermally conductive adhesive paste that was available from the heat pipe manufacturers. Two varieties of paste were available and both were aluminium powder mixed into an adhesive base. The difference between them was that one adhesive was a silicon rubber base (Thermoflex) and slightly flexible whilst the other was a more rigid epoxy resin (Thermobond). Both had a thermal conductivity of 0.9 W/m.K and had curing times of several hours. The fin/heat pipe joint was to be as shown in figure 5.3 below.

The fin hole was made by using a hole punch and die. Whilst the 10mm punch was the correct size, an oversized die of 15mm diameter, with a rounded shoulder, was used. This results in a flange with a rounded shoulder around the hole. The hole itself was slightly undersized due to the elasticity of the aluminium and this gave the fin a tight push fit onto the heat pipe resulting in increased metal/metal contact. This

design is intended to achieve a better thermal join than is possible with the poor performance of most thermally conductive adhesives alone.

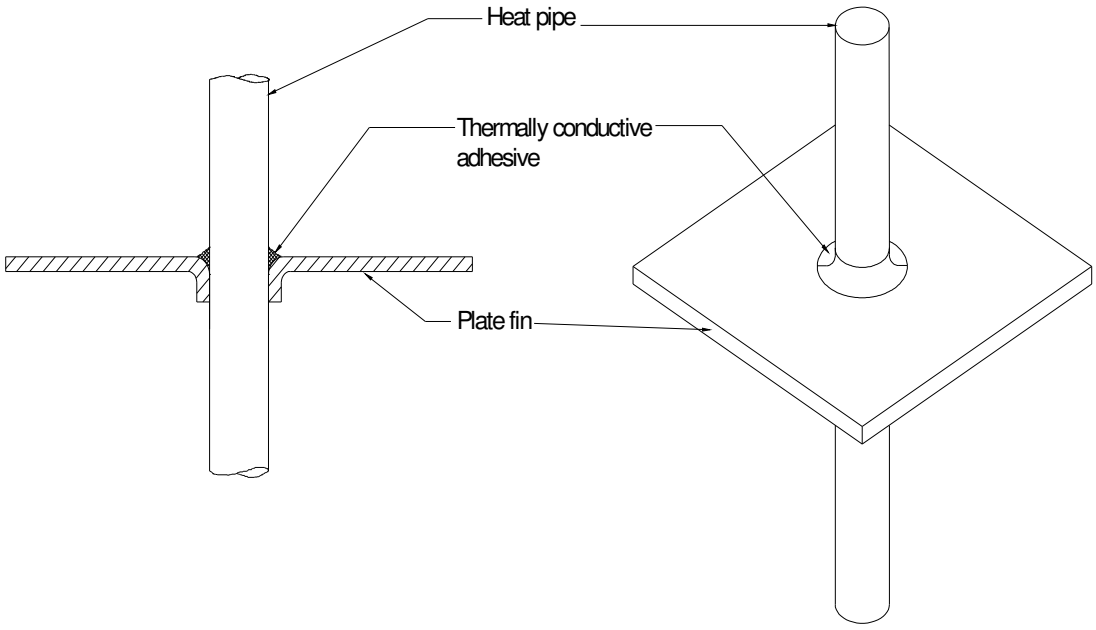

Figure 5.3 Fin fitting arrangement

The fitting process starts with placing a bead of adhesive around the heat pipe, just below the intended final position of the fin, and pushing the fin onto the bead, evenly smearing the adhesive across all the necessary surfaces. A 5mm spacer would then be placed against the fin and the fitting of the next fin would commence.

This process was followed but neither of the adhesives were sufficiently strong enough to hold the fin in place. The assemblies were left for 24 hours in a warm workshop, which was significantly more than the required curing time, after which the fins were tested for stability by being pushed lightly at one corner. The fin/heat pipe join gave after what was, subjectively, much less force than they would experience in normal handling. Further fitting attempts were made using surface degreasing, larger amounts of adhesive and longer curing times at higher

temperature. All attempts resulted in an assembly that was deemed mechanically weak and this was, probably, caused by the inadequacies of the adhesives rather than any other factor.

As the Thermobond adhesive was aluminium powder in an epoxy resin it was decided to attempt to produce a mechanically superior adhesive using the very strong SP Systems SP106 resin that was to be used for construction of the manifold body. Bronze powder was used as the thermally conductive filler. This material is a readily available from professional artist suppliers as it is used in making bronze effect sculptures. Bronze was chosen rather than aluminium because of its similar thermal conductivity (bronze 208 W/m.K, aluminium 230 W/m.K) but much lower specific heat (bronze 380J/kg.K, aluminium 910 J/kg.K). Also, bronze was preferred to copper powder as it was considered to be less chemically reactive and less likely to degrade the adhesive at a later time.

The resin and hardener were mixed in advance of mixing in the bronze powder because making a homogenous mix of resin/hardener would be much more difficult to achieve if the resin was already heavily thickened by the bronze powder. This would reduce the available working time for the mix, particularly as the laboratory/workshop was at a fairly constant 25°C. As the room was warm it was already necessary to delay the curing by keeping the mix cool in a metal tray that rested in water. As much powder was added as the mix would take and retain a usable level of plasticity. It was difficult to accurately assess the relative volumes as, because of the limited working time, only about 5 – 6ml was being prepared at a time. Also the dry bronze powder probably contained a lot of air spaces that were

filled by the resin. However, the mix ratio was approximately 70% bronze/30% resin.

An accurate “Searle’s bar” type of thermal conductivity test wasn’t practical at this time and was unnecessary as the information required was an answer to two questions:-

1. Is the bronze/resin mix as thermally conductive as the Thermobond
2. Does the bronze/resin mix have sufficient mechanical strength to reliably attach the fins to the heat pipe?

Question 1 was to be answered by a simple comparison test, as described below, and question 2 would be the “push” test that the Thermobond had already failed.

A test piece, of bronze/resin mix, was made to the dimensions 10mm diameter & length 10mm. A similar test piece was made from the remaining Thermobond in order that a comparison might be made. Each was mounted in one end of two 150mm lengths of 10mm internal diameter PVC tubing. Into the other ends were inserted a water based heat pipe so that the condenser end butted up against the internal end of the test piece. Thermocouples were attached to the external ends of the test pieces and then both heat pipes were lagged/insulated and the low evaporator ends of the heat pipes were placed in a flask of hot water. Though the water had been recently boiled its temperature wasn’t monitored as the isothermal characteristics of the heat pipe condenser meant that the base of the test pieces would be at the same temperature. This would allow a fair comparison of the test pieces by measuring the

temperatures of the external ends as read by a two channel electronic thermometer connected to the thermocouples. The general test setup is shown in figure 5.4.

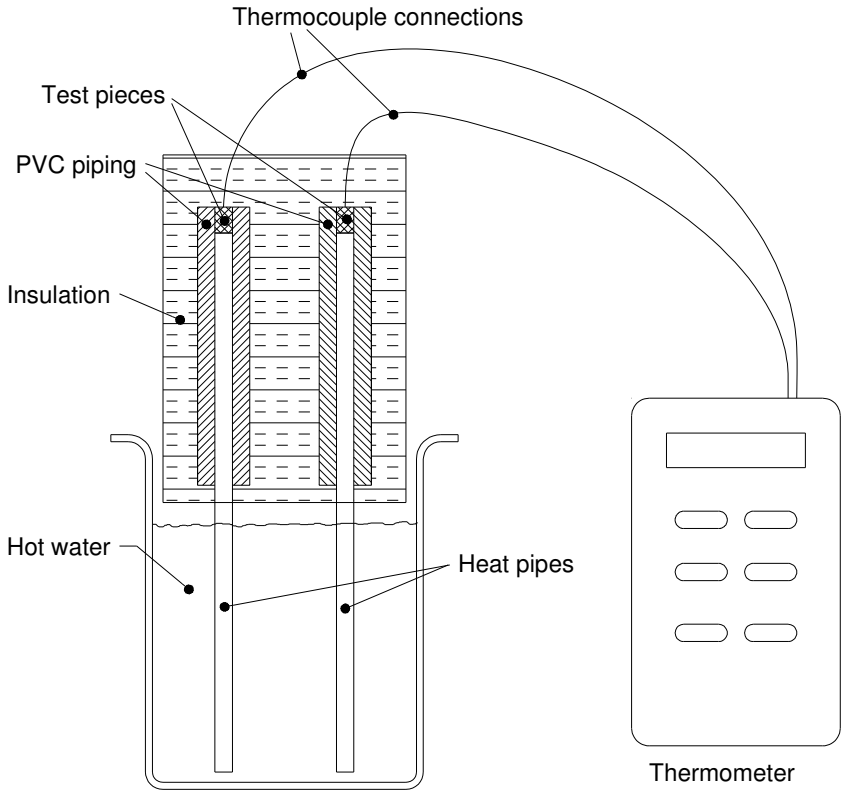

Figure 5.4 Thermal Adhesive Test Set Up

After approximately 90 s the bronze resin piece had reached 52°C whilst the Thermobond piece was at 43°C (the initial temp. was 25°C). The comparative value of this test relies on the two heat pipes having the same performance. To take account of the possibility that there was a difference between the two heat pipes, the test pieces and heat pipes were cooled down and the test repeated with the heat pipes swapped between the assemblies. Whilst the actual temperatures were different, probably due to different initial conditions, the difference between the test pieces was maintained.

The bronze resin appears to have a thermal conductivity of the order of 30 - 50% better than the Thermobond. If so, this would be about 1.2 – 1.3 W/m.K and be a

very good performance for its cost. The bronze resin would have been acceptable if it had matched the performance of the Thermobond. Exceeding it by such a substantial degree meant that it would be the preferred adhesive even if it didn't prove to be mechanically stronger. However, a portion of the same mix, as used for the thermal conductivity test, was used to attach a fin to a heat pipe and had proven to be much stronger than the Thermobond. Subjected to the same "push" test as before, whereby a corner of the aluminium fin received a thumb push acting parallel to the heat pipe axis, the fin joint was undamaged whilst the fin was distorted by the force. This test was repeated at all four fin corners and in both directions parallel to the heat pipe axis. Each time the fin itself was bent but no damage was discernable at the fin/heat pipe joint.

Subsequent experience with this adhesive has shown that it is thermally effective and very robust. No heat pipe fins have detached despite some rough handling.
It must be remembered that although this resin is successful in comparison to other thermal adhesives its performance is still very poor compared to a soldered or brazed join. A metal/metal join would have thermal conductivity values two orders of magnitude greater than these adhesives. As a result there will certainly be a reduction in performance of the primary heat exchanger compared to a similar system with soldered fins. The "shoulder" of the punched hole was intended to reduce this problem but it remains unclear as to how successful this has been. The answer to this question will have to wait until a similar finned but solder jointed heat pipe is available for comparison.

It is unlikely that a “similar finned” heat pipe will be commissioned in the near future as one further deficiency of this method is that it does not allow the fins to be tightly packed. The use of the hole punch protruding “shoulder “, the need for a spacer, unevenness in the fin plates, etc. all result in a fin spacing averaging 6mm. The manufacturers, Isoterix, have advised that they would have no trouble in achieving a fin spacing of 2mm. Clearly, whilst this thermally conductive adhesive is adequate for the current circumstances of this project, future heat exchanger designs for this project will use factory fitted finning.

The general comparative values, results and conclusions of this section are summarised in table 5.2 below.

Table 5.2 Thermal Adhesive Comparative results

Thermal Conductivity (W/m.K)	Thermobond	0.9
	Thermoflex	0.9
	Bronze/resin	1.2 – 1.3 (est)
	Aluminium	230
	copper	380
Curing time allowed	Thermobond	24 hrs
	Thermoflex	24 hrs
	Bronze/resin	24 hrs
Rough Handling Test	Thermobond	Poor Performance/Fail
	Thermoflex	Very Poor performance/Fail
	Bronze/resin	Maintained adhesion/Pass

5.4 Heat Exchanger Test Rig Design

It has been decided that the core element of the HX will be water and ethanol based heat pipes, diameter 10mm x length 250mm, with ambient air blowing over the evaporator end of length 160 mm and a condenser length of 80 mm embedded in the compressed air stream. It is now necessary to assemble a number of heat pipes into a test rig that will fully test the heat pipes and measure the change in temperature of the compressed air flow. This will be the result of both the ambient and compressed air mass flows and the temperatures of those flows. These, of course, will vary according to circumstances. Also, it will be necessary to test the various possible configurations, of heat pipes, to see how they cope with the different mass flows and temperatures.

The system chosen to investigate these configurations consists of two separate heat exchangers, each containing ten heat pipes in separate compartments, that can be connected in either a parallel or series configuration. The first heat exchanger consists of ten ethanol heat pipes which can cope with the expected sub zero temperatures in the colder upstream part of the compressed air system. The second heat exchanger consists of ten water based heat pipes and will be used downstream from the methanol heat pipes to avoid those extreme sub zero temperatures. The condenser ends of the heat pipes are finned and contained within a 100mm diameter, 600mm length, polymer tube. This tubing was sealed with glass fibre reinforced epoxy to withstand pressures much higher than the expected operational pressures.

For the experiments, the heat exchangers are contained in a box with a speed controllable fan that delivers air, at the ambient temperature, to the evaporator ends

of the heat pipes. The general form of the heat pipe test rig, individual heat exchangers and the assembled heat exchanger is illustrated in Figs 5.5 – 5.8.

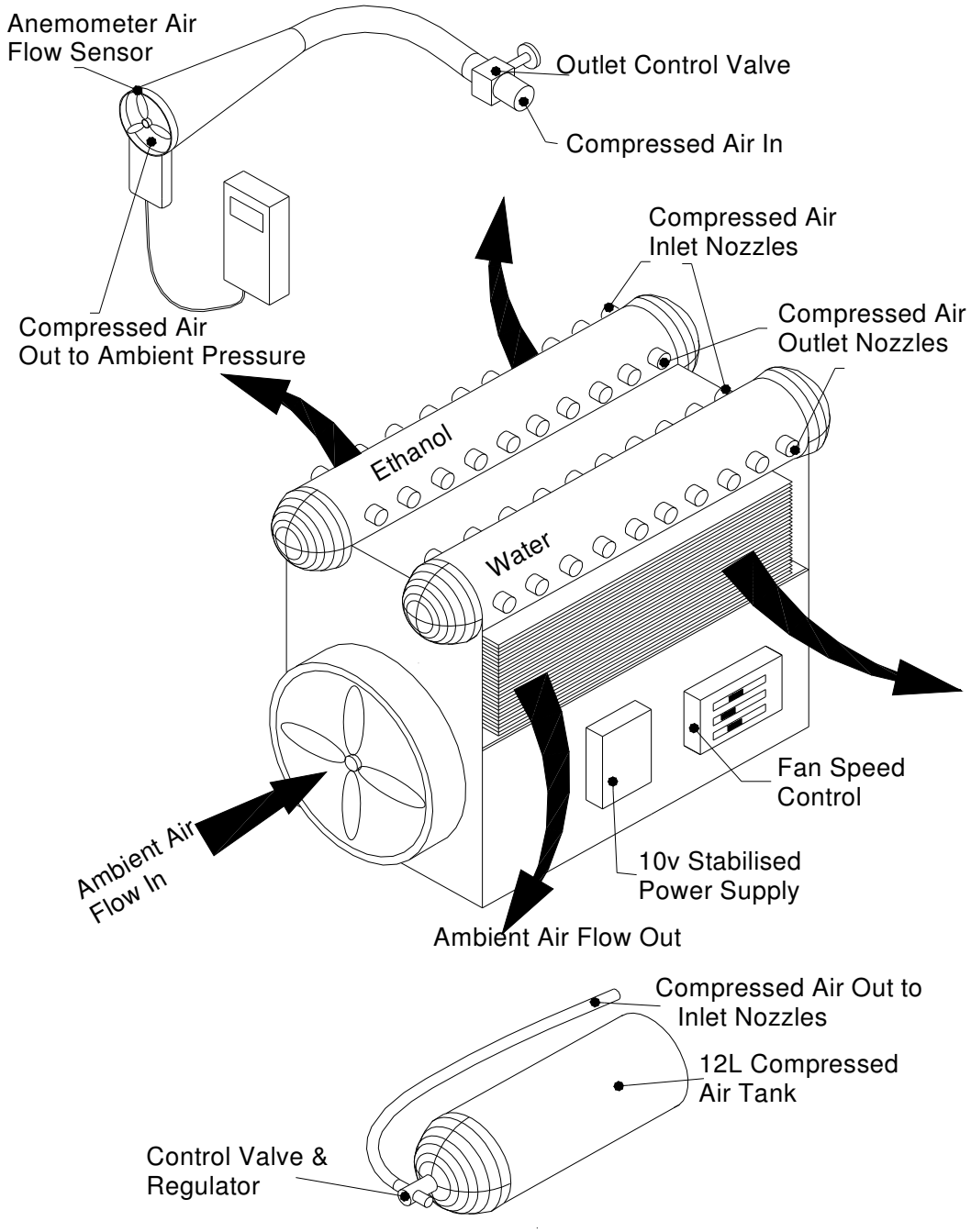

Figure 5.5 Heat Pipe Test Rig Layout

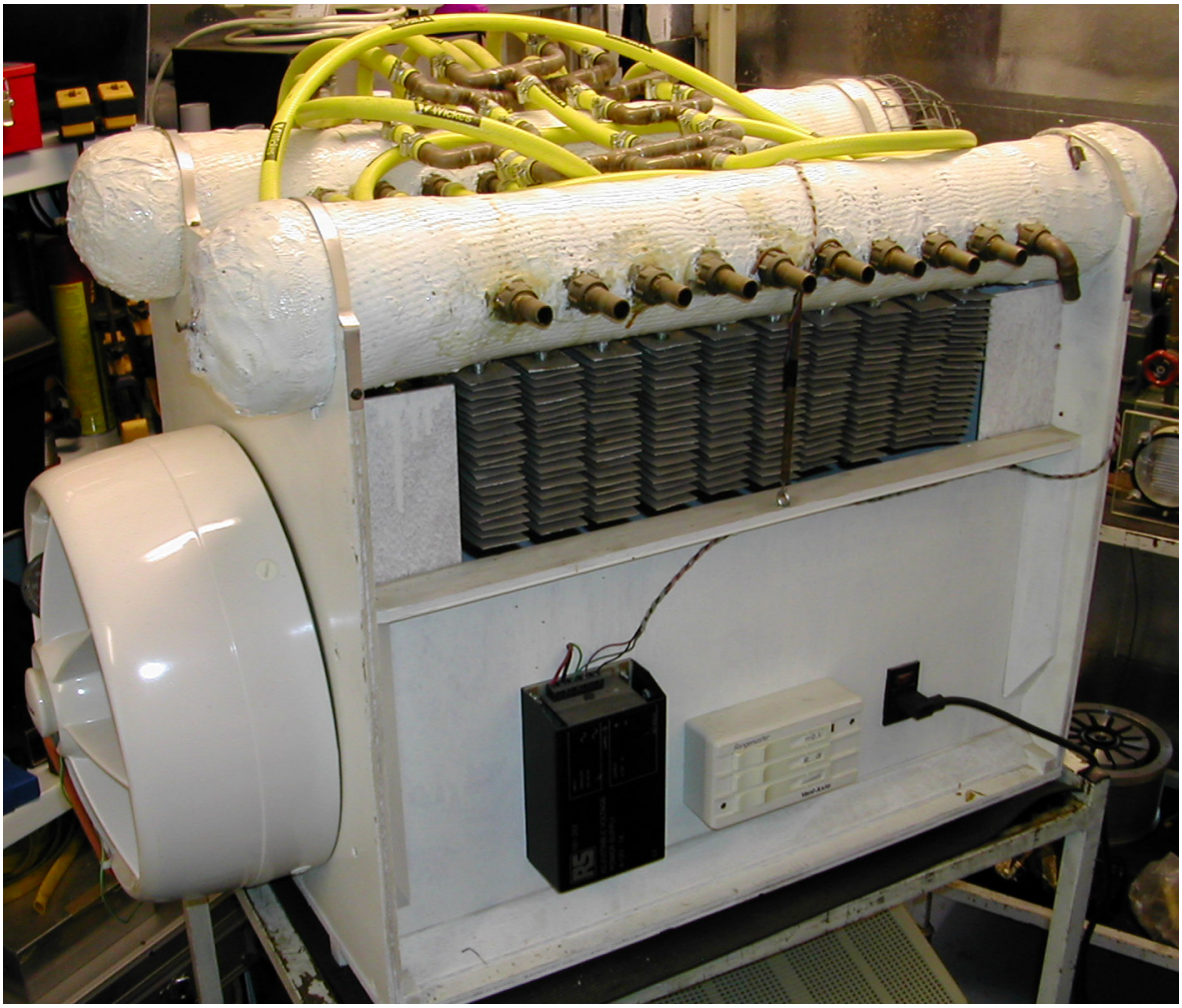

Fig 5.6 Heat Pipe Test Rig (Water Side)

The orientation of figure 5.6 is similar to that in the illustration of figure 5.5. None of the individual heat pipe connection are shown in Figure 5.5 but figure 5.6 shows the parallel inlet manifold partially connected on the ethanol side (left hand side looking from the fan end) and resting on the top.

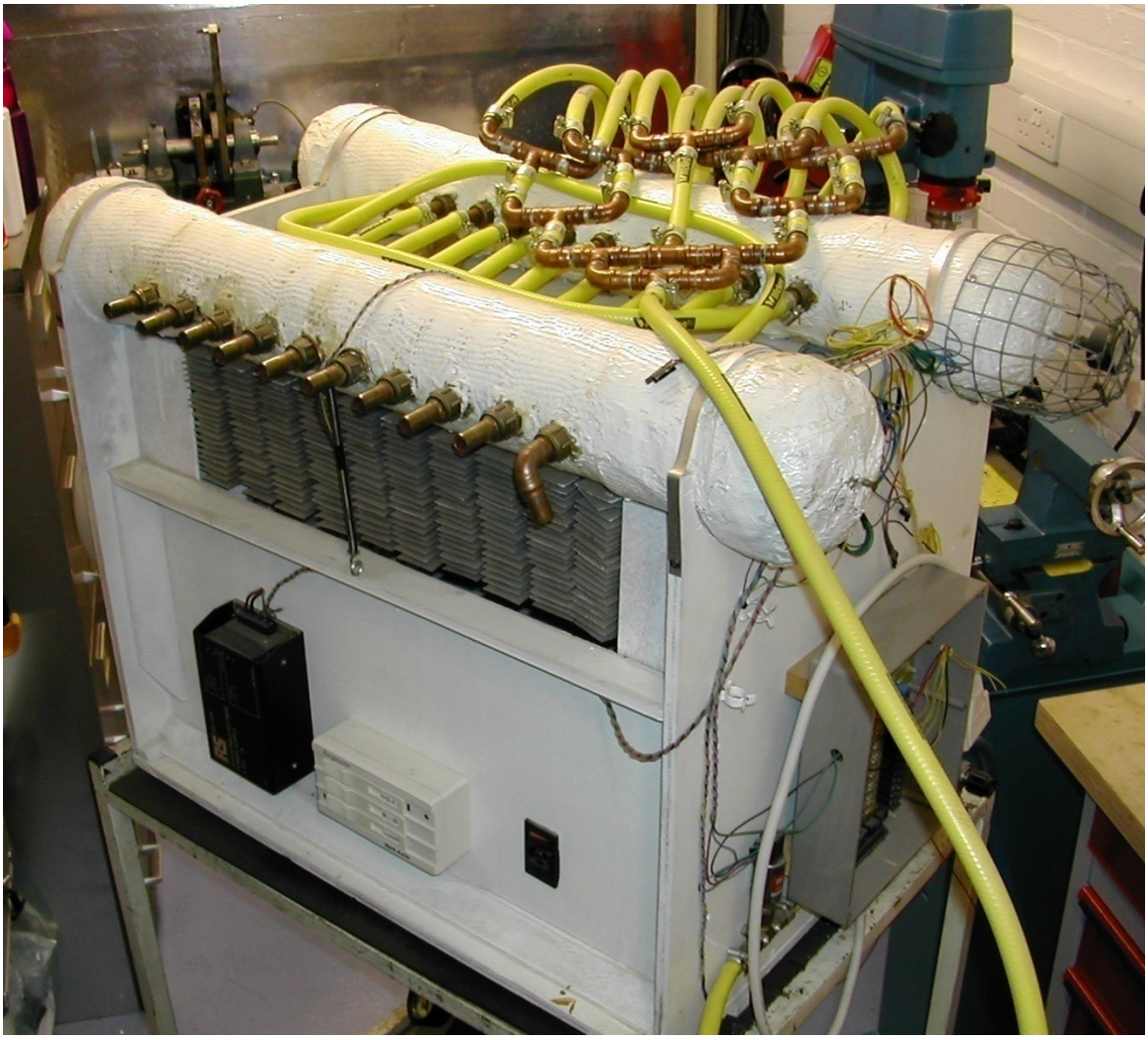

Figure 5.7 Heat Pipe Test Rig (Water Side Rear View)

Figure 5.7 is of the same side as figure 5.6 but affords a better view of the parallel inlet manifold and the parallel ethanol to water HX connections. On the rear panel is mounted the sensor connection panel that allows onward connection to the computer mounted data acquisition board.

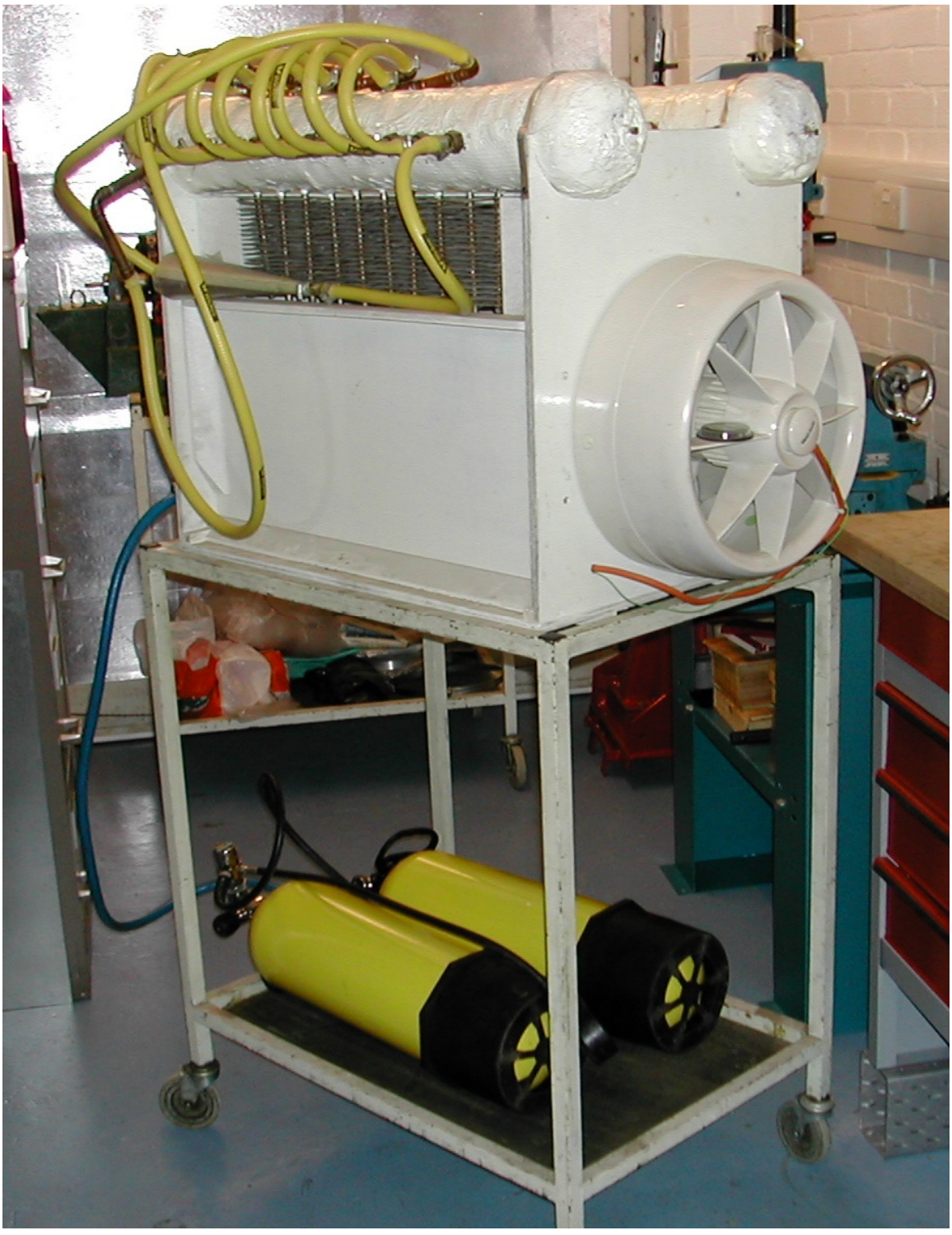

Figure 5.8 Heat Pipe Test Rig (Ethanol Side View)

The 12 litre 30 MPa storage cylinders are shown on the lower shelf of the rig's trolley.

5.4.1 Manifold Design and Construction

The heat pipe manifolds have the heat pipe condensers, with fins, contained within a pressure tight tube. The compressed air flow can only be directed across the tube over an individual heat pipe. Each heat pipe occupies a separate compartment, with its own inlet and outlet, and is separated from its adjoining heat pipe compartments by an aluminium disc. In order to prevent a damaging build up of pressure the disc is not pressure tight but does ensure that the majority of the compressed air flows across the heat pipe rather than along the tube. This can be more clearly understood from figures 5.9 & 5.10.

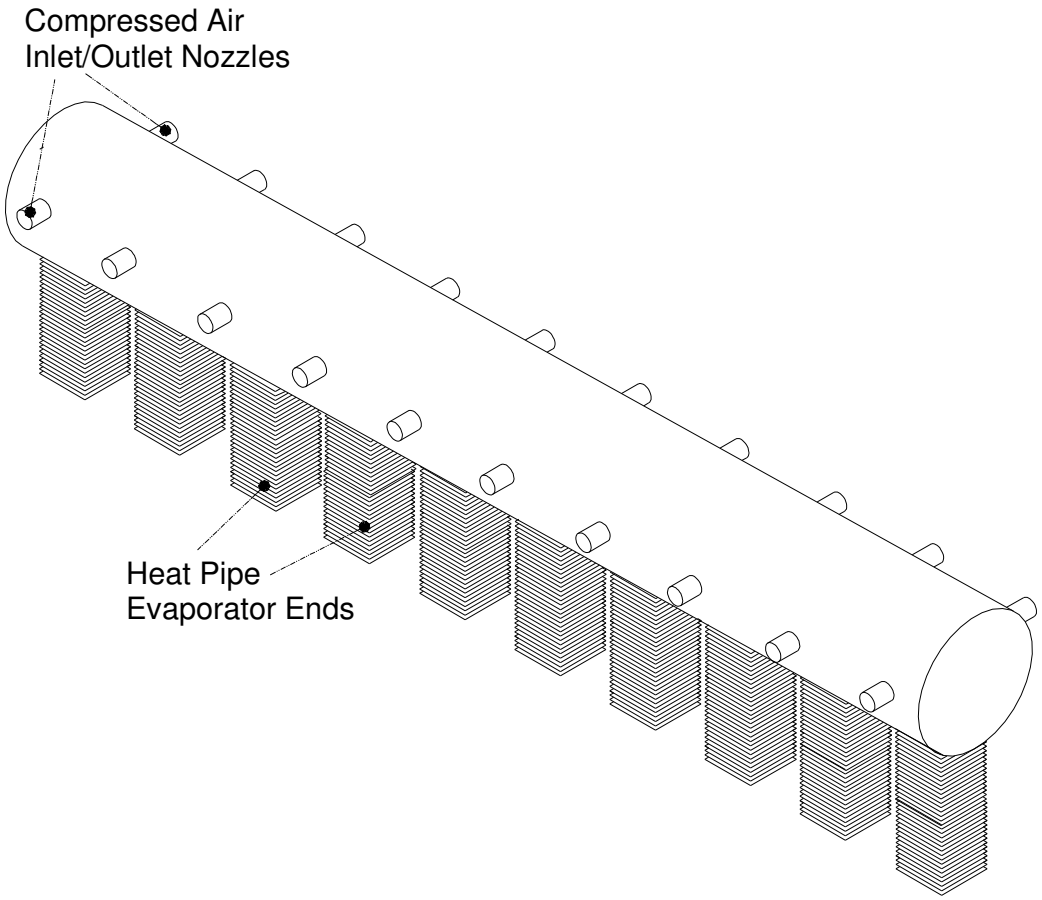

Figure 5.9 Heat Pipe Manifold

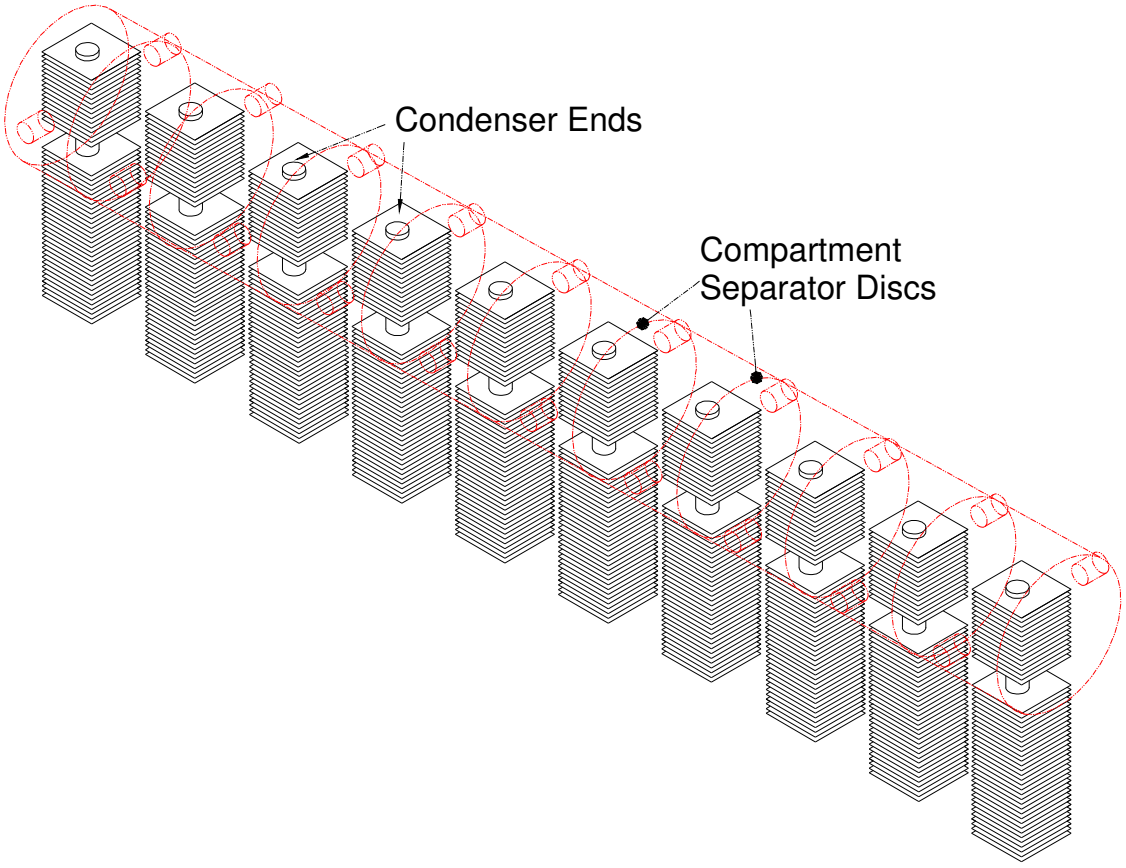

Figure 5.10 Heat Pipe manifold (with hidden detail)

In these illustrations the manifolds are flat ended whilst figures 5.5 to 5.8 show the ends as domed. The interiors of the manifolds are flat ended but this is not a good shape for the even distribution of stress in the reinforcing glass fibre epoxy. If the reinforcement had to turn through a 90° angle and then act as a thin beam, it is likely that, under pressure, some distortion would take place and some leakage would have been equally likely. To obviate this, the tubes were fitted with solid domed ends, made from MDF, which would act as thick beams. The applied reinforcement would now only have to secure the domed beams in position and would have no high stress areas.

Whilst the design is straightforward, the construction of a leak free manifold was quite demanding. The heat pipe manifolds were based on 100mm internal diameter PVC piping into which the heat pipes were fitted, after the fins were fitted to the heat pipes.

The process of fitting was as follows:-

1. A longitudinal line of 10 x 10 mm holes were drilled along the tube at 50mm intervals.
2. Directly opposite each 10mm hole a small (3mm) hole was drilled through the pipe wall and countersunk on the outer face.
3. If the small hole is considered as the 12 o'clock position and the 10mm hole as the 6 o'clock position, at the 3 & 9 o'clock positions further holes were drilled to receive the threaded ends of brass 15mm plumbing compression fittings which were to serve as inlet and outlet connections.
4. A thin straight knife cut was made along the line of the holes, so that the PVC pipe could be opened sufficiently to allow the heat pipe body to be slid into position. A 10mm unfinned gap had been left between the fins of the evaporator section and those of the condenser in order that the body of the heat pipe could be inserted in this fashion.
5. Before the heat pipes were positioned a circular wooden "shoe" with a 10mm circular hole, to match the heat pipe end, was screwed and glued to the pvc pipe at the 12 o'clock position. This was to provide a "locating" position for the heat pipe whilst it was being fitted.
6. Before the heat pipes were positioned the brass plumbing inlet and outlet fittings, which were to serve as the inlet and outlet connectors, were screwed

into their holes at the 3 & 9 o'clock positions, and secured with epoxy filler. The distribution baffle, described later, was also positioned at this stage.

7. Starting from the middle, each heat pipe was slid into place and glued into its locating shoe. After each heat pipe was positioned, its compartment separator disc was positioned.
8. Once the final heat pipe and separator disc were in place, the longitudinal slit and holes were coated in epoxy resin and allowed to close and left to cure for 24 hrs. At the same time the solid MDF domed ends were fixed in place in place also using epoxy resin.
9. Once the epoxy had cured, heavy duty tapes of woven glass fibre, impregnated with epoxy resin, were wound onto the pipe and worked into all potential leak sites. This was done in several stages and built up to approximately 4mm thickness overall. Again the assembly was allowed to cure for several days before further work was done.
10. The manifold openings were now sealed and the manifold brought, slowly, up to the working pressure of 1MPa. A number of leaks were identified and located. These were dealt with by injecting thin epoxy resin, using a syringe and narrow diameter PVC tubing passed through an inlet/outlet, into the leak area. With the manifold positioned so that the leak area was at a low point, the manifold was then repressurised for a short period. The expectation was that the pressure would drive the resin into the leak and block it. Most of the leaks were around the heat pipe body and the brass fittings and easily found. Most leaks were found and sealed but, inevitably, some remained.

5.4.2 Compressed Air Distribution Across The Condensers

Both the inlet and outlet fittings are based on the same 15mm brass plumbing fittings but the inlets have been modified to improve the distribution of the compressed air across the fins of the evaporator. Some early tests, using "chimney test smoke pellets" had shown that the air exiting, at atmospheric pressure, from the unmodified fitting formed a tight jet. Such a jet would have concentrated the air on a small section of the evaporator and its fins reducing the rate of heat transfer. This jet effect was reduced by machining a diffuser section into the interior end of the fitting but the scope for modification was limited so it was necessary to add baffles that would increase the air distribution further. Also, as air density and viscosity increase with pressure, it was unlikely that the modifications would have the same effect at the air speeds and pressures that would apply inside the manifolds. As this effect could reduce the effectiveness of the HX manifold it was decided to test the inlet geometries more rigorously.

5.4.2.1 Compressed Air Distribution Test Rig

An analogue of the interior of a single heat pipe chamber was constructed in a form that allowed different patterns inlets and distribution baffles to be tested, at high pressure, and the flow visualised.

Flow visualisation, at 1MPa, presented a number of difficulties. Conventionally, some form of smoke generation is used within the system but, at 1 MPa, the oxygen density is sufficient to achieve stoichiometric combustion. Several attempts were made using various types of smoke pellet but these burnt rapidly and without smoke. Other systems such as dry ice, glycol fogs and mineral oil aerosols were considered

but these are very pressure dependant methods that were not reliable at pressures greater than atmospheric. Also the additional equipment cost made them unattractive until other methods had been tried. Finally, it was found that injecting talcum powder into the compressed air stream provided a reliable method albeit for only a short period of 20 seconds. A schematic of the Diffuser Test Rig is shown in Figure 5.11 and a partial wire frame drawing of the test chamber is shown in figure 5.12.

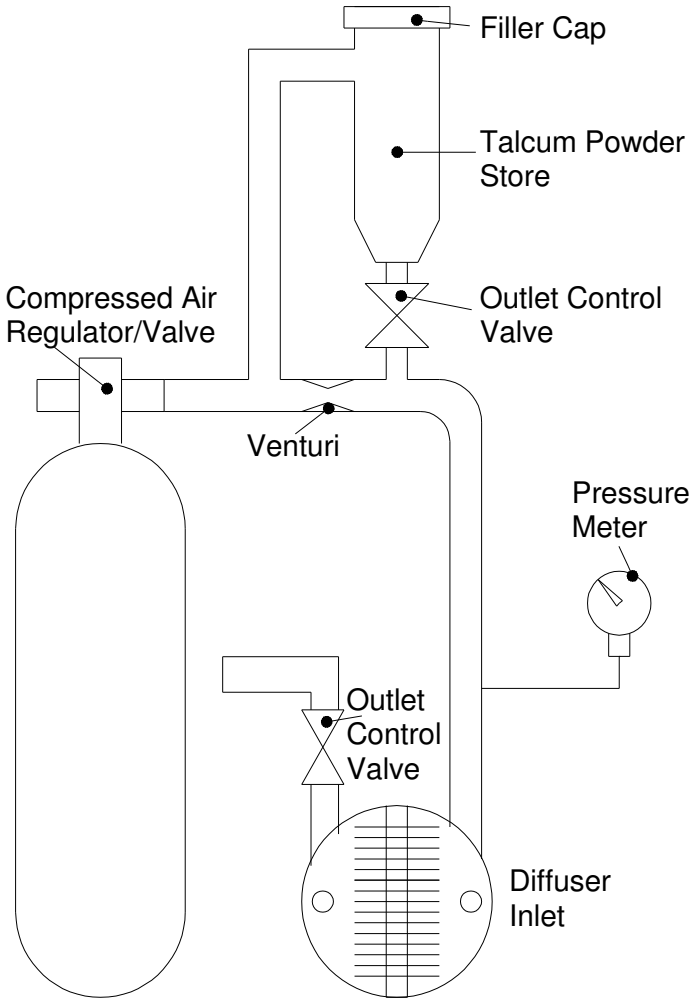

Figure 5.11 Diffuser Test Rig Schematic

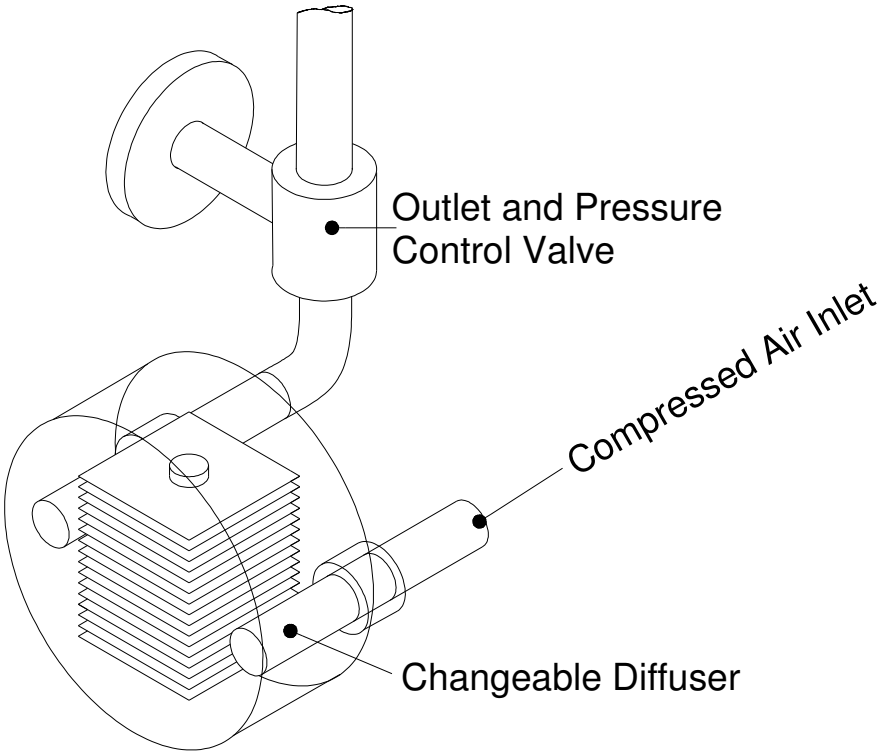

Figure 5.12 Diffuser Test Chamber

The inlet and outlet pass through a transparent endplate that seals the test chamber. This path was necessary as the short length of PVC tubing was prone to cracking when the large holes for the brass fittings were drilled in it. A piece of aluminium plate was rolled into a similar tube shape but its thin edge proved too difficult to seal at this pressure. As this design allowed the diffuser to be placed close to the tube wall there seemed to be no reduction in the accuracy of representing the real chamber, so it was adopted for the moment. The design also allowed easy changing of the diffuser.

In operation, the supply of talcum powder is placed in a store at high level. The store is at equal pressure to the compressed air outlet but the outlet from the store is at a

slightly lower pressure as it is downstream of a venturi restriction. Once a stable system pressure is established, the talcum powder store outlet valve is gradually opened and the higher pressure of the store drives the talcum into the air stream at a rate controlled by the valve. Although the flow doesn't photograph well it is stable and readily visible to the unaided eye. The store only contains enough talcum for approximately 20 seconds of operation but this is enough to get a clear idea of the flow patterns. Also longer operation would have resulted in increased build up of residual talcum in the test chamber. Most of the talcum passed through the test chamber and was captured, for re-use, in a small bin, but a small amount attached itself to the fin surfaces and needed to be cleaned out before the next test run. These were considered as useful because significant build ups were a record of areas of flow stagnation.

The air mass flow wasn't measured as it was found that the anemometer turbine was too delicate an instrument for this test. In some early tests the talcum powder contaminated the turbine, and the turbine bearings area, resulting in inaccurate readings. It was possible to blow the bearings clean, using the compressed air, and the anemometer readings returned to the pre-contamination levels, but it was clear that this meter would not be trustworthy in this context.

Photographs of the actual test chamber are shown in Figures 5.13 to 5.15.

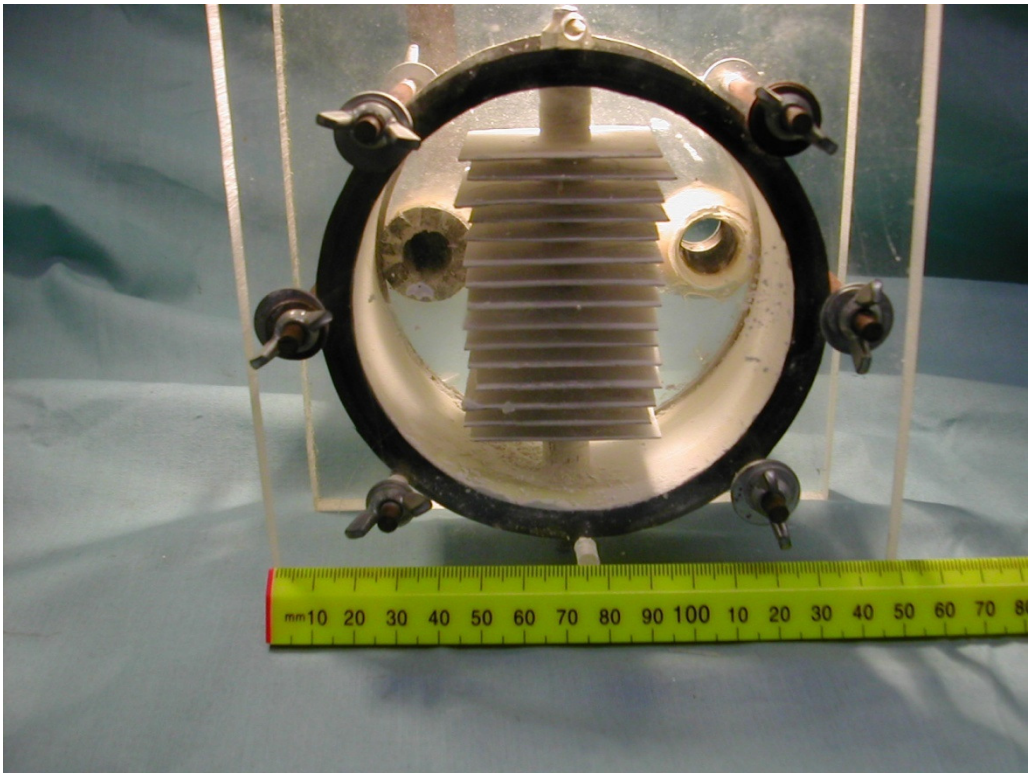

Figure 5.13 Diffuser Test Chamber (Front View)

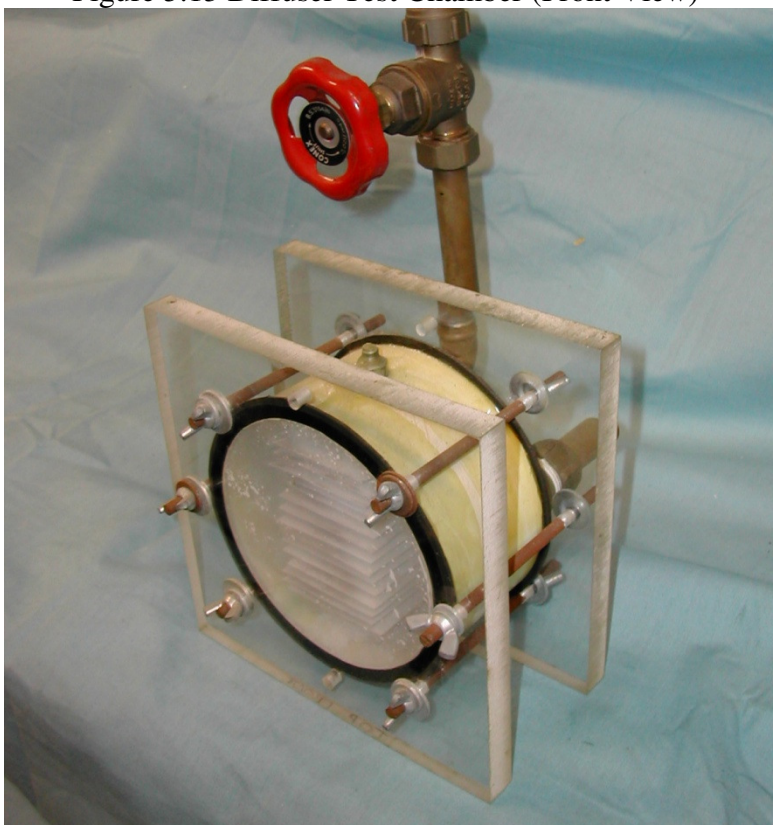

Figure 5.14 Diffuser Test Chamber (Side View)

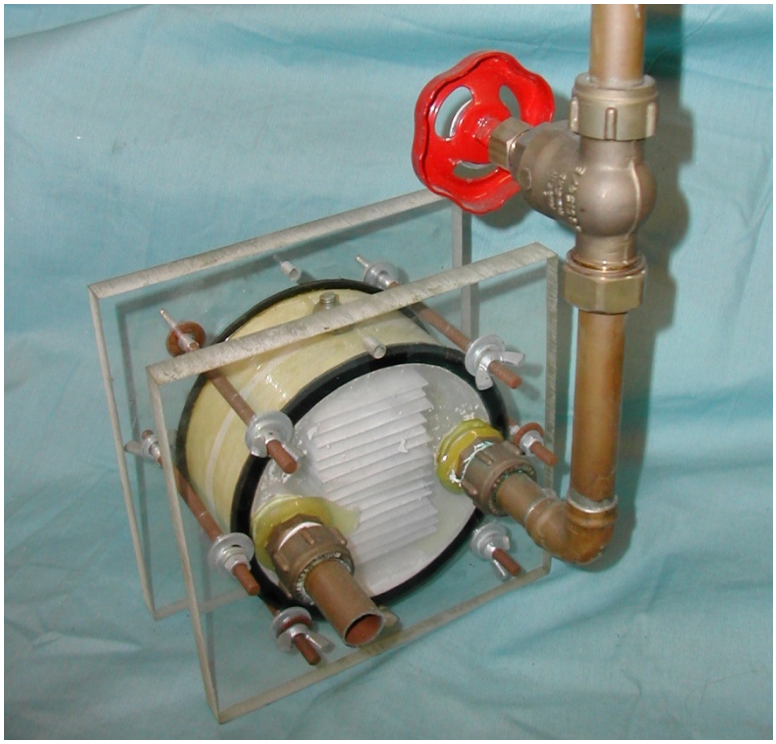

Figure 5.15 Diffuser Test Chamber (Rear View)

5.4.2.2 Diffuser Tests and Results

A digital camera was used to record the flow patterns but it was of low resolution and so all patterns were also recorded by hand drawing the patterns on a pre-drawn representation of the heat pipe fins. All flow patterns were reasonably clear, to the eye, and this indicates a laminar flow in most areas. This was unexpected as many "cloudy" areas of turbulent flow were thought likely. This is probably due to the increased viscosity of air at this pressure. All of the tested diffuser patterns left a thin layer of talcum on most surfaces. Only the significant build-ups of talcum, that were thicker than normal layers, were noted in the recordings of the flow patterns.

Various combinations of inlet shapes and baffles were tested and some are shown in figure 5.16. However, only the flow patterns associated with the basic circular inlet diffuser and the V shaped baffled diffuser (the design that was finally used) are shown here in figure 5.17.

cross T double outlet diffuser – top

+ shaped outlet diffuser – 2nd from top

simple circular hole diffuser – 3rd from top

V-shaped baffle and circular hole diffuser – bottom

Figure 5.16 Diffuser Test Pieces

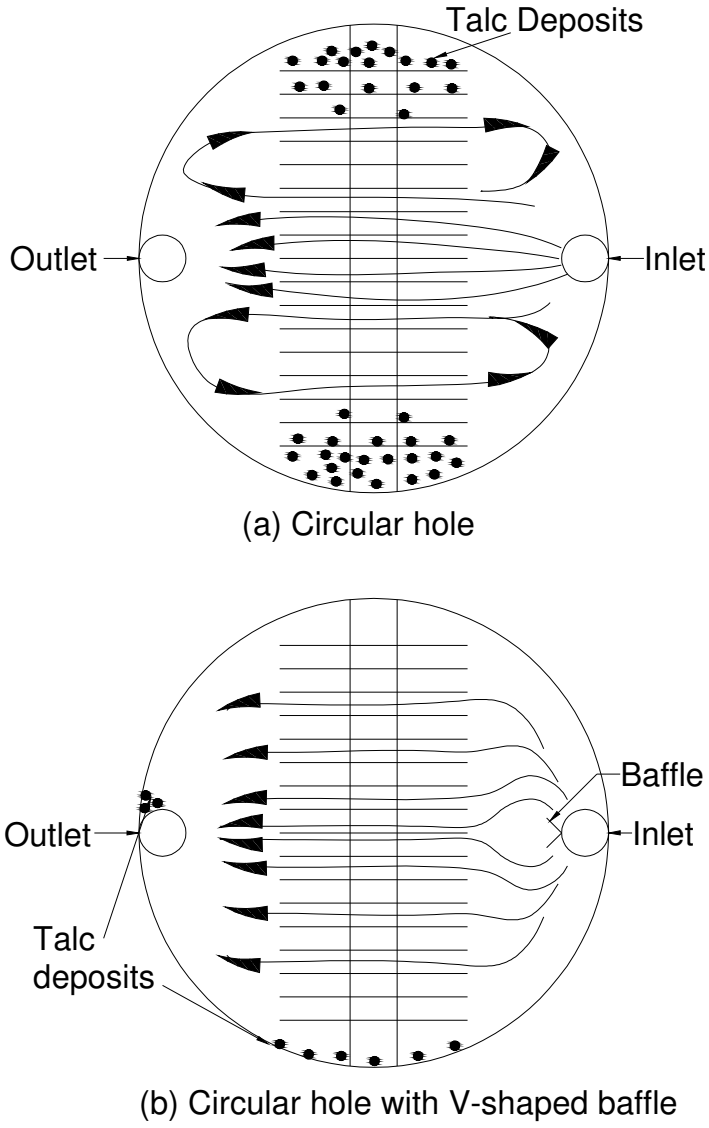

Figure 5.17 Diffuser Flows

The simple circular hole would probably be acceptable and certainly wasn't the worst of the patterns tested. As can be seen from figure 5.16(a) there were eddy patterns present above and below the main jet. There may have been a substantial mass exchange and heat flow between the main jet and these eddies but it wasn't possible to identify this with this equipment. However, this diffuser did leave

substantial deposits of talcum on the uppermost and lowermost fins, indicating that the air flow had slowed to the point of stagnation in these areas.

The chosen design was a V section plate mounted transversely across the inlet with the apex of the V facing into the flow as in figure 5.18 and the bottom test piece in figure 5.16.

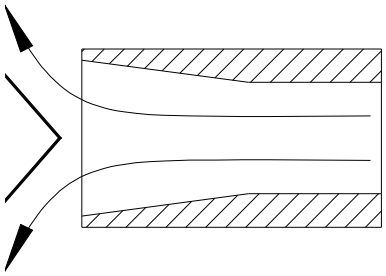

Figure 5.18 V Shaped Inlet Baffle

The included angle of the V is approximately 90° and this effectively creates two upwardly and downwardly angled diffusers. This gave rise to the pattern shown in figure 5.17(b). The flow lines shown were not as clear as shown in this drawing except for the, probable, low pressure area immediately downstream to the left of the baffle. The initial flows formed two rather diffuse fan like patterns. The re-combining of the flows along the centre line probably results from the pressure of the fans increasing as the flow speed drops immediately after they leave the diffuser. Some thick deposits of talcum did occur, at the rear of the outlet pipe and at the bottom of the test chamber, but none occurred on the fins. At the time this was taken as indicating a clean flow through all the finning, although such a flow, through the uppermost and lowermost fins, wasn't obviously visible. An alternative explanation is that no air flow was reaching those areas. This seems unlikely but could have been

tested for by placing “telltale” hanging fibres in these areas. The deflection of those fibres would have indicated a flow even if there were no talcum particles visible. However, this wasn’t done and that omission will have to be dealt with at a later date. This uncertainty notwithstanding, this design gave the widest and smoothest flow pattern of the baffles tested and was used with all the inlet diffusers.

One final point to note is that a very similar air flow pattern was achieved with a flat plate design, similarly place across the flow from the diffuser. Although this was a simpler design it wasn’t adopted as it was judged that it would have inferior mass flow characteristics compared to the V shaped baffle. This judgement wasn’t tested as there were no mass flow measurements taken. However, because the V shaped baffle would be very unlikely to exhibit mass flow characteristics inferior to the flat plate it was judged to be the safest decision for a small cost in extra construction effort.

5.5 Experiment Protocols and Results

5.5.1 Data Acquisition

Apart from the air flow sensor, which was constructed from a handheld anemometer, all temperature and pressure readings were to be taken and recorded by a PC based data acquisition system purchased from National Instruments. This was a PCL-818LS PCI card with 16 single ended channels. The temperature sensors were proprietary brand thermistors from RS Components driven by a 10V high quality stabilised power supply. The data acquisition software was Advantech Genie, also supplied by National Instruments.

Regrettably, for unknown reasons this system was never reliable enough to use. All the components seemed to work well enough but the thermistor readings would not settle into a stable output. With no compressed air flowing the temperature readings fluctuated by ± 4 or 5°C. The power supply was tested on an oscilloscope and found to be stable, as was the output from the thermistors. The PCI card was moved to a different slot and eventually to a different computer without improvement. The whole PCl-818LS system was returned to National Instruments for testing. They declared it as "working to specification".

5.5.1.2 Digital Thermometer and Thermocouples Accuracy

At this stage it was decided to put the automated data acquisition system to one side and proceed with a system of hand held digital thermometers and manual recording of data. A Kane-May 2 probe digital thermometer was already in use and a similar instrument, from the same manufacturer, was obtained. Both used thermocouples and the manufacturer's literature claimed an accuracy ± 2°C. However, the output readings could be user calibrated and this was done using melting ice as the standard. When checked against boiling water a reading of 100°C was obtained. Despite these readings an accuracy of ± 1°C has been assumed.

5.5.1.3 Anemometer Air Flow Meter Accuracy

The anemometer based air flow meter used a smoothly conical "trumpet" section to blend the compressed air outlet diameter up to the diameter of the anemometer turbine housing reducing the risk of anomalous higher speed jets causing inaccurate readings. The anemometer's manufacturer claimed an accuracy of ±3% ± 2 digits of

its full range (0.8 -30.0 m/s, res. 0.1 m/s) which corresponds to ±0.8 m/s over its range. As no standard air speed was available to check this, an attempt was made to check it by other means. The purpose of this meter was to measure the mass flow of air the total mass of which was limited by the storage capacity of the compressed air cylinders. The compressed air cylinders had a volumetric capacity of 12 litres of air at a pressure of 30MPa and a density of 314.03 kg/m^3. This was 3.77kg. The test was to run the compressed air, at a stable air speed, for a measured period. The mass flow would be the air speed times the cross sectional area (CSA) of the turbine times the density of air at sea level pressure. It was reasoned that the longer the duration of the test the less effect transient variations would have on the calculation. So a low air speed was desirable as was one with few digits making reading the meter reading easier. For these reasons 3.0 m/s was chosen as a target air speed. The open CSA was measured as 0.002m^2. This was the inside diameter of the turbine housing excluding the area of the central bearing and its three support arms.

At 1.0m/s the volume flow would be 2l/s

Air density at ambient pressure is 1.16g/l

$\therefore$ at 1m/s the mass flow should be 2.32 g/s and at 3.0 m/s it is 6.96 g/s

The cylinder had been weighed at 16.5 kg when empty. A spring balance was used for this. The same spring balance used for measuring the dynamometer torque in chapter 7. The cylinders are usually overfilled so some air is bled off, whilst the cylinder is hanging from the spring balance, until the total filled weight was 20.27 kg. Then the system was run for 540 seconds at 3.0m/s which equates to a total mass flow of 3.758 kg. 3.758/3.77 = 99.68% - an accuracy of -0.3%. The true accuracy

is not as good as this would imply. The air speed was set by manually adjusting the outlet valve, and timing only began once the air speed was approximately stable. This was hard to measure but was approximately 15 seconds. Also timing stopped shortly after the air pressure fell below that needed to sustain the required air speed of 3.0 m/s but air continued to flow at a reducing rate until the cylinder was exhausted. Again this was hard to measure but was approximately 20 seconds. In an attempt to estimate this mass flow it is reasonable to say that the flow gradually rose from zero to 3.0 m/s in 15 seconds and at the end fell from 3.0 m/s to zero in 20 seconds. Whilst the period is not known accurately it can be conservatively estimated at a total of approximately 50 seconds in which the air speed averaged 1.5 m/s, equivalent to a further 25 seconds at 3.0 m/s. This would put an upper estimate of the total mass flow as 565 seconds at 3.0 m/s = 3.932 kg. 3.932/3.77 = 104.3%. It now appears that the anemometer based system overestimates the mass flow by 4.3%.

A similar analysis to that above was attempted for higher mass flow rates. Once the flow rates were significantly higher (11 – 20 g/s) the analysis proved problematic as the "lower than nominal flow rate" periods become a larger proportion of the overall test period which fell to a minimum of 3.5 minutes. It was also clear that the anemometer was reading a reduced overall mass flow even with the above approximations applied to the initial and final flow periods. It would seem that the anemometer has a reducing response to air flow speeds, reading high at low speeds and gradually moving to a low reading at high speeds. The inaccuracy seems to be approximately symmetrical around a minimum at 12 – 14 g/s with an under reading

of 4-5% at 21 g/s. However, that would be hard to be more precise than that with the current equipment.

The only remaining issue is the question of how accurate was the spring balance used for the initial weighing of the compressed air bottles. The major accuracy issue was in the reading of the dial which was graduated in Newtons. The dial had a range of 0-200 N graduated in 1N increments. It was therefore necessary to translate from Newtons into kg. The spring balance has a reading adjustment control and this allowed the reading to be calibrated. Using a standard calibration weight of 5kg, the spring balance was adjusted to read 49 Newtons (9.81 N = 1kg). Several weighing tests have shown that the reading does not alter over time or with small changes in temperature, assuming the adjustment control has not been disturbed. Once the pointer has stabilised a reading accuracy of 1 N is practical and the reading is appears to be very accurate in that it is highly repeatable. The accuracy of reading is ±1 N = 0.1 kg. Applying this to the calculated value of 3.77kg for the mass of stored air gives a range of 3.77 ±0.1 kg (3.67 – 3.87kg). This would change the accuracy of the air flow meter readings to a range of between 95% and 105%.

It would seem that the air flow measurements are accurate to a value of the order of ±5% which can be regarded as reasonably accurate for the purposes of the current project. For this reason the measurements and calculations reported will be the actual values measured without any correction factor applied. The range of uncertainties will be noted on the graphs by the use of error bars.

5.5.2 Results

The results reported here are all for a set of given conditions, although it is possible to test the rig over a whole range of inlet and outlet pressures, temperatures and mass flow rates. The conditions chosen are for an initial compressed air storage pressure of 300 bar, entry pressure to the heat exchangers of 6 bar, atmospheric air temperature at entry to the heat exchanger of 20°C, and atmospheric air speed across the heat pipe evaporator of 2m/s. The primary variable is the mass flow rate of the compressed air, in grams per second, passing over the heat pipe condensers within the tubular casing (effectively its velocity variation), and the connection arrangement (series or parallel) for the heat pipes themselves. The measurable output is the energy gain in Watts, of the air flow, as it leaves the heat exchangers (the product of the heat capacity rate and the temperature rise of the compressed air). Thus the results reported here are the final readings of each test being the maximum rate of heat gain achieved in these conditions.

No attempt has been made to calculate the total energy gain for the total mass flow. This is not particularly interesting as much of the early part of each test is confounded by the compressed air absorbing heat from the mass of the system, its thermal inertia. The purpose of these tests is to ascertain the performance of the heat pipe once the compressed air has reached its lowest temperature. Each compressed air cylinder allows for ten minutes of testing which is sufficient time to achieve stable values. Heat flow into the system through the walls of the storage cylinder, connecting pipes and inlet manifold would also warm the air before it reaches the heat pipes, further reducing the temperature gradient across the heat pipes. Whilst desirable in a working vehicle in these tests it reduces the extremes against which the

heat pipes are tested. To reduce this effect all cold pipes and surfaces, other than the heat pipes, are insulated by lagging.

5.5.2.1 Series Connection

A schematic of the heat pipes, connected in series, is shown in Figure 5.19.

A summary of the results is presented in Table 5.3 and graphically in Figure 5.20.

Each one of the readings shown are the average result of at least three experiments. However, all of the runs returned extremely similar results indicating a high level of repeatability of the experiments.

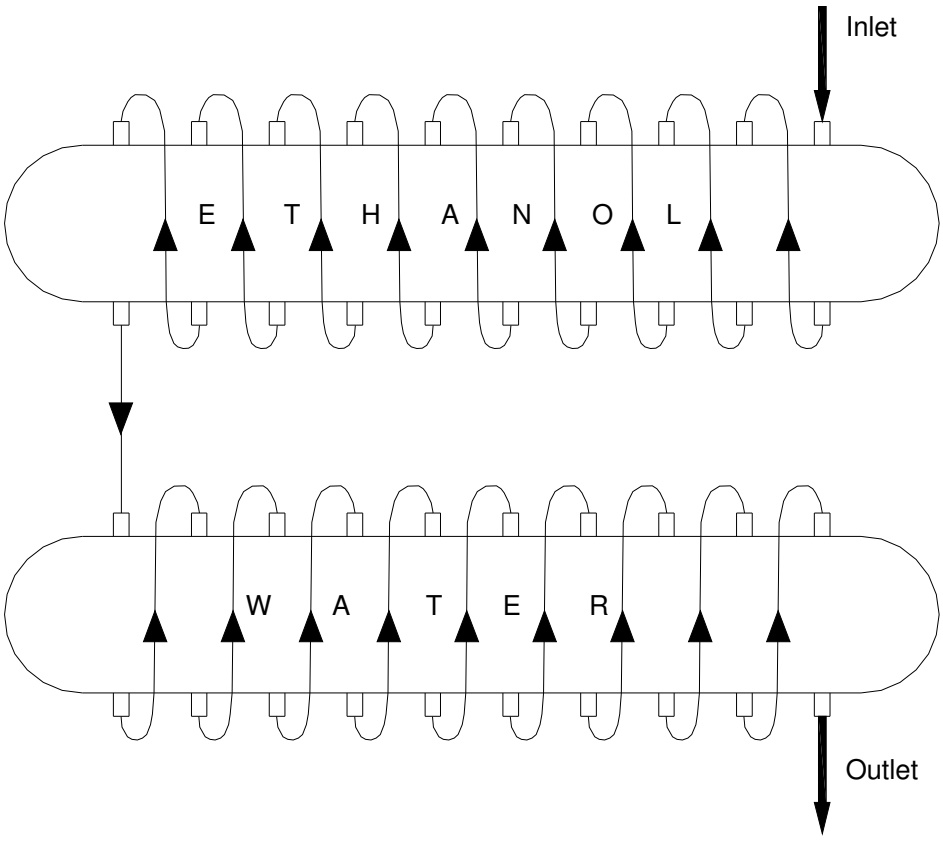

Figure 5.19 Schematic of Series Connections

Table 5.3 Energy Gain for Range of Pressurised Air Flows (series connection)

Flow Rate of Pressurised Air (g/s)	Temperature at Inlet to Ethanol Manifold (°C)	Temperature Between Heat Exchangers (°C)	Temperature at Exit from Water HP Manifold (°C)	Energy Gain Rate (Watts)
7.0	-27	17	20	332
8.6	-29	14	20	427
11.4	-33	12	19	609
13.9	-36	10	18	758
20.1	-38	9	17	1127

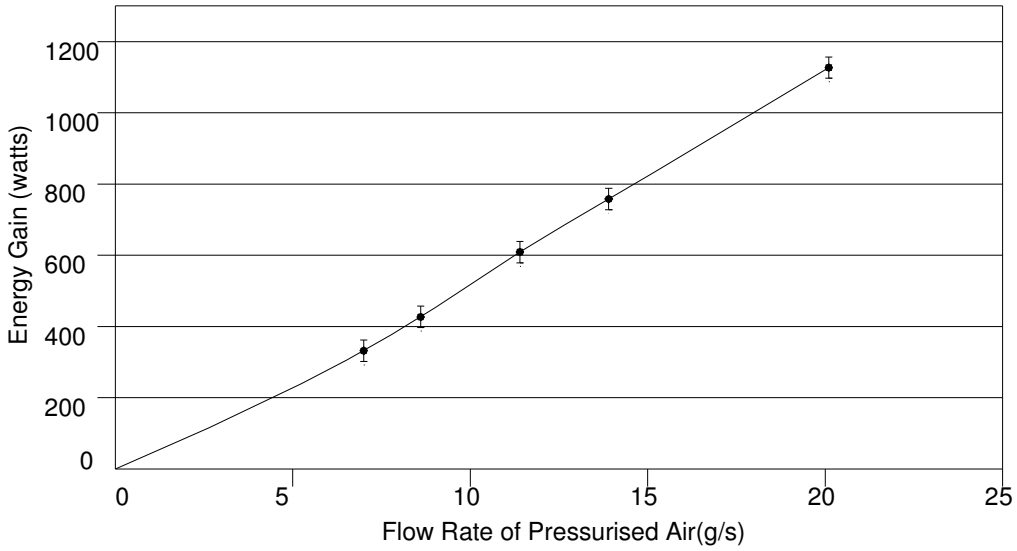

Figure 5.20 Graph of Table 5.3 Results

The implication of Fig 5.20 is that the greater the air flow through the heat exchangers, the greater is the energy gain, perhaps unsurprisingly, and that the relationship between the two variables is a reasonably linear one. In fact a better straight line is obtained if the origin is ignored as in figure 5.21. Here the extension, of the results straight line, now passes through the X axis at the 1.5 g/s point. A possible explanation is that the air flow sensor is consistently under reading by about 1%. However, as noted in 5.5.1.2 above, the anemometer is more likely to be over reading the flow. Alternatively, it is possible that the graph is not linear at very low flow rates

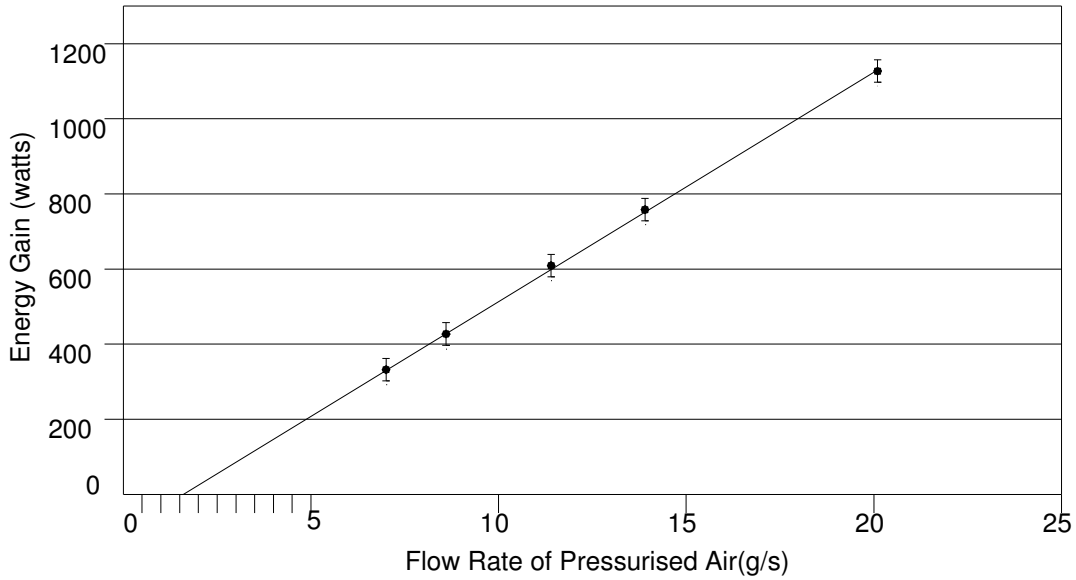

Figure 5.21 True Straight Line Graph of Table 5.3 Results

due to thermal effects. Assuming the anemometer is accurate, the most likely explanation is that 1.5 g/s, or more, is bypassing the heat pipes but is reaching the anemometer. The only path by which this is likely is around the edges of the aluminium discs used to separate the heat pipe compartments. These were not sealed as it was thought that if a pressure difference built up, between compartments, some irreparable damage might be done. It is possible that there is a leakage of approximately 1.5 g/s along the edges of these compartments. If this is the case it is only a problem for the test rig with separate compartments and not for a practical vehicle HX. It is not possible to clarify this point, at the moment, as it is difficult to achieve stable conditions, at very low flows, with the present test rig. It might be possible to pressurise the manifolds whilst all inlet and outlets, except the endmost connections, are blocked, and to test for a flow. The risk of damage still remains and this will not be attempted until all other test runs have been completed.

5.5.2.2 Parallel Connection

A schematic of the heat pipes, connected in parallel, is shown in Figure 5.22. The rather complex inlet manifold was designed to distribute compressed air equally to all 10 individual heat pipe inlets. Earlier, simpler, designs were inadequate in this respect. A summary of the results is presented in Table 5.4 and graphically in Figure 5.23. Again, the readings are an average of at least three runs. Given the linear trend displayed in Fig 5.21, for series connection, only higher mass flow rates are presented for parallel flow because they are more relevant to a practical application.

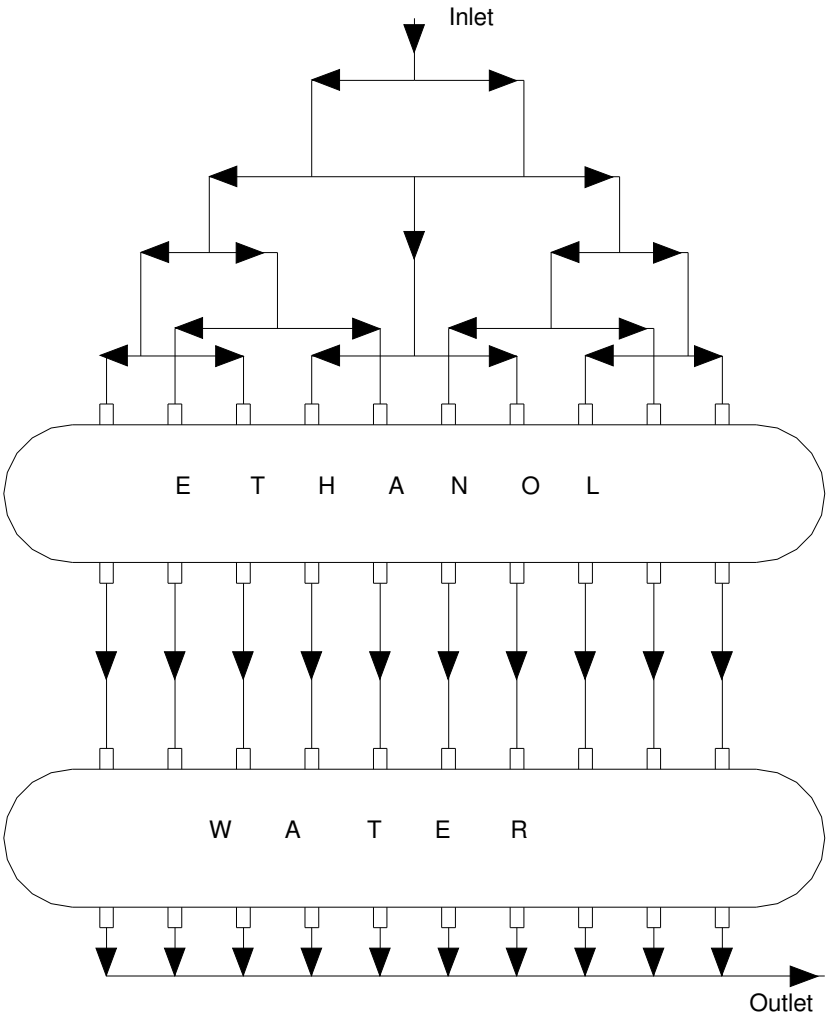

Figure 5.22 Schematic of Parallel Heat Pipe Connections

Table 5.4 Results of Parallel Connections Tests

Flow Rate of Pressurised Air (g/s)	Temperature at Inlet to Ethanol HP Manifold (°C)	Temperature at Exit from Ethanol HP Manifold (°C)	Temperature at Exit from Water HP Manifold (°C)	Energy Gain Rate (Watts)
18.5	-29	5	15	822
19.7	-33	8	15	955
20.2	-35	10	15	1010
20.9	-36	11	15	1080
21.1	-36	11	15	1114

Note. One of the tests at 20.9 g/s was accidentally carried out without the ambient air fan switched on. The tests are noisy and the omission was only noticed at the end of the test. In all other respects the test was normal and yielded comparable results to the other tests at that flow speed. This indicates that this system is able to extract sufficient heat from the ambient air without a forced air flow, perhaps by generating a convective flow from the temperature difference.

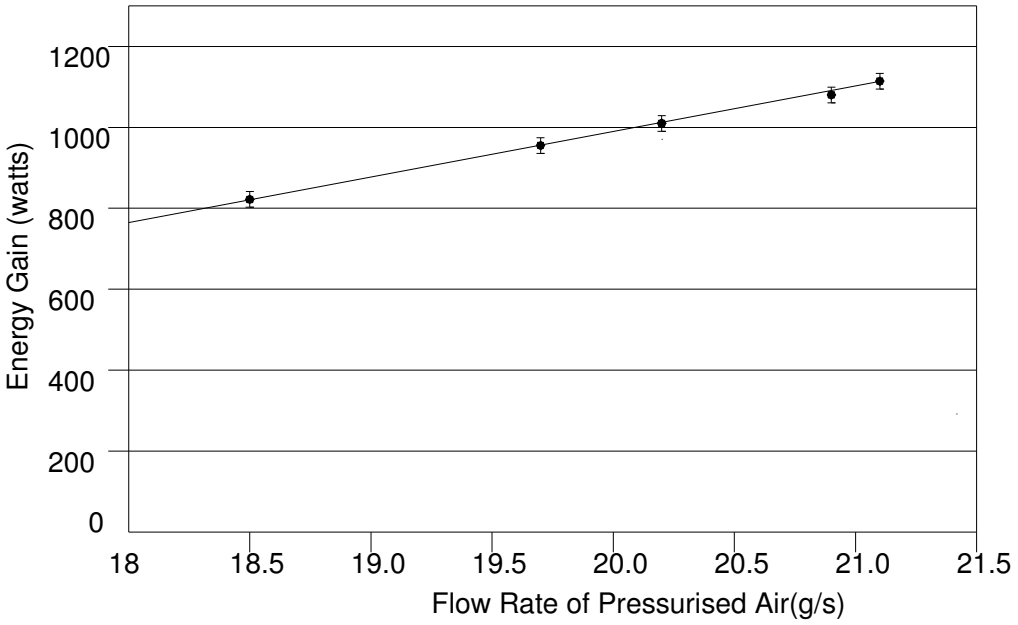

Figure 5.23 Graph of Table 5.4 Results

Again, the relationship exhibited between the flow rate of compressed air and the energy gain through the heat exchangers is linear. Generally speaking, this linearity of relationship is to be expected as, at these pressures, air is a reasonable approximation of an ideal gas. What is interesting is that such linearity is shown so clearly in these results despite the potential of many practical factors, (air leaks, fin arrangements and manual timing of data collection, etc.) to give rise to inaccuracies. This delivers confidence in the robustness and stability of the equipment and the repeatability of the results.

With regard to the question of the graph line not passing through the origin, with the parallel configuration all the adjoining chambers should be at similar pressures and leakage between chambers should have been reduced. Although not shown here, the problem has worsened with this configuration and the original “blow by” explanation is not supported.

The circumstances of this discrepancy suggest that compressed air is getting through the HX without being heated but it is remaining in the system until it leaves via the air flow sensor. It does not appear to be a simple leak. The “blow-by” explanation (going directly from inlet to outlet, bypassing the heat pipe) could work for a series configuration but should have been greatly reduced with all the compartments at a similar pressure. It seems that the compressed air is passing through the heat pipe compartment but a proportion of it is not being heated and there is some indication that the problem worsens with compressed air flow speed. The foregoing leads to the explanation that a proportion of the compressed air is passing through the HP fin array whilst experiencing little or no heat transfer.

The fabrication technique for the fin array prevented the fins from being closer than 5mm to each other and so it is possible that air passing through the middle of that space would receive little heat. The effect would increase with air flow speed and transverse distance from the heat pipe as the outer parts of the fin are cooler. It seems that the solution to this problem is to have the fin separation reduced. This solution will have to wait until the next iteration of this design.

5.5.2.3 Higher Flow Rates (parallel connections)

The flow rate, from the storage cylinder, is limited by the flow capacity of the pressure regulator. Therefore, it is not practical to increase the flow rate, of the compressed air, beyond the values achieved in tables 5.3 & 5.4. However, it is possible to explore the performance of the heat exchangers at higher flows by passing all of the available compressed air through one set (1 x ethanol & 1 x water) of heat pipes. Taking this approach, with the connection flowing from the ethanol to the water HP, the three results in table 5.5 are representative of what is achievable. This result should be read in conjunction with tables 5.3, 5.4 & 5.6. In table 5.4 a similar mass flow results in a maximum energy gain of 1114 watts which equates to a 13.8% energy gain. In this example the energy gain is only 10%, probably as a result of the reduced air to heat pipe contact time.

As there are ten heat pipes in each manifold, the “Equivalent” columns in table 5.5 (the last two) are the mass flow rate and energy gain multiplied by a factor of 10 to show the potential performance of the whole rig.

Table 5.5 Energy Gain from a Single Ethanol/Water Heat Pipe Set

Flow rate of Pressurised air (g/s)	Temperature at Inlet to Ethanol Manifold (°C)	Temperature at Exit from Water Manifold (°C)	Energy gain (Watts)	Equivalent Flow Rate for ten HP sets (g/s)	Equivalent Energy Gain (Watts)
18.1	-33	10	781	181	7810
19.5	-36	14	910	195	9100
21.1	-36	14	985	211	9850

The final column indicates that if the flow rate of 211g/s could be achieved then the HX could deliver an energy gain of nearly 10kW

5.5.2.4 Additional Small Tests

5.5.2.4.1 Two Ethanol Heat Pipes in Series

The parallel tests delivered a slightly worse performance than the series tests and the detail temperature measurements indicated that the bulk of the heat transfer was being achieved by the ethanol heat pipes. Two tests were carried out to see how two ethanol heat pipes compared to the 1x ethanol + 1x water arrangement and the results are in table 5.6 below.

Table 5.6 Two Ethanol Heat Pipes in Series - Results

Flow rate of Pressurised air (g/s)	Temperature at Inlet to 1st ethanol HP (°C)	Temperature at Outlet from 1st ethanol HP (°C)	Temperature at Outlet from 2nd ethanol HP (°C)
18.1	-36	10	10
19.5	-33	14	13

These results appear counter-intuitive and require some further explanation. The 18.1 g/s run was the second of two consecutive runs. The first of these runs used two adjoining ethanol HPs and provided results that appeared nonsensical in that the second HP/final outlet temperature was several degrees cooler than the middle

(1st HP outlet/2nd HP inlet) temperature. This seemed to require that the downstream HP be cooling the flow and this was not considered possible with this configuration. The only practical explanation was that a significant portion of the compressed air flow was bypassing one, or both, of the heat pipes. That is travelling directly from the first inlet to the final outlet, around the edges of the aluminium separator discs without receiving much heat transfer. The second run took place about 20 minutes later but this time using the two endmost heat pipes that were separated by eight intervening HP compartments. It was judged that any blow-by that took place would be limited by the greater number of barriers between the compartments and would also be partially warmed thus reducing the cooling effect.

The rig was still cool from the first run when the second run commenced and because of this progressed more quickly to the low temperatures shown. The third run took place several days later but still using the configuration of the second run. In both of those runs the second HP is still showing anomalous behaviour and it is presumed that cold air blow by is still a factor albeit much reduced in effect. The important information to take from these runs is that the bulk of the heating of the compressed air is being carried out by the first/upstream HP. This implies that a single ethanol HX can do most of the heating of the compressed air and that a second downstream HX (water or ethanol based) may be useful but is not essential.

5.5.2.4.2 High Humidity Low Temperature Test (parallel configuration)

The temperatures and humidity of the test laboratory were stable and comfortable and so humidity was not judged to be an important initial condition for the laboratory experiments. However, it was possible that at low temperatures and high humidity water could freeze on the HP evaporators so a test of the HXs response to these conditions was desirable. No environmental chambers were available so the test had to be delayed until the appropriate ambient conditions, essentially a cold foggy day, occurred in central London. This only occurred twice in the period of these tests and the results of the test, during the most extreme of those days, are shown in table 5.7.

Table 5.7 High Humidity Low Temperature Test Results

Flow rate of Pressurised air (g/s)	Temp. at Inlet to ethanol HP (°C)	Temp. at Outlet from ethanol HP (°C)	Temp. at Outlet from Water HP (°C)	Ambient Temp. (°C)	Humidity (%)
18.3	-45	-10	-3	5	98

The point of major interest is that although a great deal of condensation formed on the evaporator fins, during the six minute test, no frost formed. Possibly the enthalpy of evaporation/condensation prevented this and a longer test would have seen freezing take place although, channelling the condensate to drip off the fin would probably reduce or prevent that. Another interesting point is that although the water heat pipes were unlikely to be contributing much heat the temperature at the water HP outlet had risen 7K, from -10°C to -3°C. Even in the low pressure interior of the HP where would be little evaporation at those temperatures. If the heating was due to the water HPs they would be performing better than at higher temperatures. It is

more likely that that heating arose from the conversion of kinetic energy of turbulence to heat, but this would be difficult to test.

5.5.3 Discussion of Results

It should be remembered that the mass flow readings were only accurate to ±5% and the digital thermometer readings to ±1°C. This equates to a variation of ±7% in the final values which would commonly be considered a reasonable level of accuracy for this type of experiment. As mentioned in section 5.5.2.1 the results produced a very linear graph and this shows a very stable, and repeatable, response from the equipment. There remains the problem of the graph passing through the Y axis below origin. Considering this in the light of the system accuracy, simply taking the higher values (increasing the basic readings by 7%) would result in the graph line passing through Y axis above the origin. This would mean that the discrepancy is within the accuracy of the system. However, the anemometer did seem to exhibit a high reading at low speeds and a low reading at high speeds. If this is the case it would have the effect of rotating the graph line anti-clockwise about the centre of the data set. This would in turn have the effect of lowering the point of intersection with the Y axis and increasing the discrepancy. This is unlikely to be solved without a re-design of the heat pipe fin array and a more accurate method of assessing mass flow.

The encouraging aspect of the results is that they show that the ethanol heat pipes can perform in a satisfactory manner as the compressed air flow is increased. In other words it is practical to maintain a high thermal flow into the system using the ethanol HX alone. Ethanol, as mentioned earlier, cannot transport heat as rapidly as the water heat pipes. Despite this lower capacity the need to include ethanol heat

pipes cannot be avoided if water heat pipes are to be included in the system. This does not necessarily have to be the case, as can be seen from table 5.3, because the methanol heat pipes on their own accounted for a 47K rise in temperature. If further tests, at lower ambient temperatures, make it clear that they enable the high capacity water heat pipes to maintain their performance despite temperatures of -40°C and lower, then water heat pipes will remain part of the design. However, the implication of table 5.5 is that, even at high flow rates, the ethanol heat pipes are not approaching the conditions at which their performance will start to deteriorate whereas the water heat pipes appear to be operating at their lower limits and are contributing a very small proportion of the heat gain. It is possible that an entirely ethanol heat pipe HX would be a more effective design. A possible explanation of the parallel configuration graph not passing through the origin might be that the ethanol heat pipes are working well and the water heat pipes are not working at all.

A compressed air car has the potential to operate in a wide range of climates and conditions. Whilst the heat exchanger has not been tested at sub-zero ambient temperatures it is clear that the ethanol heat pipes would continue to function. It may be that a vehicle that regularly operated in a colder environment would need an all ethanol heat exchanger but would otherwise be able to perform as normal. Frosting is not an automatic event at 0°C as air at low or sub zero temperatures is often very dry. However, should the HX ceased to operate, say through blockage by driven snow, the Compac would only lose 10-13% of its energy (table 5.8 below) and power levels should be unaffected.

The energy gain in tables 5.2, 5.4 & 5.5 needs to be put in perspective. The energy being recovered is equivalent to that rejected to the atmosphere in the process of compressing the air into the cylinders. Taking a gram of air, stored at 30MPa, as containing approximately 475J the flow of the energy of compression can be derived from the mass flow. The energy gain can therefore be expressed as a proportion of the energy of compression. Table 5.8 presents the energy gain in this way related to the results of the heat exchangers previously described in tables 5.3, 5.4 & 5.5.

Table 5.8 Energy Gain as a Proportion of the Energy of Compression

Heat Exchanger Connection	Flow Rate of Air (g/s)	Energy Gain (Watts)	Energy of Compression (Watts)	Energy Gain (%)
Series	7.0	332	3315	11.1
	8.6	427	4072	11.7
	11.4	609	5377	12.8
	13.9	758	6530	13.1
	20.1	1127	9404	13.6
Parallel	18.5	822	8586	10.6
	19.7	955	9142	11.7
	20.2	1010	9375	12.1
	20.9	1080	9699	12.5
	21.1	1114	9832	12.8
Max Flow	21.1	9850	98320	10.0

As the energy gain improves with an increasing flow rate, as a proportion of the total energy available, this holds promise for the much larger flow rates required of a practical vehicle. Again the implication is that the ethanol heat pipes are working below their optimum level at these lower flow rates. The maximum flow rate example is of the order that would be required by a practical vehicle but delivers a slightly lower proportion of energy gain than the lower flow rates. The reason for this is unclear but is most likely due to poorer heat transfer at the higher flow speeds.

Generally speaking, the proportion of the energy gain is encouraging. The heat recovery system is providing a 13% gain in energy availability for a probable weight gain of 5kg (30 heat pipes, each pipe and fin weighing 100g plus casing, etc.). The best performance in these tests was 1127 Watts. If this were to be supplied by a 30 heat pipe HX weighing 5kg, its specific power output would be 225W/kg and its equivalent energy storage density for a 1 hour running period would be 225Wh/kg. At the beginning of this chapter it was estimated that a HX would have to achieve at least 80W/kg in order to match the energy store and justify the weight of its inclusion and it would seem that this target is readily achievable. Adding the above energy storage value and heat exchanger weight to those same figures for the compressed air cell yields a system specific energy storage value of 81Wh/kg.

5.6 Recuperator & Air Conditioning

A recuperator is a counterflow HX that is used to scavenge heat, from hot gases leaving a system, in order to heat cold gases entering that system. Usually applied to boiler systems this form of heat exchange has some value in this context where there is a substantial temperature gradient between the compressed air stream, as it leaves the storage cell, and the outlet stream as it leaves the motor. It is accepted that the benefit of this is not immediately obvious. Although a substantial temperature gradient does exist between these two gas streams it is smaller than the gradient that exists between the compressed air and the ambient air. The advantage arises from the fact that the air stream, from the storage cell, was filtered in the original compression process and is now has a low water content.

In section 5.5.2.4 Additional Tests above it was indicated that the risk of the primary heat exchanger frosting up was smaller than expected. Nevertheless, the test was limited in duration and the risk remains for longer periods of use in a real vehicle. The recuperator would use the dry outlet air to warm the air leaving the storage cell, before it enters the primary HX. There would be no risk of frost forming on the recuperator surfaces and the early heating would reduce the risk of frost forming on the primary HX.

A similar concept was considered in the liquid Nitrogen based Cryocar project [Williams, 1997b] and was called an “Economizer”. In the case of the Compac outlet stream the available heat would be similar to the heat required to warm the inlet air as, by definition, the heating requirement of the compressed air stream two streams will be approximately equal to the heat available from the outlet stream, in stable driving conditions. A theoretically 100% efficient recuperator could have heat circulating in a cycle that would require no input from the ambient air. A more realistic HX of 50% efficiency would take much of the load from the primary HX and greatly reduce the risk of the primary HX frosting up in a cold wet climate. This efficiency could be achieved by a tubular shaped “shell & tube” HX that would fit under the vehicle floor. It could be placed in this convenient position as it doesn’t need to be exposed to the ambient air flow as does the primary HX.

As the outlet stream would consist of clean dry air that, after passing through the recuperator, is cold, it would make a good source of ventilation air if the vehicle is also in a climate that requires air conditioning. If further long durations tests show that frosting can occur, it is likely that the recuperator would be considered a

necessity. In that case the cold ventilation air would amount to free air conditioning which, in a normal system, would be a complex and expensive system that drains power from the vehicle engine.

This idea has not been tested yet but it is a simple concept that could be achieved with existing designs of proprietary HX equipment at low cost. Such tests will have to wait until a large compressed air store is available to enable the necessary long duration tests.

5.7 Conclusions

The heat pipe HX has proven that a very useful increase in enthalpy can be achieved with a lightweight HX and that the HX can be justified on the basis of that performance alone. As no comparison, with any other design of HX, has been attempted it cannot be said that the HX must be heat pipe based. At the very least a question mark must be placed against the use of water based heat pipes in the light of the results of the tests showing that most of the enthalpy increase was achieved by the ethanol heat pipes.

The current pressures and flow rates may be adequate for city driving but higher pressures should be explored. The maximum pressure of operation was limited by the regulator valve. This valve will now be modified to allow higher pressures and higher flow rates to be tested with the existing. Once these tests have been completed it is the intention to form the existing heat pipes into a single “series” configuration HX design and attempt to modify the heat pipe fin array to reduce the “blow by”

problem. Also, the possibility of finding a high pressure, but lightweight, flat tube and fin HX for comparison, has not yet been abandoned.

6.0 Regenerative Braking System

A pivotal element of all zero emission vehicles is a braking system that can capture the kinetic energy of the vehicle that is usually lost as heat through a conventional braking system. This is known as a regenerative braking system (RBS). In the process of driving an electric battery vehicle current is drawn from the battery and applied by the electronic control to the motor. Within the motor, magnetic fields of the correct polarity are created in order to turn the motor armature in the correct direction and provide the torque to drive the vehicle wheels. Under braking, this process can be reversed. Instead of electricity being used to create torque, torque is used to create electricity. The electronic motor controller switches off the armature field so that the armature conductors are now driven, by the wheels, through the stator magnetic field. The current that is created is then supplied to and stored in the battery. Such a system can increase the driving range of an EV by 10-15% [Dhameja, 2002c]. These systems commonly have a cyclic efficiency of approx 50% but some experimental systems, using super capacitors, claim much higher efficiencies of 90+% .

Whilst an RBS can be made to work with any type of electric motor it should also be able to operate to the maximum power required of the braking system in order to absorb as much energy as possible. This raises a number of practical problems that must be dealt with if an RBS is to operate efficiently [OECD,1993].

The most notable are listed below:-

1. Overheating of the motor under hard braking
2. Rechargeability of the battery subject to high currents
3. Driver perceptions of brake system's behaviour/response
4. In the event of a fault, the RBS should fail safe and braking be unaffected.

1 & 2 are closely linked to the RBS of an electric vehicle but 3 & 4 apply to all braking systems.

When considering the design of an RBS, for a Compac, it would be rational to attempt some physical corollary of the electric vehicle RBS. The act of engaging the brakes would convert the compressed air motor to a pump/compressor which would then drive air into the compressed air store. However, there are a number of problems with this process. The current design of compressed air motor, in this project, uses ports for the induction and exhaust of the compressed air stream, strategically placed to provide the necessary timing of port opening and closing. If the motor were to also serve as a compressor, this reliable, and simple to build, design would have to be replaced by a valve arrangement. Whether electrically or mechanically controlled, these valves would have to increase complexity and costs, and would probably reduce reliability.

Perhaps, more importantly, it is inevitable that there would be a variable pressure in the compressed air store and a varying back pressure would result in a varying braking effect. If the main store were to be used it would be at different states of charge in the course of its use. If a separate, smaller, store were to be used, the back pressure would increase as the store filled in the course of the braking process. This

varying brake effect would violate the requirements of problem 3, and possibly 4, above.

The reasons given above are, probably, the reasons that, to date, no air car design has attempted an RBS. An interesting RBS design, using compressed air has recently been proposed [Lee, 2009] in which an IC piston engined vehicle converts the piston engine to a compressor under braking and it is possible that this might be used with a Compac that uses a piston motor. However, the problem of varying braking effort and the effect on driver perceptions have yet to be investigated for this design.

In the course of this project a number of options have been explored for an essentially mechanical RBS but for the reasons given above, and the sheer mechanical complexity required for such a system, it was accepted that such a system was beyond the resources of this project. However, because a zero-emissions vehicle must be considered incomplete without an RBS, non mechanical alternative systems were considered.

An electro-mechanical system would be more achievable. This considered the use of a generator/battery system, much as used in the electric vehicle, which then drove an electric motor and compressor. Although a generator and battery are already required as part of the normal equipment of such a vehicle, larger and more robust versions would be required and the system would be only slightly less complex than the mechanical system already considered and discarded. Using the following representative efficiencies a calculation of the probable efficiency of such a system is possible.

Expected Component Efficiencies

generator (85%)

battery (75%)

motor (85%)

compressor (50%)

0.85 x 0.75 x 0.85 x 0.50 = 0.27 - System efficiency (27%),

Whilst it is possible that increased system efficiency might be achievable with more efficient components, this would only be possible at much greater expense and would still be unlikely to reach 50%. It would seem that this, and similar systems, are not worthwhile.

However, the concept of the primary HX, of chapter 5, for warming the compressed air flow suggested a non-mechanical system for reclaiming the braking energy. In an ordinary braking system, the kinetic energy is converted to heat and rejected to the atmosphere. It is a requirement, of any friction based brake, that the temperature of the brake components is substantially above the ambient temperature, otherwise little useful heat transfer could take place. If this thermal energy could be transferred to the compressed air flow, which will be at or below the ambient temperature, then the increased enthalpy would result in increased work done as the air expands through the air motor. As a purely thermal process of heat transfer, losses could be minimal and good insulation could result in high efficiency levels. It was decided to proceed with an investigation of the major elements of the system as proposed in Ditmore [1995] and Ditmore et al [1997b].

6.1 Basic System Design

The basic concept is to use ventilated disc brakes as air pumps and to channel the hot air, through insulated ducting, to a heat pipe mediated thermal store using a water/alcohol mixture as the storage medium. An array of water based heat pipes would induct the heat into the storage medium from the hot air from the brakes. Further water based heat pipes would extract the heat, transferring it to the compressed air flow shortly before it enters the motor. A schematic of the initial concept is shown in Figure 6.1.

(Note: direct water cooling of the brake discs would probably capture more heat than this system. However, this has been attempted before by motor sports engineers and it is a system no longer in use. The reasons for this are not readily available but are probably related to reliability problems surrounding the highly stressed rotary joint required to carry the water feed and return. Water cooled brake callipers are available but their purpose is solely to cool the brake fluid and only a fraction of the kinetic energy is disposed of through this route.)

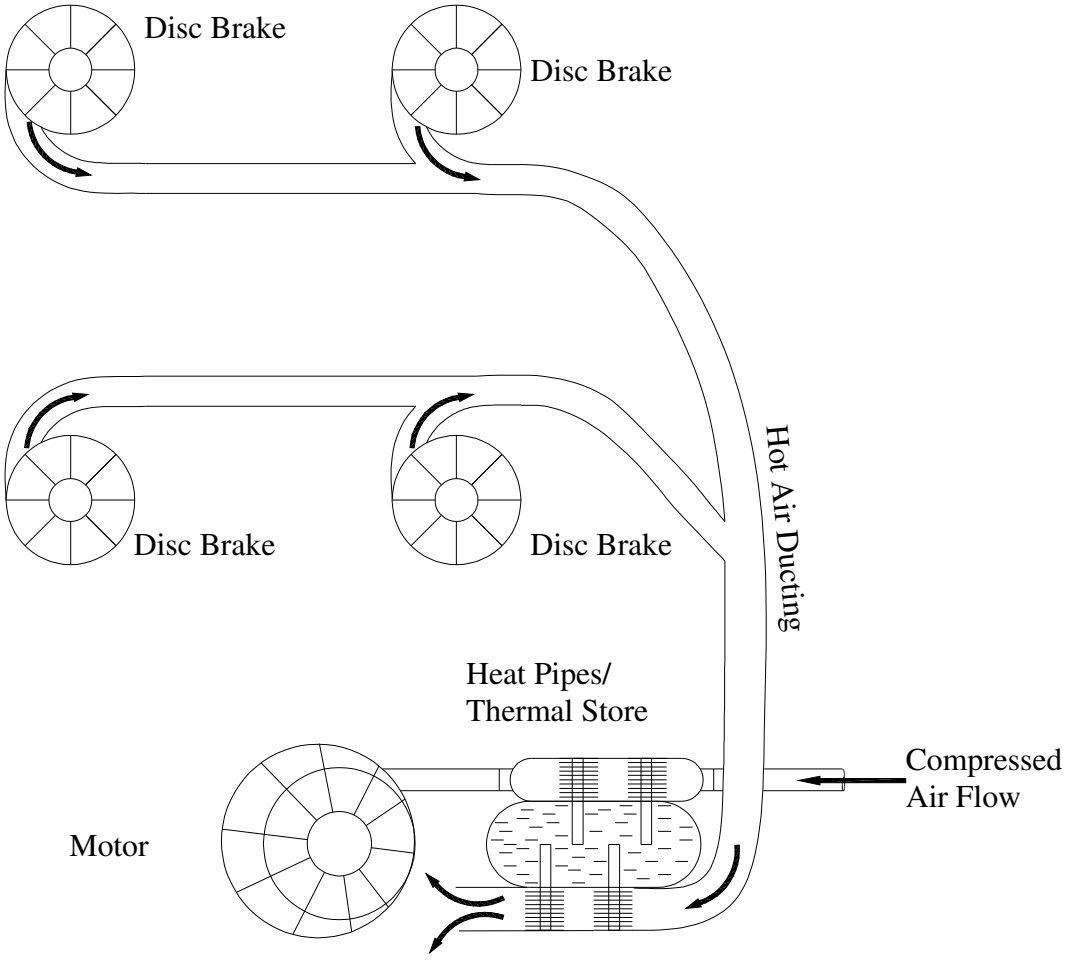

Fig 6.1 Schematic of Thermal Regenerative Braking System

The intention is that the RBS be based on a normal braking system with ventilated brake discs, as in Figure 6.2. This type of brake disc is normally reserved for high performance automobiles as its design allows the rapid dissipation of heat resulting from hard braking. The disc design is essentially that of a centrifugal fan/pump that draws cool air in at its centre, accelerates it across its fins and ejects hot pressurised air at its perimeter.

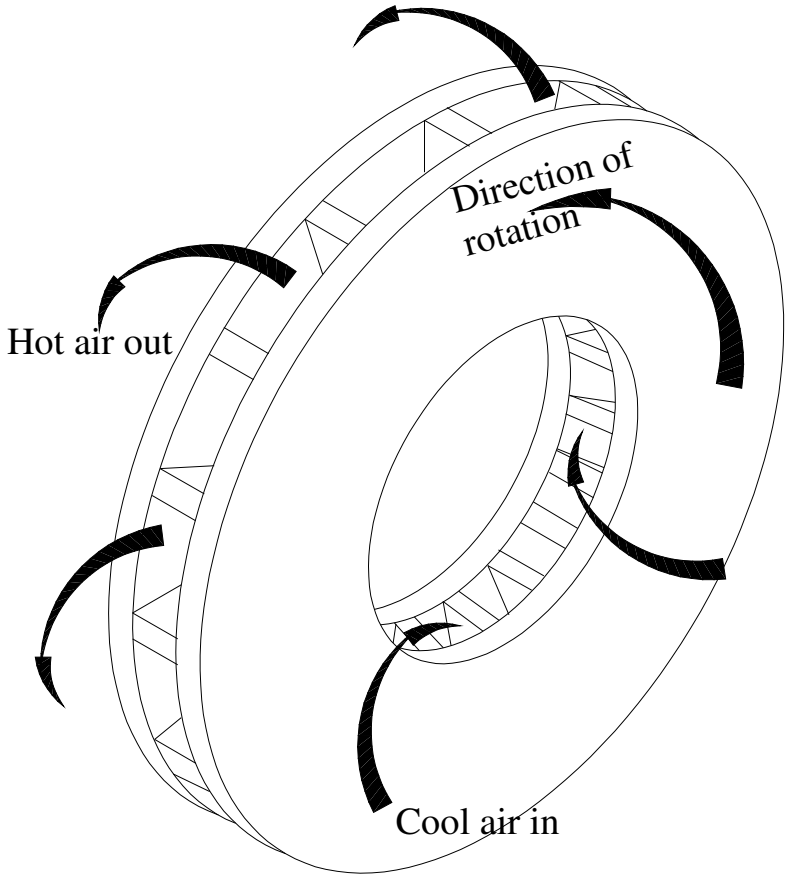

Figure 6.2 Air Flow Through a Ventilated Disc Brake

A shroud, shown in Figure 6.3A, envelopes the brake disc, as shown in Figure 6.3B. This shroud captures the hot air, heated and accelerated by the brake disc, and channels it to the ducting system. The shroud shown here is indicative of the concept but the real shroud would have to accommodate the brake calliper and other suspension components.

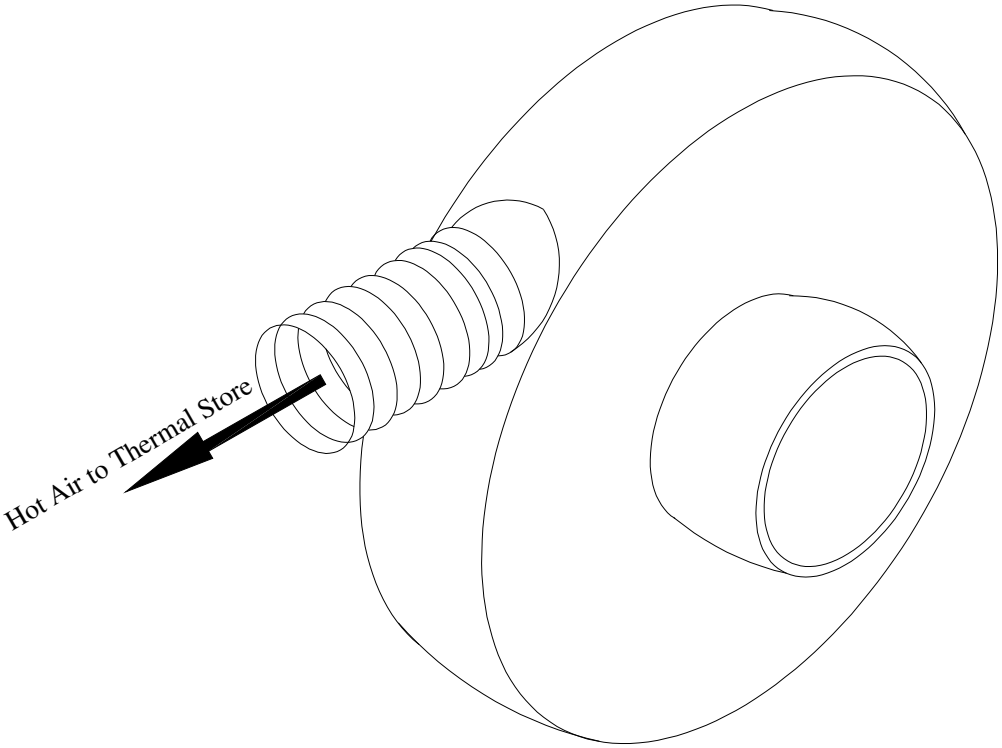

Figure 6.3A Disc Brake Shroud

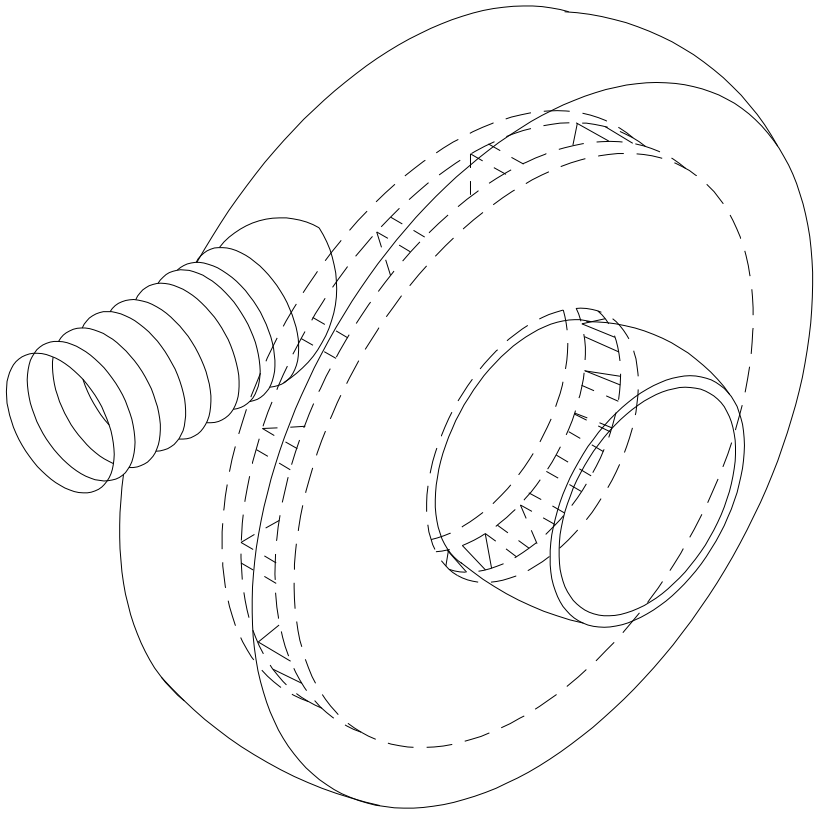

Figure 6.3B Disc Brake and Shroud

The (insulated) hot air ducting channels the air to the heat pipes and thermal store. The purpose of the store is to act as a thermal "surge" tank that prevents heat from flowing through the system at undesired high speeds. It is axiomatic that when the brakes are being used the motor is not being driven. If there were a heat pipe heat exchanger directly connecting the RBS air stream with the compressed air stream to the motor, much of the heat of braking would be lost. Initially some of the heat would travel through the motor, as it slows down, without doing any useful work. Subsequently, heat would be put into a stagnant air stream whilst the vehicle is stationary. This would increase the pressure in the induction manifold. This would allow leakage of energy by thermal paths and through gas leakage through the motor's imperfect seals. Also, it is desirable to keep the induction manifold at atmospheric pressure whilst the vehicle is stationary. Without this the motor is straining against the brakes or it will be necessary to include a clutch mechanism in the design.

With the heat store intervening between the two sets of heat pipes a delay is built into the system. Heat transfer will not take place until a useful temperature difference has built up between the heat store and the compressed air stream. The rate of temperature increase will depend on the energy available from braking, the rating of the heat pipe array, the mass of the heat storage medium and its specific heat. All of these elements can be modified in advance to achieve a desired range of temperature gradients suitable for a specific vehicle. A layout of the thermal store is shown in Figure 6.4. This layout shows only two induction heat pipes and two extraction heat pipes but it is expected the number would vary according to design requirements.

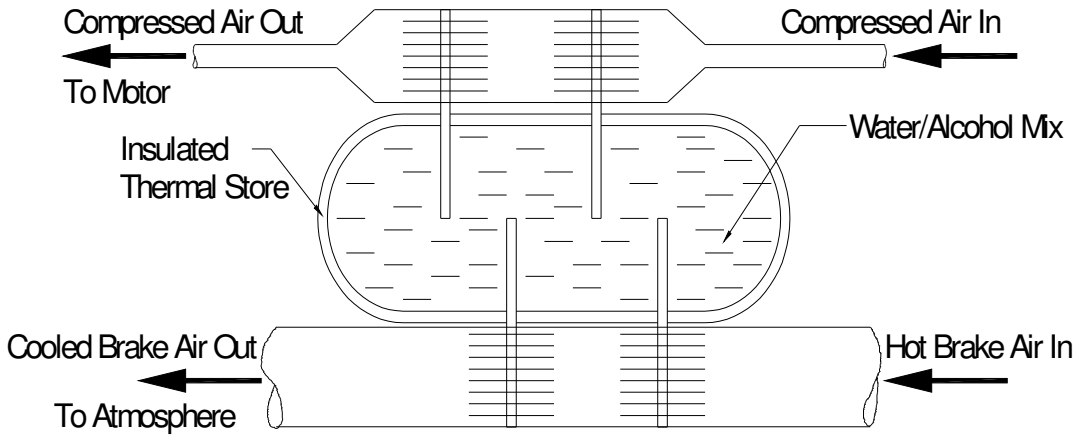

Figure 6.4 Heat Pipe Thermal Store

It is expected that water based heat pipes will be used for conveying the heat into and out of the store and a water/alcohol mix would be the heat store medium. Water based heat pipes have a higher individual rating than alcohol heat pipes and so fewer would be required to achieve the desired overall rating so reducing system size and cost. However, if sub-zero temperatures were to be regularly expected alcohol heat pipes would be preferred. A water/alcohol mix, for the heat store medium, would be required to avoid freezing and varying the ratio would vary the mixture's specific heat allowing "tuning" of the system response by varying the mass and specific heat. A purely water storage medium would be advantageous as its high specific heat would enable higher heat storage and maintain a higher temperature gradient for the induction heat pipes. For obvious reasons this would be limited to warm climes.

The primary advantage of this design of RBS is that it is functionally a normal brake system and so obviates the problems enumerated in the first section of this chapter.

Particularly, driver perceptions, braking performance and reliability will be the same as for an otherwise identical system without the RBS elements.

6.2 Initial Experiment Design

The major question to be addressed by experiment is whether the proposed design is capable of scavenging sufficient energy in order to make the system worthwhile. This begs the question what is meant by "sufficient" and "worthwhile". At this stage no clear answer can be given but a useful target would be the common 50% efficiency claimed for electric vehicle RBSs. It is not expected that the experimental rig would achieve 50% efficiency as it will only have two induction heat pipes. It is expected to provide the prospect of 50% efficiency if further heat pipes were added. The question of how many heat pipes, and whether it is a practical design, will be addressed once the experimental data is available.

It is not required to test the warming of the compressed air stream and the heat extraction performance of the heat pipes as this has been sufficiently tested in the chapter on the primary air to air heat exchanger. Also, logically speaking, the heat from the heat store has no where else to go but into the compressed air stream (assuming good thermal insulation of the heat store). Varying the number of heat extraction heat pipes will vary the rate at which heat is transferred from the store to the compressed air stream but virtually all of the heat stored will eventually be transferred into the compressed air. It is not clear that the rate of heat extraction is an important question as it is unlikely to have a substantial effect on the power of the motor or vehicle. There is no particular advantage to rapidly transferring the heat into the compressed air stream. It is simply that the heat should not be allowed to

accumulate in the store for a long time. The important initial question is, what is the rate of heat transfer into the heat store using the available design and could this be expanded into a practical design?

6.3 Design of Experimental Rig

To answer this question required a heat store of known volume and specific heat with at least two induction heat pipes. As with the primary heat exchanger, the fins were attached with the thermally conductive bronze/epoxy resin mix. Also required was a heat source with a known power output and thermocouples to provide an accurate assessment of the heat store and air flow temperatures. Finally, as a check of the air mass flow, an anemometer would be required to assess the air flow speeds. A drawing of the experimental heat store is shown is figure 6.5 and figure 6.6A & B are photographs of the actual heat store.

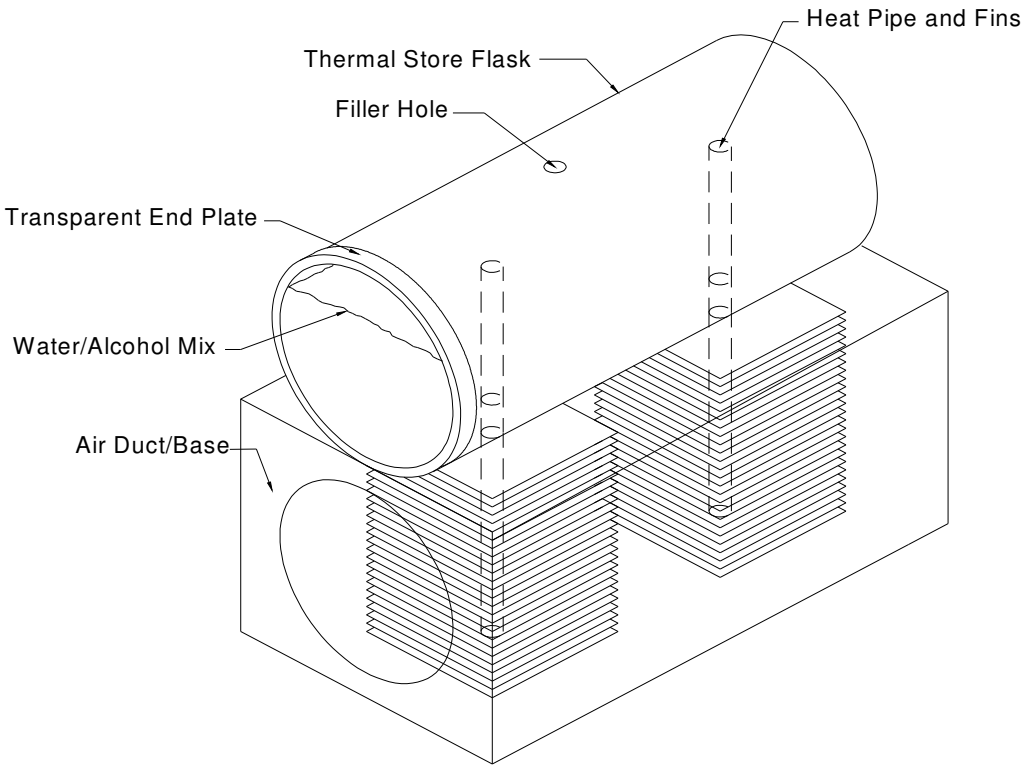

Figure 6.5 Heat Store for Experimental Rig

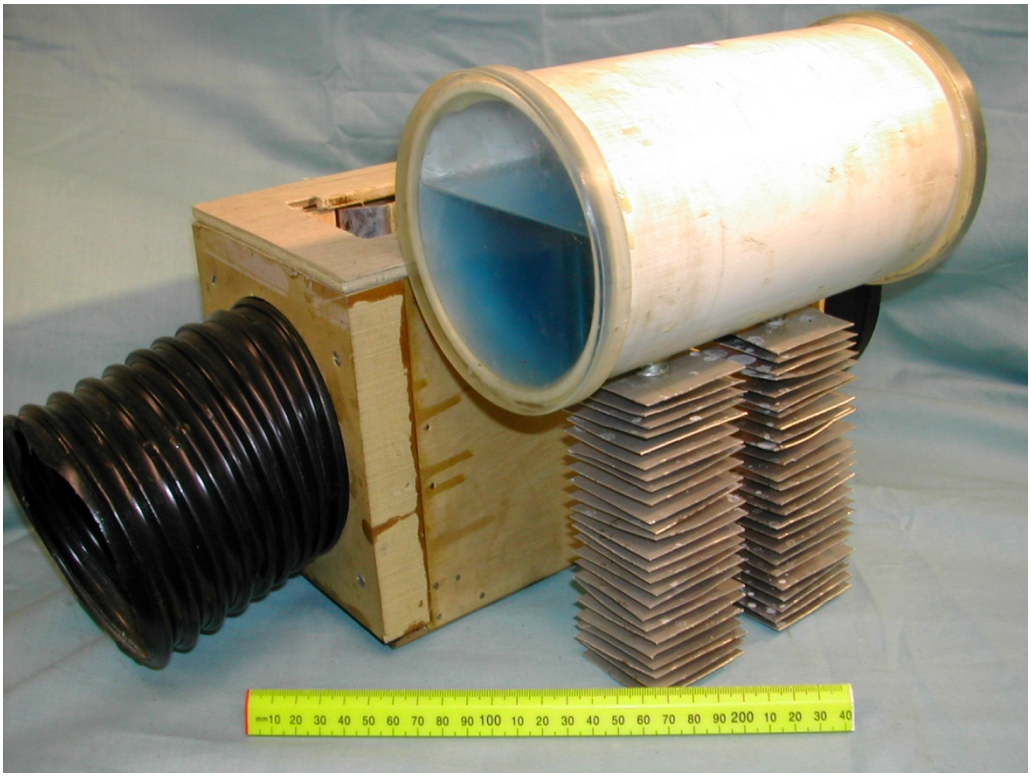

Figure 6.6A Actual Heat Store (Store separate from duct manifold)

Figure 6.6B Heat Store & Duct Manifold Assembled

6.3.1 Experimental Heat Store Construction Details

The |heat store was built of a 200 mm length of PVC tubing of 100mm ID, with end caps of transparent Perspex.

The heat storage fluid was 1 kg of water and 0.5kg of ethanol/anti-freeze. Taking the C_p of water as 4.2 kJ/kg.K and the C_p of ethanol as 2.44kJ/kg.K the C_p of this mixture is 3.6kJ/kg.K and the thermal storage of the 1.5kg mass is 5.42kJ/K. The final design of heat store is expected to absorb the entire kinetic energy of the vehicle under emergency braking which in chapter 3 was calculated as 96.5 kJ @50kph and 420.5 kJ @90kmh. If all the braking energy were to be transferred to the heat store without any being transferred to the compressed air flow, braking from 50kph would raise the 1.5kg heat store temperature by 18K and 90kph would raise it by 78K. If a starting temperature of 20°C is assumed, the heat storage mass is barely sufficient to absorb the heat of a worst case scenario without boiling and is therefore a reasonable mass for the purpose of the experiment.

The heat pipes are water based and of the same dimensions (12mm D x 250mm L) and capacity as those used in the primary heat store. Aluminium (50mm x 50mm) fins were bonded to the lower (evaporator) section only. The upper (condenser) section was left unfinned. This was because horizontal fins would have blocked the vertical convection of the heat storage fluid. An attempt was made to attach vertical fins but this proved unreliable and made the fitting of the heat pipes more difficult. The attachment of the evaporator fins was achieved using the thermally conductive bronze/epoxy adhesive used in the primary heat exchanger.

Four K type thermocouples were used to measure the air flow temperature and heat store temperature. Referring to Fig 6.7 below, the first thermocouple (TC1) at the hot air inlet, the second (TC2) midway between the two heat pipe fin arrays, the third (TC3) at the outlet and the last (TC4) in the heat store. The anemometer was placed at the outlet. The thermocouples and anemometer were all connected to hand held meters, their readings recorded manually. The two channel meters, reading the thermocouples, were supposedly calibrated to an accuracy of ± 2°C but allowed self calibration. Both were tested against melting ice and boiling water and each adjusted to read 0°C and 100°C at the appropriate time but it was assumed that the accuracy would be limited to ±1°C as with the primary heat exchanger experiments. The anemometer manufacturer claims that it is calibrated to an accuracy of ±3% ± 2 digits of its full range (0.8 - 30.0 m/s, resolution 0.1 m/s) which corresponds to ±0.8 m/s at the upper limit of its range. A calibration certificate is provided to this effect. In these tests only 14% of its range was used which corresponds to a reading of ±0.1 m/s. This was trusted as there was no standard available to compare it to. A drawing of the experiment layout is shown in figure 6.7 and photographs in 6.8A, B & C.

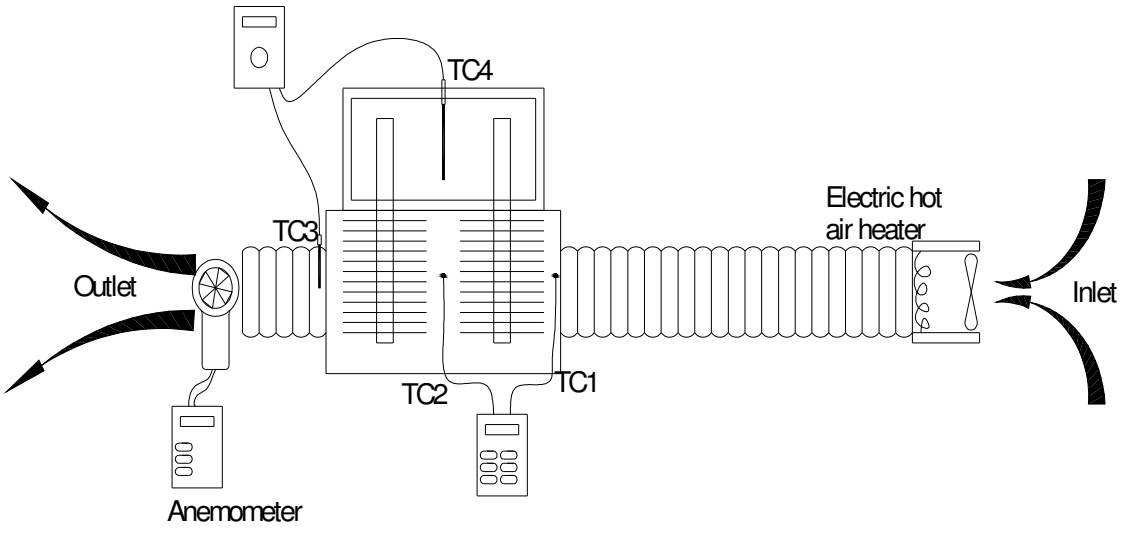

Figure 6.7 Layout of Heat Store Experiment Rig

The heat source was an electric hot air gun with a nominal maximum power output of 1kW. This device wasn't calibrated nor instrumented in any way as the temperature and air flow readings would supply the necessary data, and approximate data would be sufficient the answer the initial question.

Preliminary testing, of the heat store with the heat source, had shown that there was no performance difference between ducting the hot air over each fin array at the same time, in parallel, or passing it over them in series. As this was also one of the conclusions from the testing of the primary heat exchanger it was decided to limit the ducting manifold design, and experiments, to a series configuration as this was perceived as easier to construct.

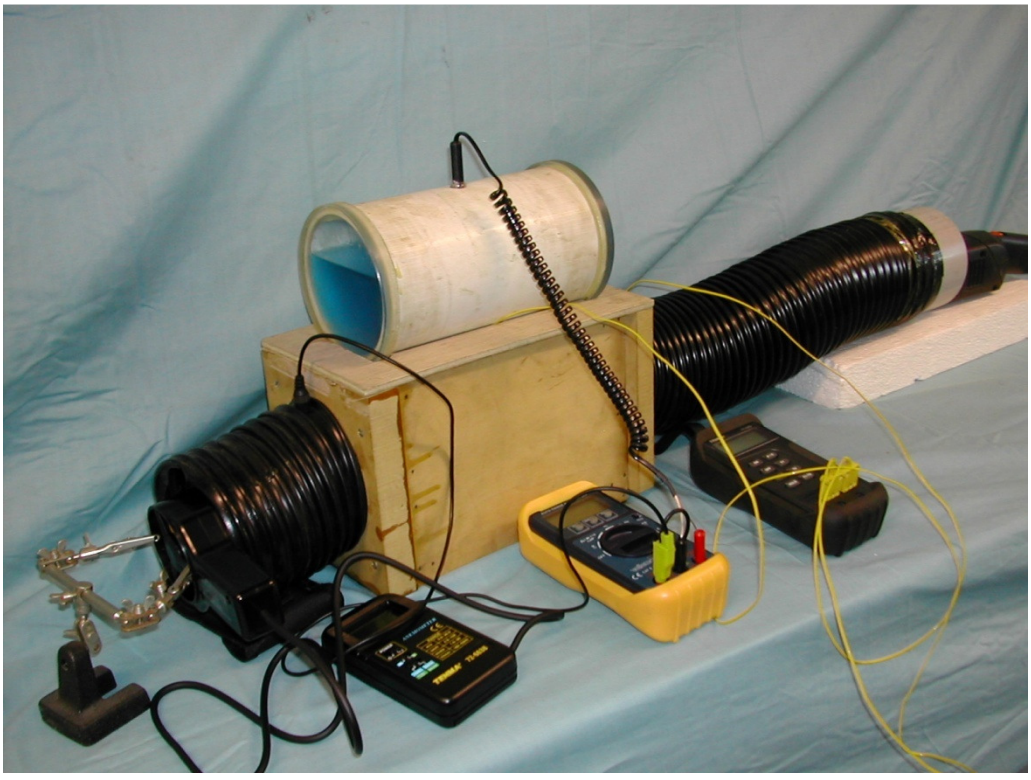

Fig 6.8A Heat Store Test Rig (left view)

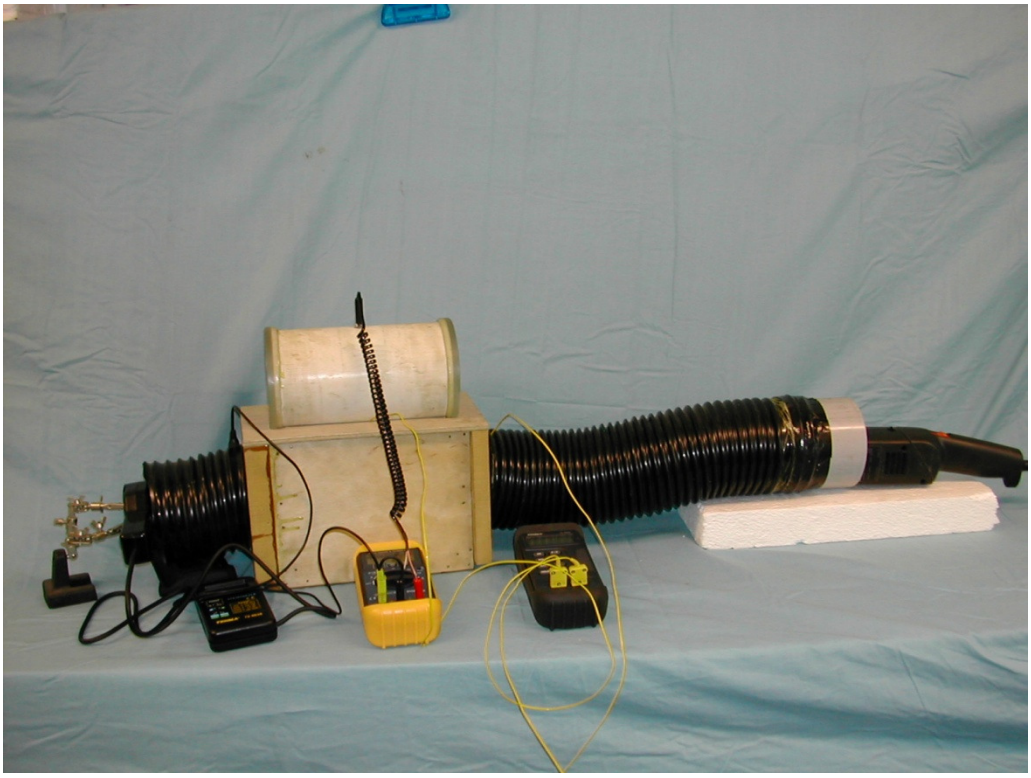

Fig 6.8B Heat Store Test Rig (front view)

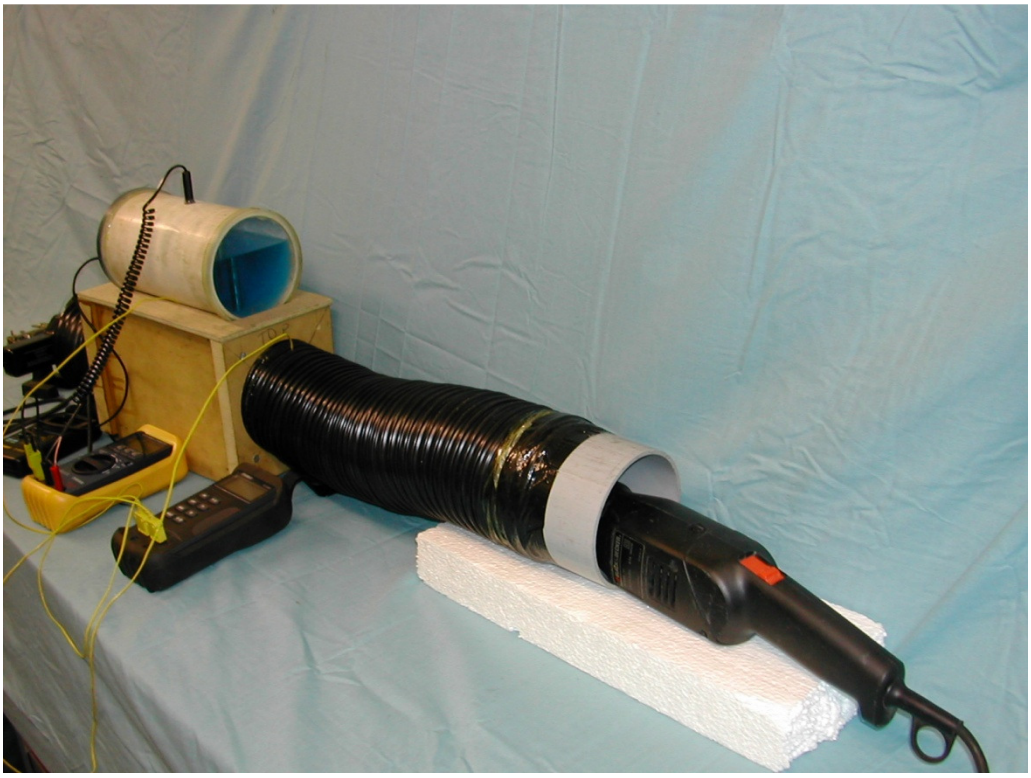

Fig 6.8C Heat Store Test Rig (right view)

The air heater has three settings. The first was low air speed, no heating. The second was low air speed with low heating. The third and final setting was the highest air speed at the highest level of heating. An attempt was made to test the output of the heater by connecting it to a 10A ammeter. This read 3.5amps at full power which at 230V implies an output of approximately 800W. A further heater test using the anemometer (4.7m/s) and thermocouples ($\Delta T \approx 30K$) in a smooth 80mm tube, (Reynolds number calculated at about 21,000, so fully turbulent), indicated 770W. Because of these preliminary readings the subsequent values, obtained in the full test rig, were accepted.

6.4 First Tests and Results

The initial experiment's procedure was to simply run the air heater at its two "hot" settings and measure the heat store's temperature change against time.

Table 6.1 Heat Storage Results at Low Heat/Power Setting

	Thermocouple Temperature °C				Initial
Time (s)	TC1 (inlet)	TC2 (mid)	TC3 (out)	TC4 (store)	Conditions
0	25	25	25	25	
30	38	34	32	25	Air Speed
60	39	36	35	25	V_{out} 2.2m/s
120	39	37	36	26	
180	39	37	37	26	Air temp
240	39	38	38	26	25°C
300	39	38	38	27	
360	39	38	38	27	

In this test the outlet was a rectangular shape of dimensions 160 x 80mm, not the circular outlet in figs 6.5 & 6.6, so the cross sectional area is 0.160 x .080 = 0.0128m^2. At 300K the density of air is 1.16 kg/m^3 and at 350K it is 1 kg/m^3 (Sychev et al, 1987) Interpolating, the density (ρ) of air is taken as 1.08kg/m^3. The mass flow is given by the equation

$$\dot{m} = \rho \times A \times V_{out} \qquad \text{Eqn. 6.1}$$

$$= 1.08 \times 0.0128 \times 2.2 = 0.0304 \text{kg/s.}$$

The equation for heat flow is

$$\dot{Q} = \dot{m} \times C_{p\,(air)} \times \Delta T \qquad \text{Eqn. 6.2}$$

Taking $C_{p\,(air)}$ as 1.007 kJ/kg.K and ΔT as (temp TC1 - ambient temp) the heat provided by the heat gun was

0.0304 x 1.007 x (39 – 25) = 0.429 = 429 Watts

The highest rate of heat absorbed through the heat pipes was

0.0304 x 1.007 x (38 - 32) = 0.184kJ/s = 184 Watts (efficiency η 43%) highest

but more representative is

0.0304 x 1.007 x (39 - 38) = 0.031kJ/s = 31 Watts (η 7%) lowest

Taking $C_{p\,(HS\ mix)}$ as 3.61 kJ/kg.K the heat absorbed by the heat store was

1.5 x 3.61 x (26 – 25) = 10.83kJ

Table 6.2 Heat Storage Results at High Heat/Power Setting

	Thermocouple Temperature °C				Initial
Time (s)	TC1 (inlet)	TC2 (mid)	TC3 (out)	TC4 (store)	Conditions
0	25	25	25	25	
30	41	39	38	25	Air Speed
60	41	40	40	26	V_{out} 3.5m/s
120	41	40	40	26	
180	41	40	40	27	Air temp
240	41	40	40	27	25°C
300	41	40	40	28	
360	41	40	40	28	

For the “high” heat source setting the same calculations are

1.08 x 0.0128 x 3.5 = 0.0484kg/s

The heat provided by the heat gun was

0.0484 x 1.007 x (41 - 25) = 0.78kJ/s = 780 watts

The rate of heat absorbed through the heat pipes was

0.0538 x 1.007 . (41 - 40) = 0-054kJ/s = 54 watts (η 7%)

The heat absorbed by the heat store was

1.5 x 3.61 x (28 – 25) = 16.25kJ

6.4.1 Interim Conclusions

It was calculated earlier that emergency braking from 50 kph would require a storage capacity of 96kJ. It can be seen from these measurements that this system isn’t approaching the required performance and average efficiencies are single figure percentage values

The “heat absorbed” values were achieved after 300 seconds but a realistic brake system would, probably, have cooled down to the ambient temperature by this time. The heat pipe performance was disappointing and was falling far short of that achieved with the primary heat exchanger and the downstream heat pipe seems to be ineffective after a short period of time. Also the temperature differences being generated by the heat source were below those expected. This was at least partly due to it performing 13% below its nominal rating of 1kW but was also due to the high air speed/mass flows being generated.

The requirements for the next series of tests were :-

1. Check downstream heat pipe for functionality, is it working?
2. Check heat source for a malfunction that would explain its low heat output.
3. Increase temperature differences.
4. Reduce air mass flow

6.5 Second Series of Tests

Downstream Heat Pipe. This was tested by reversing the orientation of the heat store, in the manifold, so that the downstream heat pipe now receives the hot air stream first. The results are not reproduced here as they were nearly identical to the first test. Therefore it must be concluded that the heat pipe is functioning correctly and it was not the source of the systems poor performance.

One explanation of the poor performance of the downstream heat pipe, compared to the ostensibly identical heat pipes of the primary heat exchanger, is the configuration

of the condenser. In the present configuration the condenser is without finning and heat is extracted by passive convection of the liquid. The primary heat exchanger has horizontal fins with the compressed air driven over the fins. This implies that, despite the difficulty of fitting fins, a method of applying fins should be developed. Additionally, some form of forced convection would probably be beneficial. Finally, the decision to have a solely series design may have to be revisited. However, this will require the heat store to be completely rebuilt and so will be left until the present series of tests have been completed.

The heat source was checked for any obvious deficiencies but it appeared to be functioning as well as it could. Its poor performance was put down to poor design/build quality. Unfortunately, a better heat source wasn't readily available so the tests continued with this design until a superior design could be obtained.

Using the present rig the first desirable change was to restrict the air flow through the heat gun and rig by reducing the area of the induction vents/ports. This was achieved by partially blocking these areas, reducing them to approximately half their previous area. With the heat gun on maximum power this would have the effect of reducing the cooling air flow and so increasing the temperatures at the manifold inlet. The air speed on the maximum setting fell to that of the minimum setting

With this modification completed, the air speed on the maximum setting fell to that of the minimum setting. A further test was run and the results are shown in table 6.3 below.

Table 6.3 Restricted Air Flow Test Results

	Thermocouple Temperature °C				Initial
Time (s)	TC1 (inlet)	TC2 (mid)	TC3 (out)	TC4 (store)	Conditions
0	25	25	25	25	Air Speed
30	49	46	44	26	V_{out}
60	50	47	45	27	
120	50	47	45	28	Air temp
180	51	48	46	33	25°C
240	51	48	46	34	

The mass flow rate = 1.08 x 0.0128 x 2.15 = 0.030kg/s.

The heat provided by the heat gun was

0.030 x 1.007 x (51 - 25) = 0.78kJ/s = 780 Watts

The rate of heat absorbed through the heat pipes was

0.030 x 1.007 x 5 = 0.099kJ/s = 151 Watts (η 19%)

The heat absorbed by the heat store was

1.5 x 3.61 x (32 – 25) = 37.9kJ

6.5.1 Second Test Results – Interim Conclusions

These results are a clear improvement on the earlier tests with efficiency at 19% and heat stored increased to 37.9 kJ. The efficiency of heat scavenged is increased by about 300% and the amount of heat stored by 230%, in 240 seconds at which time the temperatures seem to stabilise. However, the heat stored is still only about 40% of the heat (96kJ) to be generated in a 50kph emergency braking event. If it is assumed that the 96kJ are entirely absorbed into the braking system and the disc

braking system takes 90 seconds of motoring to cool down, then the RBS should be absorbing heat at a rate of about 1kW. The rate of 151 Watts achieved implies that an array of 12 heat pipes could achieve the desired efficiency. It must also be noted that the downstream heat pipe continues to underperform.

A twelve heat pipe heat store could be built at an affordable price and might be made compact enough for a small vehicle. However, the higher energy resulting from braking at higher speeds would have to be allowed to escape. A further re-design of the system was planned which might capture all of the energy from all braking scenarios that were likely for this type of vehicle.

6.6 Redesigned Regenerative Braking System

There seems to be two answers to the problem of the heat being lost. The essential problem is that the hot air doesn't spend enough time in contact with the heat pipe and fins to transfer the heat to the heat store. The two options are;-

1. Reduce the size of the outlet so that the transit time, of the hot air, is increased to minutes.
2. Close the system so that the hot air is continually recycled through the disc brake and heat store manifold with all of the available heat being gradually extracted

Option 1 has the attraction of simplicity but a simple fixed area outlet would be a compromise. A small area outlet would almost certainly cause overheating of the system in circumstance of high ambient temperatures or regular braking. A large area outlet would lower efficiency by allowing too much heat to escape during more

normal usage. A thermostatically operated air valve, that would open gradually, would probably be able to solve this but would increase the complexity of the system and would still reduce efficiency by releasing the heat to the atmosphere.

Option 2 would require additional space for additional piping and a second flexible connection to the disc brake but would trap the air so that a large proportion of the heat could be scavenged. Again, there remains the risk of overheating in extreme conditions but in most driving scenarios a high level of efficiency could be achieved if the system were correctly insulated. The option of a thermostatically operated valve could also be applied to this system, as a safety valve, and need not have a complex graduated response as required for option 1.

The lack of an available, and appropriate, valve system and the compromise this would necessitate meant that the closed system to recycle the hot air was the system with the best prospects. That the existing rig could be readily modified also meant that it was an immediately testable option. An amended schematic of the intended design is shown in figure 6.9.

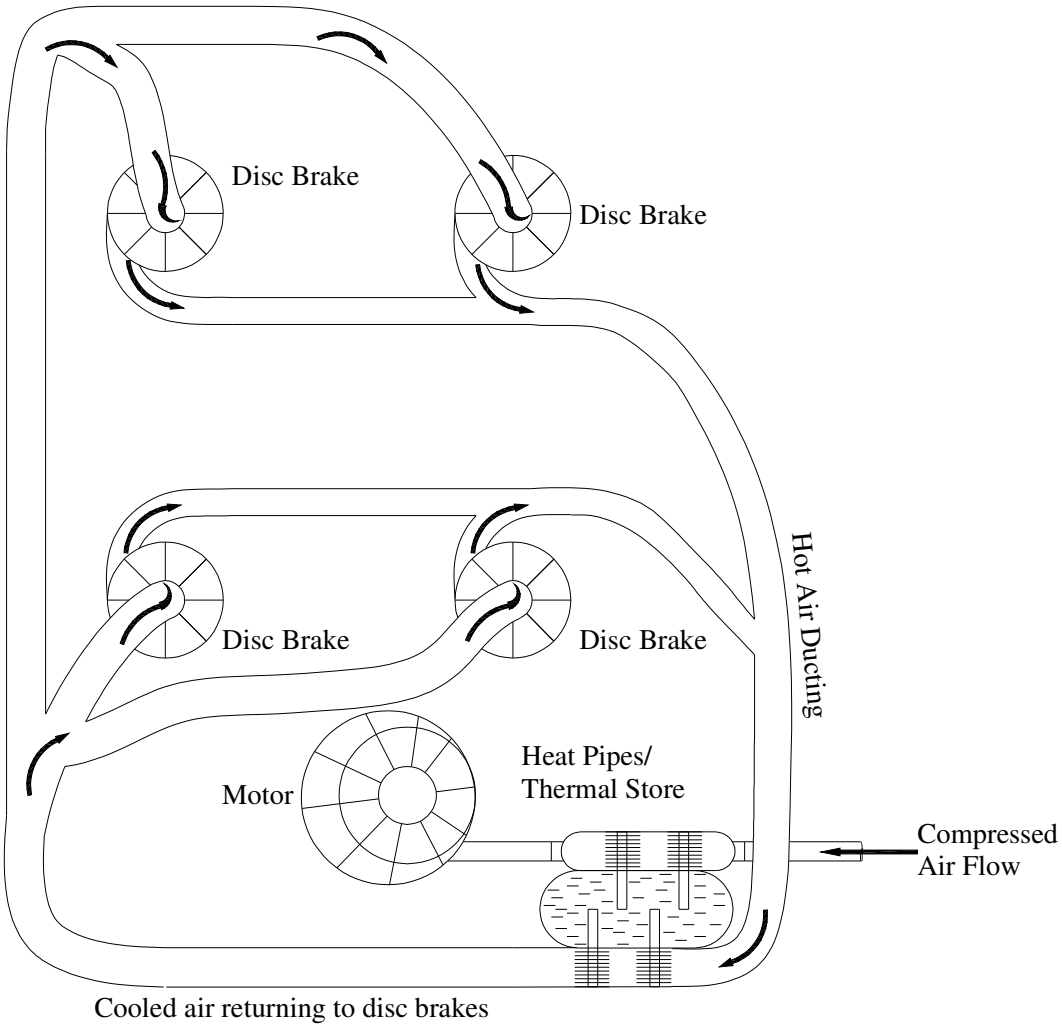

Figure 6.9 Schematic of "Closed" Regenerative Braking System

It is not intended that the system be air tight, only that there will be no substantial exchanges of air between the system ducting and the local environment. It will operate at ambient pressure and any pressure changes, due to temperature changes, will be very short lived. The disc brake shroud will be changed along the lines of that in figure 6.10.

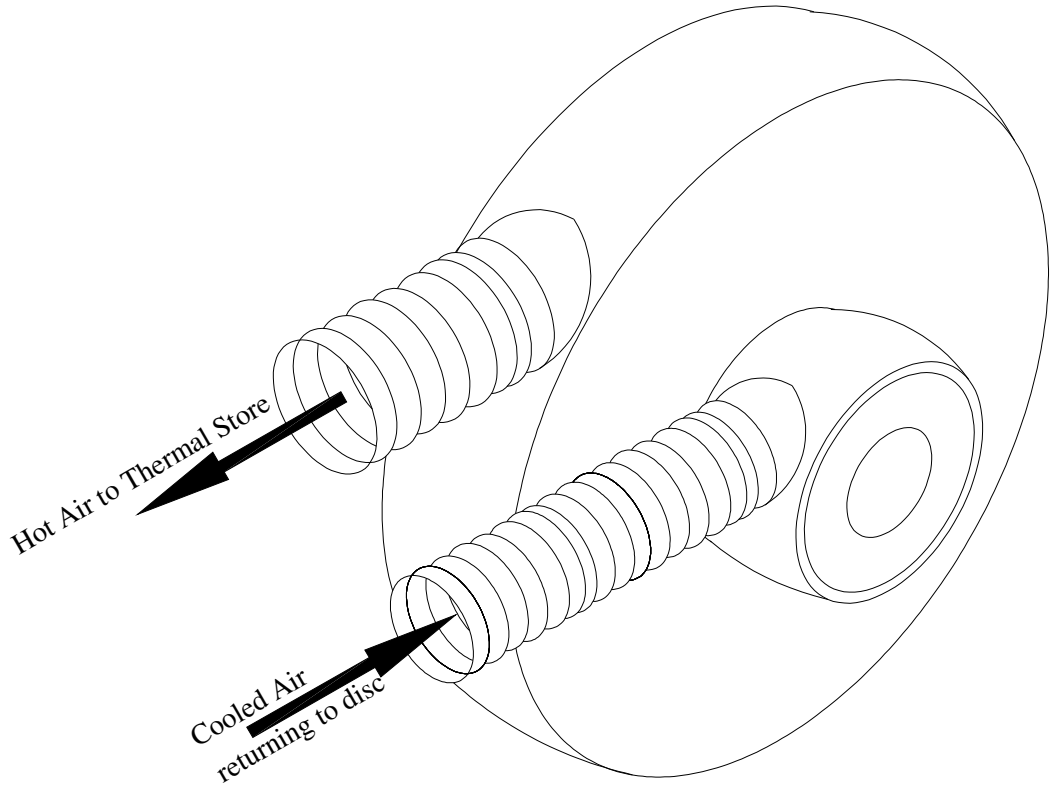

Figure 6.10 Closed System Disc Brake Shroud

6.7 Closed System Experiment Design

In this experiment it was intended to test the effect of trapping an equivalent amount of heat as that produced by the front brake discs. This would be achieved by enclosing the electric heater within the closed ducting system and by running it at full power for the time necessary to deliver the amount of energy equivalent to an emergency braking manoeuvre (100kJ/780W = 128s). The ducting was insulated and made of a polymer so it was necessary to ensure the temperatures didn't exceed the melting point of this material. 150°C was considered to be the safe limit. Figure 6.11 is a photograph of the altered experimental rig.

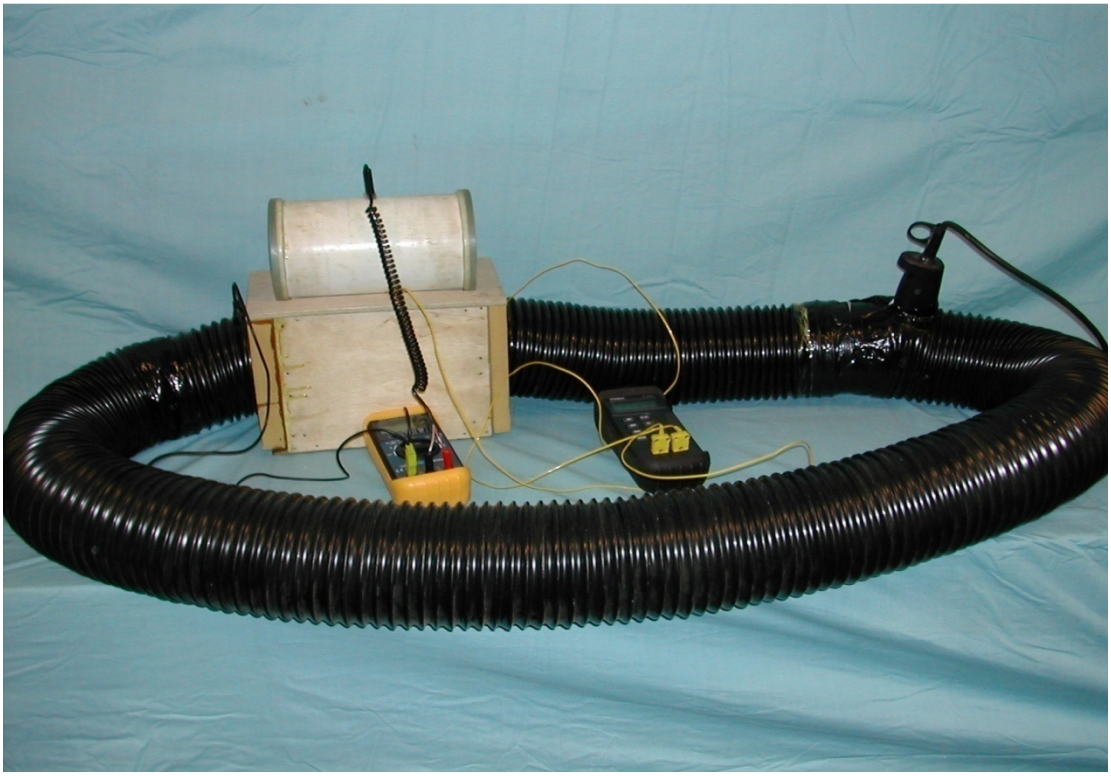

Figure 6.11 Closed Heat Store Test Rig

6.7.1 Energy and Temperature Limits

It was assumed that the kinetic energy of the vehicle would be dissipated evenly by the two front brakes. The kinetic energy of the vehicle was calculated, in chapter 3, as 96kJ (50 kph) and 312.5kJ (90kph) so one brake disc would produce about 50kJ, in braking from 50kph, or about 160 kJ if it were braking from 90kmh. Immediately after braking most if not all the energy would be stored in the brake disc assembly. Assuming the assembly weighs approximately 5kg (some available brakes were weighed to obtain this figure) and is made of cast grey iron (a common material for brake discs, specific heat 440J/kg.K) then the temperature of the brake assembly would be between 135°C and 380°C. These temperatures are probably higher than

those obtained in reality as normal private passenger vehicle specification brake pads are subject to a temperature limit of approximately 300°C, although higher performance road specification brake pads operate up to 450°C.

With this RBS element of this project the lack of an independently verified temperature profile of a braking system has been a source of consideration. It would have been helpful to know the range of temperatures experienced by a braking system before, during and after a braking manoeuvre. This is not readily available in the literature, probably because a manufacturer would regard this as commercially sensitive information. Some relatively recent papers [Cueva, 2003 & Eltoukhy, 2006], seeking to simulate wear characteristics in cast iron disc brakes, have quoted a maximum value of 240°C for normal road use. It is not certain that this is a relevant value as this was obtained from a normally ventilated system and is unlikely to be representative of a closed system. As a closed braking system is probably unique it is unlikely that any better data will be available from any other source. Therefore, this temperature value will be used as a desirable limit until better data is available. In any case it is certainly beyond the safe temperatures that can be handled by the polymers used in the construction of the test rig. What this does make clear is that a practical system would need to be built of materials that would not deteriorate at 250-300°C. This must include the flexible connections to the disc brake shroud.

For the moment the current test rig materials cannot deal with the temperatures that would result from a 90 kph braking manoeuvre so the tests will be limited to simulating a 50 kph braking manoeuvre.

It can be seen from the test results that the system air temperatures did not reach the temperature of 135°C predicted for the brake assembly. This was not a cause for concern as the system as a whole would not be expected to operate at the same temperature as the brake assembly, although some localised high temperatures close to the brake might be expected. What would be expected is a gradual air temperature rise once the vehicle starts to move again and heat gradually transfers from the brake to the air and from the air to the heat store.

6.8 Closed System Test Results

The results of the tests are shown in table 6.4

Table 6.4 Closed System Test Results

	Thermocouple Temperature °C				Initial
Time (s)	TC1 (inlet)	TC2 (mid)	TC3 (out)	TC4 (store)	Conditions
0	22	22	22	22	
125/0	96	67	63	24	Air Speed
120	78	63	59	31	V_{out} 3.5m/s
240	77	61	57	33	
360	68	61	58	34	Air temp
480	68	61	58	35	22°C
600	65	61	58	35	

The heater was turned to the cool setting after the 125 seconds necessary to deliver 100kJ into the system. This time is noted as 125/0 in Table 6.4. As can be seen, there is a steady increase in the temperature of the heat storage fluid as the air continues to circulate around the system although no more heat is being added to the system.

The energy transferred to the heat store was

1.5 x 3610 x (35-22) = 70,395J (η 70%)

The average rate of heat absorption is

70,395J/600 seconds = 117W

and is comparable to that in previous tests.

6.9 Observations and Conclusions Regarding Closed System Tests

- The most significant outcome of these tests must be the final efficiency value of 70%. Although obtained over a period of several minutes, this shows that even a basic system as this can achieve superior efficiencies to those exhibited by the highly developed RBS common amongst electric vehicles. It was achieved using initial temperatures that were probably not as high as would occur in a real braking system and, therefore, with a lower average temperature gradient than might be expected in a real system.
- Gas bubbles formed inside the heat store and particularly on the heat pipes themselves. The bubbles would have an insulating effect, reducing the heat transfer from the heat pipes to the storage fluid again reducing the efficiency of the system. The development of a finning arrangement for the heat pipe condenser would reduce this and must form part of a practical system.
- A temperature gradient formed within the heat store. This was noticed when the thermocouple probe TC4 was moved vertically and it was necessary to ensure that the probe measurements were always taken at the same height within the store. It was mentioned earlier that assisted convection might be beneficial, and this should be investigated.

- At the end of the experiment, the heat store fluid expanded sufficiently to cause a substantial overflow from the filler hole. Once the fluid had returned to the ambient temperature it had contracted to the point of the top of the heat pipe condensers being exposed. Perhaps this should have been expected. It was considered and allowance had been made for expansion, but, obviously, not enough. With hindsight an expansion tank should have been included in the design. This would have allowed the fluid to expand and contract whilst leaving the main tank full.
- The ducting manifold did not allow testing of the heat pipes in parallel mode. It was a mistake to close off this option so early in the testing procedure, given the poor performance of the downstream heat pipe.

7. Design and Testing of the Prime Mover

This project has used a unique design of motor for converting the energy of compressed air into mechanical movement. That design is a rotary multi-vane expander with many aspects of its geometry being variable, some whilst the expander is in operation. This chapter describes the origins and design criteria that have lead to that design. The purpose of this expander design was to maintain a high level of efficiency across as wide a range of operating speeds as was practical.

7.1 Initial Design Considerations

The appropriate basic design of the prime mover was not immediately clear. Past Compac designs have used some form of piston/cylinder arrangement but have not been particularly successful. Some have adopted this arrangement because it was the most readily available in the form of existing machines that could be adapted. Others have constructed their own design but based on steam engines or IC engines. Various forms of turbine have been used for motive power in the past and so there was every reason to think that a useful design would be practical for this application.

There are two basic types of machine for converting the expansion of gases into mechanical work. Known as expanders, one type is a positive displacement process that directly uses the pressure of expansion, e.g. a piston/cylinder arrangement. The other converts the enthalpy to kinetic energy and then to mechanical work, e.g. a turbine. Large scale comparisons of such machines are few but a useful study was carried out by Curran [1981] focussing on Rankine cycle engines using various organic working fluids. None of these were for mobile installations and so no comparison of system weight or cost was attempted. However, the purpose of the

study was to compare system capabilities and performance. The general conclusions were that low speed (≤ 5000rpm) machines were predominately positive displacement designs and high speed machines (≥ 5000rpm) were turbines. Also, the low speed designs had a power output in the order of 10kW, although some could achieve 100kW, whilst all of the turbines power output was ≥10kW.

Further comparisons have been attempted using the Mach number and Reynolds number, of the working fluid at the inlet to the machine, and two further parameters, the specific speed and specific diameter. Barber and Prigmore [1981] discovered that the Mach and Reynolds numbers have only secondary effects on the performance of the expander which could now be represented by the two parameters, specific speed and diameter.

The specific speed is a measure of the rotational speed of the expander's rotor, for a specified volume flow rate and enthalpy change through the expander and is defined in equation 7.1.

$$N_s = \frac{NQ^{1/2}}{(\Delta h)_{is}^{3/4}} \qquad \text{Eqn.7.1}$$

The specific diameter can be regarded as a measure of the size of the machine and is defined in equation 7.2.

$$D_s = \frac{D(\Delta h)_{is}^{1/4}}{Q^{1/2}} \qquad \text{Eqn.7.2}$$

In an earlier study Balje [1962] used these parameters to compare expander types in the form of N_s-D_s diagrams. These are not reproduced here but the indication was that in the low specific-speed regime positive displacement expanders exhibited superior efficiency to that of single stage turbines. Balje also found that rotary

positive displacement (rotary piston and multi vane) expanders exhibited about the same efficiencies as the pressure staged single disc turbines, of a similar specific diameter, but at only one third to one quarter of the tip speed values. It is also known that the efficiency of a turbine will reduce if it operates at speeds other than its design speed and, as a consequence, normally require a substantial gearbox to match the turbine speed to that of the driven equipment.

The above studies had an interest in evaluating expanders for use in solar energy Rankine cycle systems. In these systems a solar collector would heat an organic refrigerant that would then drive an expander that would in turn power a pump or generator. Because of the intermittent nature of the power source it was concluded that turbines would always suffer from low off design speed efficiencies and that positive displacement expanders had several advantages in this type of application. These are: (1) high efficiency (2) moderate operational speeds and large speed reducing gearboxes not required (3) good off design performances (4) only simple control systems required (5) low cost (6) compact and (7) can be built with normal workshop technologies. A Compac would also benefit from these requirements and would have similar variations in power output that would make a turbine an inefficient prime mover. For these reason it was concluded that any form of turbine must be excluded from the range of designs to be considered further.

There are three types of positive displacement expanders in common use. These are the reciprocating piston expander (RPE), the rotary piston (the Rootes two lobed rotors and the Lysholm helical screw system) expander (RoPE) and the rotary multi vane expander (MVE). It must be acknowledged that reciprocating pistons have been

developed to a high standard and to a lesser extent the RoPEs have seen much development as pumps. The MVE is used as a small rotary actuator in industrial systems but is seen as a cheap low efficiency device and has received little development. Nonetheless, rotary positive displacement expanders could compete with the reciprocating expander because of two advantages. The first is that the rotary designs use ports rather than the poppet valves of reciprocating designs. These ports have much superior breathing characteristics and avoid the complicated, and expensive, valve timing gear required for poppet valves. The second advantage is that rotary designs are inherently better balanced than reciprocating machines because oscillating masses such as connecting rods and crankshafts are unnecessary. This translates into mechanical simplicity, compactness, lower weight and less cost.

From the foregoing it would appear that the rotary designs were appearing as clear leaders as the basis for a Compac prime mover but that is not the case. The superior breathing characteristics of ports are desirable but some of the poor characteristics of poppet valves could be overcome by simply increasing the pressure in the inlet pathway. In IC engines this requires a compressor but in a Compac the compressed air is stored at 30 MPa. As the system has to use a throttling valve to regulate the air pressure to a much lower level, supplying a higher inlet pressure is simply a matter of adjusting that valve. Such valves, and the poppet valves, are isenthalpic devices and, in reality, little or no energy is lost across the valve. There would still be some back pressure caused by the exhaust valve but this is not a disadvantage that would obviously block the concept.

That the mechanical complexity of reciprocating designs is great, compared to rotary designs, is an accurate assessment but not a practical barrier for the purposes of this project. Small 4-stroke engines are readily and cheaply available and could be converted to expanders by changing the valve timing drive gears and the camshaft. Presumably something of this nature was done by the early Compac pioneers referred to in chapter 2. On the other hand, although superficially simple, the RoPEs require very accurate and complex machining to manufacture their rotors to high standards and tolerances to prevent substantial leakage. Also, they are not readily available. Furthermore, RoPEs normally have higher specific speeds than RPEs and will probably need a multi ratio gearbox for matching power and speed to demand.

The MVE is a rotary, low-speed, positive displacement machine that remains simple in design and cheap to manufacture. It would be an ideal machine in many respects except that the current examples are small air motors, operating at low expansion ratios and low efficiencies. They are common devices in industrial applications and their low efficiency (early values were 25 – 35%) is tolerated because they operate for only short periods and therefore total energy consumption is small. Also the poor efficiency is balanced by the low cost, high reliability and compactness. In the early 1970's several studies [Gill & Shouman, 1976] were carried out to improve the understanding of sliding vane air motors. These succeeded in improving their efficiency to over 50%. Gill and Shouman concluded that by controlling tolerances and using appropriate port timings the efficiency could be raised to well above 80%. Badr, et al [1984a] refers to several studies that quantify the power losses in air motors. 65% of power losses were due to the pressure drop at the inlet, 20% of the losses were due to leakages and the remaining 15% were due to friction and outlet

pressure drops. Although these do not refer directly to energy efficiency they provide some indication of what factors should be considered and their relative importance. The pressure drop across the inlet will, probably, be isenthalpic, as with a throttling valve, and does not represent a loss of energy from the system. Therefore, real losses may be confined to the 35% represented by the 20% leakages and 15% friction and outlet pressure drops and these are the areas to address when considering efficiency improvements.

Leakages and friction can be reduced by improved tolerances and attention to seals but pressure losses through the outlet is an old problem and will increase with increased inlet pressures. This problem is addressed further in section 7.3.

7.1.1 The Cranfield Vane Expander Group

At this point it is useful to mention the vane expander research programme at the Cranfield Institute of Technology, UK. which was set up in the late 1970s. O. Badr , mentioned above, was a founder member of that group. At the time there was much interest in using Rankine cycle systems to convert low grade heat, from solar collectors, into work or electricity. All of the machines mentioned in 7.1 above were considered as potential converters for such systems. Many academics were interested in using the MVE as it was perceived as having a number of desirable features and these were summarised at the end of Badr, et al, (1984b), as follows:

(1) Simple Construction
    Easily machined to tight tolerances
    Conventional shaft seals and bearings
    Easily lubricated
    Self Compensating for wear
    Compact, lightweight and rugged
    Requires little maintenance
(2) Low Noise and Vibration

Low speed
No dynamic valves or gear train required
Intrinsically balanced

(3) Potentially High Brake Efficiency over wide ranges of
Shaft powers
Speed
Working fluid mass flow rates
Available energy inputs

(4) High Torque at Low or Zero Speed
Self starting under load
Speed compatible with driven equipment
Smooth torque production without the need for a flywheel

(5) Relatively High Volumetric Expansion Ratios
Range up to 10 via a single stage expansion
Easily adjustable expansion ratios

Of the remaining problems to be solved, the mechanical problems were: "Reduction of breathing problems and the corresponding problem of optimal port timing," and "inherently high internal leakage losses and frictional dissipations of the expanders".

The Cranfield vane expander group was set up to address these final problems by investigating two existing designs and constructing mathematical models of them. The mathematical models cannot be considered a particularly successful as they underestimated the two MVEs output by 26 - 40%, Badr et al, [1985d]. However, their investigations did quantify the major sources of losses although no significant design solutions to those problems were suggested or attempted. Those solutions that were attempted were improved tolerances/fitting of the vanes to their space and improved port timing.

It might be thought that the above list of advantages made a clear case for pursuing the MVE design, but it must be understood that the machines to which this list applied were quite small. They were usually of less than 10kW output and the

Cranfield units were both less than 2kW. All were for static installations and closed Rankine cycle systems. It was not clear that the advantages of this design would apply to a larger, more powerful, mobile installation operating on the Brayton cycle.

7.1.2 Friction Losses

Friction and viscous drag are not substantial sources of losses for RoPEs as the intermeshing rotors are machined to high tolerances to ensure that they maintain pressures without actually touching. Only the bearings are lubricated and suffer from viscous drag. This is not the case for either the RPE or the MVE. Both pursue increased pressure sealing by forcing metal seals onto moving metal surfaces.

In the case of the RPE, the sealing system is similar to that used for a piston IC engine and the losses are proportional to the piston speed and the reaction force from the pressure above the piston. This latter force causes an increase in side thrust resulting from the crankshaft and connecting rod angle.

In the case of the MVE the major source of friction is at the vane tip and stator casing interface and the total friction is related to the vane tip speed [Badr, et al 1985e]. As an indication of the losses, in that study, reductions in mechanical efficiency are mostly due to friction. At 3000 rpm mechanical efficiency was approximately 85%. There was not much friction involving the vane ends which do not normally touch the endplates. This is because the vane is normally shorter than the internal axial length of the MVE. The purpose of this is to reduce friction and reduce the risk of the vane expanding and jamming between the endplates.

A long consideration of the detailed sources of friction losses is warranted in any machine design and there are number of friction reduction techniques and materials that could be applied to these machines. That will be done in a later chapter but here a more general consideration of friction losses is appropriate. In air motors the handling of such losses could be different from that of similar machines operating with different working fluids and temperature regimes. The Rankine cycle machines examined by the Cranfield vane expander group operated at a temperature of approximately 110ºC. Air motors operate at temperatures at or below the ambient temperature and it is part of the system proposed in this project that low grade heat from the environment be drawn into the system by the cool working fluid (chapter 5). The process of friction quickly converts the kinetic energy of the moving components into heat that will raise an air motor's temperature. As the compressed air stream is never at more than 5 -10ºC below the ambient temperature it could act as a coolant if part of that stream were circulated through a cooling jacket adjacent to the area where the friction is being produced. After absorbing the waste heat the cooling stream would be passed on to the motor inlet and would expand through the motor doing more work than if it had been left at its original lower temperature, thus reclaiming the energy that would be lost to friction.

This is not to say that friction in air motors shouldn't be tackled in the usual ways. It still has the undesirable effect of reducing the motor's power output. The cooling jacket would also have the effect of reducing motor power by producing drag and reducing the air mass flow. This could be overcome by adjusting the regulator valve, and increasing the air stream pressure, at no energy cost, as explained in 7.1 above.

If the heat of friction can be reclaimed in this way, and there is no reason why at least part of it can't, then the friction producing differences, between the designs, are of limited value when trying to separate them from the standpoint of efficiency.

7.1.3 Loss of Pressure in the Outlet Stream

A straightforward consideration is the loss of pressure energy through the outlet stream. This has long been a concern to design engineers dealing with Rankine cycle engines. The problem is that in order to maximise power the mass flow of the working fluid must also be maximised. This is always achieved by ensuring the input high pressure stream should be at as high a pressure as is practical. As operational power requirements vary, that pressure will vary and if the ratio of input pressure to the ambient pressure exceeds the expansion ratio of the machine then there will be a substantial drop in pressure along the outlet tract, representing a loss of energy to the atmosphere. The conventional solution to this problem is to have a large expansion ratio resulting in a large, often slow moving, machine. Steam engines used a double expansion process whereby the high pressure exhaust stream from a small high pressure cylinder was passed to the inlet of a large low pressure cylinder. A similar arrangement was used in the "Spirit of Joplin" Compac (Pneumacom, 1994). Whilst this improves efficiency during high pressure usage, during low power low pressure usage, such as low speed city motoring, a vacuum would occur in the final expansion stage resulting in a loss of power.

The conflicting requirements of power and efficiency across a wide range of operating conditions arise from the fixed geometry of the engine designs and could be solved by a design that used a variable expansion ratio (VER). For piston engine

designs, the technology would be similar to that required for a variable compression ratio (VCR), a highly desirable feature for IC engines. VCR designs varying the position of crankshaft journal bearings, the length of crankshaft throw, the length of the connecting rod and the height of the piston crown have all been attempted by capable engineers and manufacturers. These are complex mechanisms and, for reasons of reliability or cost, none of these designs have been applied beyond the laboratory, as is evidenced by the fact that there is no VCR system in widespread use today.

When considering the matter of a VER for the rotary machines described so far, it must be noted that the RoPEs have a fixed geometry that is even less conducive to variation than the RPE and it is hard to see how any form of VER would be practical with them. However, the general form of the MVE has been used as a variable displacement hydraulic pump [Parr, 1991], see Fig 7.1, and a similar mechanism could act as a reliable VER for an MVE.

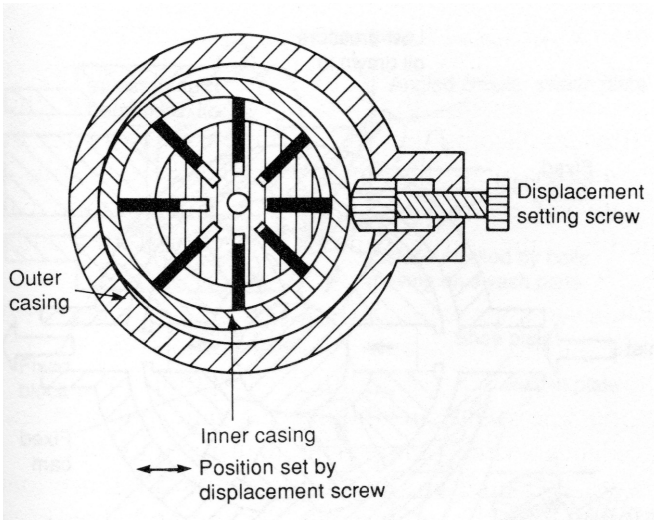

Figure 7.1 Variable Displacement Vane Pump

The axis of the internal rotor is fixed but the casing can be moved laterally allowing the minimum and maximum extension of the vanes to be varied which also varies the

minimum and maximum capacities of the chambers between the vanes. The primary purpose here is to vary the hydraulic fluid displacement and power requirements of the pump. However, It can be seen that any lateral offset will have the effect of reducing the volume of the smallest chamber whilst increasing the volume of the largest chamber and thus increasing the expansion/compression ratio if used with acompressible fluid.

7.1.4 Internal Leakage Losses

It is essential that a Compac prime mover has low air leakage at low vehicle speeds. It is expected that such vehicles will be used primarily for city commuting and will need to perform well at low speeds. If a large gearbox is to be avoided then high torque at low speeds is essential and low leakage, to maintain efficiency, is highly desirable.

There appears to be no air leakage data available for a conventional IC piston engine acting as an air motor but, as they are designed to contain the high pressures of combustion, it should be presumed that the level of sealing is good. The static torque, of an IC engine, would be a useful proxy indicator of its sealing quality as both are related by the pressure that the piston rings exert on the cylinder wall. A small single cylinder spark ignition engine was available for inspection, and, with some lubrication and its spark plug removed to prevent pressure build up, its static torque was measured at approximately 8.5 Nm. This was considered to be quite high and was taken to indicate good sealing. In an attempt to measure leakage directly the same engine had its driveshaft locked in place with its poppet valves closed and its cylinder pressurised via the spark plug mounting hole. There was a lot of leakage

from several areas (crankcase, inlet and exhaust tract) and so it wasn't possible to measure the leakage from around the piston. The problem was presumed to be poor sealing by the poppet valves.

The RoPEs are designed to seal well at higher shaft speeds but it is generally accepted [Badr, O. et al, 1984a] that they do not seal well at low shaft speeds and, apart from making the currently close tolerances even closer, there is no clear way to improve the design.

The current designs of MVEs do not seal well at most speeds but this is considered to be a problem of low build/design quality [Badr, et al, 1985c]. The Cranfield Vane Expander group identified six main pathways for internal leakages and these were all considered to be capable of being improved. The group applied some of their general recommendations to an existing design of circular MVE and obtained an isentropic efficiency of approximately 73.2% [Badr, et al, 1986]. This was due to several optimisation procedures and not due solely to their anti-leakage recommendation (improve vane tolerances). The mathematical models that were developed out of these studies suggested that a fully optimised MVE could achieve an isentropic efficiency of 90%. It should be noted that these models consistently underestimated the measured performance of the actual machines.

7.1.5 Basis for Final Design of Prime Mover

The RPE was a competitive machine which, given the length of it development history, was no surprise. Scavenging of the heat created by friction and careful control of the inlet pressures to prevent excessive outlet pressures would yield an

efficient machine. However, the valve mechanism is complex and absorbs power, creates friction - the heat of which would be hard to recapture and the whole machine tends to be large, heavy and complicated. These latter characteristics all increase cost. Nonetheless, the ready availability of used examples made it an attractive prospect for conversion to air motor operation. The further downside to such a project is that the design solutions are relatively simple, are reasonably certain to work moderately well and would, therefore, add little knowledge to that about an already well understood machine.

The MVE is not a well developed machine but its potential advantages, enumerated in 7.1.1 above, make it an attractive prospect for many applications. The work of many researchers, including the Cranfield Multi Vane Expander group, has mapped out the path to a more efficient machine but that group's efforts were the last significant effort to appear in the literature. Reports have appeared concerning new applications but the machines used are essentially the same as those investigated by the Cranfield group. In the course of the consideration of these machines it was realised that there were a number of possibly innovative solutions to the problems previously identified. These solutions will be detailed in later sections but it seemed possible to build a machine that could have many aspects of its geometry able to adapt to its operating conditions. Some adaptation could be implemented whilst the motor was in operation and this presents the prospect of a control system that could optimise some of the motors parameters whilst it is operating in a real world system.

The project remains focussed on a practical automobile system but the smaller Rankine cycle systems, of the type focussed upon by the Cranfield group, would

benefit as well. It is this prospect of building a genuinely useful research machine, for a broadly applicable design, that has made the MVE the clear choice as the prime mover for this project.

7.2 MVE Design Overview

There are five major design requirements to be met by the proposed MVE. These are:

1. A variable expansion ratio.
2. Variable port timing.
3. Reduce leakage around the vanes.
4. Reduce leakage around the rotor.
5. Capture and re-use the heat of friction.

All of the major components are shown in Figure 7.2.

To achieve the first requirement, a VER, the rotor axis will be fixed with the axle in rigid bearings enabling a reliable power take-off, but the stator position can be offset, in a fixed radial plane, by 15mm. This enables the vane extension to vary from 0 mm to 30 mm at full offset but also for the vane extension to be 15mm at all positions placing the rotor in a balanced, neutral, state. This is close to the design in Figure 7.1 but it has only one casing. In the constructed machine a screw mechanism, attached to the endplates and mounting frame, varies the offset but locks it in position for each experimental run. It is intended that this mechanism be replaced by a more robust system that enables the offset to be varied whilst the motor is in operation. It is also intended that the control mechanism for the offset be set to maintain a pre-determined outlet pressure.

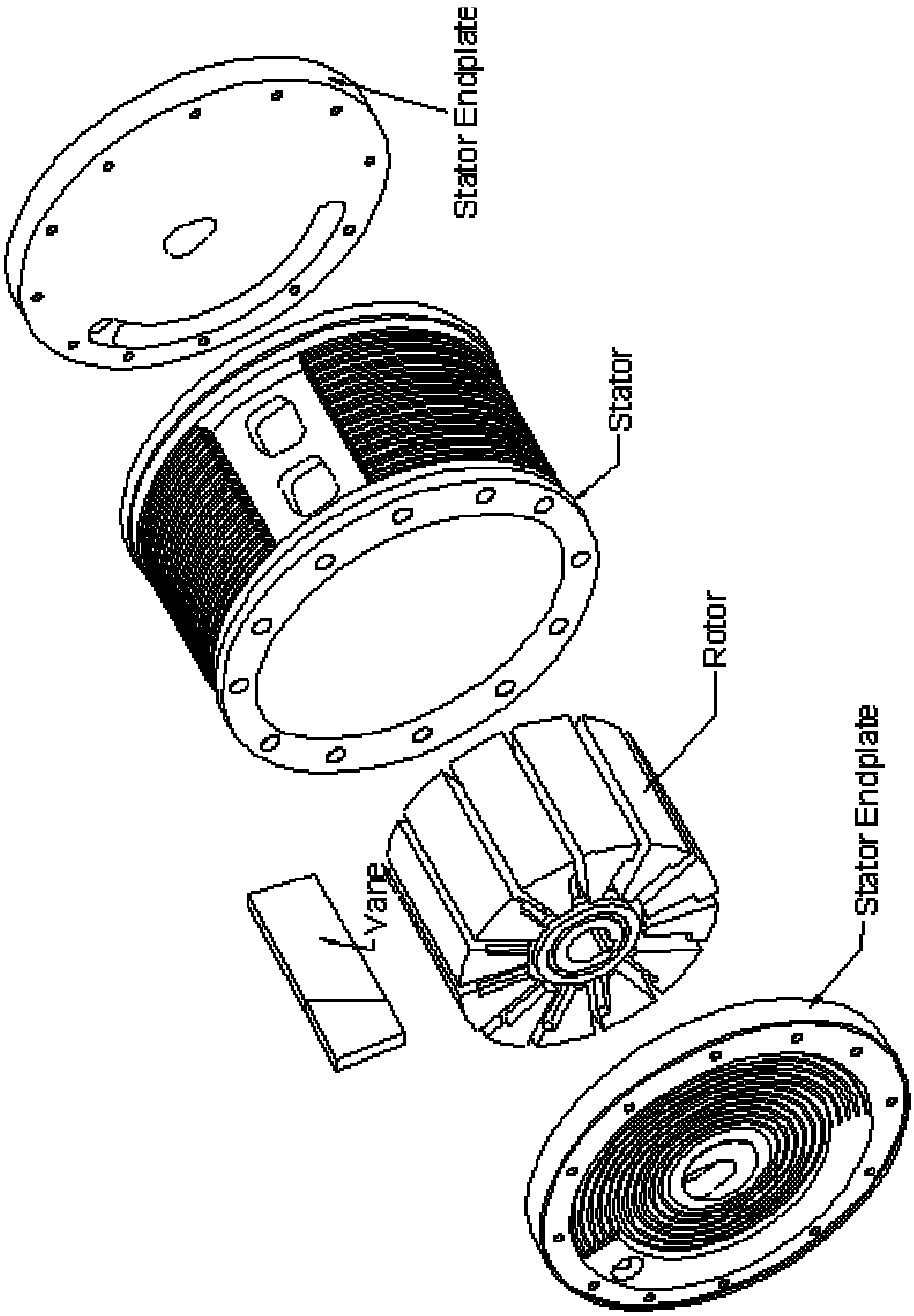

Figure 7.2 Air Motor – Major Components

Figure 7.3 The Major Machined Components of the Air Motor

The second function of variable port timing is achieved by having the inlet ports in the stator casing and the outlet ports in the endplates. The endplate fixing bolts are placed at 30º intervals and so the inlet and outlet ports can be separated in 30º increments. More importantly, the endplate axle hole is trianguloid with a 30º apex angle, which enables the casing to be rotated in relation to the radial offset plane. This means the port timing can be changed, in relation to the rotor, over a 30º range. Currently this is achieved by varying the length of brackets supporting the casing but a screw mechanism, that could rotate the casing in fine increments, is certainly possible.

The third and fourth requirements are guided by the Cranfield group's identification of the leakage paths through the MVE, [Badr, et al, 1985c] quoted below.

"The most significant of these are:

1. Along the axial clearances between the rotor and the two endplates.
2. Along the tips of the vanes via the radial clearances created between the tips of the vanes and the stator cylinder if there is a loss of contact, especially at low rotational speeds, i.e. when the centrifugal forces, experienced by the vanes, are small.
3. Via the axial clearance gaps between the sides of the vanes and the endplates.
4. Through the radial clearance region between the rotor and the sealing arc of the stator cylinder. [Refers to the shortest path from the inlet, against the direction of rotation, to the outlet. Only partly relevant to this design].
5. Through the pressurising slots on the trailing faces of the vanes and the clearance regions between the faces of the vanes and the side walls of the rotor's slots.
6. From the high pressure chambers in the rotor slot cavities, beneath the vanes, through the axial clearance regions between the rotor and the two endplates"(p.6).

The third requirement of reduced leakage around the rotor vanes is to be addressed by vanes of variable axial length and spring assistance to tip sealing at low speeds. The Cranfield group identified leakage around all the edges of the vanes as major internal leakage pathways. Tip leakage was primarily a problem at low speeds as centrifugal effects ensure good sealing at higher speeds. Normal designs have a pressure bleed pathway, either in the vane or the vane slot, carrying pressurised working fluid to the base of the vane slot from the high pressure side. This increases pressure at the base of the vane, pushing it against the stator wall but also promotes pressure leakage around the vane and rotor. In early designs helical springs were used but problems were experienced with them distorting and binding in the vane slot. The pressure bleed technique was not ideal but was reliable. This technique may be used in the future of this machine but the current method is to use a double leaf spring that takes up little space and is resistant to binding.

Leakage around the sides of the vanes was caused by loosely fitting the vanes in order to avoid excessive friction and binding of the vane between the two endplates. The design used here involves a three part vane that will expand axially driven by the pressure from the wedge shaped middle vane component. At zero to low rpm the source of that pressure will be the spring acting at the base of the vane but the vane will be driven more forcefully once the centrifugal force becomes dominant.

The fourth requirement of reducing the leakage around the rotor ends is to be dealt with by some steel reinforced butyl rubber seals of complex shape and construction but otherwise normal design.

The fifth and final requirement is to capture the heat produced by friction and use it to increase the enthalpy of the compressed air stream. The compressed air stream is to be divided before it reaches the motor. One stream will go direct to the inlet ports and the other will first go to the cooling jackets in the endplates and then to the cooling jacket surrounding the periphery of the stator, at the end of which it reaches the inlet ports. The cooling jackets consist of finned galleries adjacent the areas of highest friction. These are machined into the outer faces of the endplates and the periphery of the stator and are, initially, open to the atmosphere. Once the motor is to be assembled they are sealed by covering plates that also carry the pipe connections.

No attempt has been made to model the heat transfer in the cooling jacket. The design is predicated on the presumption that the heat will build up, in the metal components, until an equilibrium point is reached with the rate of heat transfer into the compressed air flow. The design has attempted to place an air flow across most of the areas that would conduct heat out of the motor. This hasn't been achieved 100% of the time as the edges of the casing are potential pathways that structural integrity requires remain as solid metal. Also it is expected that some heat will be transferred into the compressed air stream within the motor. This is not a problem for the air within the expanding chambers as this would cause further work to be done. However, any heat transferred on the low pressure outlet side would be lost in the exhaust stream.

7.3 Motor Components

Whilst the general design of the motor components have adhered to some of the recommendations of the Cranfield group, it cannot be said that the motor that was built was entirely the preferred design. Many of the major dimensions of the stator and rotor were

largely determined by the available aluminium stock and a larger diameter design would have been preferred in order to increase the torque delivery and reduce any gearbox requirements. One of the effects of this is that the exact expansion ratio must be calculated from the final built dimensions rather than be specified in advance. This and other effects will be noted in the following sections.

7.3.1 Rotor and End Seals

The rotor was machined from a solid bar of aluminium 175 mm in diameter and 150 mm axial length. These dimensions were partly dictated by the available size of tube for the stator which had an internal diameter if 200 mm. This placed limits on the practical size of the the vanes and rotor. Additionally, Badr, et al, [1986], calculated that the ideal rotor aspect ratio (length/radius), for the machine most comparable to this design, was 1.3. This was the AR that delivered the peak of isentropic efficiency for the investigated conditions. Being a Brayton cycle machine, those conditions were not directly comparable to an air motor and , furthermore, the investigated machine's isentropic efficiency wasn't sensitive to higher AR values and it was judged that, for various practical reasons, 1.6 was a good compromise value. For similar practical reasons of fitting in a useful vane length and the necessary rubber seals, the diameter of 174mm (radius 87 mm) and a rotor length of 150mm were chosen. They were also chosen because they were close to that envisaged for a commercial product and were the maximum dimensions that would fit on the dynamometer. These dimensions provide an AR of 1.72 which was considered a practical compromise. Figure 7.4 shows an isometric drawing of the rotor and Figures 7.5 & 7.6 are photographs of the finished rotor. The full technical drawings, with dimensions, are in appendix B.

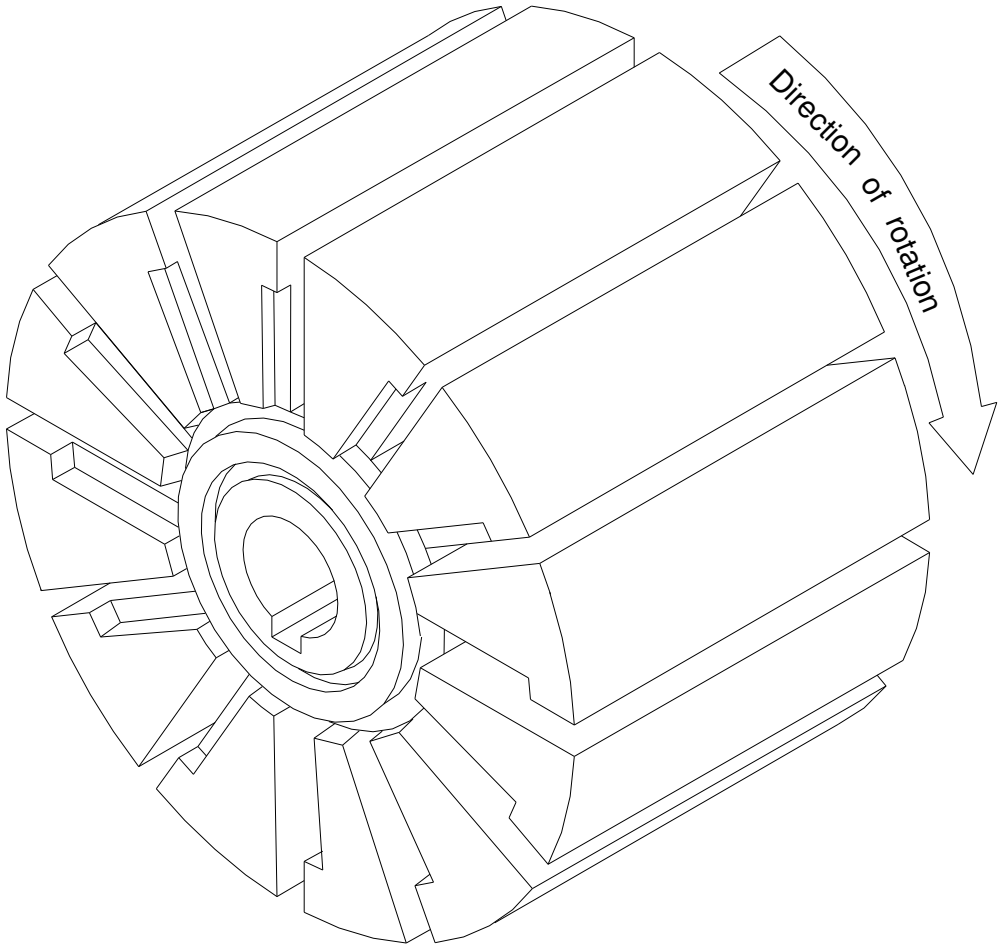

Figure 7.4 Air Motor Rotor

The choice of the number of vanes (12) needs to be justified as this seems to be the maximum that commercial machines use whilst the Cranfield group preferred eight. The reasons for this number was not well developed as their primary reason for preferring fewer vanes was a criterion named the “leakage efficiency”, [Badr, et al, 1985c]. This related the leakage around a chamber’s vanes to its volume. For a given length of vane edge, if a chambers volume was smaller than another chamber then its leakage efficiency would also be smaller. This was useful for their computer models but it did mean that an MVE with more chambers for the same capacity would score poorly on leakage efficiency. Underpinning this judgement was their belief that any leakage from a vane/chamber was a bad thing and in most cases this was

true. However, leakage from a high pressure chamber to a low pressure chamber that was still expanding would be isenthalpic and the working fluid that moved would expand into the new chamber, increasing the pressure there and doing work. The leakage is only a loss if the final expanding chamber has its pressure raised significantly above the minimum pressure required to keep the waste air moving out of the system. The Rankine cycle systems that they were investigating had higher than necessary outlet pressures and this was recognised as a problem.

An undoubted problem with increased vane numbers is increased friction but the design under consideration here will attempt to reuse that heat. A probable benefit of increased vane numbers is reduced overall leakage due to more barriers between the high pressure areas and the low pressure areas. This was intimated by one of the Cranfield groups other criteria, "leakage power," which related actual power output to the "leakage efficiency" and graphed it with the number of vanes as the variable. In this case the indicated power increased with the number of vanes. Little consideration was given to this finding.

In the design being pursued in this project increased vane numbers should increase efficiency and power and also spreads the stress of the torque producing pressure over more vanes, potentially improving reliability. Also, Badr, et al [1986] found that the expansion ratio is loosely proportional to the number of vanes. So, a higher number of vanes equates to a greater expansion ratio. For these reasons a higher than average number of vanes was chosen.

Figure 7.5 Air Motor Rotor

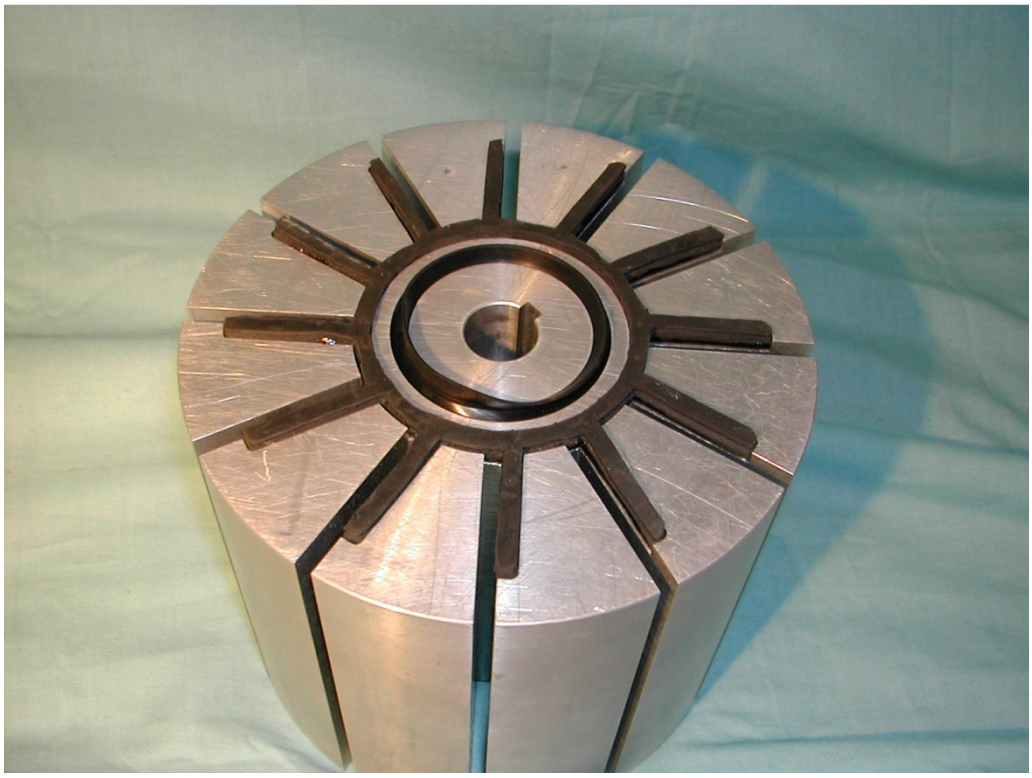

Figure 7.6 Rotor Endface with Butyl Rubber Seals Fitted

Figure 7.6 shows the rotor with the butyl rubber seals fitted. Both are “V” section seals with the mouth of the V facing the high pressure side. The inner seal is a commercial product and something similar is used on most MVEs to place a seal between the rotor and endplate axle hole. The twelve armed “spider” seal is unique to this design and is designed to block the leakage path (Cranfield No.1) between the rotor and endplates. This leakage flow path is shown in Figure 7.7.

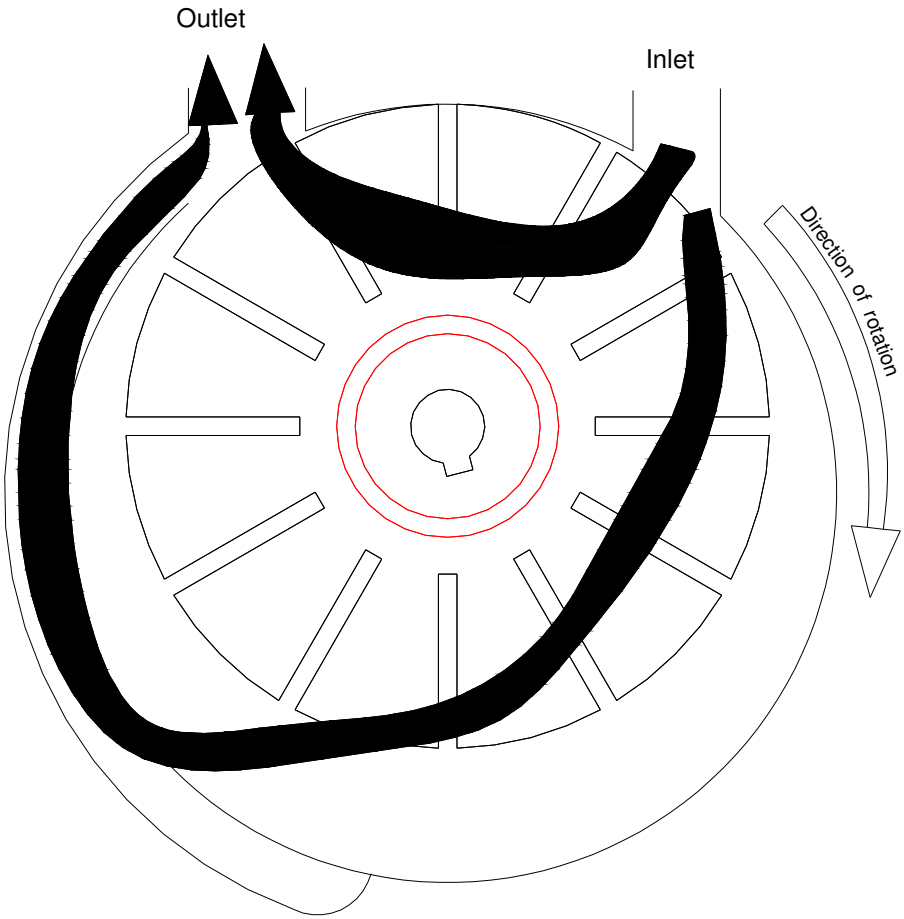

Figure 7.7 Leakage Flow from Inlet to Outlet Via the Rotor Endface (without spider seal).

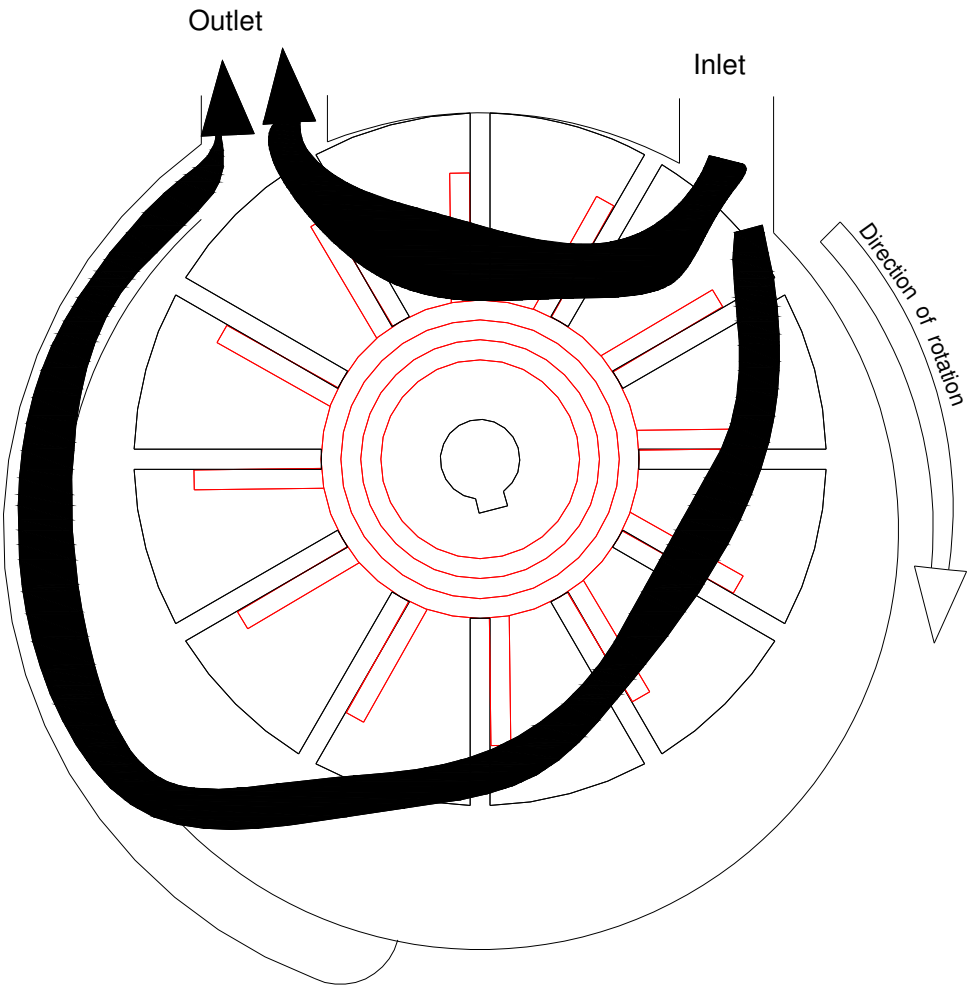

Figure 7.8 Leakage flow from inlet to outlet via the rotor endface (with spider seal).

The relationship to the spider seal is shown in Figure 7.8 above. The illustration should be considered in the context of the various vane positions. For the smallest chamber volumes, and the highest pressures, the vanes are almost fully retracted, sandwiching the seal between the vane and the seal location trench. The seal and vanes act together to block the high pressure flow. At the greatest vane extension positions, the largest chamber volumes and lowest pressures, the seal blocks the lowest part of the pathway and the vane blocks the upper part. The seal arm doesn't extend to the periphery of the rotor as it was preferred to have solid aluminium at this point for maximising the positive location of the vanes.

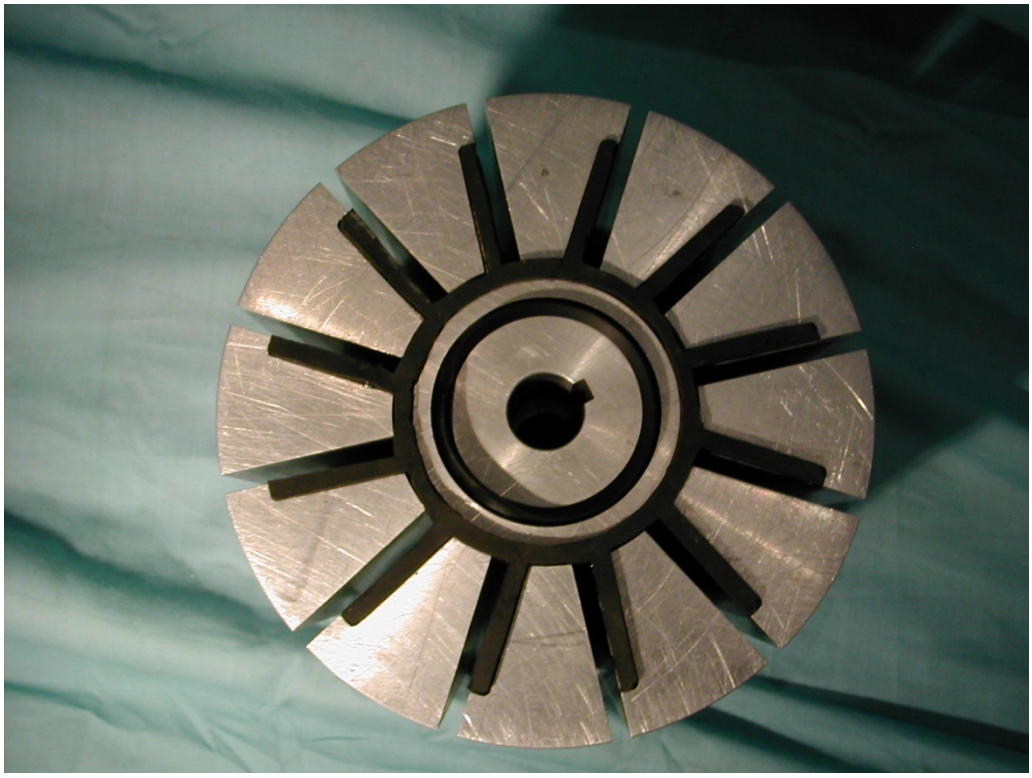

Figure 7.9 Rotor Endface with Butyl Rubber Seals Fitted

Figure 7.9 is a photo with a more clear orientation than Figure 7.6 showing the seals as they appear in the drawing in fig 7.8. The seals are held in place, on the rotor, by peg like extensions of the metal reinforcement that extend down from the seal arm tip. These extensions locate in corresponding holes in the rotor seal trench. Otherwise, there are no fixing or locating methods, other than the seal trench itself, and the seals are removable with little difficulty.

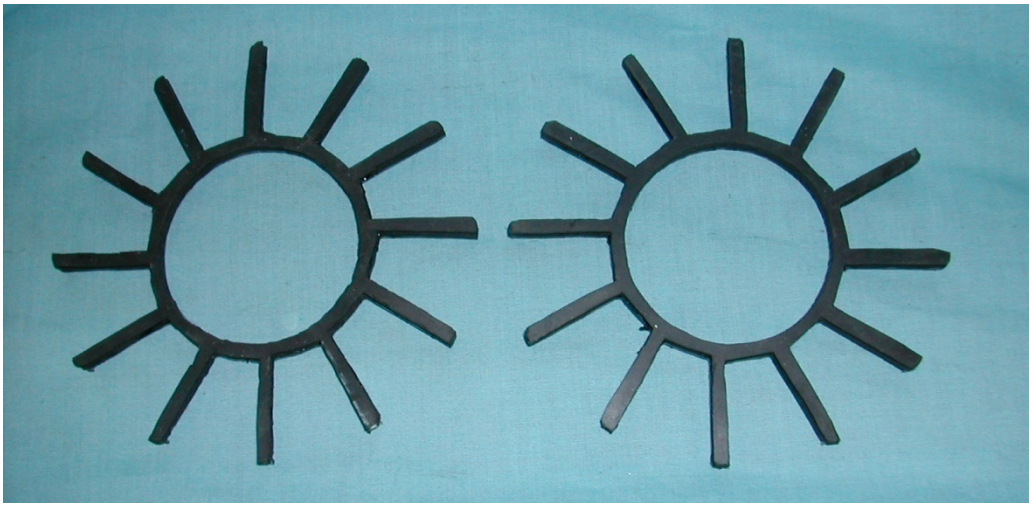

Figure 7.10 Both Spider Seals – Butyl Rubber Side

Figure 7.10 shows both spider seals together and it can be seen that they are not identical, with the arms being purely radial. They are mirror images of each other representing the pattern required for the left hand and right hand trenches that must trail the vane slots. Figure 7.11 below shows the same seals but with one reversed to show the metal reinforcement attached to the underside of the rubber seal. The attachment is by a cyanoacrylate adhesive.

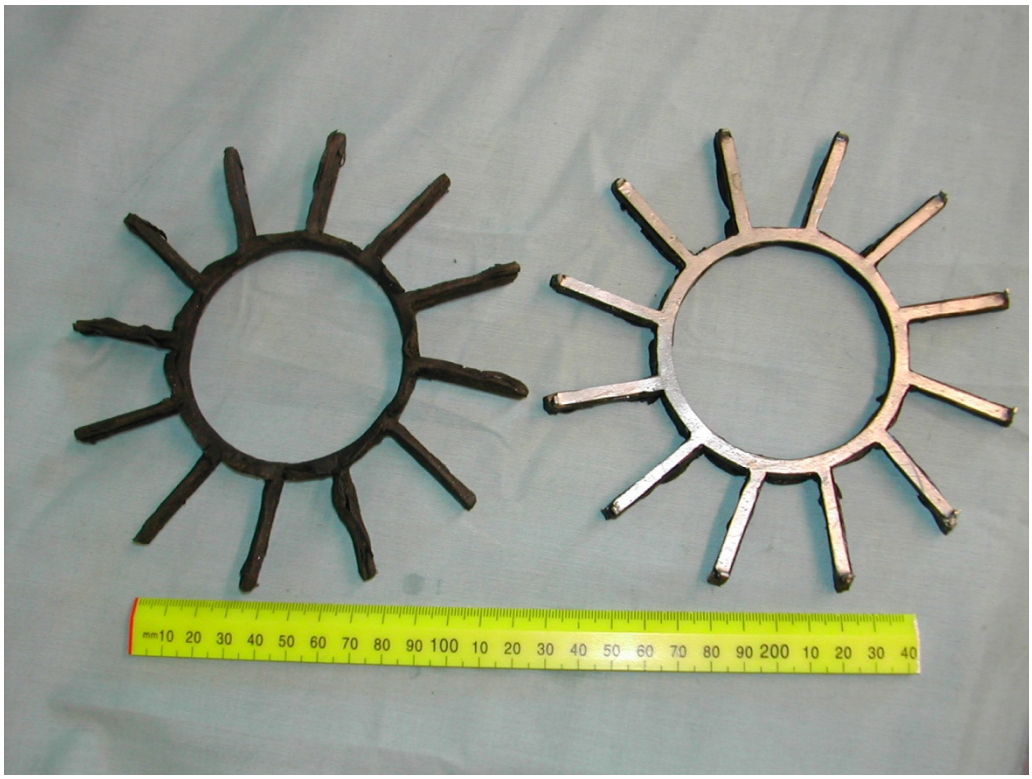

Figure 7.11 Spider Seals – one showing the steel reinforcement attached to the underside

7.3.2 Adaptive Vanes with Spring Assistance

Pathways 2, 3 & 5 of the Cranfield leakage analysis refer to the leakage around the vane tips, between the stator wall, around the sides between the vanes and the endplates and, finally, between the vane and rotor slot.

The first of these is leakage around the vane tips whilst the MVE is operating at low speed. The past solution to this problem was to have a pathway, for the pressurised working fluid, to be machined into the surface of the vane on its high pressure side. This would leak high pressure fluid into the area at the base of the vane pushing the vane upward against the stator wall. This was of limited effectiveness as the Cranfield investigators could hear the vane "judder" at low speeds. In the conclusions of Badr, et al, [1985c], it was suggested that spring assistance might be helpful at low speeds but no design of springing system was suggested. It was mentioned earlier that this "high base pressure" system replaced earlier helical springing systems that had proven unreliable due to distortion and binding of the springs. Furthermore, this system was adopted although it clearly promoted increased leakage and is the cause of the leakage pathway number 5.

For the current design it was decided to attempt a reliable "spring only" system. This was because sealing the rotor slots against leaks to the downstream low pressure side was perceived as much more difficult than simply placing another sealing arm, of the spider seal, on that side. Helical coiled springs were not considered for the reasons already mentioned. The photographs of the final design are shown in figures 7.12 & 7.13.

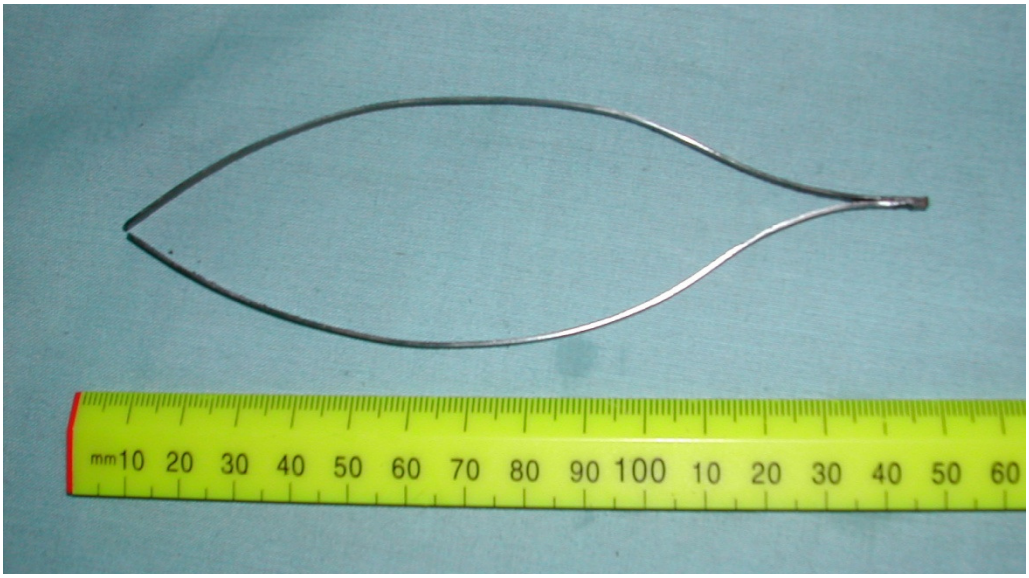

Figure 7.12 Vane Support - Double Leaf Spring

The spring is constructed from two plain spring steel elements of dimensions 150 x 4.5 x 1 mm spot welded at the left hand end. The width across the span of the two curves is 45mm and the right hand ends are free to move independently. The upper and lower springs have, as closely as possible, identical curves which are as smoothly curved as possible in order to minimise any stress concentrations when the spring is compressed. The intention of the spring design is that it floats freely in the rotor slot but slightly compressed between the base of the rotor slot and the vane at its maximum extension. The centre of the curves bear upon the centre of the base of the vane and the centre of the base of the rotor slot. The spot weld maintains the stability of the two springs in relation to each other but otherwise the springs can move within the slot. The springs will be kept flat, across their 4.5 mm width, when pushed against the base faces of the vane and slot and should be able to slide in the rotor slot without binding. When fully compressed the springs will be flattened against the base of the vane slot. When flat the length of the springs will be the same as the axial length of the rotor. This will occur once every revolution and will have the effect of centring the

spring in the rotor slot. The spring ends are radiused in order to prevent gouging of adjacent surfaces. Figure 7.13 shows three springs in different orientations.

Figure 7.13 Double Leaf Springs in Various Orientations

The springing rate of these springs has not been measured accurately but they require a force of approximately 0.6 kg to compress them completely which would be 0.013 N/mm.

The remaining leakage path, number 3, through the clearance gaps between the sides of the vanes and the endplates, cannot be adequately dealt with by the Cranfield suggestion of improving the fits and tolerances. This is due to the requirement that the axial length of the vane is a sliding fit at the vanes highest temperature, in order to prevent the vane and rotor seizing. Current rotary vane machines use a vane design that is a solid plate and little effort has been put into improving this design. However, a similar mechanism, the rotor apex seal of a Wankel engine, Figure 7.14, has been developed to adapt to the available space whilst wearing to a better fit. The common designs for the tip seal [Yamamoto, 1981] are shown in

Figure 7.15, the top most (7.15a) being the earliest design and the bottom most (7.15c) being the latest design.

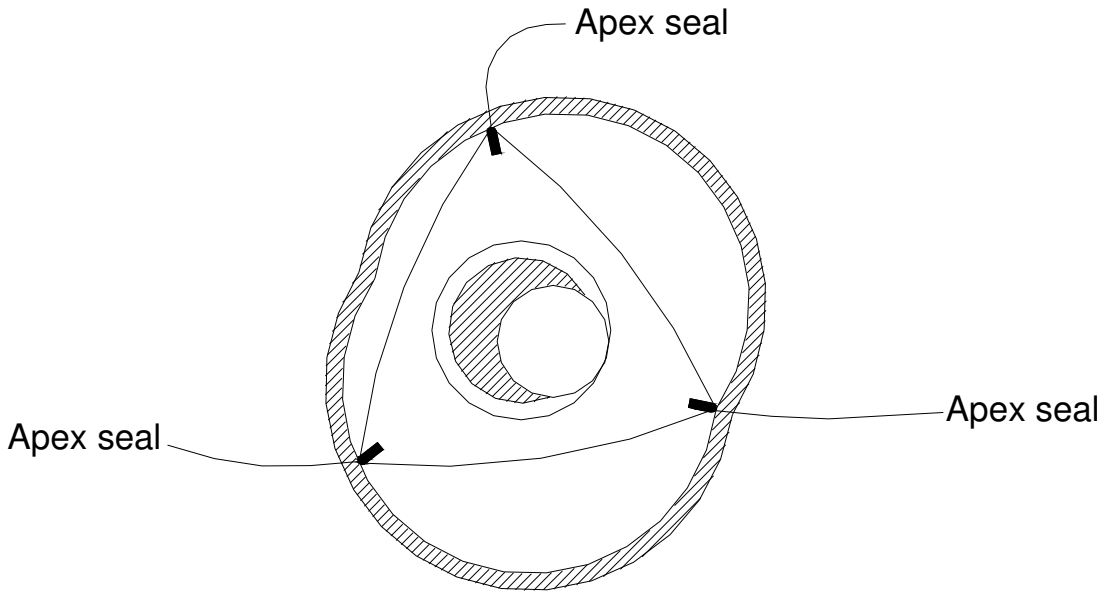

Figure 7.14

A simple schematic of a Wankel engine - showing the position of the three apex seals.

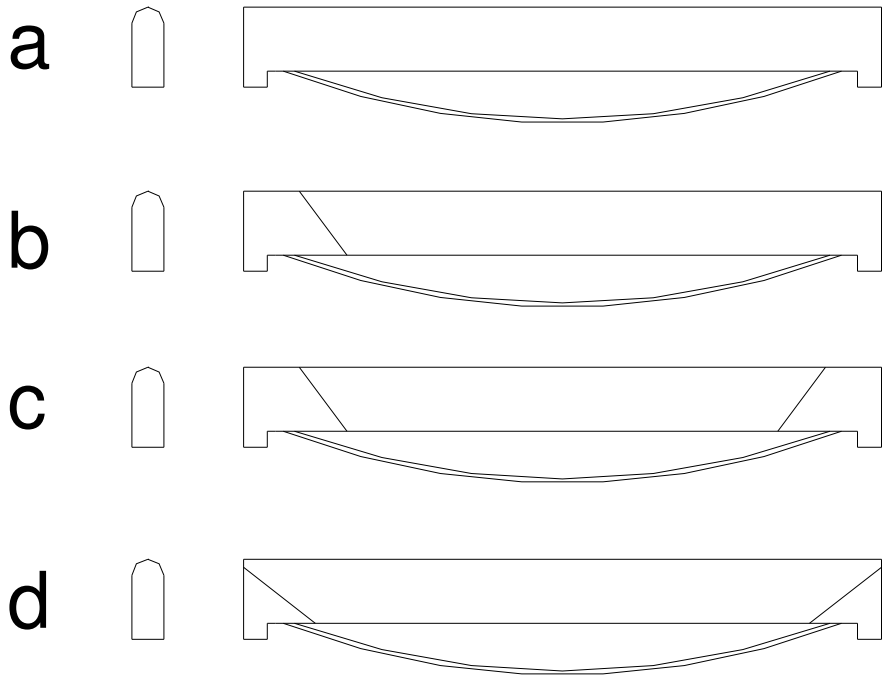

Figure 7.15 Wankel Engine Apex Seal Set

The tip seal designs are not directly applicable to a rotary vane machine as the aspect ratio is very different and there isn't the same degree of sliding in a tip seals dynamics. An effective compromise design is shown in Figure 7.16. This is a two piece design after the form in Figure 7.15b except that the smaller piece has become the largest in order that the two part leaf spring may apply a radial force at its centre so as to cause the two part vane to widen and bear against the rotor housing endplates.

The vane material is mild steel and photographs of the complete vane set are shown in Figures 7.17 - 7.19.

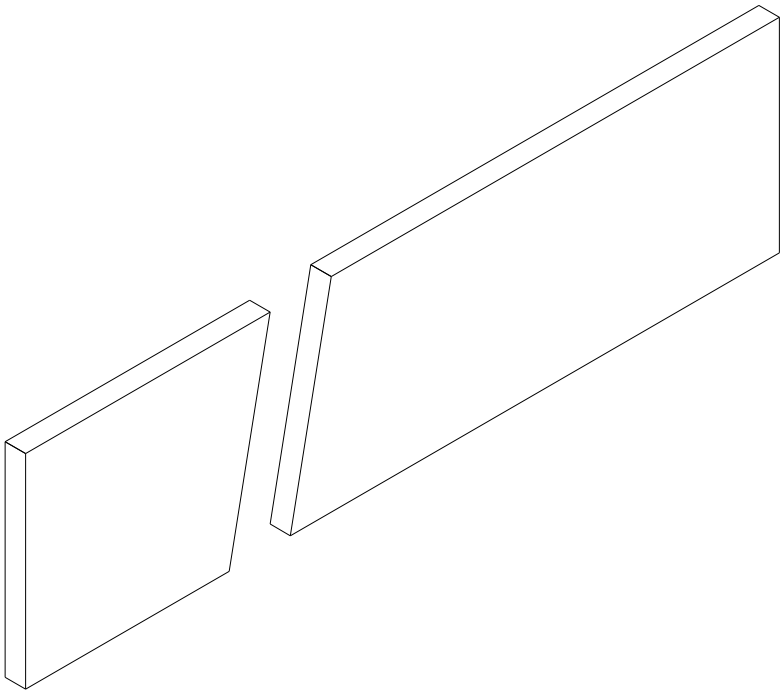

Figure 7.16 Vane Set – Isometric Drawing

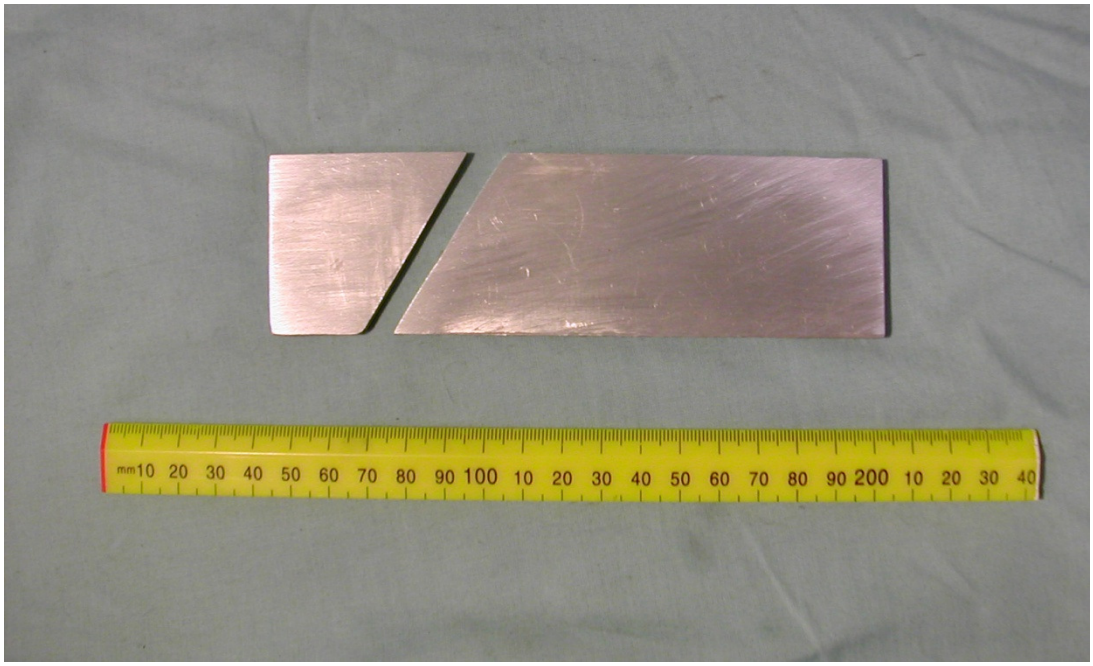

Figure 7.17 Vane Set – Separated

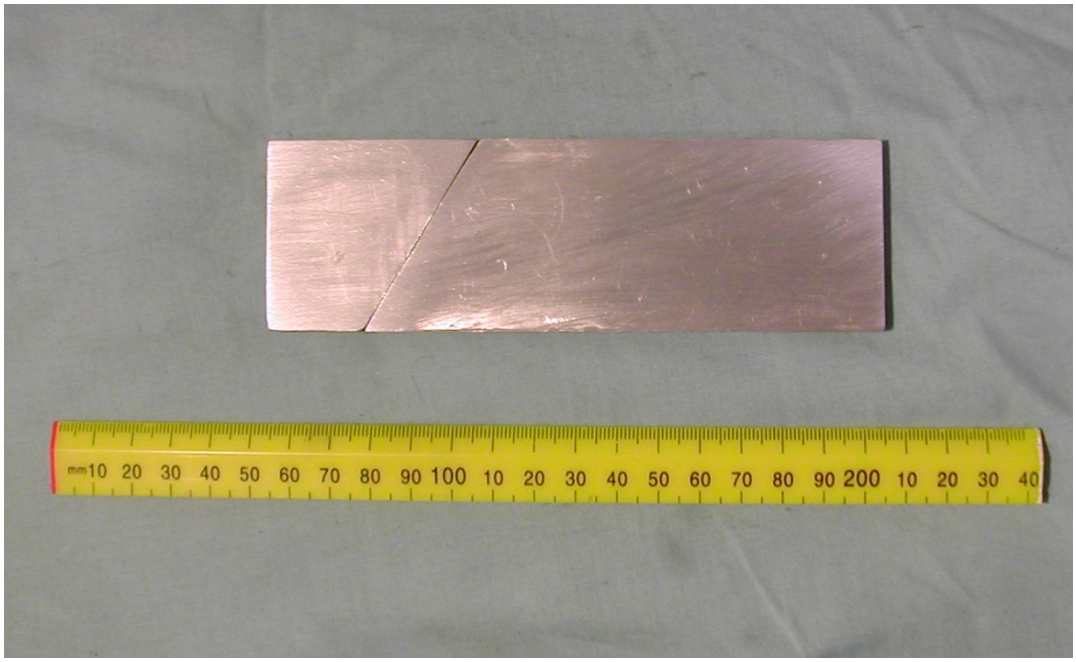

Figure 7.18 Vane Set – Closed

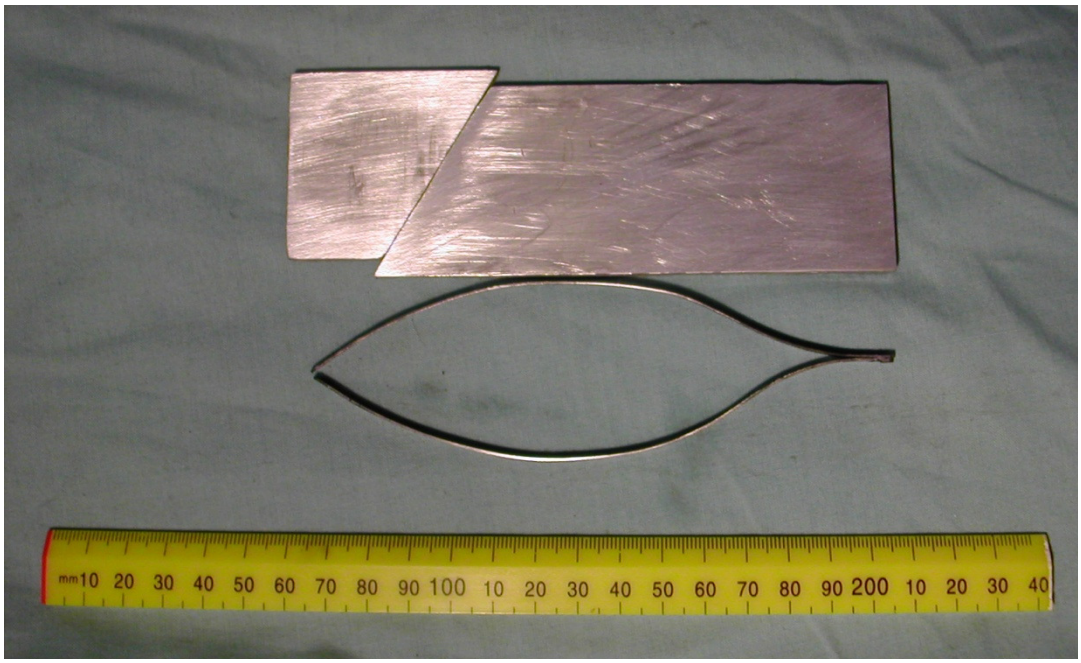

Figure 7.19 Vane Set – Offset with spring

7.3.3 Stator (Casing and Endplates)

The casing and endplates need to fulfil a large number of functions and, consequently the components are of complex shape and appearance. The major functions are:

1. Provision of a variable expansion ratio.
2. Provision of variable port timing.
3. The capture and re-use of heat generated by friction

Subsidiary functions are the provision of inlet and exhaust ports, provision of lubrication for the rotor and vanes and the placement of mounting and adjustment brackets. The systems providing the major functions will be dealt with separately and the subsidiary functions will be included where appropriate.

7.3.3.1 Variable Expansion Ratio

The VER is to be achieved by moving the combined casing and endplates laterally in a plane that is radial to the rotor as shown in Figure 7.1. If that plane is aligned with two diametrically opposite vane sets, those vanes will be the least and most extended vanes. The least extended vane can be considered the 0º position of the rotor.

A screw mechanism will push the casing toward the rotor. The point at which the screw mechanism bears on the casing will be varied according to the requirements of port timing but will not be varied whilst the motor is in operation. The illustration, in Figure 7.1, shows an inner and outer casing with only the inner casing moving and, presumably, a seal being formed between the end edges of the inner casing and the endplates of the outer casing. The outer casing would carry a simple bearing for the rotor axle. This design was intended for a hydraulic pump and, apart from being a heavy design, this would create problems with sealing the inner casing to contain high pressure gas. A single casing design has been adopted and this has a number of advantages for the variable port timing which will be considered in that section. However, with regard to the VER it does mean that a large non-circular axle hole must be used in order to accommodate the movement of the casing. A simple elongated sausage shaped hole, aligned with the radial plane, would have been sufficient but for the additional demands of the variable port timing. Consequently, a trianguloid (for want of a better term) hole was used to accommodate those movements. Figure 7.20 shows an orthographic side view of one of the endplates with the direction of the VER radial plane shown.

It is planned to identify the lowest pressure, in the largest final chamber volume and the outlet area, associated with the peak of efficiency and power. Once known, this pressure threshold would be a direct indicator of whether the inlet pressure was too high, or low, for the current adjusted ER. The control system would be set to adjust the VER mechanism to a higher, or lower, ER if this pressure threshold was not met. That pressure outlet is shown in Figure 7.20

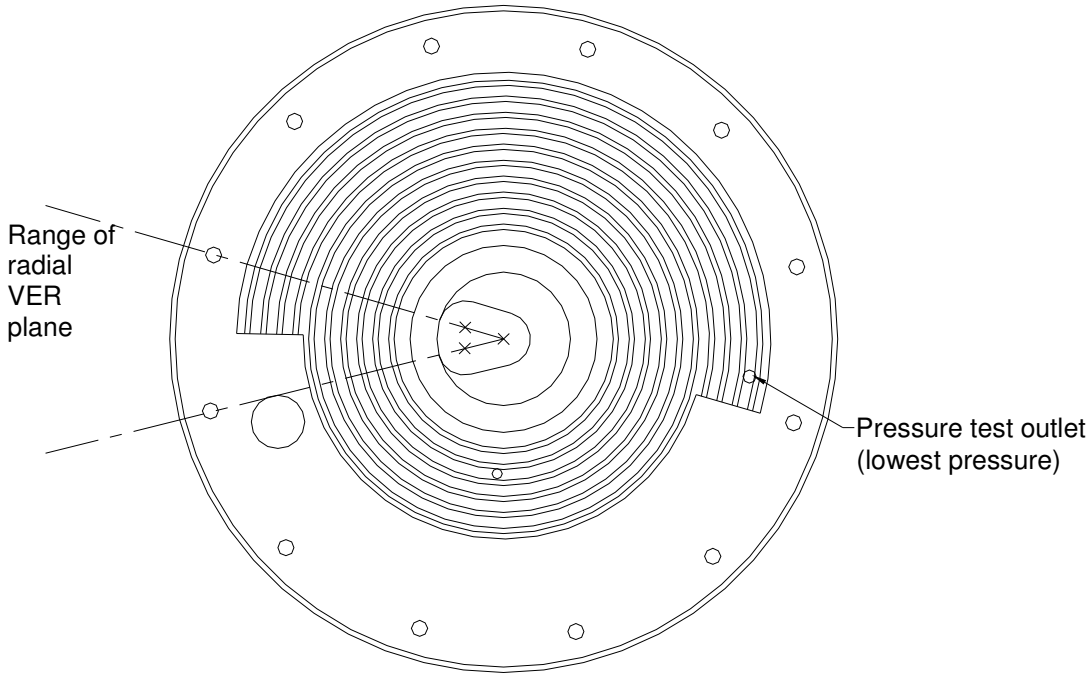

Figure 7.20 Endplate – orthographic side view with VER plane

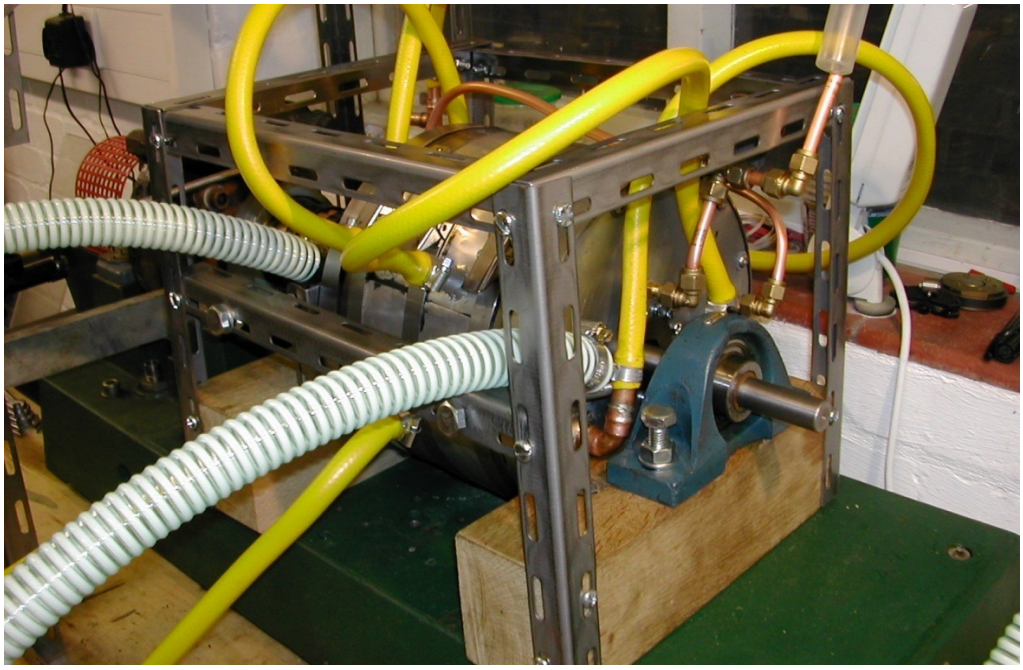

Figure 7.21 Assembled Motor

(the VER adjustment bolts are visible on the front frame lower cross beam)

7.3.3.2 Variable Port Timing

The variable port timing (VPT) mechanism does not control how long the ports are open. That is a fixed characteristic of the port angles (Inlet 30º, Outlet 150º) and the motor speed. The VPT mechanism is concerned with the opening point of the ports in relation to each other and the smallest and largest chamber volume positions (the VER radial plane). In Badr, et al, [1986], the Cranfield group considered that varying conditions of inlet pressures and temperatures required different inlet and outlet timings to optimise performance. It is unlikely that the same holds true for this machine but it is possible that the VER would benefit from altered timing. Because of this possibility the motor was designed so that it could be investigated.

The mechanism is simple enough. Referring to Figure 7.20, the endplate fixing bolts are placed at 30º intervals and, consequently, allow the endplates to be rotated in 30º increments in either direction. This adjustment requires the motor to be removed from the test rig and partially dismantled. The trianguloid axle hole, see the centre of Figure 20 and the photograph in Figure 7.22, allows the whole casing to be rotated around the axle for a further range of 0 - 30º. Currently this rotation is achieved by changing the length of the stator mounting brackets. In the future a screw adjustment of those brackets is intended but it is also conceivable that a more sophisticated mechanism could rotate the stator whilst it is in operation. Between the fixing bolt adjustment and the 0 - 30 º fine adjustment mechanisms, the relationship between the rotor's VER radial plane and the inlet ports can be varied to any desired degree.

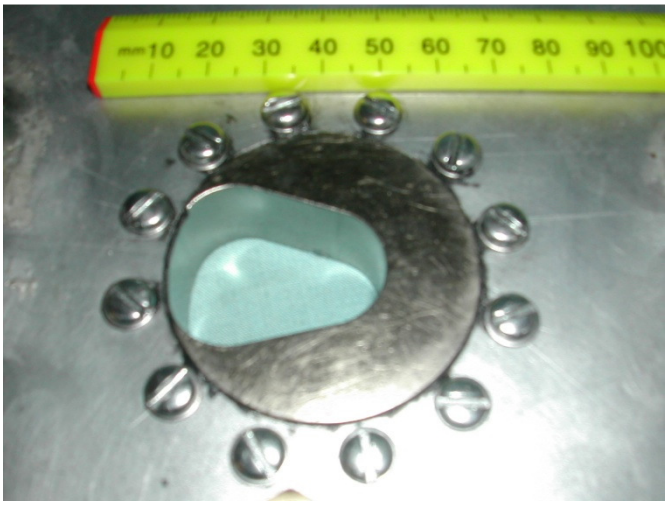

Figure 7.22 Trianguloid Axle Hole

The relationship between the rotor's VER radial plane and the outlet can only be varied by the fine adjustment mechanism.

The angle between the inlet and outlet ports can only be varied by the "bolt hole" mechanism, i.e. in 30º increments.

It is advantageous for the outlet port to open as soon as possible in order to allow waste air with little energy in it to be released from the system. In order to achieve an early opening for the fixed port a trench has been milled into the inner face of the endplate, from the position of the port to the approximate position of the largest rotor chamber volume. This is shown in Figures 7.23 & 7.24. It is also advantageous for the port opening to be as large as practical. It can be seen from Figures 7.23 & 7.24 that there is only one port per side and it might be considered that this is too few. It is intended to increase the number of outlet port openings in the future but, for the present, the number is restricted to one per side to limit constructional and operational problems. Those problems are:

- Fitting additional outlet fittings to the endplate covers whilst avoiding leaks from the endplate cooling jacket.
- Avoiding structural weakening in a potential high stress area.
- Potential air resonance problems.

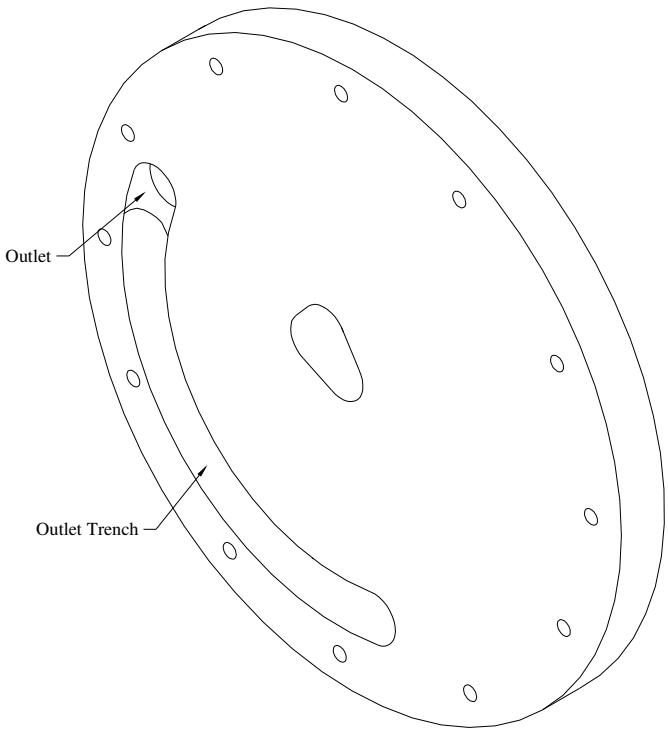

Figure 7.23 Endplate – interior detail

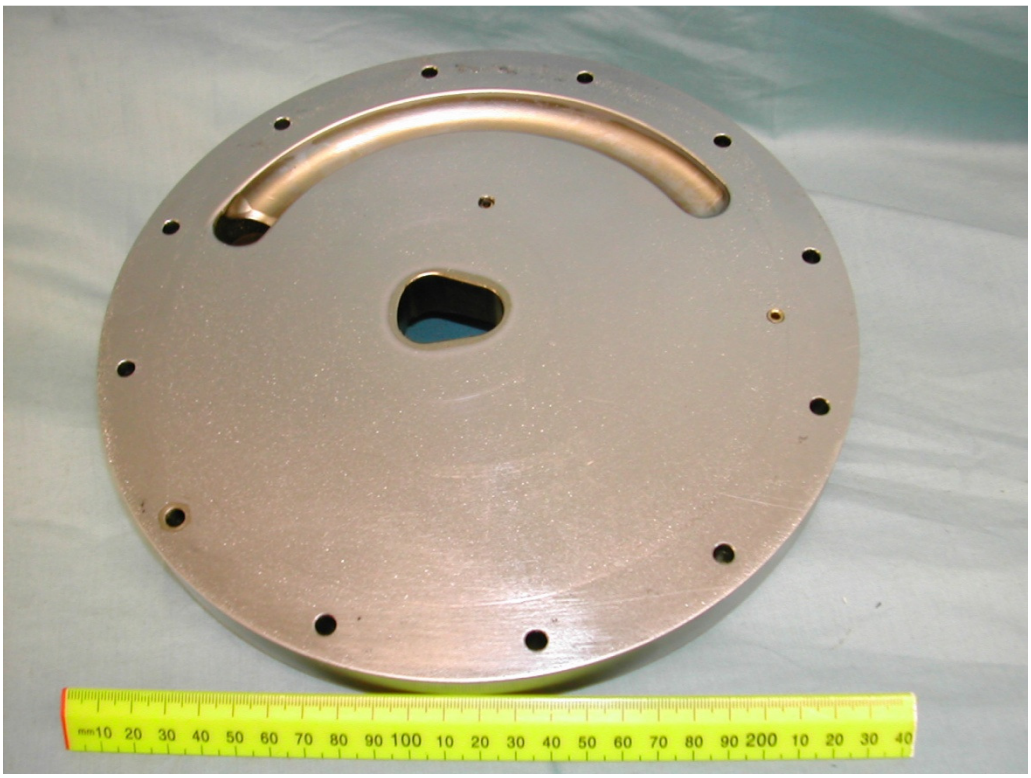

Figure 7.24 Endplate – interior detail photo

7.3.3.3 Re-using the Heat Generated by Friction

As the working fluid reaches the motor it is approximately 10ºC below the ambient temperature. This forms a useful low temperature reservoir into which the heat of friction can be transferred. The heat available from this source can be substantial. In Badr, O. et al, [1985e] the Cranfield group calculated that the friction losses were the cause of a reduction of mechanical efficiency (defined as power output/power expected) from 95% at 1500 rpm to 65% at 4500 rpm. Whilst they didn't quote actual power losses, the maximum power output of their machine was 8 kW at 3500 rpm (Badr, O. et al, 1986) at which speed the mechanical efficiency was 80%. This implies that the frictional losses produce 2 kW of heat, at least in that particular machine. Losses of this order would substantially raise the temperature of the body of the motor, creating a temperature gradient sufficiently steep

enough to guarantee that the heat would quickly transfer to the compressed air coolant. It is likely that some of this heat would have been transferred to the expanding air within the motor anyway (that is less likely to have happened with the Cranfield groups machine as the working fluids inlet temperature was 80 - 140ºC). However, even if only 50% of the heat loss travels outwards it would be a worthwhile improvement in efficiency to capture and re-use this.

As stated earlier the means to achieve the capture of this heat is to machine fins onto the external areas adjacent to the rubbing areas. These are around the periphery of the stator casing and the outer faces of the endplates and are shown in Figures 7.23 to 7.29. Full technical drawings are to be found in Appendix B.

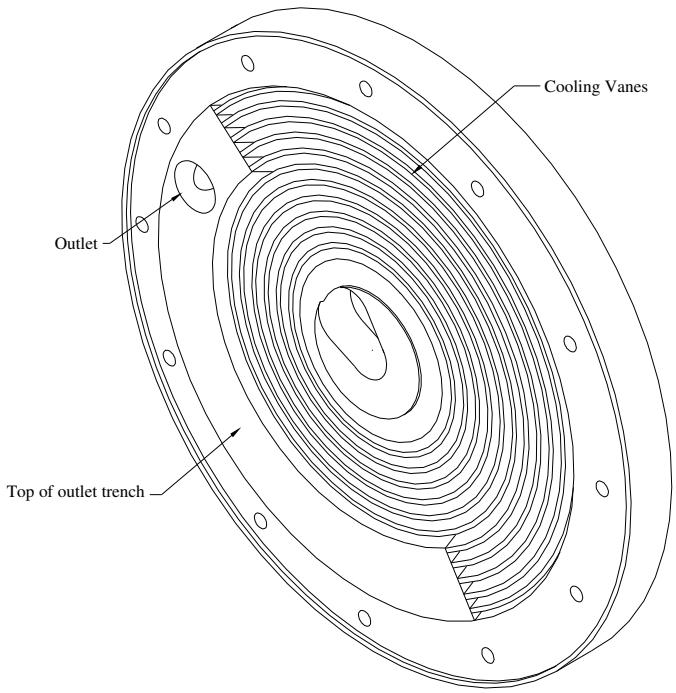

Figure 7.25 Stator Endplate – Exterior detail

The surface patterning seen in the photographs is the result of zinc plating. This was a necessary pre-requisite to having the interior surfaces hard chrome plated. The chrome plating is necessary to protect the aluminium surface from wear but is also intended to lower the friction coefficient of those surfaces. Even if all the friction produced heat was recaptured the instantaneous power output would still have been reduced, so friction reduction is always worthwhile.

The endplate covering plates are zinc coated steel and the pipe connections are copper plumbing fittings soldered into place.

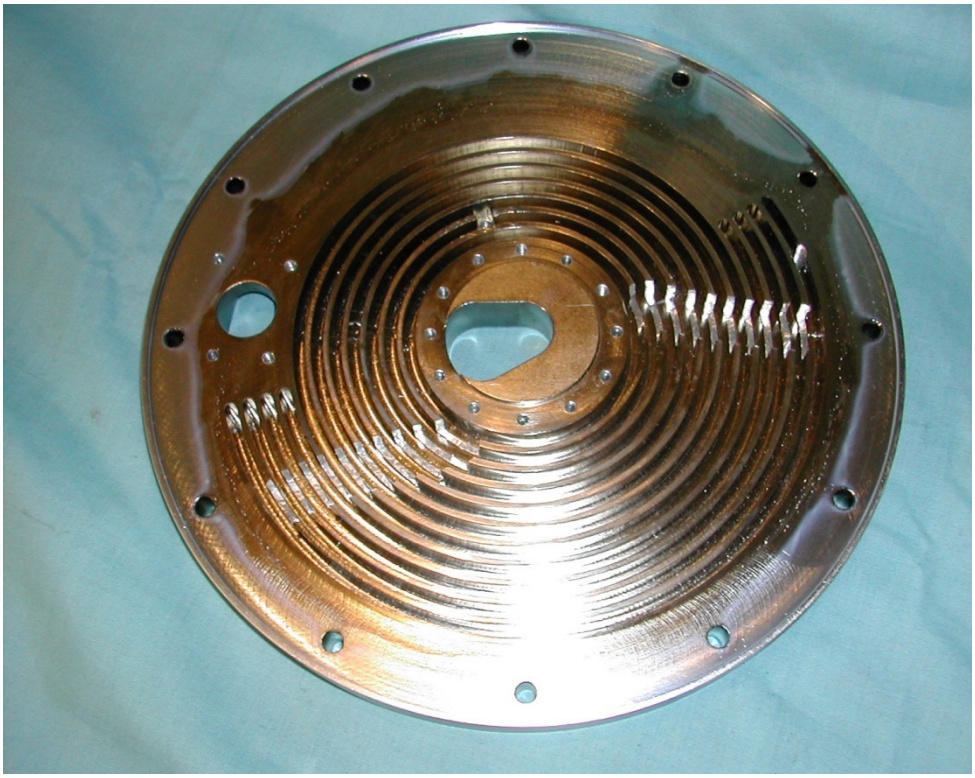

Figure 7.26 Endplate – Exterior detail photo

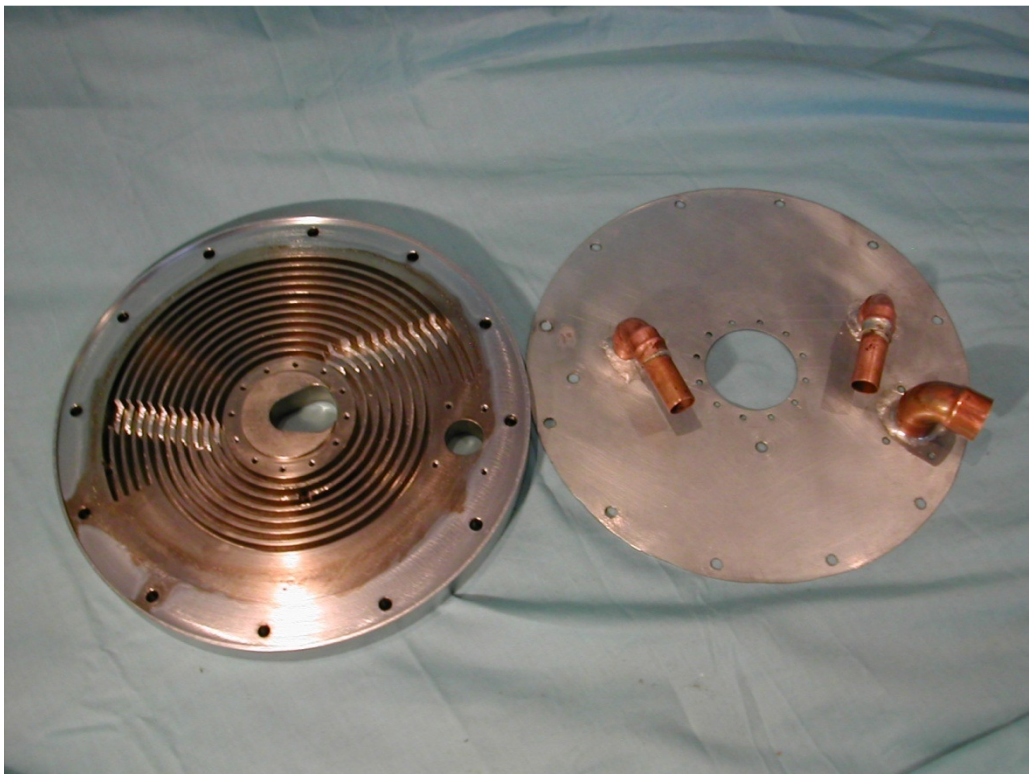

Figure 7.27 Endplate with Covering Plate – in same orientation

In figure 7.27 it can be seen that the cooling fins have been partly milled away on almost opposite sides of the endplate. This is not shown in the technical drawings as it was done after a trial assembly indicated that more clearance was required for the air flow to spread evenly across the fins. It can be seen that the reduced finning area coincides with the positions of the compressed air inlet and outlet pipe connections on the covering plate. The endplate with the covering plate fitted is shown in 7.28 below. The small pipe fittings are for compressed air coolant in and out. The large fitting is for the low pressure outlet.

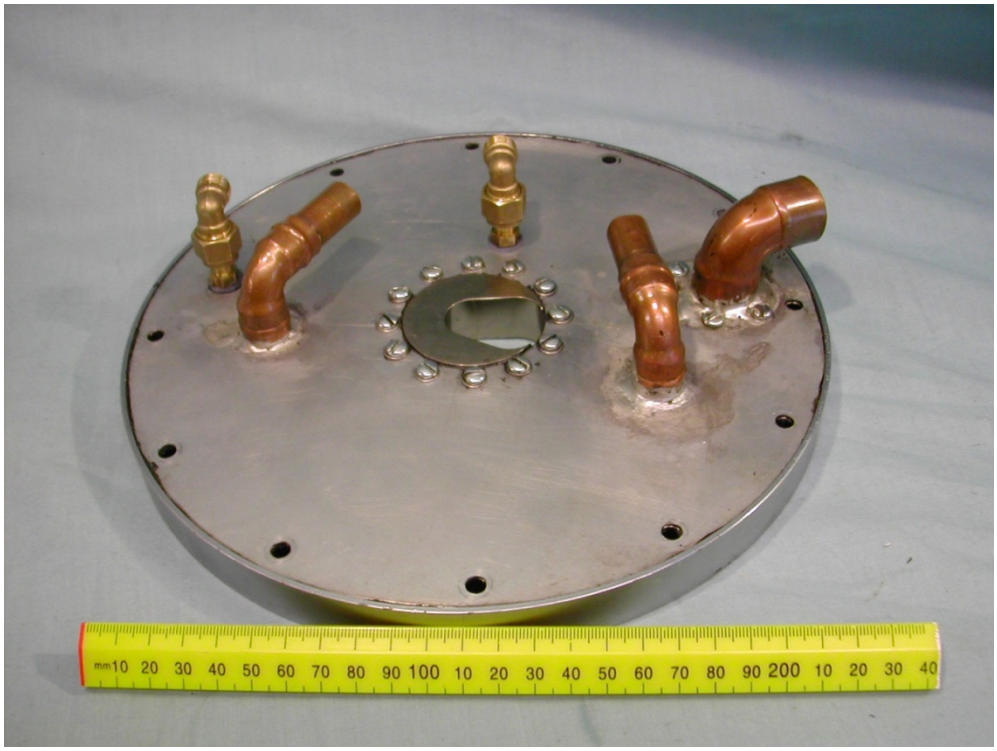

Figure 7.28 Endplate with covering plate fitted

The stator casing has more finned area than both the endplates and this is shown in figures 7.29 and 7.30.

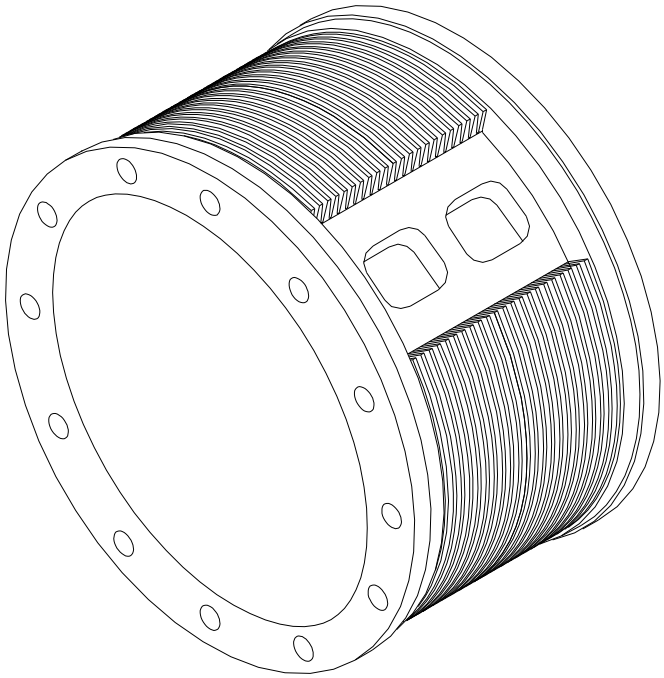

Figure 7.29 Stator Casing (isometric view)

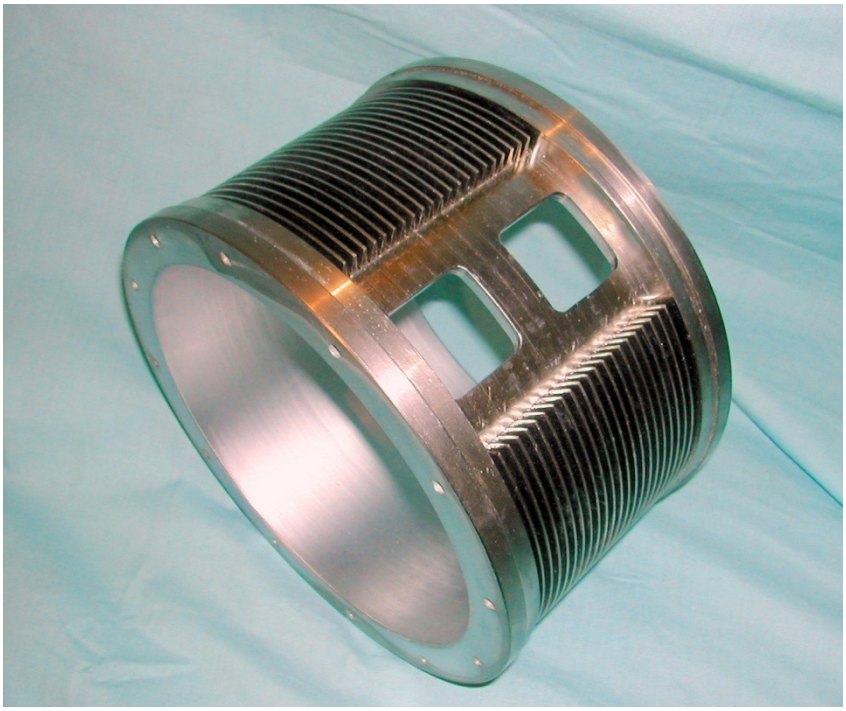

Figure 7.30a Stator Fin Detail – photo

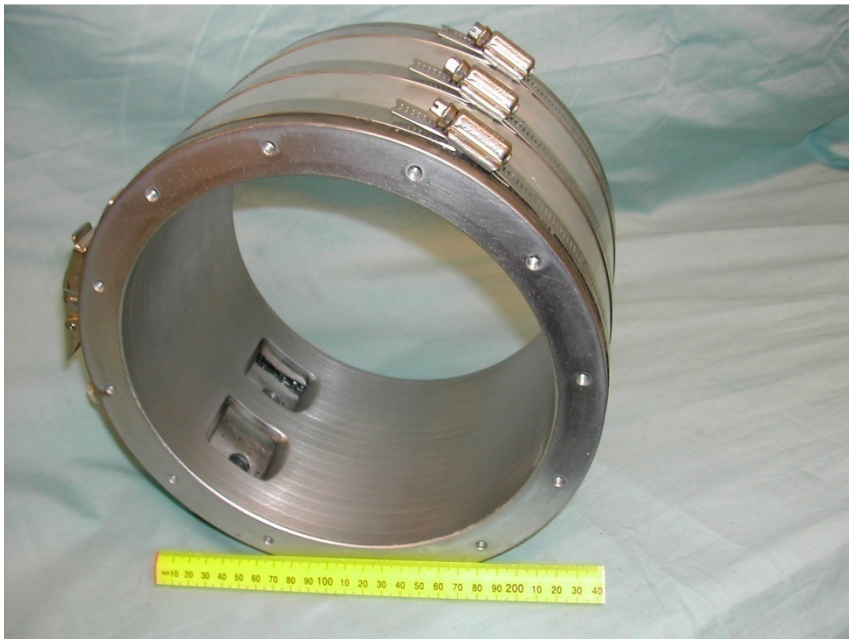

Figure 7.30b Stator with Casing fitted - photo

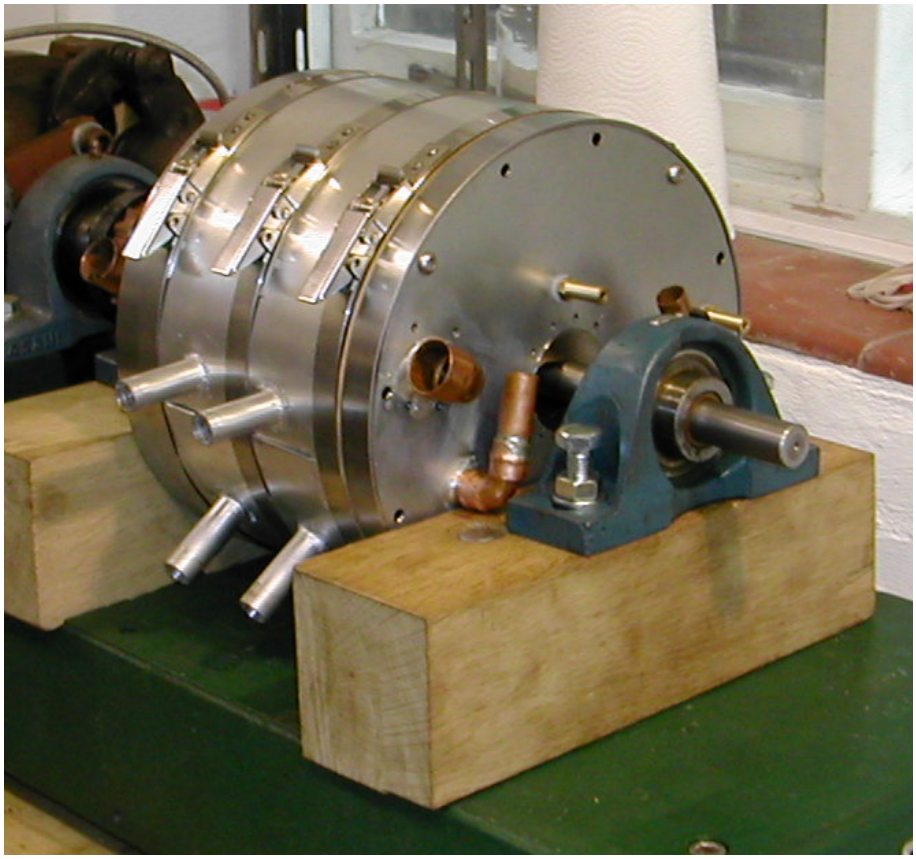

Figure 7.31 Motor Partially Assembled

Figure 7.31 shows the motor only partly assembled but the stator casing covering plate is in place and secured, held in place by three Protex stainless steel bandclamps. The curved covering plate is aluminium. The pipe connections are also aluminium and have been welded into position. The upper pair of pipes feed air, from the endplates, to the casing peripheral cooling jacket. The lower pair of pipes feed air directly to the inlet ports. The bandclamps are the sole method for securing the casing covering plate. No screw fasteners are to be used.

7.4 Testing Rig

The test rig is a converted TecQuipment dynamometer. The green painted cast iron bed is all that remains of the original equipment. The original torque measuring equipment was based on a fluid (water) clutch and was limited to approximately 3 kW. This was considered inadequate and it was converted to a disc brake with a 330 mm torque arm, a load cell and an oil piston damper. The load cell reads up to 25 kg with an accuracy of ±2%.

The pressure of the compressed air stream is read at several points with Wika Bourdon pneumatic gauges with 50 mm displays and an accuracy of ±2.5% of the full span of the display.

Temperatures of the various air flows are to be measured by thermocouples and read by Tenma Digital Thermometers of an accuracy of ±0.2%.

All readings will be manually noted and no data acquisition system is to be used.

A photograph of the full test rig is shown in Figure 7.32 and various closer views are shown in Figures 7.33 & 7.34 and a schematic of the test rig is shown in Figure 7.35.

The lubrication is achieved by the injection of light machine oil, at the base of the rotor vanes on the low pressure side of the rotor, by a syringe pump on the left hand side of the motor. See Figure 7.33. The oil is extracted from the outlet air stream by a cyclonic filtration system. The white polymer sump for this system can be seen on the far left of Figure 7.32 and the anemometer air flow sensor can be seen mounted on the top outlet from that sump. It is intended that an electrically pumped oil recirculation system be eventually fitted.

Figure 7.32

Motor

Test Rig

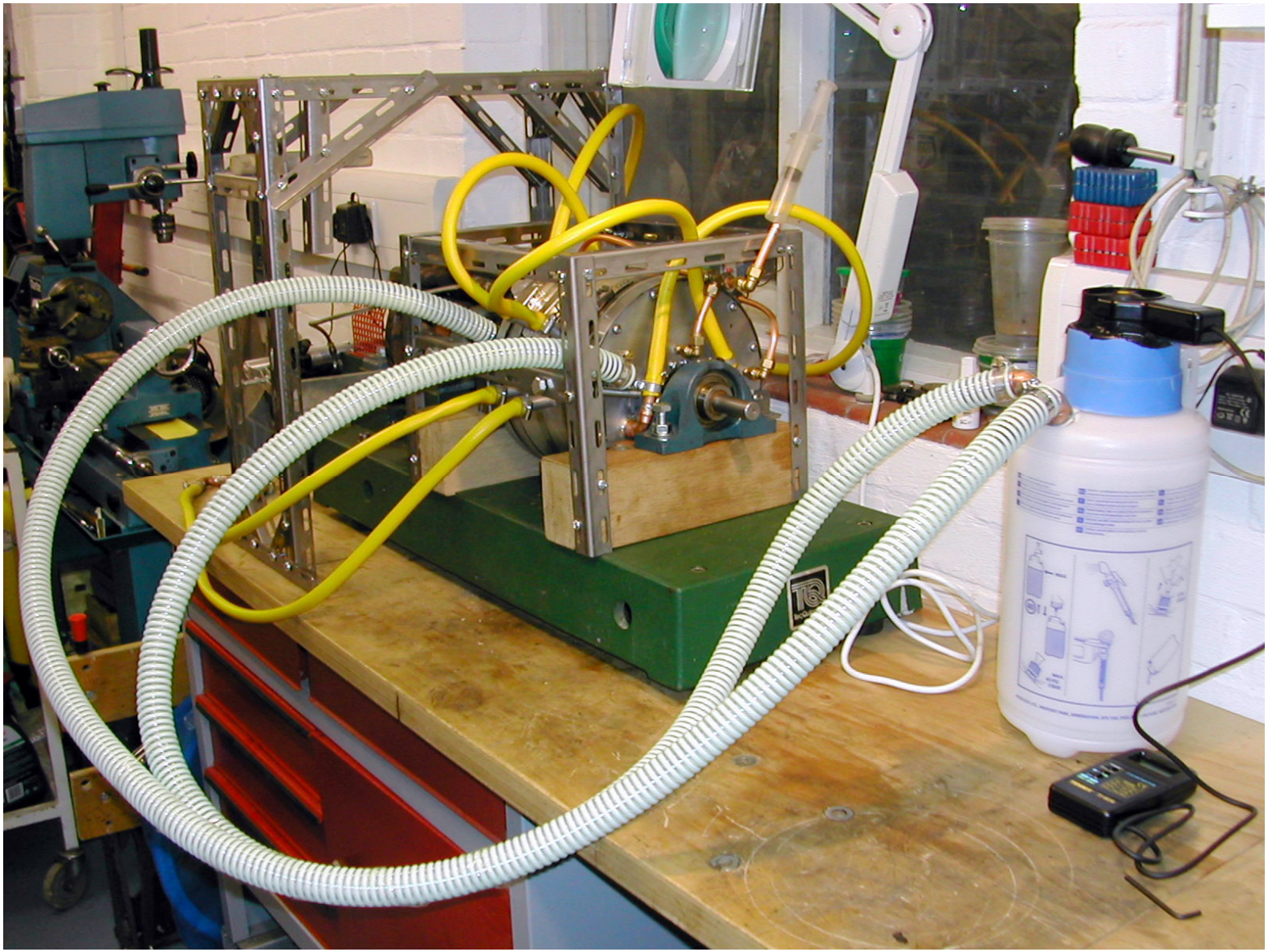

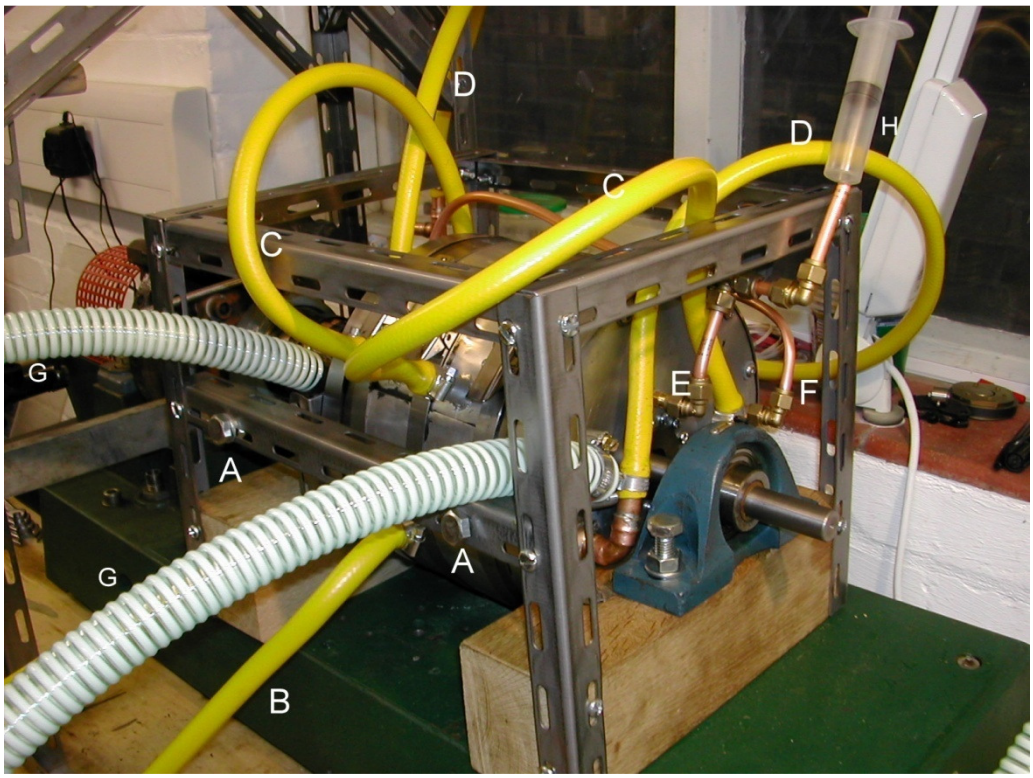

Figure 7.33 Test Rig – detail right hand side (motor, air inlets and outlets, oil in)

In Figure 7.33 the motor is shown fully assembled and surrounded by the frame and compressed air feed pipes. The key to the elements in Figure 7.33 is:

(A) VER offset adjustment screws.

(B) Compressed air (CA) direct to inlet ports (see also 7.34 below).

(C) CA coolant – endplates to stator casing.

(D) CA coolant – to endplate inlets.

(E) Lubricant inlet.

(F) Low pressure chamber, pressure takeoff.

(G) Low pressure outlet from motor to lubricant sump and air flow sensor.

(H) Lubricant injector syringe.

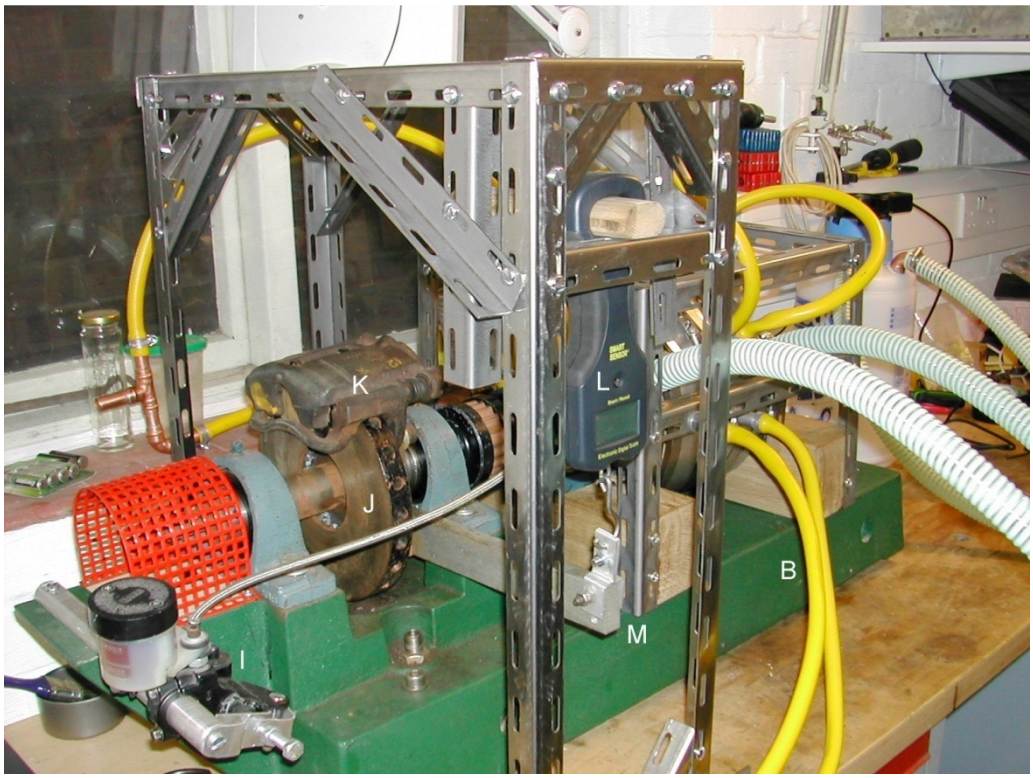

Figure 7.34 Test Rig – detail left hand side (disc brake, torque arm & load sensor)

The view of the rig from the left side shows the detail of the disc brake torque measurement equipment. The key to the elements in Figure 7.34 is:

(B) Twin CA inlets direct to the main inlet ports.

(I) Hydraulic brake cylinder with screw adjustment.

(J) Brake disc.

(K) Disc brake calliper.

(L) Load sensor.

(M) Torque arm.

7.5 Results

The test rig is still in the process of being modified to make the equipment more usable and accurate. The motor will stall if the disc brake is engaged before the motor gets up to speed and will race, suddenly, if the brake is then disengaged. The start up procedure is to open the main cylinder valve fully whilst the regulator valve is set at a moderate pressure and the disc brake is fully disengaged. The regulator valve is then gradually set to a higher pressure so that the motor is rotating at a substantially higher speed than the expected final reading speed. The disc brake is then gradually engaged and the regulator valve manipulated until a stable speed, torque and air flow reading is achieved. Currently it takes approximately two minutes to adjust the disc brake and air flow valves so that a relatively stable state of operation is reached and useful readings can be taken. As a test run lasts less than 4minutes this is very limiting. The range of expected modifications is dealt with under "further work".

Nonetheless, measurements have been obtained and an attempt has been made to assess the motor's initial mechanical efficiency η_{mech} defined as power out/power available .

The initial conditions of the test run were:

Ambient temperature 15ºC

Humidity 55%

Storage cylinder pressure 30 MPa

Storage cylinder temperature 15ºC

The equation for the power output in Watts is given in Equation 7.1 below

$$\frac{\text{Torque (Nm)} \times 2\pi \times \text{Rotational Speed (rpm)}}{60} = \text{Power (W)} \qquad \text{Equation 7.1}$$

The torque arm load sensor reading was in kilograms and was from a one third metre torque arm. This was converted to Nm by (m x 9.81)/3. The load sensor reading was stabilised at approximately 19 kg and so the torque was 62 Nm.

For the test run the settled speed of rotation was approximately 400 rpm.

Power = (62 x 2π x 400)/60 = 2,597 W

To calculate the power in the compressed air flow it was decided that the energy storage equation (equation 3.8) would be used to calculate the energy available from 1g of compressed air in the state measured at the inlets. To get the power available, that value would be multiplied by the air mass flow.

Equation 3.8 $P_o \times V_o \times \ln(V_o/V_f)$

The inlet pressure P_o = 750,000 Pa

The original volume V_o = 1.22×10^{-4} m^3 (1g @ 750 kPa)

The final volume V_f = 8.65×10^{-4} m^3 (1g @ 100 kPa)

Using these values in equation 3.8 gives;

$750{,}000 \times 1.22 \times 10^{-4} \times \ln(1.22 \times 10^{-4}/8.65 \times 10^{-4}) = -179$ J/g

The negative sign represents energy leaving the system.

The air mass flow was calculated from the air flow sensor. The cross sectional area of the air flow sensor has been measured as 0.002 m^2 and its flow speed reading was 7.1 m/s. Taking the density of air as 1.16 kg/m^3 this equates to an air mass flow of -- 16.47 g/s.

Power available - 179J/g x 16.47 g/s = 2948 J/s = 2,948 W

$$\eta_{mech} = 2,597/2,948 = 88\%$$

7.5.1 Conclusions

The η_{mech} value of 88% is a surprisingly good result for this stage of the testing but this should be seen in the light of the Cranfield group's results. Their value for η_{mech} of 80% was for a speed of 3500 rpm, [Badr, et al, 1986]. At lower speeds, of between 1500 – 2000 rpm, it rose to above 90% , probably as result of reduced friction. No values were provided for speeds below 1500 rpm.

This result also compares well with the Cranfield machines in that it has achieved good power at low speeds. However, it must be remembered that this is effectively one test run on a test rig that is still being developed. The stated readings from the sensors are approximate median values of readings that were changing/oscillating, particularly the load sensor. There was a clear tendency for the torque to reduce whilst the speed increased. This may be the result of heating effects in the disc brake mechanism.

For the moment this result must remain provisional until it is repeated with the improvements noted in the section on further work.

8. System Overview, Overall Conclusions and Further Work

8.1 System Overview

Until now this thesis has focussed on the individual elements that compose the Compac but an overall view of the system is required to put them all into perspective, particularly with regard to its competitor, the electric battery car. Table 8.1 estimates the Compac's

system efficiency using the measured values for the motor and heat exchanger and reasonable values for the efficiency of an electric motor driving a multi stage compressor with a water based heat exchanger. The efficiency value for the electric motor is similar to that used in earlier chapters whilst the efficiency for the compressor is typical of modern compressors water adsorption technology with water cooled heat exchangers. By comparison Atlas-Copco [2009] claim 100% efficiency for their Carbon Zero range of compressors. Although these additionally scavenge waste heat for water and space heating both are processes that could be implemented in a domestic or light commercial situation. It is expected that the Compac's compressor would be working relatively slowly, compressing something of the order of 0.2 – 0.25 kg of air a minute, and would be using a cold water counter flow heat exchanger. This means that it would take 6 - 8 hours to recharge a 250 litre store to 30MPa and would allow sufficient time for good heat transfer to take place.

Table 8.1 Compac System Efficiency

Compressed Air Car		
Element	Element efficiency	Running efficiency
Compressor Motor	85%	85%
Compressor & heat exch	90% (-10%)	76.5%
Heat Pipe Scavenge	+13%(+10%)	86.5%
Air Motor	88% (-10%)	76%

The right hand column titled "Running efficiency" shows the change in system efficiency after each element has affected the process. The final value in the air motor row is the final system efficiency of 76%. In table 8.2 below the Compac elements have been

adjusted to show some likely improved values and compared to the system efficiency of an electric battery vehicle.

Table 8.2 Comparison of Improved Compac and the Electric Battery Vehicle

Compressed Air Car			Electric Battery Vehicle		
Element	Element efficiency	Running efficiency	Element	Element efficiency	Running efficiency
Compressor Motor	85%	85%	Transformer & Control	90%	90%
Compressor & heat exch	90% (-10%)	76.5%	Battery	75% (-25%)	67.5%
Heat Pipe Scavenge	+15%(+11.5%)	88%	Motor control gear	90% (-10%)	60.75%
Air Motor	90% (-10%)	79%	Veh Motor	85% (-15%)	51.6%

The Compac efficiency has increased by a small amount, to 79%, but whichever value is used the system efficiency for the electric battery car is much lower. The major cause of this is the poor charge/discharge cycle efficiency of the battery. 75% is typical of a new battery operating at 20°C. If the battery were old or cold or both, the efficiency would be much worse. This is an unsurprising conclusion as the electrochemical battery is known to be the weakest component of electric vehicles but it is useful to have such a clear difference between the systems.

It should be noted that these figures omit a value for a transmission unit. Electric vehicles use only a limited transmission, usually in the form of an epicyclic gear cluster with a differential, although some use multiple motors with a direct connection to the wheels. The decision on the transmission requirements for the Compac will have to wait until full torque curves have been constructed for the air motor but it seems likely that those requirements will be similar to those of the electric battery vehicle. The advantage of an epicyclic system is that it is compact, assuming only a single stage is used, and can

provide a reverse gear function. Typical mechanical efficiency is 95-98% per stage and thus whether or not this element is included in the comparison has little effect on the outcome.

8.1.2 Auxiliary Systems and Parasitic Loads

The Compac has few auxiliary systems and these can be summarised as follows:-

1. Passenger space cooling
2. Passenger space heating
3. Power assisted steering
4. Power assisted braking
5. Electrical system

Passenger space cooling has been referred to in several of the earlier chapters as it is one of the benefits of a Compac that air cooling is available as a by product of its normal operation. It is the intention that the dry air from the motor outlet be passed across a "recuperator" heat exchanger in order to minimise the risk of frosting (section 5.6). Subsequently, this cooled air stream could be used for space cooling, by passing it to the passenger space, with no energy cost to the motive power system. The only caveat to be considered is that the outlet air stream may contain some residual fumes from the lubrication oil, polluting the passenger space. This does not seem to be the case with the motor tests so far and it is likely that the recuperator would act as a distillation system that would cause any residual fumes to condense out. Nonetheless, if it did become a problem, a further heat exchanger and an electrically driven fan could be used to cool the passenger space without the need to inject the motor outlet air. Although the fan would represent a small energy cost it would be much less than that of a conventional compressor based air conditioning system.

Passenger space heating is more problematic as there is no simple way to generate heat from the compressed air flow. However, the problem is not unique to the Compac. All electric battery cars have to deal with the same problem and many diesel vehicles suffer from poor heating at initial start up and, because of this, two broad solutions are available. These alternatives are to use an electrically powered heater or a liquid fuel based combustion heater. Electric car heaters are available up to 200W and a new technology, Positive Temperature Coefficient (PTC), is particularly efficient as it is self regulating. In respect of combustion heaters there are several suppliers of diesel fired air heaters [Bosch, 2008b] for small boats and cars. However these are expensive and add complexity and the need for refuelling. The most viable solution appears to be the use of an electric heater despite the fact that it adds a parasitic load to the electrical system which must be supplied from the motor via an alternator.

Power assisted steering (PAS) is commonly supplied with compact cars and it is reasonable that drivers would expect the Compac to provide this option, although it is not clear that such a lightweight vehicle would need it, even in low speed city driving. In the past PAS was hydraulically powered and for larger vehicles it still is. For reasons of fuel economy compact cars now use electric power assisted steering that is demand oriented, supplying power only when it is needed. The hydraulically powered systems were powered by a pump that was constantly driven while the engine was turning thus representing a substantial parasitic loss. The new electric systems may demand a substantial load (approx. 40A) from the battery but it is intermittent and represents a small long term load on the alternator and the motor. The exact load varies with driving style and conditions but $1/10^{th}$ of the instantaneous load, about 4A, is considered reasonable.

Power assisted braking, particularly anti-lock braking, is considered a necessity in all modern vehicles and is controlled electronically. The power assist can be any one of a wide variety of systems but for a Compac the obvious power source is compressed air. Pneumatic braking systems for large commercial vehicles are highly developed and represent an intermittent demand rather than a constant load. The electronic control unit also is an intermittent demand.

The electrical system must supply power and energy for all of the above systems and also supply the lighting and infotainment systems. Of these two systems the headlamps are potentially the most demanding. If halogen lights were used they would demand 55W per headlight beam and this would be a continuous demand in low light conditions. This can be reduced to 19W per headlight if modern LED systems are used and this would appear to be the future for all headlight systems.

The “infotainment” systems, radio and music players, satnav, phone etc. can be large continuous loads or intermittent loads that fall to zero. An estimate of 100W continuous load has been made for this element.

Whilst all of the loads identified would, initially, be supplied by the battery it is good practice to size the alternator to be able to supply the expected maximum load by itself. This is particularly the case with the Compac which generates no power whilst it is motionless but may still be powering the heating lights and infotainment equipment and will have to compensate by generating a larger amount of power once the Compac resumes motion. Using the foregoing approximations heating would require 200W,

lighting 50W, infotainment 100W, steering – possibly as much as 400W intermittently plus another 100W for miscellaneous fans and other demands would result in a total demand of 850W. In a 12V system this would require at least a 70A alternator. Taking the Bosch KCB1 90A alternator as typical of compact alternators, this can deliver a part load of 80A, at 13.5V, at an efficiency of 65% at 2000rpm. At higher speeds and currents the efficiency falls to 50-55%. [Bosch, 2008c]. This would mean that the alternator load on the motor would be 1660W at 2000rpm. This is a substantial load on a motor that would only be producing approximately 30kW at the time. However, it is sustainable for short periods and would be unlikely to occur often as the alternator regulator is designed to minimise engine load in order to improve fuel economy.

8.1.3 The Compac as a Hybrid

The problems of limited energy and range can be addressed by hybridising the Compac with an IC engine in much the same way that is being currently attempted with the electric battery car. However, the Compac is particularly suited to this form of hybridisation as the waste heat of the IC engine can be reclaimed by using it to heat the compressed air flow.

In hybrid form the vehicle is intended to operate as a switchable series-parallel hybrid. In "commute" mode the vehicle will operate on the CA motor only. An optimised internal combustion engine (ICE) of 20 kW output will be started when (A) the CA charge falls below a predefined pressure or (B) high loads are applied or (C) the driver demands full power. The ICE will also be capable of driving a compressor to recharge the CA cell when the vehicle is parked. In this mode there would be no scavenging of the waste heat so fuel efficiency would be reduced.

The general layout of the proposed CA hybrid is shown in fig 8.1

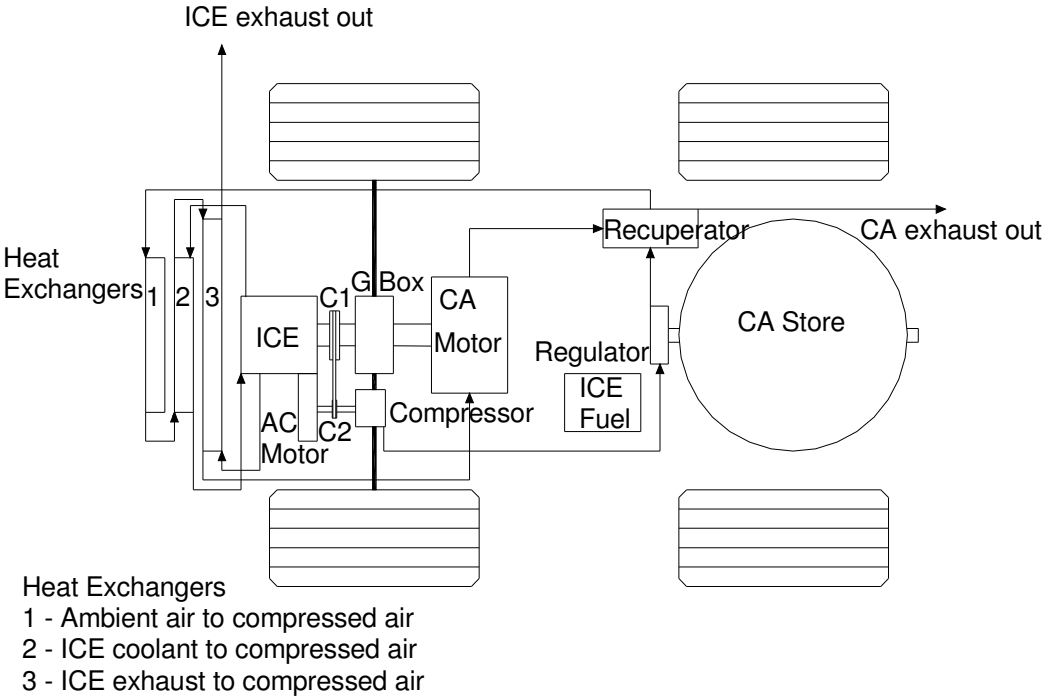

Fig 8.1
Compac Hybrid General Layout

In hybrid operation the CA stream is regulated down to a maximum of ten bars but may be any pressure between zero and ten bars according to the driver's demands.

Before entering the CA motor the CA stream passes through three heat exchangers. The first is the ethanol and low pressure water heat pipe HX described earlier. At the outlet from this HX 1 the CA stream is expected have been warmed to within 10ºC of the ambient temperature.

The second HX is intended to receive heat from the internal combustion engine (ICE) cooling system and is also expected to be a water based heat pipe system. However, as

the ICE is also intended to operate the compressor whilst the vehicle is parked, a further ordinary “radiator” type HX may be required to provide a heat sink when the CA stream isn’t present. This consideration may make HX 2 uneconomical and a simpler system would be an entirely separate conventional cooling system with the radiator placed ahead of HX 1. Whilst the vehicle is moving the HX 1 would benefit from the warmed ambient air flow. Whilst parked, and in compressor only mode, the ICE radiator would be cooled by an electric fan as in a conventional system.

HX 3 is intended to recover some of the heat lost in the ICE exhaust and is expected to operate over a wide temperature range. The condenser end of the heat pipes would be receiving CA at a temperature lower than ambient whereas the evaporators could be at 400ºC. This range would require at least two, possibly three, types of working fluid. At the low temperature end of the counterflow HX, water based pipes are desirable for their high capacity but are limited to evaporator temperatures of about 200ºC. Once the CA flow reaches these temperatures an organic fluid such as Dowtherm A (useful range 150 - 350ºC) [Reay, 2006] would be required. This fluid has a useful range that overlaps with water and the final working fluid, Mercury, with a range of 250 - 650ºC. After HX 3 the CA stream proceeds to the CA motor and the ICE exhaust is released to the atmosphere.

The waste heat to CA HXs 2 & 3 have yet to be modelled mathematically, for size, weight and capacity, but it seems clear that at least 15 kw of waste heat would be captured and reused. For an ICE as described (20 KW output, 35% efficiency) this represents 50% of the energy in the exhaust stream and a substantial increase in ICE system efficiency, to approximately 60%.

8.2 Aims and Achievements

The project must be considered to be broadly successful in that all of its aims, from section 1.1, have been met.

- The requirements of a lightweight compressed air storage cell were identified and a design, optimised for the criterion of weight, was completed.
- A working heat pipe heat exchanger test rig was constructed and it was successful in confirming that it was possible to reheat the cold compressed air to a useful degree whilst air flows were comparable to those that might be expected in a Compac.
- It was confirmed that a regenerative braking system, using a heat pipe based thermal store, could be constructed for a Compac and have comparable, or superior, performance to RBS systems used in current electric and hybrid vehicles.
- A working compressed air motor has been designed, built and tested and it appears to have great potential for high efficiency.

The overall conclusion is that a Compac should be considered at least as practical as any currently available design of electric battery vehicle. However, that isn't a particularly high standard to meet and a number of further studies and developments should be pursued in order to place the design of a future Compac on a more sound basis.

8.3 Future Work

8.3.1 Pressure Storage Vessel

The general structure, material and shape of the pressure vessel was identified and optimised for minimum weight. The shape identified was a sphere, which for reasons of minimum surface to volume ratio and minimal hoop stress, was clearly the form of minimum weight. However, the more complex demands of product design might cause a large sphere to be considered an awkward shape to accommodate within the design of a small automobile. For this reason the weight penalty of using vessels with more convenient form factors should be explored.

The first options to be explored will be single cylinders of increasing length/width aspect ratios but of identical volume. Starting with a sphere (aspect ratio = 1) the weight to volume relationship will be traced for each aspect ratio up to a practical length limit. It is possible that the use of multiple pressure vessels would be commercially acceptable and multiple cylinders are used for high pressure hydrogen storage in experimental hydrogen driven vehicles. It will be necessary to repeat the first study for the same volume divided into two vessels and more, probably limited to a maximum of five vessels.

More unusual vessel geometries should also be explored. An ovoid holds the potential for being a weight efficient compromise between the sphere and cylinder forms. A toroidal (doughnut like) form has been used as a lightweight portable breathing air store and this should also be considered. These unusual geometries are too complex to be dealt with by the simple hoop stress equations and will have to wait until an FEA computer program is available.

The value of these different geometries cannot be decided by engineering analysis and, finally, will be subjectively evaluated through financial cost and convenience of design.

8.3.2 Primary Heat Exchanger

The compressed air flow and heating experiments were limited to lower pressures and flow rates by the limitations of the regulator valve. The outlet pressure of the regulator valve can be altered but this is a normal part of the equipments operation. It was intended to enlarge the channels within the regulator to improve mass flow. It was also intended to modify its regulator mechanism to allow higher pressures to be delivered. These alterations haven't been attempted as they would cause the cylinder to empty more rapidly. If the double cylinder linkage is obtained, these modifications will be attempted and this will allow an investigation into the higher power regimes that could be expected to arise in normal motoring.

The problem of the "blow by" effect remains and some further investigation is warranted. The favoured explanation of the effect is that the compressed air flow through the heat pipe condenser fins is laminar and that the air at the centre of the flow between two fins, furthest from the fin surfaces, is receiving little heat. If this is the case then inducing turbulent flow should reduce the effect. It may be possible to modify the inlet baffles so that some turbulence is created before the flow enters the fin array. This could be investigated using the existing diffuser test chamber but any design must be limited to modification that can be effected through the inlet without dismantling the heat exchanger.

Although the heat pipe based heat exchanger performed its functions to a good standard, the lack of an alternative design prevents a useful comparison being achieved. Therefore, the search for a commercially available alternative will continue.

8.3.3 Regenerative Braking System

The final version of the RBS test rig achieved an efficiency of 70% heat captured over a period of 600 seconds, and stored. This leaves a further 30% of the heat to be captured. The losses were, most likely, through the walls of the ducting and the heat store. The heat store can be insulated but the ducting is already large and insulation would take up further space in what would be a small vehicle. An alternative is to shorten the ducting by placing the heat store close to the brake. This would require a separate heat store for each brake but the length of ducting would be greatly reduced. The individual heat stores would be of a similar size to the test rig heat store but with the modifications detailed at the end of Chapter 6.

8.2.4 MVE Prime Mover

Vane Tolerances. The rotor vanes were specified to have a close sliding fit to the rotor slot and the fit was good in dry, non-lubricated, conditions. However, once the light machine oil was added the vanes motion became restricted both in the sliding action within the slot and in expanding action adapting to the stator length. A degree of metal removal alleviated this problem, for the test run, but it remains capable of improvement. It is intended to reduce the thickness of the vanes and to loosen the fit of the tongue and groove mechanism, and to use an oil of lower viscosity. This latter change should also reduce losses due to viscous drag.

Vane Pressure Spring. The springs may be providing useful additional pressure but it was not clearly so. They did not provide sufficient force to overcome the initial tightness caused by the lubricant, although that was considerable. The subsequent loosening, of the vanes, improved their performance and it is to be hoped that further loosening will enable them to perform better. Constructing springs capable of greater force must be considered.

Dynamometer Disc Brake. The disc brake experienced some stick/slip juddering and this caused substantial variation in the load sensor readings. It is intended to increase the effectiveness of the damper (a tighter piston and more viscous oil) and to introduce an anti-vibration link between the sensor and the torque arm. Overheating, at the brake disc/brake pad interface, may be a problem and this will be investigated with a view to adding fan assistance to the air flow. Standard maintenance such as a change of brake fluid and checking for air bubbles will be carried out first but this seems an unlikely cause considering the short time span involved.

Short Test Run Time Span. The short period of test possible with one air cylinder reduces the effectiveness of each test. Two cylinders are available and joining them together to feed one regulator will double the amount of time available. It is believed that this is a readily available linkage, albeit expensive, that is used by professional scuba divers.

Enhanced Regulator Valve. The outlet pressure of the regulator valve can be altered but this is a normal part of the equipments operation. It was intended to enlarge the channels within the regulator to improve mass flow. It was also intended to modify its regulator mechanism to allow higher pressures to be delivered. These alterations haven't been

attempted as they would cause the cylinder to empty more rapidly. If the double cylinder linkage is obtained, these modifications will be attempted.

Accessibility of Sensors. The sensors and their visual displays are distributed across the test rig and checking them, whilst operating the valves and disc brake, promotes reading errors. It should be possible to bring all of the sensor displays and rig adjustment mechanisms into close proximity so that little movement is required to check and note displayed values whilst the test rig is being operated.

Plan of Further Studies. A full range of torque, power and efficiency curves are required for this design in its present configuration (port timing and offsets) in order to characterise the motor. Particular attention is to be paid to increasing the motor's speed range and noting the limits of its breathing capabilities. It was always intended to increase the number of outlet ports and this will done in two port, one per side, increments. At each increment the aforementioned studies will be repeated.

References

Atlas Copco, 2009	Atlas Copco, Carbon Zero Compressors brochure, 2009, p7/18 copy of TUV certificate dated 17/6/2009. PDF copy available at :- http://www.atlascopco.com/microsites/Images/Carbon%20Zero%20brochure_EN_tcm428-925566.pdf
Badr, et al, 1984a	Badr, O. O'Callaghan, P. W., Hussain. M., Probert, S. D.: Multi-Vane Expanders as Prime Movers for Low Grade Energy Organic Rankine Cycle Engines, Applied Energy, Vol 16/2 (1984) 129-146
Badr, et al, 1984b	Badr, O. O'Callaghan, P. W., Hussain. M., Probert, S. D.: Multi-Vane Expanders as Prime Movers for Low Grade Energy Organic Rankine Cycle Engines, Applied Energy, Vol 16/2 (1984) PP145
Badr, et al, 1985a	Badr, O. O'Callaghan, P. W., Probert, S. D.: Multi-Vane Expanders: Geometry and Vane Kinematics, Applied Energy, Vol 19 (1985) 159-182
Badr, et al, 1985b	Badr, O. O'Callaghan, P. W., Probert, S. D.: Multi –Vane Expander Performance: Breathing Characteristics, Applied Energy Vol 19 (1985) 214-271.
Badr, et al, 1985c	Badr, O., Probert, S. D., O'Callaghan, P. W.: Multi-Vane Expanders: Internal Leakage Losses, Applied Energy, Vol 20 (1985)1-46.
Badr, et al, 1985d	Badr, O., Probert, S. D., O'Callaghan, P. W.: Performances of Multi-Vane Expanders, Applied Energy, Vol 20 (1985), 207 – 234.
Badr, et al, 1985e	Badr, O., Probert, S. D., O'Callaghan, P. W.: Multi-Vane Expanders: Vane Dynamics and Friction Losses, Applied Energy, Vol 20 (1985), 253 – 285.
Badr, et al, 1986	Badr, O., Probert, S. D., O'Callaghan, P. W. Selection of Operating Conditions and Optimisation of Design Parameters for Multi-Vane Expanders, Applied Energy, Vol 23 (1986), 1 - 46.
Balje, 1962	Balje, O. E., A study on design criteria and matching of turbomachines: Part A – Similarity relations and design criteria of turbines, Trans. ASME, Journal of Engineering for Power, 84(January, 1962), pp. 83 – 102.
Barber and Prigmore, 1981	Barber, R. E. & Prigmore. D. E., Solar Energy Handbook (Ed. Kreider, J. F.), Chapter 22 Solar Powered Heat Engines, McGraw Hill, 1981, ISBN 007035474X
Boese & Hencey,1972	Boese, H.L, and Hencey Jr., T.R., Non Polluting Motors Including Cryogenic Fluid as the Motive Means, US Patent No., 3,681,609,

	Aug. 1, 1972.
Boese, 1981	Boese, H.L., Cryogenic Powered Vehicle, US Patent No. 4,294,323, Oct. 13, 1981.
Bosch, 2008a	Robert Bosch Gmbh, Automotive Handbook, 7th Edn, pp430 - 433 Distributer - John Wiley and Son, ISBN 978-0470519363
Bosch, 2008b	Robert Bosch Gmbh, Automotive Handbook, 7th Edn, p988 Distributer - John Wiley and Son, ISBN 978-0470519363
Bosch, 2008c	Robert Bosch Gmbh, Automotive Handbook, 7th Edn, pp1014-1015 Distributer - John Wiley and Son, ISBN 978-0470519363
Bozic & Milton, 2011	Bozic, G., Milton, B., Design Concepts and Performance Simulation of a Compressed Air Hybrid Vehicle
BNCB, 1976	British National Coal Board, Automotive Engineering, Jan 1976.
CARB, 2008	California Air Resources Board, California Code of Regulations, Rulemaking to consider adoption of the 2008 amendments to the California zero emission vehicle regulation (March 27, 2008).
CARB, 1992	California Air Resources Board, California Code of Regulations, Zero Emission Vehicle Regulations, 1992, plus subsequent amendments.
Carvalho, 2008	Carvalho, L. O., Exergetic analysis of of compressed air for vehicular propulsion, SAE Technical Paper, 2008-36-0315.
Cengal, 1989a	Cengal, Y. A., Boles, M. A., Thermodynamics: An Engineering Approach, 1989, P762-816, McGraw-Hill. Original source – Kobe, K. A., Lynn R. E. Jnr., Chemical Review, Vol 52, pp 117-236, 1953.
Cengal, 1989b	Cengal, Y. A., Boles, M. A., Thermodynamics: An Engineering Approach, 1989, P 57 , McGraw-Hill. ISBN 0-07-010356-9
Chen et al, 2011	Chen, H., Ding, Y., Li, Y., Zhang, X., Tan, C., Air-Fuelled zero-emission road transport, Applied Energy, Vol 88, 2011, pp337-342.
Cohen, 2001	Cohen, D., Mantell, S. C., Zhao, L., The effect of fiber volume fraction on filament wound composite pressure vessel strength, Composites Part B: Engineering, 2001, pp 413-429, Elsevier.
Curran, 1981	Curran, H. M. Use of Organic Working Fluids in Rankine Engines, J. Energy 5(4) July-August, 1981, pp218-223

Creutzig et al, 2009	Creutzig, F., Papson, A., Schipper, L., Kammen, D.M., Economic and Environmental Evaluation of Compressed-Air Cars, Environmental Research Letters, Vol 4 (2009) 044011, 9pp.
Daily Mail, 2002	Daily Mail, 4th September 2002, Press release from MDI publicising their compressed air car.
Dhameja, 2002a	Dhameja, S., Electric Vehicle Battery Systems, Pub. Newnes, 2002, pp 23-42, ISBN 0-7506-9916-7.
Dhameja, 2002b	Dhameja, S., Electric Vehicle Battery Systems, Pub. Newnes, 2002, Appendix E, ISBN 0-7506-9916-7.
Dhameja, 2002c	Dhameja, S., Electric Vehicle Battery Systems, Pub. Newnes, 2002, pp 45 , ISBN 0-7506-9916-7.
Dietrich & Jacob, 1999	Dietrich, F. M., Jacob, W. L, Survey and Assessment of Electric and Magnetic Field (EMF) Public Exposure in the Transportation Environment, Electric Research and Management Inc., 1999, pp 4.22-4.49, report prepared for and owned by US department of Transport, copies available from the National Technical Information Service.
Ditmore, 1995	Ditmore, H. R., An Innovative Compressed Air Car of Practical Performance. Unpublished final year project report for the degree of B.Eng (Hons) Mechanical Engineering at the University of Westminster, May 1995.
Ditmore. et al, 1997a	Ditmore, H. R., Marquand, C. J., McVeigh, J.C., An Innovative Power Pack and Motor for a Compressed Air Car of Practical Performance, International Journal of Ambient Energy, pp 36 – 42,Vol 18, Number 1, January 1997.
Ditmore et al, 1997b	Ditmore, H. R., Xystri, E., Marquand, C. J., McVeigh, J.C., The Performance of an Innovative Power Pack for a Compressed Air Car, International Conference on Energy and the Environment, Cyprus 12-14 October, 1997.
Ditmore et al, 2007	Ditmore, H. R., Marquand, C. J., The Performance of a Power Pack for a Compressed Air Car, Proceedings 6th International Colloquium Fuels 2007, pp171-181, Stuttgart, 10-11 Jan, 2007. ISBN3-924813-67-1
Ditmore, 2009	Ditmore, H.R., Development of a Compressed Air Energy Storage System For a Plug-In Hybrid Vehicle, Proc. Low Carbon Vehicles, pp159-167, 2009, Pub. IMechE. ISBN 978 1 84334 560 2.
Ehsani, 2009	Ehsani, H., Gao, Y., Emahdi, A., Modern Electric, Hybrid Electric and Fuel Cell Vehicles, CRC Press 2nd Edition, 2009, pp380-388,

	ISBN 978-1420053982.
Fetchenko, 2010	Fetchenko, Michael., Ovonics Battery Company, NiMH for Consumer, Vehicle and Stationary Applications, Proceedings of Batteries 2010, 29th September 2010.
Gill and Shouman, 1976	Gill, W. and Shouman, A. R., State of the Art Review of Sliding Vane Machinery, ASME paper No. 76-DET-90, Design Engineering Technical Conference, Montreal, Canada, 1976.
GRP Tubing, 2009	GRP Tubing trade website, 2009, http://grptubing.com/index.php?option=com_content&view=article&id=51&Itemid=110
Hesselgreaves, 2001a	Hesselgreaves, J.E., Compact Heat Exchangers, 2001, Pub. Pergamon/Elsevier, Oxford, UK. ISBN 0-08-042839-8
Hesselgreaves, 2001b	Hesselgreaves, J.E., Compact Heat Exchangers, 2001, pp76-77, Pub. Pergamon/Elsevier, Oxford, UK. ISBN 0-08-042839-8
Hesselgreaves, 2001c	Hesselgreaves, J.E., Compact Heat Exchangers, 2001, pp78, Pub. Pergamon/Elsevier, Oxford, UK. ISBN 0-08-042839-8
Hightech, 1999	Borroni-Bird, Chris, Daimler Chrysler Hightech Report 1999, pp17, Pub. Daimler Chrysler AG Communications, D-70546, Stuttgart, Germany.
Higuchi, 2005	Ken Higuchi, et al, Development and flight test of metal-lined CFRP cryogenic tank for reusable rocket, *Acta Astronautica*, *Volume 57, Issues 2-8*, *July-October 2005*, *Pages 432-437*
HSE, 2002	United Kingdom Health and Safety Executive, Specification for Fully Wrapped Carbon Composite Containers, Document Code HSE-AL-FW2, Version 5, 2002.
IEA,1993	International Energy Agency, Cars and Climate Change, Organisation for Economic Co-operation and Development, 1993, pp110-113, ISBN 92-64-13804-8 http://www.iea.org/textbase/nppdf/free/1990/cars_climate1993.pdf
ISO, 2002	Standard ISO1119-3:2002, Gas cylinders of composite construction -- Specification and test methods -- Part 3: Fully wrapped fibre reinforced composite gas cylinders with non-load-sharing metallic or non-metallic liners, International Organization for Standardization, Geneva, Switzerland.
Isoterix 2002	Isoterix Ltd (now Thermocore Europe Ltd): Heatpipe Cooling Solutions, Power Electronics Europe, Issue 4, 2002, p23-25.

Jacazio et al, 1979	Jacazio, G, Piombo, B. Romitti, and A. Sola, A., The Optmisation of the Performance of Sliding Vane Type Air Motors, Proceedings of the Fifth World Congress on Theory of Machines and Mechanisms, Montreal, Canada, pp.607-10, 1979.
Jensen, 1980	Jensen, J., Energy Storage, Newnes-Butterworths, 1980, P.50-51, ISBN 0-408-00390-1
Jensen, 1984	Jensen, J., Sorensen, B., Fundamentals of Energy Storage, 1984, pp 46-54, J. Wiley and Sons Ltd. ISBN 0-471-08604-5,
John, 2003a	John, V., Introduction to Engineering Materials, Table 1.3. ISBN-13: 978-0333949177, 2003, Palgrave MacMillan.
John, 2003b	John, V., Introduction to Engineering Materials, Section 21.3. ISBN-13: 978-0333949177, 2003, Palgrave MacMillan.
Kawahara, 1996	Kawahara, G., & Mekleskey, S. F., Titanium Lined, carbon Composite Overwrapped Pressure Vessel, P.6, Proceedings of 32nd AIAA Joint Propulsion Conference, AIAA 96-2751, 1996, American Institute of Aeronautics and Astronautics
Knight, 1876	Knight, E.H., Knight's American Mechanical Dictionary, pp 602-604, 1876 Edn, original Pub. Hurd & Houghton. Currently available from Algrove Publishing Ltd, Ontario, Canada, ISBN 1-894572-85-8. See also pp 620-622 of a free, searchable, E-book version available from the Princeton Digital Library at :- www.princetonimaging.com/library/mechanical-dictionary/
Lamarre, 1991	Lamarre, L., Alabama Cooperative Generates Power From Air, Electric Power Research Institute, Dec 1991, pp12-19.
Mattick et al, 1975	Mattick, W., Haddenhorst, H. G., Weber, O., & Stys, Z. S., Huntorf, The World's First 290MW Gas Turbine Air-Storage Peaking Plan, Proc. of 37th American Power Conference, Illinois Institute of Technology, 1974, pp379-389.
Minder & Pfluger,2001	Minder, C. E., Pfluger, D H., Leukemia, brain tumours and exposure to extremely low frequency electromagnetic fields in Swiss railway employees, American Journal of Epidemiology, Vol 153, issue 9, May 1, 2001, pp 825-835.
Parr, 1991	Parr, A., Hydraulics and Pneumatics, Newnes/Butterworth-Heineman Ltd. Oxford, UK., PP 45-47, ISBN 0750607939.
Pneumacom, 1994.	Pneumacom Inc. Spirit of Joplin, Press release reported in New Scientist, pp. 21 , 6/8/94.

Popov, 1978	Popov, E. P., Mechanics of Materials, 1978, pp 290-291, ISBN 0-13-571158-4, Prentice Hall, USA, New jersey.
Reay, D., 2006.	Reay, D. and Kew, P., Heat Pipes, 2006, P.109, Butterworth-Heinemann, 5th Edition. ISBN 13: 978-0-7506—6754-8
Sychev, et al., 1987a	Sychev, V. V., et al, Thermodynamic Properties of Air, National Standard Reference Data Service of the USSR, 1987, Hemisphere Publishing Corporation, ISBN 0-89116-610-6
Sychev, et al., 1987b	Sychev, V. V., et al, Thermodynamic Properties of Air, pp 3 – 21, National Standard Reference Data Service of the USSR, 1987, Hemisphere Publishing Corporation, ISBN 0-89116-610-6
Ter-Gazarian, 1994a.	Ter-Gazarian, A., Energy Storage for Power Systems, 1994, Pub. Peter Peregrinus Ltd, Institute of Electrical Engineers, UK, pp 100 – 101, ISBN 0-86341-264-54.
Ter-Gazarian, 1994b.	Ter-Gazarian, A., Energy Storage for Power Systems, 1994, Pub. Peter Peregrinus Ltd, Institute of Electrical Engineers, UK, pp. 109, ISBN 0-86341-264-54.
Toray, 2008	Toray Industries, Inc., Company literature, "Toray's Strategy for Carbon Fiber Composite Materials" PDF available at HTTP://www.toray.com/ir/pdf/lib_a136.pdf#page=12
US DOE/ OTTNRE 2001	US DOE / Office of Transportation Technologies and National Renewable Energy Laboratory, "Future US highway energy use: a fifty year perspective" 2001
US DOT, 2007	United States, Department of Transport, DOT-CFFC BASIC REQUIREMENTS (FIFTH REVISION) Appendix A, Basic Requirements for Fully Wrapped Carbon-Fiber Reinforced Aluminum Lined Cylinder(DOT-CFFC), March 2007 (fifth revision), P. 6.
Williams, J., 1997a	Williams, J.: Cryogenic Automobile Propulsion: Heat Exchanger Design and Performance Issues, AIAA paper 97-0017, 1997.
Williams, J., 1997b	Williams, J. et al: Frost-Free Cryogenic Heat Exchangers for Automotive Propulsion, AIAA Paper 97-3168.
Yamamoto, Y., 1981	Yamamoto, Y. Rotary Engine, 1981, Pub. Sankaido Co. Ltd., 5-5-18, Hongo, Bunkyo-ku, Tokyo, Japan

Author's publications	
Ditmore, 1995	Ditmore, H. R., An Innovative Compressed Air Car of Practical Performance. Unpublished final year project report for the degree of B.Eng (Hons) Mechanical Engineering at the University of Westminster, May 1995.
Ditmore. et al, 1997a	Ditmore, H. R., Marquand, C. J., McVeigh, J.C., An Innovative Power Pack and Motor for a Compressed Air Car of Practical Performance, International Journal of Ambient Energy, pp 36 – 42,Vol 18, Number 1, January 1997.
Ditmore et al, 1997b	Ditmore, H. R., Xystri, E., Marquand, C. J., McVeigh, J.C., The Performance of an Innovative Power Pack for a Compressed Air Car, International Conference on Energy and the Environment, Cyprus 12-14 October, 1997.
Ditmore et al, 2007	Ditmore, H. R., Marquand, C. J., The Performance of a Power Pack for a Compressed Air Car, Proceedings 6th International Colloquium Fuels 2007, pp171-181, Stuttgart, 10-11 Jan, 2007. ISBN3-924813-67-1
Ditmore, 2009	Ditmore, H.R., Development of a Compressed Air Energy Storage System For a Plug-In Hybrid Vehicle, Proc. Low Carbon Vehicles, pp159-167, 2009, Pub. IMechE. ISBN 978 1 84334 560 2.

Appendices

Appendix A – Primary Heat Exchanger Test Results

Series Connected – Test 1			
Initial Pressure 300 bar		**Ambient Temp 20°C**	
Flow Rate 3.0 m/s		**Mass Flow 7 g/s**	
Reading	**Inlet to Ethanol HP temp °C**	**Midway temp °C**	**Outlet from Water HP temp °C**
1	**20**	**20**	**20**
2	**-10**	**20**	**20**
3	**-24**	**19**	**20**
4	**-27**	**17**	**20**
5	**-27**	**17**	**20**
6	**-27**	**18**	**20**

Series Connected – Test 1a			
Initial Pressure 300 bar		**Ambient Temp 20°C**	
Flow Rate 3.0 m/s		**Mass Flow 7 g/s**	
Reading	**Inlet to Ethanol HP temp °C**	**Midway temp °C**	**Outlet from Water HP temp °C**
1	**20**	**20**	**20**
2	**-9**	**20**	**20**
3	**-24**	**19**	**20**
4	**-27**	**18**	**19**
5	**-27**	**17**	**19**
6	**-27**	**17**	**19**

Series Connected – Test 2			
Initial Pressure 300 bar		**Ambient Temp 20°C**	
Flow Rate 3.7 m/s		**Mass Flow 8.6 g/s**	
Reading	**Inlet to Ethanol HP temp °C**	**Midway temp °C**	**Outlet from Water HP temp °C**
1	**20**	**20**	**20**
2	**-21**	**20**	**20**
3	**-27**	**18**	**20**
4	**-29**	**14**	**20**
5	**-29**	**14**	**20**
6			

Series Connected – Test 2a			
Initial Pressure 300 bar		**Ambient Temp 20°C**	
Flow Rate 3.7 m/s		**Mass Flow 8.6 g/s**	
Reading	**Inlet to Ethanol HP temp °C**	**Midway temp °C**	**Outlet from Water HP temp °C**
1	**20**	**20**	**20**
2	**-20**	**20**	**19**
3	**-27**	**18**	**19**
4	**-29**	**15**	**19**
5	**-29**	**14**	**19**
6			

Series Connected – Test 3			
Initial Pressure 300 bar		**Ambient Temp 20°C**	
Flow Rate 4.9 m/s		**Mass Flow 11.4 g/s**	
Reading	**Inlet to Ethanol HP temp °C**	**Midway temp °C**	**Outlet from Water HP temp °C**
1	**20**	**20**	**20**
2	**6**	**14**	**20**
3	**-8**	**8**	**19**
4	**-21**	**-2**	**19**
5	**-33**	**-12**	**19**
6			

Series Connected – Test 3a			
Initial Pressure 300 bar		**Ambient Temp 21°C**	
Flow Rate 4.9 m/s		**Mass Flow 11.4g/s**	
Reading	**Inlet to Ethanol HP temp °C**	**Midway temp °C**	**Outlet from Water HP temp °C**
1	**20**	**20**	**20**
2	**6**	**14**	**20**
3	**-9**	**9**	**19**
4	**-22**	**-1**	**19**
5	**-34**	**-12**	**19**
6			

Series Connected – Test 4			
Initial Pressure 300 bar		**Ambient Temp 22 °C**	
Flow Rate 6.0m/s		**Mass Flow 13.9g/s**	
Reading	**Inlet to Ethanol HP temp °C**	**Midway temp °C**	**Outlet from Water HP temp °C**
1	**22**	**22**	**22**
2	**11**	**18**	**22**
3	**-1**	**15**	**21**
4	**-13**	**12**	**20**
5	**-26**	**11**	**19**
6	**-38**	**10**	**18**

Series Connected – Test 5			
Initial Pressure 300 bar		**Ambient Temp 20°C**	
Flow Rate 8.7 m/s		**Mass Flow 20.2 g/s**	
Reading	**Inlet to Ethanol HP temp °C**	**Midway temp °C**	**Outlet from Water HP temp °C**
1	**20**	**20**	**20**
2	**-29**	**12**	**18**
3	**-38**	**9**	**17**
4			
5			
6			

Series Connected – Test 5a			
Initial Pressure 300 bar		**Ambient Temp 20°C**	
Flow Rate 8.7 m/s		**Mass Flow 20.2 g/s**	
Reading	**Inlet to Ethanol HP temp °C**	**Midway temp °C**	**Outlet from Water HP temp °C**
1	**20**	**20**	**20**
2	**9**	**15**	**18**
3	**-30**	**12**	**18**
4	**-38**	**9**	**17**
5			
6			

Parallel Connected – Test 6			
Initial Pressure 300 bar		**Ambient Temp 20 °C**	
Flow Rate 9.1 m/s		**Mass Flow 21.1 g/s**	
Reading	**Inlet to Ethanol HP temp °C**	**Midway temp °C**	**Outlet from Water HP temp °C**
1	**20**	**20**	**20**
2	**-26**	**20**	**20**
3	**-30**	**18**	**18**
4	**-34**	**18**	**17**
5	**-36**	**11**	**15**
6			

Parallel Connected – Test 6a			
Initial Pressure 300 bar		**Ambient Temp 20 °C**	
Flow Rate 9.1 m/s		**Mass Flow 21.1g/s**	
Reading	**Inlet to Ethanol HP temp °C**	**Midway temp °C**	**Outlet from Water HP temp °C**
1	**20**	**20**	**20**
2	**-26**	**20**	**20**
3	**-31**	**18**	**18**
4	**-34**	**18**	**17**
5	**-36**	**11**	**15**
6			

Parallel Connected – Test 7			
Initial Pressure 300 bar		**Ambient Temp 22°C**	
Flow Rate 9.0 m/s		**Mass Flow 20.88 g/s**	
Reading	**Inlet to Ethanol HP temp °C**	**Midway temp °C**	**Outlet from Water HP temp °C**
1	**22**	**22**	**22**
2	**15**	**18**	**20**
3	**-25**	**16**	**17**
4	**-32**	**13**	**17**
5	**-34**	**11**	**17**
6	**-36**	**11**	**15**

Parallel Connected – Test 8			
Initial Pressure 300 bar		**Ambient Temp 20°C**	
Flow Rate 7.8 m/s		**Mass Flow 18.1 g/s**	
Reading	**Inlet to Ethanol HP temp °C**	**Midway temp °C**	**Outlet from Water HP temp °C**
1	**20**	**20**	**20**
2	**-17**	**18**	**17**
3	**-25**	**14**	**17**
4	**-28**	**7**	**16**
5	**-29**	**5**	**15**
6			

Parallel Connected – Test 9			
Initial Pressure 300 bar		**Ambient Temp 22°C**	
Flow Rate 8.5 m/s		**Mass Flow 19.7 g/s**	
Reading	**Inlet to Ethanol HP temp °C**	**Midway temp °C**	**Outlet from Water HP temp °C**
1	**22**	**22**	**22**
2	**4**	**19**	**20**
3	**-15**	**13**	**18**
4	**-33**	**8**	**15**
5			
6			

Parallel Connected – Test 9a			
Initial Pressure 300 bar		**Ambient Temp 22 °C**	
Flow Rate 8.5 m/s		**Mass Flow 19.7 g/s**	
Reading	**Inlet to Ethanol HP temp °C**	**Midway temp °C**	**Outlet from Water HP temp °C**
1	**22**	**22**	**22**
2	**5**	**18**	**20**
3	**-16**	**12**	**18**
4	**-33**	**8**	**15**
5			
6			

Parallel Connected – Test 10			
Initial Pressure 300 bar		**Ambient Temp 22°C**	
Flow Rate 8.7 m/s		**Mass Flow 20.2 g/s**	
Reading	**Inlet to Ethanol HP temp °C**	**Midway temp °C**	**Outlet from Water HP temp °C**
1	**22**	**22**	**22**
2	**7**	**19**	**19**
3	**-14**	**14**	**17**
4	**-35**	**10**	**15**
5			
6			

Max Flow 2 x ethanol pipes in series – Test 11			
Initial Pressure 300 bar		**Ambient Temp 22°C**	
Flow Rate 8.4 m/s		**Mass Flow 19.5 g/s**	
Reading	**Inlet to Ethanol HP temp °C**	**Midway temp °C**	**Outlet from Water HP temp °C**
1	**22**	**22**	**22**
2	**-2**	**21**	**20**
3	**-15**	**19**	**19**
4	**-25**	**16**	**16**
5	**-29**	**14**	**14**
6	**-33**	**14**	**13**

Ethanol to water HP pathway 1 – Test 12			
Initial Pressure 300 bar		**Ambient Temp 22°C**	
Flow Rate 7.4 m/s		**Mass Flow 17.2 g/s**	
Reading	**Inlet to Ethanol HP temp °C**	**Midway temp °C**	**Outlet from Water HP temp °C**
1	**22**	**22**	**22**
2	**-17**	**13**	**17**
3	**-24**	**9**	**15**
4	**-26**	**5**	**14**
5	**-29**	**2**	**13**
6	**-30**	**1**	**12**

Low Temperature - High Humidity – Test 13		**Humidity 98%**	
Initial Pressure 300 bar		**Ambient Temp 5°C**	
Flow Rate 7.9 m/s		**Mass Flow 18.3 g/s**	
Reading	**Inlet to Ethanol HP temp °C**	**Midway temp °C**	**Outlet from Water HP temp °C**
1	**5**	**5**	**5**
2	**-5**	**--**	**3**
3	**-15**	**--**	**1**
4	**-19**	**--**	**0**
5	**-25**	**--**	**-2**
6	**-32**	**--**	**-3**
7	**-45**	**--**	**-3**

Low Temperature - High Humidity – Test 14		**Humidity 80%**	
Initial Pressure 300 bar		**Ambient Temp 9°C**	
Flow Rate 8.1m/s		**Mass Flow 18.8 g/s**	
Reading	**Inlet to Ethanol HP temp °C**	**Midway temp °C**	**Outlet from Water HP temp °C**
1	**10**	**9**	**9**
2	**-7**	**0**	**0**
3	**-14**	**--**	**0**
4	**-21**	**-6**	**-3**
5	**-28**	**--**	**-3**
6	**-38**	**--**	**-3**

Appendix B – Engineering Drawings for MVE

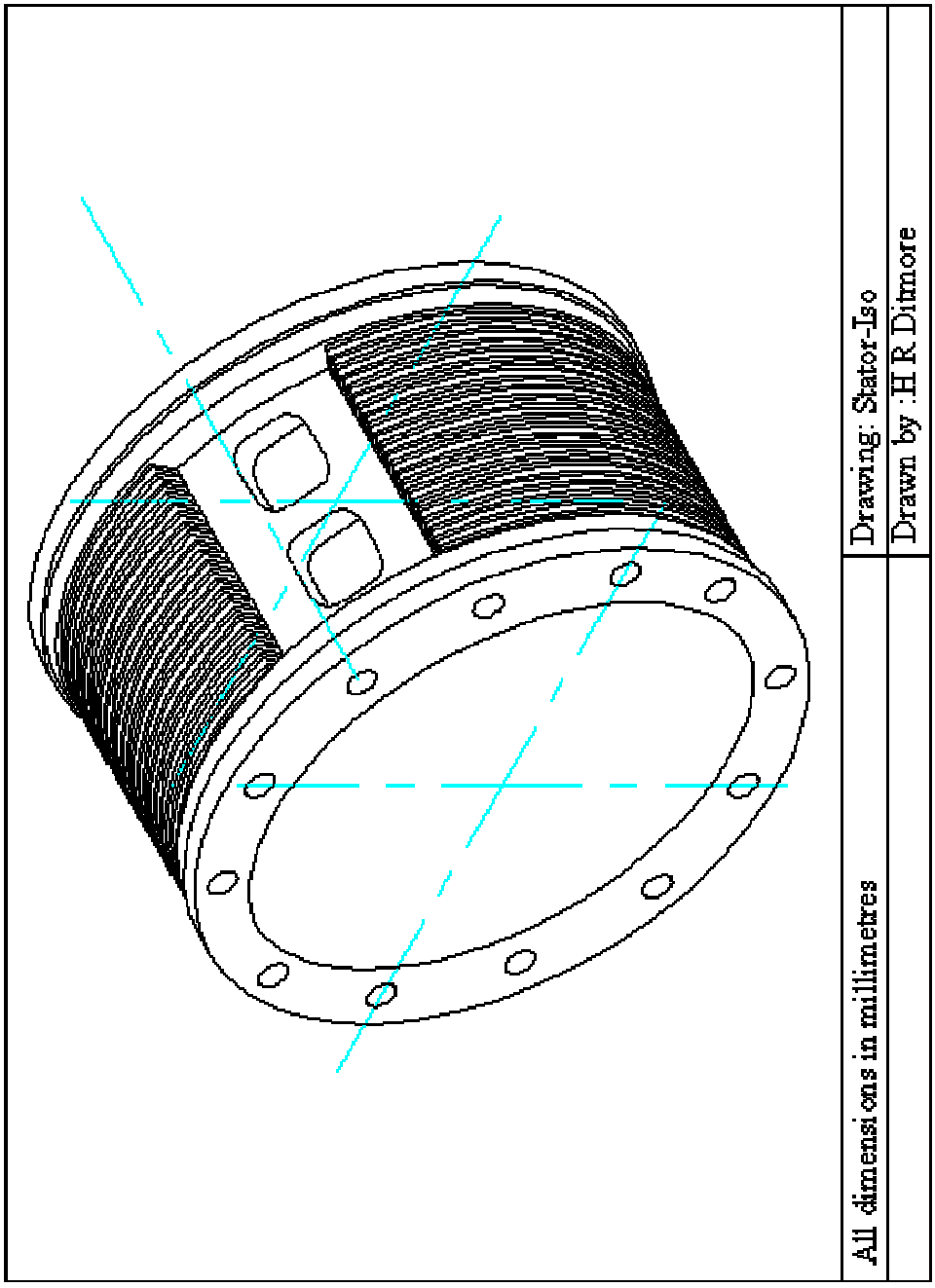

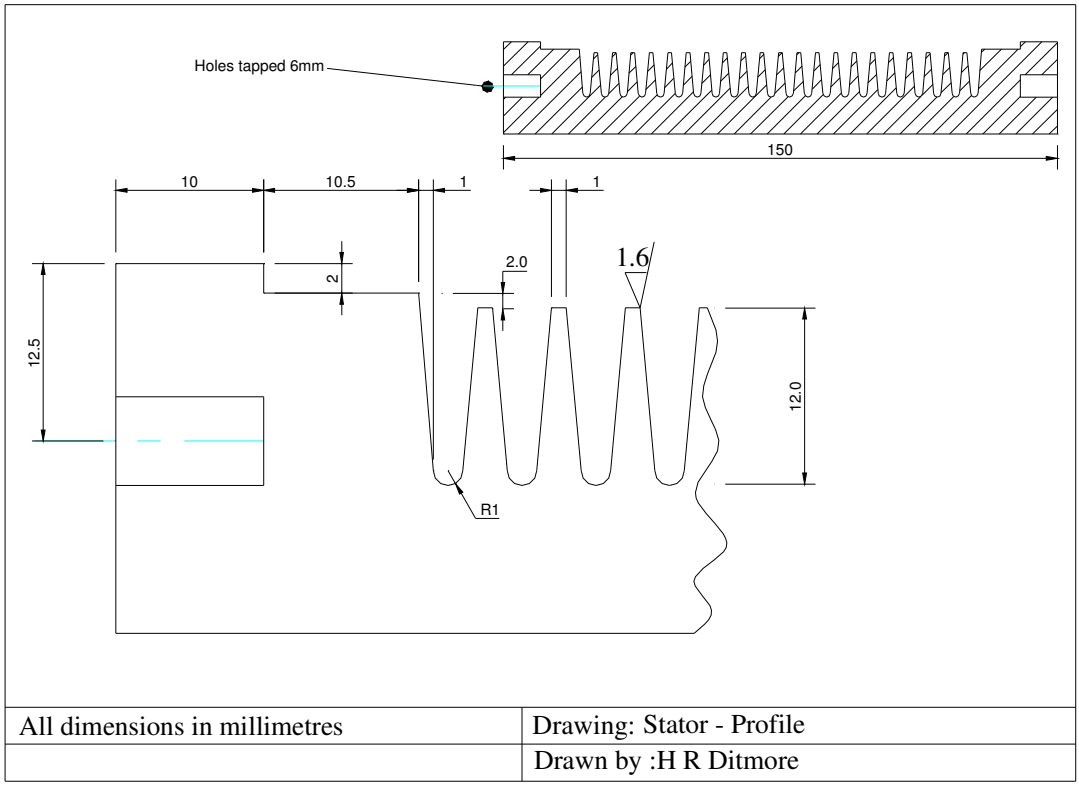

All dimensions in millimetres	Drawing: Stator - Profile
	Drawn by :H R Ditmore

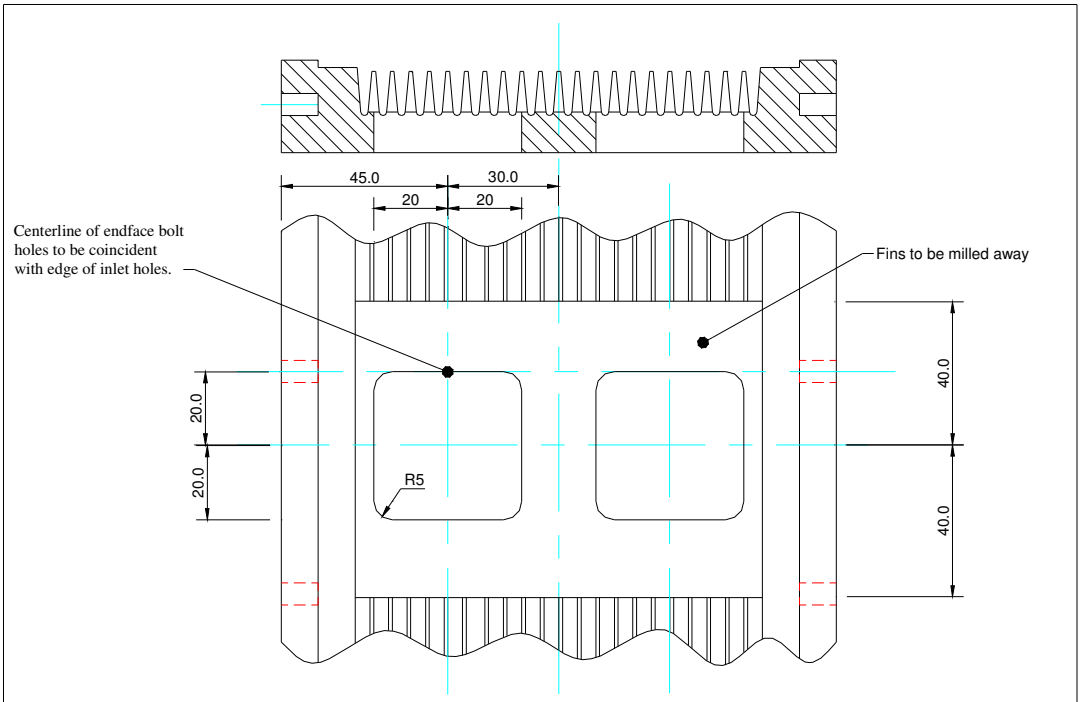

All dimensions in millimetres	Drawing: Stator-Inlet
	Drawn by :H R Ditmore

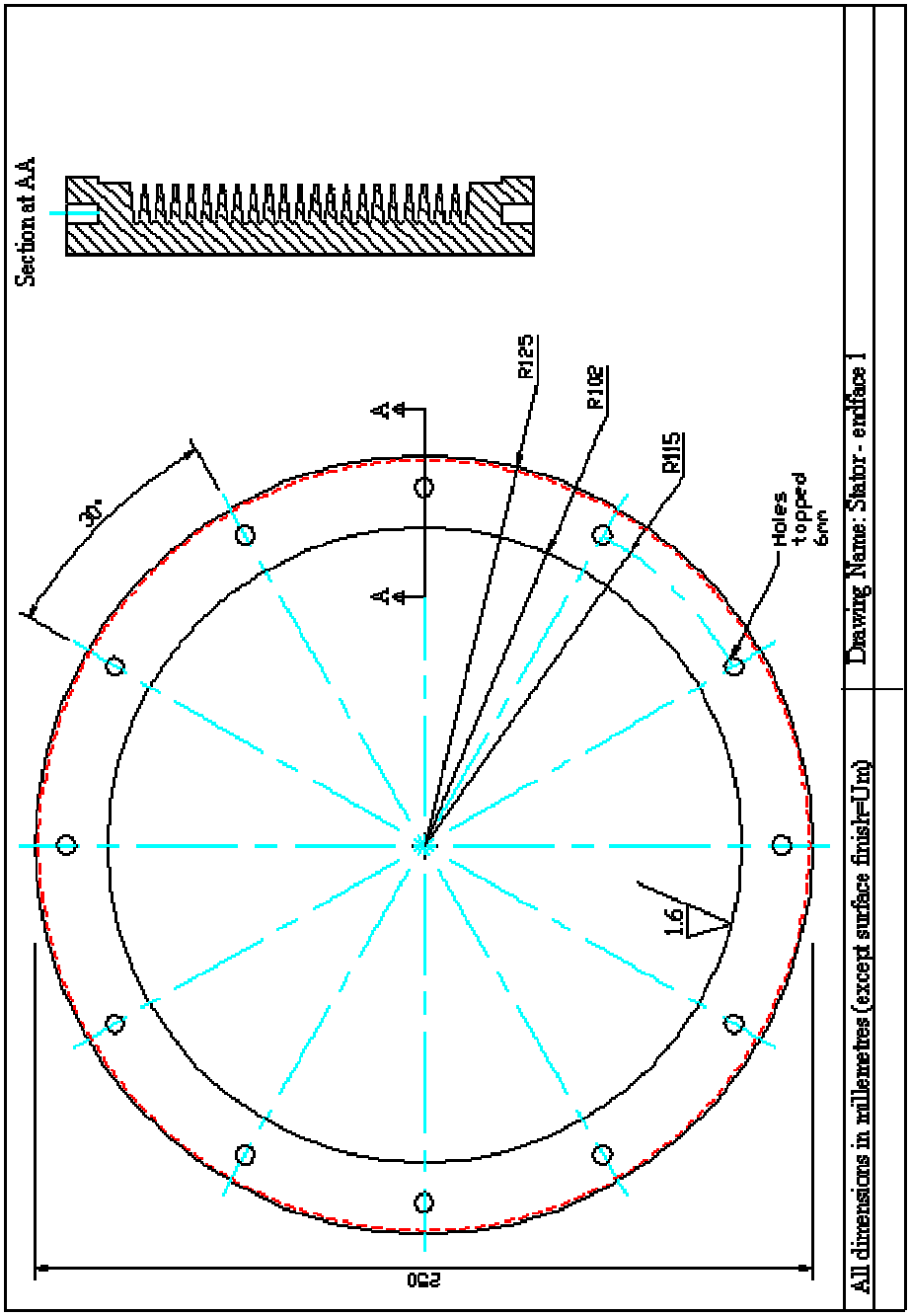
Section at AA
A
A
R125
R102
R115
Holes
topped
6mm
30°
1.6
250
All dimensions in millimetres (except surface finish=Um)
Drawing Name: Stator - endface 1

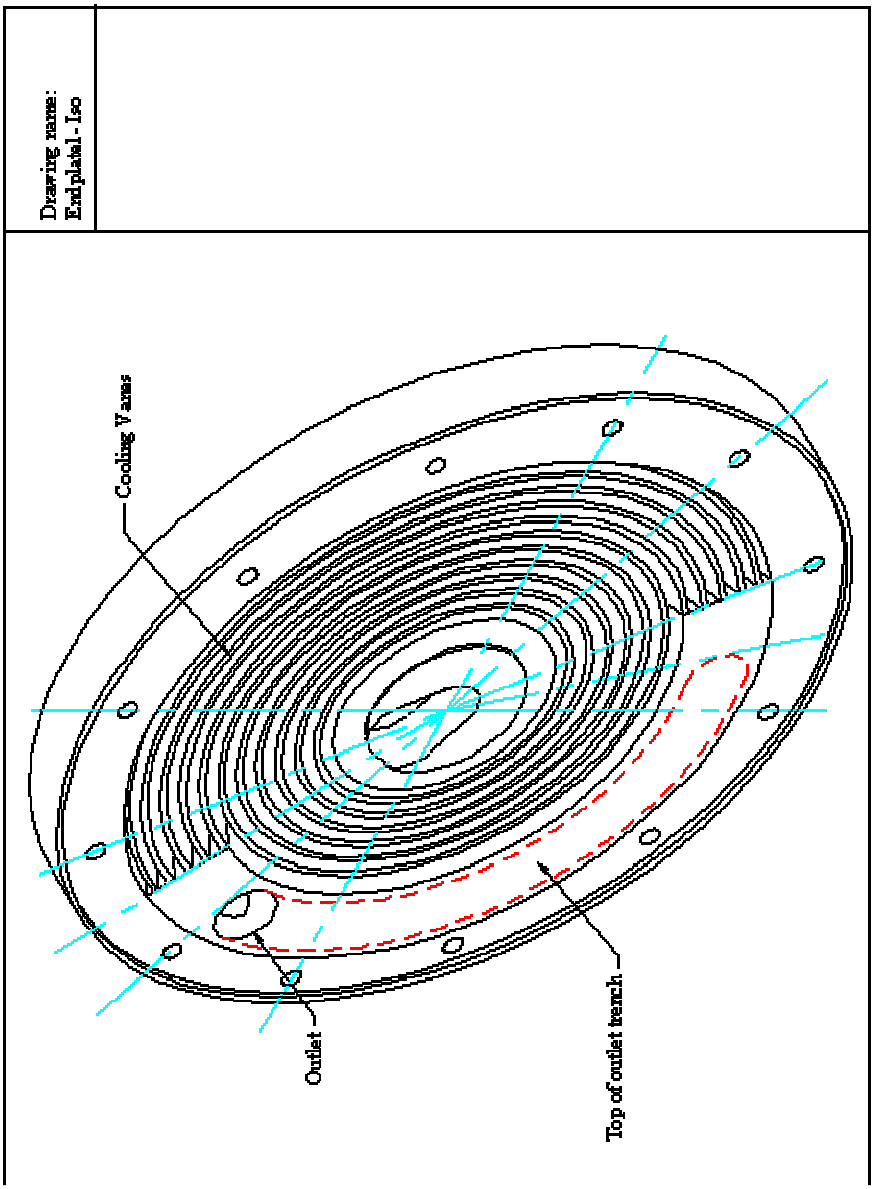
Drawing name:
Endplate1-Iso
Cooling Vanes
Outlet
Top of outlet trench

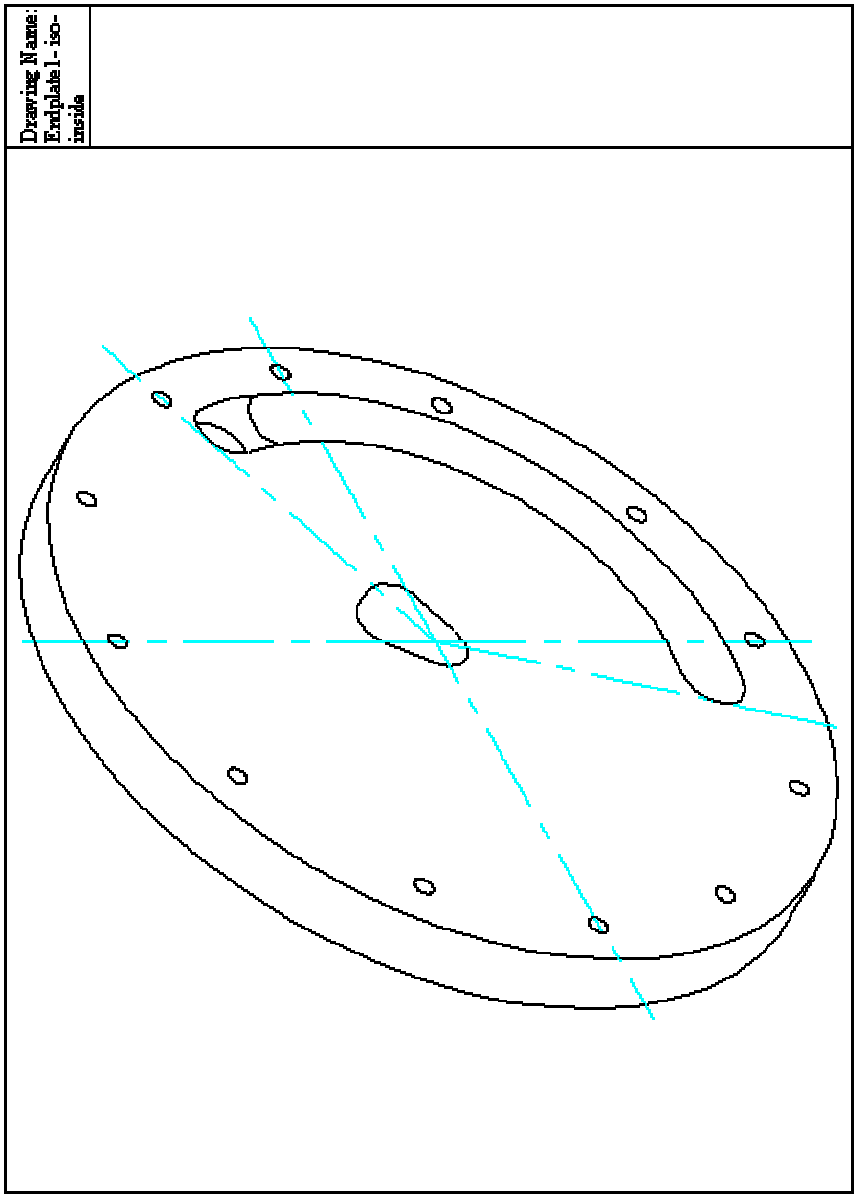
Drawing Name:
Endplate1 - iso -
inside

Section X-X
X
X
Drawing: Endplate 1 - outside
Drawn by: H R Dimmore
All dimensions in millimetres
Not to scale

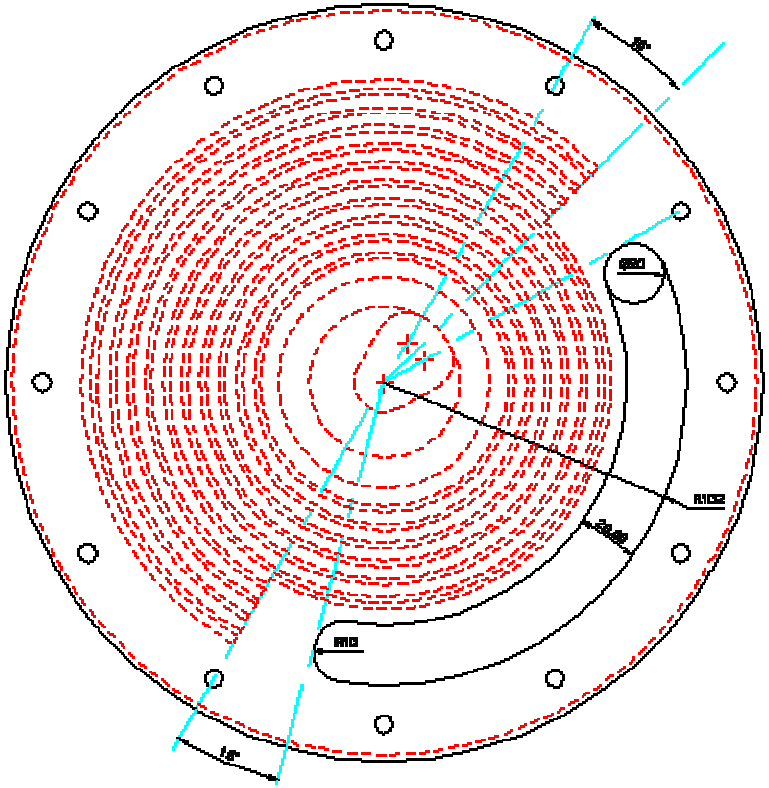

All dimensions in millemetres		Drawing Name: Stator endplate1 - inside
Not to scale		Drawn by: H R Ditmore

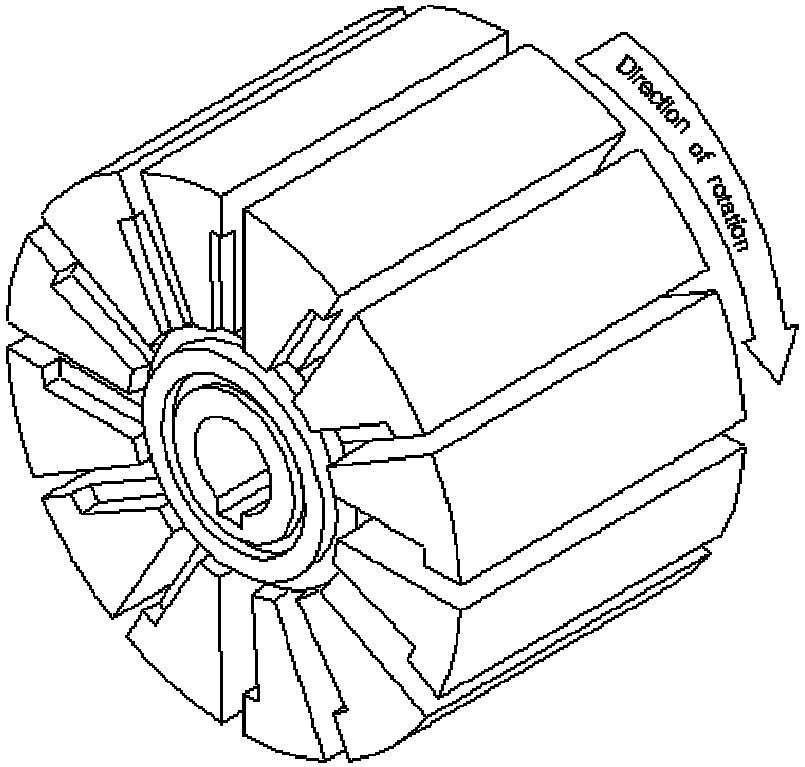

All dimensions in millimetres	Drawing: Rotor - isometric
	Drawn by :H R Ditmore

The outer seal trench (in red with radial components) is to be 5mm wide and 5mm deep in the circular section. In the radial sections, the trenches are to be 5mm wide and 5mm deep. The radial trenches are always to be on the side of the trenches trailing the direction of rotation.

The inner seal trench (in red) is to be approx 5mm deep by 5mm wide.

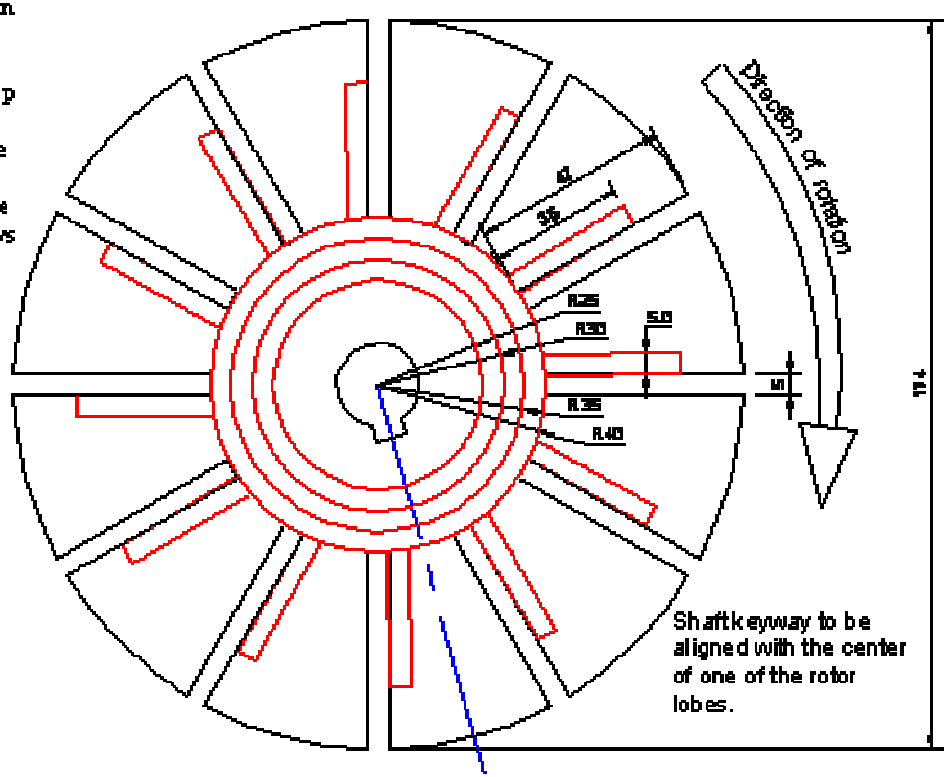

Shaft keyway to be aligned with the center of one of the rotor lobes.

All dimensions in millimetres	Drawing: Rotor - endface 1
	Drawn by: H R Ditmore

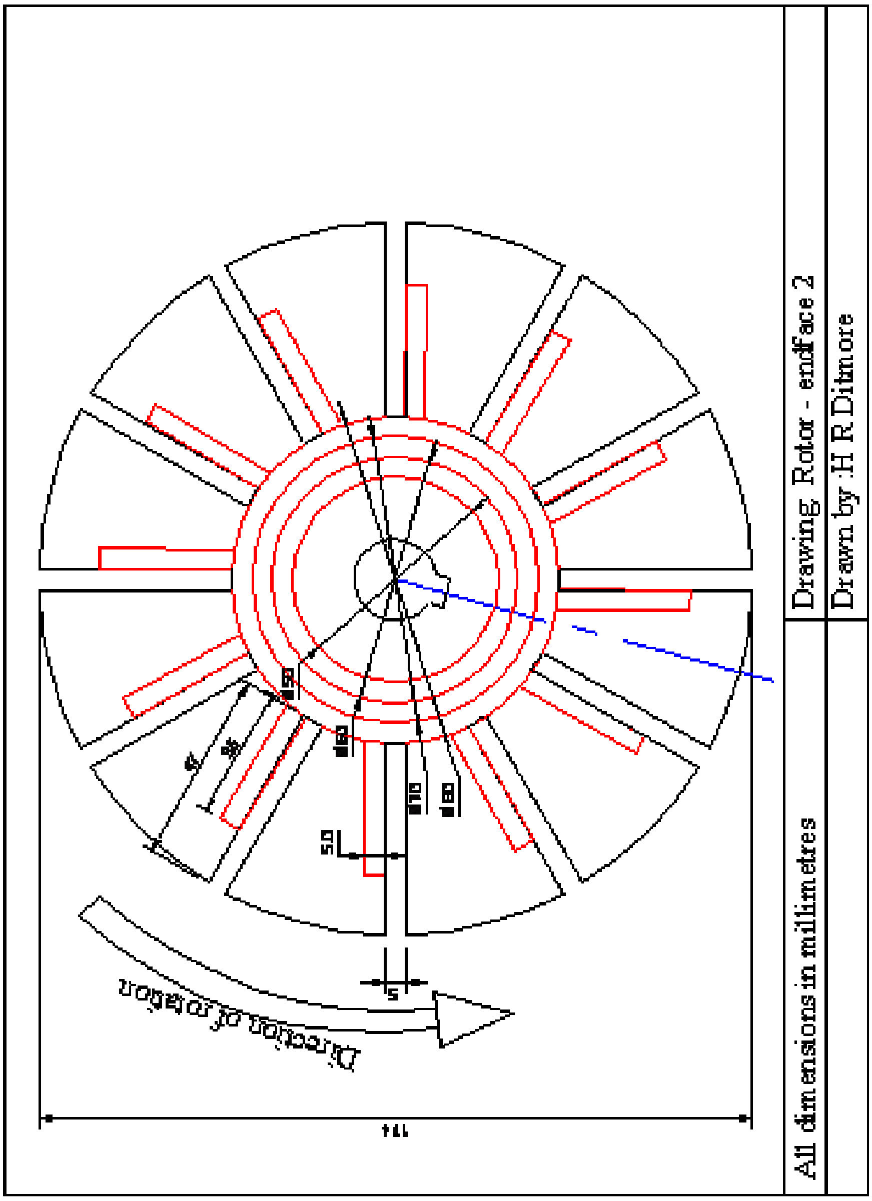
Drawing Rotor - endface 2
Drawn by :H R Ditmore
All dimensions in millimetres
Direction of rotation

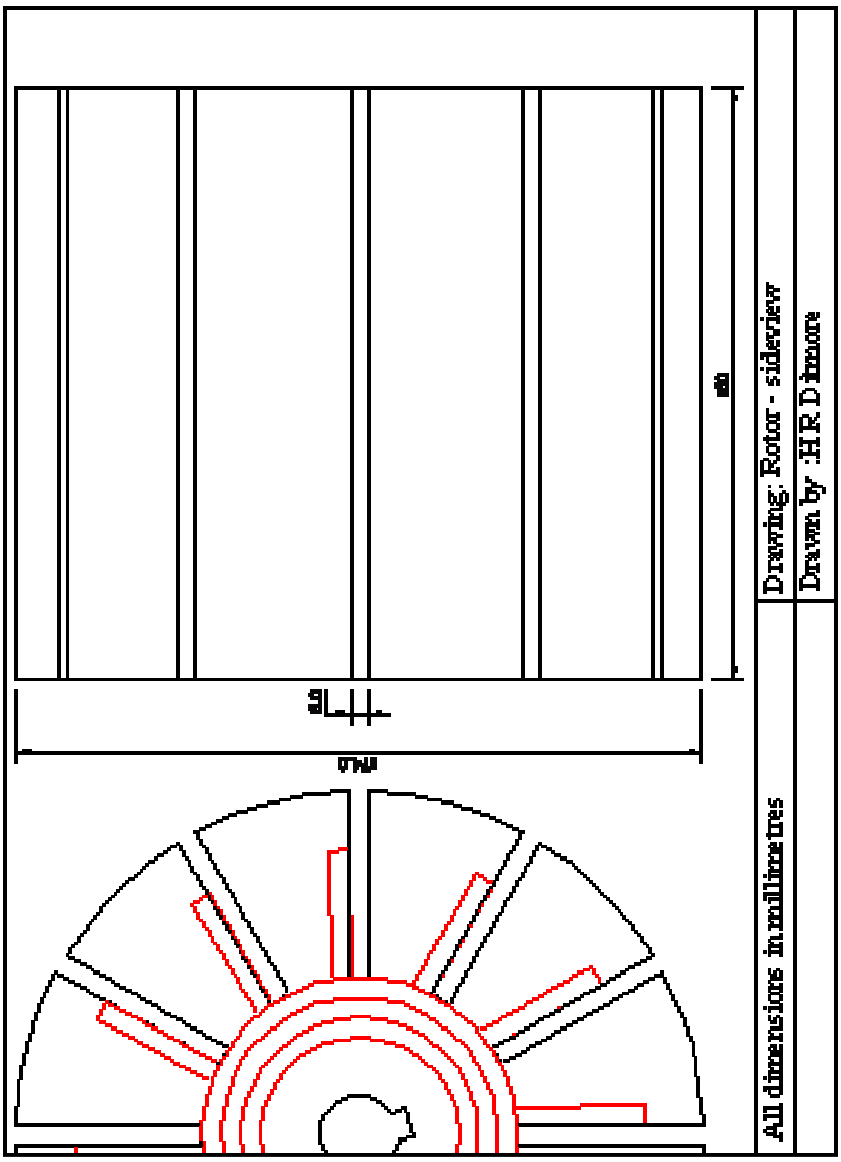
All dimensions in millimetres
Drawing: Rotor - sideview
Drawn by :HR Dinsmore

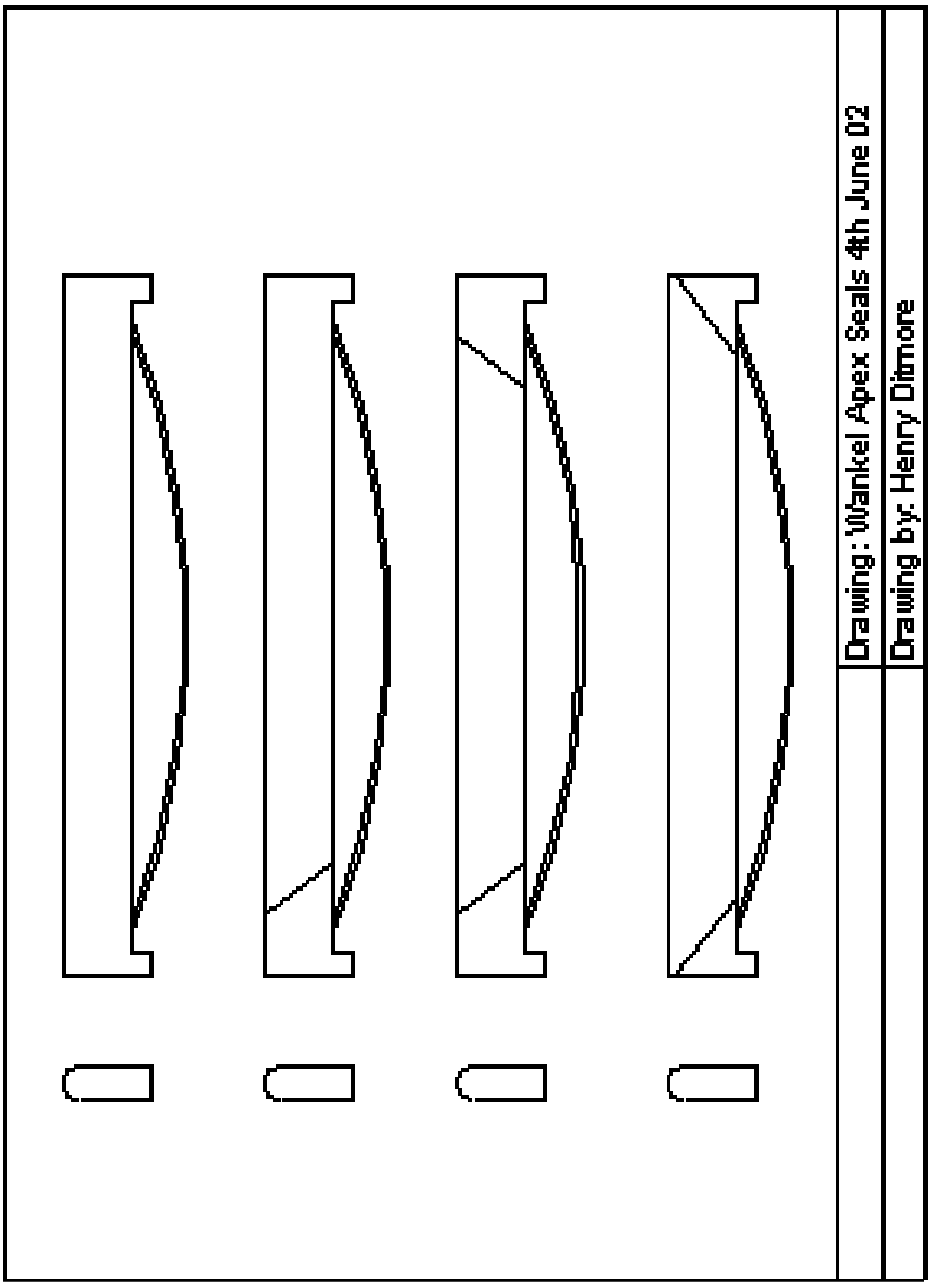
Drawing: Wankel Apex Seals 4th June 02
Drawing by: Henry Dimore

The vane is to be constructed from 5mm brass plate and to be an easy running fit (H9/c9) in the rotor vane slot.

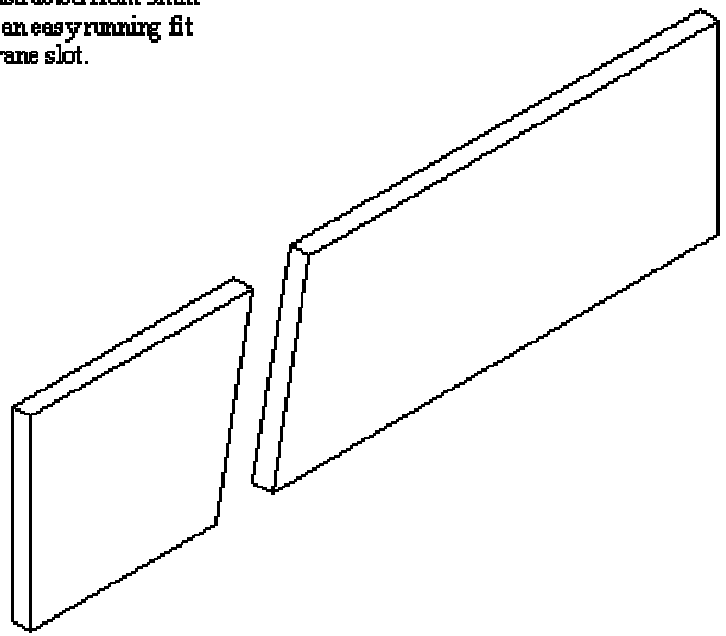

All dimensions in millimetres	Drawing: Vane set - iso
	Drawn by :H R Ditmore

47
150
58°
50
66°
All dimensions in millimetres
Drawing: Basic vane set
Drawing by H R Dimmre

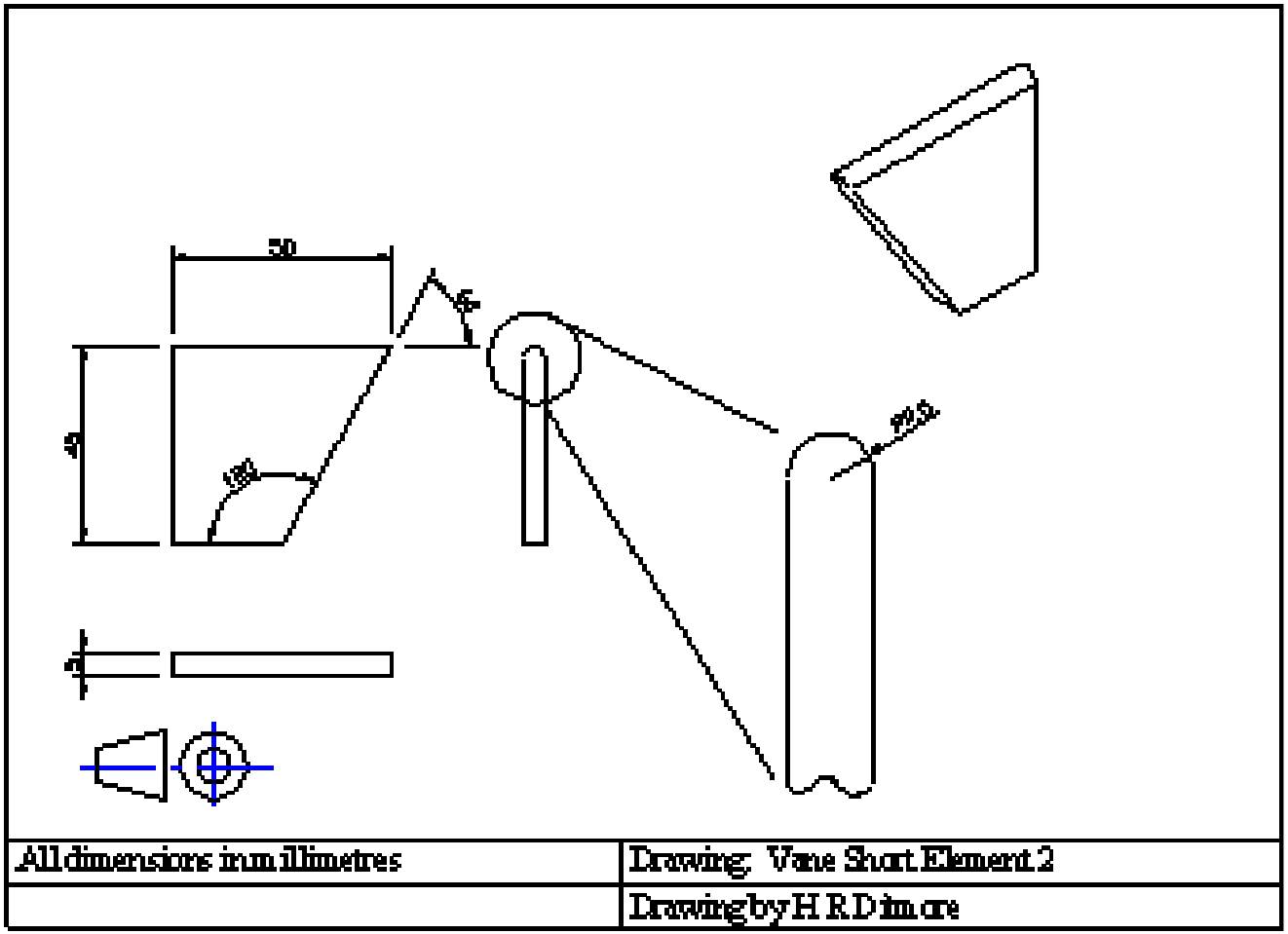
30
6
45
15°
R2.5
All dimensions in millimetres
Drawing: Vane Short Element 2
Drawing by H R Dinmore

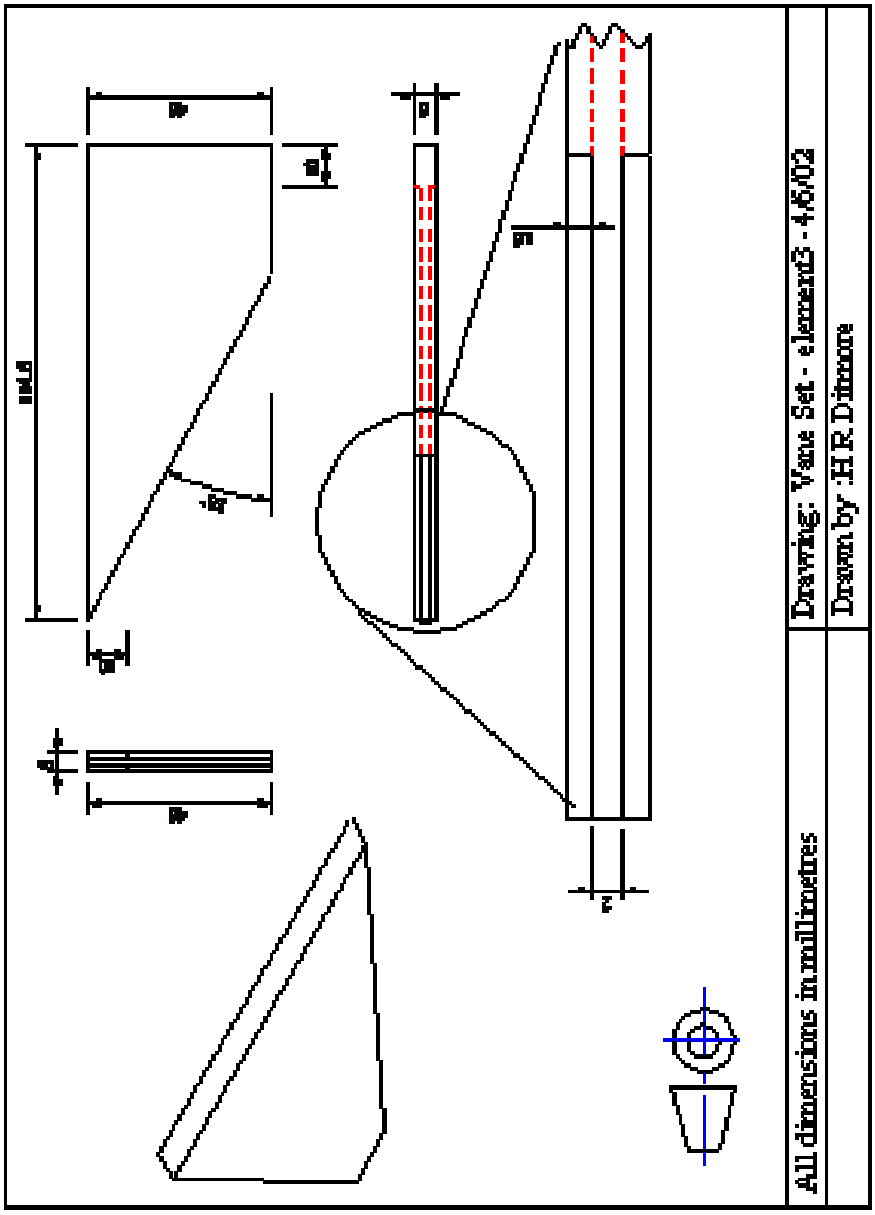
All dimensions in millimetres
Drawing: Vane Set - element3 - 4/6/02
Drawn by :H R Dimmore